IJAE

Italian Journal of Anatomy and Embryology

FIRENZE
UNIVERSITY
PRESS

Discovery and development of the cardiovascular system with a focus on angiogenesis: a historical overview

Gianfranco Natale[1,2] and Guido Bocci[3,*]

[1] Dipartimento di Ricerca Traslazionale e delle Nuove Tecnologie in Medicina e Chirurgia
[2] Museo di Anatomia Umana "Filippo Civinini", Università di Pisa, 56121, Pisa, Italy
[3] Dipartimento di Medicina Clinica e Sperimentale, Università di Pisa, 56126, Pisa

Abstract

In comparison with other organs, the beating heart and the red color of blood flowing inside vessels not only were arguments for anatomical research but also inspired metaphorical as well as symbolical considerations. Indeed, for a long time the cardiac pump was thought as the seat of passions and a haemocardiocentric theory developed, especially in Aristotle's philosophy. After the Galen's medicine, new anatomical observations were shown in the Renaissance period, with modern descriptions of the cardiovascular system by Leonardo da Vinci and Vesalius. Descartes' mechanistic view confirmed the discovery of the blood circulation by Harvey, and microscopic investigations unrevealed the capillary network. Most of these studies mainly described blood vessels as static anatomical structures and said little about their formation and development. Then, at the end of the 18th century, Hunter introduced the concept of angiogenesis in *in vivo* experiments, leading to the modern embryological research. The beginning of angiogenesis era was characterized by the first microscopical evidences of capillary formation and the discovery of the angioblasts by Sabin. The evolution of angiogenesis concept occurred in the '70s of 20th century with the pivotal work by Folkman and the onset of research on pro-and anti-angiogenic factors which characterized the next two decades of angiogenesis field. New models of neovascularization have been recently proposed such as the vasculogenic mimicry and the vessel cooption to explain the non-angiogenic tumor growth and the antiangiogenic drug unresponsiveness. Future trends are dealing with the role of angiogenic process and immunity.

Introduction

At the dawn of great civilizations men's curiosity and technology were addressed to the discovery of the nature and its phenomena, and philosophy appealed human conscience with fundamental questions about the meaning of life. Then, living beings were not an exception in this exploration. In particular, the human body gained the interest of scientists and thinkers, because of its special debatable nature: simple material object or the seat where human and divine meet? Anatomical dissection was

* Corresponding author. E-mail: guido.bocci@med.unipi.it

performed not only to know structure and organization of the human body, but also to ascertain the secrets of its spiritual nature. Among the different systems explored, the cardiovascular one was the most intriguing and fascinating. Indeed, its holistic organization, and dynamic and functional features, forcefully evoked long-lasting extraordinary theories. The concept of blood "circulation" also needed a long time to be correctly assessed. If anatomy and physiology of the cardiovascular system advanced more or less at the same time, the concept of vessel formation, as well as other anatomical structures, was more difficult to be understood, and it was mainly developed in the embryological field. After the first modern descriptions of foetal blood vessels, dating back to the Renaissance period, it was necessary to wait for the embryological studies of the 19th century to obtain the fundamental concept of angiogenesis. Since then, a large body of evidence was provided, and the modern molecular biology also allowed to discover many factors and mechanisms involved in blood vessel formation, especially in an attempt to modulate this process in cancer disease.

The cardiovascular system: concepts and theories before the 20th century

Ancient times: the cardiovascular system between science and philosophy

Since ancient times, the beating heart and the red blood flowing inside an intricate network of vessels drew men's attention and fantasy. The position of the heart in the centre of the body also contributed to assign a crucial importance for this organ. In particular, perceptible palpitations due to efforts and emotions evoked extraordinary roles for such a vital organ, whose inactivity just coincides with death. For these reasons, the cardiovascular system not only was considered in an anatomical and medical context, but was also endowed with metaphorical as well as symbolical, anthropological, mythological, magical and religious significance. Indeed, for a long time the cardiac pump was thought as the seat of passions, intelligence and soul.

In prehistoric times, about 15,000 years ago, the Paleolithic man realized a stylized heart of mammoth and bison on the wall of the Pindal cave in Spain, and Niaux cave in France. This suggests that the abstract thinking of our ancestors understood the importance of the heart for life when killing animals during hunt. In ancient Mesopotamic civilizations the heart was also recognized as the seat of the soul or spirit, the will and conscience. A very special consideration was elaborated by Egyptian civilization, when the heart was also symbolized into two hieroglyphic signs and was the only organ to be left inside the mummies or replaced with a scarab beetle amulet reporting a dedicated inscription. Again, the judgment of the dead was the process including the famous and typical scene of psychostasia or weighing of souls, when the weight of the heart was compared with that of a feather. In the famous Smith and Ebers papyri, the pulse was directly correlated to the heart activity. Interestingly, the latter papyrus also reported the description of a type of "vessel-tumor", related to the wound of a blood vessel (Latronico, 1955; Marinković et al., 2014; Natale et al., 2017).

Ancient Greek philosophers and scientists gave a great contribute to the development of technology and medicine. In the Homeric era two types of soul were distinguished. One type was named *psyche*, a sort of impalpable breathing entity which was associated to any particular part of the body. It was silent during active life. The

other type was tripartite into different body souls, named *thymos*, *noos* and *menos*, and active during waking life. All were differently located into the chest and in the proximity of the heart. Concerning the identification of a pivotal organ within the human body, two main theories took place. More correctly, in the 5th century BC an encephalocentric theory arose in the pre-socratic era. In the embryology of Anaxagoras the brain was recognized as the first living organ. Again, according to Alcmaeon of Croton, from the school of Pythagoras, as well as to Hippon of Samos, Diogenes of Apollonia and Philolaus of Croton, the brain was considered the most important organ, the mental activity depending on its function. Later, the eclectic physician Hippocrates of Kos (c. 460-370 BC) confirmed the importance of the brain. He described the tumor growth associated with solid columns of infiltrating cancer cells and swollen blood vessels tortuously arranged around the tumor itself, reminiscing the claws of a crab. This impressive iconography of newly formed pathological vessels was particularly referred to breast cancer, and Hippocrates named the tumor *karkinoma* (the Greek name for crab). In the meantime, the famous philosopher Plato (c. 427-347 BC) considered the incorporeal and immortal soul as tripartite: irascible, located in the chest, with the heart as a guardian; concupiscible, located in the abdomen, near the liver; and rational, located in brain, the head having a hierarchical supremacy over the other parts of the body. However, by the Greeks a hemocardiocentric theory was also proposed, stimulated by the suggestive and rooted notion that the heart activity just coincides with life. In the opinion of Empedocles of Agrigento (5th century BC), thoughts originated in the chest, in particular in the blood circulating around the heart, which was considered the centre of *pneuma* (breath and soul). The Empedocles' theory had a great fortune and diffusion and was later incorporated into the authoritative doctrine of the famous Aristotle (384-322 BC). According to the philosopher from Stagira, the brain was described as cold and bloodless, insensitive to touch, unconnected with the sense organs. The soul was the form of the body and the mind did not need an anatomical basis to perform its activity. Apart from the intellectual soul (*nous*), which was immaterial and belonged only to humans, the other soul faculties resided in the heart, considered the seat of life principle, movement and sensation. On the contrary, the brain had the mere function to temper the warmth emanating from the heart, the source of the innate, vital heat. Veins, arteries, and nerves were not distinguished and they were mere paths from the heart to the sense organs and muscles. Aristotle also noted that a chicken decapitated can live and walk for several minutes or more, but with a heart lesion the death is immediate. Furthermore, alterations of the state of mind associates with changes of cardiac rhythm, then the heart was assumed more important and, unlike Plato, considered the supreme organ (Manzoni, 1998; Crivellato and Ribatti, 2007; Santoro et al., 2009; Natale et al., 2017).

Aristotle was also a scientist and he dedicated a particular attention to the description of the natural world. He classified several animal species and investigated natural phenomena in living beings. In this respect, he is generally considered a pioneer in biological studies. His interests mainly dealt with animal locomotion, respiration, aging and sensations. Within a vitalistic epigenetic vision, his embryological studies deserve a particular mention, and some interesting observations allowed Aristotle to be credited with the first description of blood vessel formation. The philosopher noticed that the cardiovascular system is the first structure to appear during chick development. In his *Historia animalium* (History of Animals) he clearly stated

that *the first signs of the embryo are seen after three days and three nights… and the heart is no bigger than just a small blood spot in the white. This spot beats and moves as though it were alive.* More in depth, he understood that blood vessel formation and distribution were related to heart development and function, with the blood flowing inside this system to nourish the whole organism. Then, body growth just depended on the ongoing development and organization of blood vessels and the heart was the first organ to appear during organogenesis and the centre of that system (Crivellato and Ribatti, 2006; Crivellato et al., 2007; Ribatti et al., 2015).

The physician Diocles of Carystus (4th century BC) reinforced the central position and importance of the heart, as the seat for hearing and understanding. He described the auricles, improving the anatomy of this organ, and attributed to these appendages the role of sensory organs. However, he also recognized the involvement of the brain in cognitive functions. In particular, the right half of the brain was the centre for sensation and the left for intelligence, thus anticipating the modern concept of cerebral dominance. These ideas were also accepted by Praxagoras of Cos (born c. 340 BC) and his disciples. This physician had the great merit to distinguish arteries from veins. Nevertheless, only veins were thought to transport the blood, whereas arteries were involved in the distribution of the *pneuma* (Crivellato and Ribatti, 2007).

Later, during the Hellenistic period (3rd century BC), the Alexandrian medical school distinguished itself for a remarkable progress, especially in anatomy, and two principal figures emerged: Herophilus of Chalcedon (335-280 BC) and Erasistratus of Ceos (310-250 BC). These scientists had the opportunity to dissect corpses and vivisect animals and probably human bodies from criminals. This activity led to improve not only anatomy, but also physiology, with the description of the arterial pulse depending on the heartbeat. Finally, the neuroanatomical studies allowed to assign cognitive functions to the brain (encephalocentric theory) to the detriment of the heart, and blood vessels were distinguished from nerves. However, against the evidence of the facts, arteries were still believed to transport a vital spirit. Erasistratus also described a peculiar structure characterized by a network of veins, arteries and nerves, named *triplokia*. (Latronico, 1955; Crivellato and Ribatti, 2007; Natale et al., 2017).

During the Roman period, the ancient knowledge was elaborated by one the most important figures of the western medicine: Galen of Pergamon (2nd century CE) (Fig. 1). His observations and descriptions were dogmatically accepted for about fifteen centuries. One of his most famous physiological theories just concerned the cardiovascular system, which was not regarded as a circulatory one. Apart from the heart, Galen's theory also assigned a pivotal role to the liver, responsible for blood formation and movement (Azizi et al; 2008; Limet, 2010; Aird, 2011). However, in the Middle Ages the influence of Byzantine and Islamic medicine, and the development of the *Schola Medica Salernitana*, favored a new approach. Even if without a practical repercussion, Mondino de Luzzi (c. 1270-1326) dared to propose the dissection of human corpses.

New insights into the anatomy of the cardiovascular system were provided by Islamic medicine. In *The Canon of Medicine* the famous Avicenna (980-1037) admitted the connection between arteries and veins, and a peripheral network of very small vessels was postulated: *The good blood ascends into the superior vena cava, and its subsequent course is into smaller and smaller veins: and finally into the finest hair-like channels …*

Figure 1. Frontispiece of Galen's *Omnia quae extant opera* (1576). Library of Medicine and Surgery, and Pharmacy. University of Pisa.

according to the decree of Allah. Ibn al-Quff (1233-1286) also hypothesized the presence of communicating fenestrations between arterial and venous systems: *These fenestrations are hidden from the eye*. Ibn al-Nafis (c. 1210-1288) was the first to describe the pulmonary circulation (Azizi et al; 2008; Limet, 2010; Aird, 2011; Natale et al., 2017).

Renaissance of the cardiovascular system

The first scientific and accurate anatomical drawings of the heart and blood vessels were realized by Leonardo da Vinci (1452-1519) in the 15th century. This year we just celebrate the achievements of Leonardo, one of the greatest polymath of all times, who died five-hundred years ago. He revolutionized Renaissance painting, taught and technology, inspiring many important artists and scientists, and his innovative dissections on human corpses anticipated the anatomical revolution by Vesalius. Leonardo invented the anatomical iconography, with remarkable drawings and informative descriptions. He also adopted descriptive models taken from other fields. Then, the anatomical description was inspired by Ptolemy's geography and Leonardo

considered the human body as a new territory to be explored and named: *Thus, in 15 entire figures, you will have set before you the cosmography of this lesser world on the same plan as, before me, was adopted by Ptolemy in his cosmography; and so I will afterwards divide them into limbs as he divided the whole world into provinces.* In particular, blood vessels suggested such an approach: *Here shall be represented the tree of the vessels generally, as Ptolemy did with the universe in his Cosmography; then shall be represented the vessels of each member separately from different aspects.* Leonardo was fascinated by the heart and its valvular functions, and about one fourth of his anatomical drawings, mainly from the Windsor manuscripts, was dedicated to the cardiovascular system. His astonishing embryological drawings of fetuses and newborns are also very famous. Then, after Aristotle, Leonardo also faced the dynamic changes occurring during development, including blood vessel rearrangement. He thought that the fetus had no cardiopulmonary activity: *To this child the heart does not beat, and it does not breathe because it lies continually in water.* Leonardo described the presence and formation of the intricate vascular network interconnecting the fetus with his mother: *The «vene massime» of the child in the uterus. Explain how the veins of the uterus ramify in the uterus, and which and how many they are, and which enter the placenta, and which of them are torn asunder in the separation of the child from the uterus. The veins and arteries of the uterus of woman have such a mixture of contacts with the extreme veins of the navelstring of her child […], as the «vene miseraice» ramifying in the liver, have with the ramification of the veins which descend from the heart into the same liver, and as the ramifications of the veins of the lung have with the ramifications of the trachea, which refresh them. But the veins of the child do no ramify in the substance of the uterus of its mother, but in the placenta, which takes the place of a shirt in the interior of the uterus, which it coats, and is connected (but not united) to this by means of the cotyledons etc.* More interestingly, he also provided the description of a blood vessel that collapses when its function after birth ends. It is the case of the fetal umbilical vein, whose remnant is represented by the round ligament of the liver: *When the umbilical vein is in operation, for which it was created, it attains the principal site in Man, that is, the middle of the body, as well for height as for breadth. But when such vein was afterwards deprived of its office, it drew itself apart together with the liver, created and then nourished by it. And this upper part of the umbilical vein was pushed through the change of the middle of the liver, which through the increasing of the milt, created on the left side [this liver] was driven into the right side and carried with it the upper part of the umbilical vein, which was joined to it* (Vangensten et al., 1911-1916; Aird, 2011; Shoja et al., 2013; Loukas et al., 2016; Kemp, 2019; Laurenza, 2019).

Leonardo noticed different patterns of vessel ramification and in the pre-microscopic era intuitively perceived the existence of capillaries: *Of the ramifications of the veins are two sorts, i.e. simple and compound ones; simple is the one which goes on ramifying infinitely; compound is it, if from the two ramifications a single vein is generated, as you see* n m *and* m o, *branches of two veins which join in* m *and compose the vein* m p, *which goes to the membrum* (Fig. 2). More in depth, he clearly defined these narrower blood vessels: *…per le istrette ramificazion delle vene capillare* (through the narrow ramifications of capillary veins). Leonardo also dealt with blood vessel ramification and distribution: *Always are the ramifications of the vessels so much bigger as they originate in a bigger trunk, that is the principal ramifications; the same continues in the ramifications of the ramifications till the end.* Then, although unaware of the geometrical and mathematical significance of such observations, Leonardo's drawings illustrated and anticipated the modern

Figure 2. Different types of venous ramification according to Leonardo da Vinci (see text for a full description). From Vangensten et al. (1911-1916; volume IV, folio 8 recto). Library of Medicine and Surgery, and Pharmacy. University of Pisa.

concept of fractal formation and distribution of natural structures, such as rivers and blood vessels (Scianna et al., 2013). More recently, the "self-similarity logic" concept, dealing with a hierarchical multi-level organization in which very similar rules (logic) apply at each level, has been also proposed as a unitary scheme to describe many features of the formation of the vascular system and its remodeling processes (Guidolin et al., 2011).

In the Renaissance period, the father of modern anatomy, Andreas Vesalius (1514-1564), in his masterpiece *De Humani corporis fabrica* (On the Fabric of the Human Body) corrected the Galen's assumption that great blood vessels moved from liver to supply all parts of the body and doubted the existence of interventricular pores. In the same period, the philosopher and theologian Michael Servetus (1511-1553) and the anatomist Realdo Colombo (1516-1559) rediscovered the pulmonary circulation and firmly denied a communication between the two cardiac ventricles (Azizi et al; 2008; Limet, 2010; Aird, 2011).

Embryological studies favored the discovery of more dynamic features of the cardiovascular system. In the work *De foramine* (Foramen Ovale), Leonardo Botallo (1530-1587) provided a more complete description of the interatrial foramen ovale. His name was also associated with the ductus arteriosus, connecting the main pul-

monary artery to the proximal descending aorta. Giulio Cesare Aranzio (c. 1530-1589) dedicated some researches to the study of umbilical vessels and in the work *De humano foetu libellus* (Book on the Human Fetus) described the ductus venosus, which shunts the fetal umbilical vein blood flow directly to the inferior vena cava. Because of incorrect ideas about blood circulation, Girolamo Fabrici d'Acquapendente (c. 1533-1619) was not able to discover some features of the fetal vascular system. However, his embryological studies, published in *De formato foetu* (The Formed Fetus) (1600) and *De formatione ovi, et pulli tractatus accuratissimus* (Accurate Treatise on the Formation of the Egg and of the Chick) (1621), are noteworthy. He realized that after birth the umbilical cord and its vascular content dried up and disintegrated, having accomplished their function within the womb. In another work, *De venarum ostiolis* (Valves of Veins) (1603), he fully described anatomy and function of venous valves (Aird, 2011).

In the work *Peripateticarum quaestionum libri quinque* (Five Books of Peripatetic Questions), Andrea Cesalpino (1524-1603) introduced for the first time the concept of "circulation" applied to the cardiovascular system and also mentioned the presence of very small blood vessels, named *capillamenta* (hair-like vessels). But the important step in the history of the cardiovascular anatomy and physiology is represented by the notion of a systemic circulation of the blood, which is propelled by the heart, finally regarded as a muscular pump. The famous author of this mature account of the blood circulation as a closed circuit was William Harvey (1578-1657), who published his fundamental observations in the work *Exercitatio anatomica de motu cordis et sanguinis in animalibus* (An Anatomical Exercise on the Motion of the Heart and Blood in Living Beings) (Azizi et al; 2008; Aird, 2011).

Heart and blood vessels in the scientific revolution: mechanism and microscopic investigations

The French philosopher René Descartes (1596-1650) based his explanation of the world, including living beings, on a mechanistic model. Against Harvey's opinion, he postulated a heat theory to explain cardiac movements and blood circulation, through distillation, agitation, rarefaction and fermentation of particles (animal spirits), as reported in his work *Description du corps humain* (Description of the Human Body): *So I will say here that the heat in the heart is like the great spring or principle responsible for all the movements occurring in the machine*. Then, the development of a fetus was a mechanistic process, as well, according to an epigenetic model that included differentiation and growth (Heitsch, 2016). Concerning the development of the human body, Descartes described the parts of the body which are formed in the seminal material. The substance forming the blood also induced the development of the heart and subsequently the great artery originating from the heart to which it came back through another pathway: *As soon as the heart begins to form in this way, the rarefied blood leaving it makes its way in a straight line in the direction of least resistance, viz. towards the region of the body where the brain forms later on; and the path taken by the blood begins to form the upper part of the great artery. Now, because of the resistance produced by the parts of seminal material which it encounters, the blood does not travel very far in a straight line without being pushed back towards the heart along the same path by which it came. But it cannot return down this path, because the way is blocked by the new blood which*

the heart is producing. Then, in the same way blood vessels are formed: *I do not need to explain the formation of arteries and veins, because I have nothing else to say. Blood vessels are formed according to this general mechanism. When a little part of the seminal material reaches the heart, the pathway it creates is a vein, and the pathway created by the blood coming from the heart is an artery. When these blood vessels are far from each other, vein and artery appear separated, because the extremities of the artery are not visible anymore.*

Malpighi described the network of pulmonary capillaries that connect the small arteries to the small veins, then completing the closed circuit postulated by Harvey. However, this discovery did not fully clarify the vascular nature of capillary networks in particular organs, such as uterus, spleen and cavernous tissues in genitals. For example, some scientists, such as the above-mentioned Hunter and other anatomists, including Georges Cuvier (1769-1832), Friedrich Tiedemann (1781-1861), Bartolomeo Panizza (1785-1867), Ernst Heinrich Weber (1795-1878) and Pierre Augustin Béclard (1785-1825) recognized the vascular nature of the cavernous tissue. In the 18th century alternative hypotheses were also reported. For instance, in the case of erectile tissues of genitals, with particular attention to the male urethra, the presence of a non vascular spongy tissue with cellular texture (cellular theory) was postulated by some authors, such as Albrecht von Haller (1708-1777), Guichard Joseph Duverney (1648-1730), Herman Boerhaave (1668-1738) and Marie François Xavier Bichat (1771-1802). According to this theory, the cavernous tissue was conceived as consisting of a loose and elastic tissue arranged in several cellular cavities into which, during erection, blood was poured from the arteries, and from which it was afterwards removed by veins. Finally, thanks to improved injection techniques, Paolo Mascagni (1755-1815) and Alessandro Moreschi (1771-1826) provided accurate works on this subject, demonstrating the vascular nature of the cavernous bodies. Finally, in 1899 Victor Vecki von Gyurkovechky (1857-1938) confirmed the vascular theory, histologically demonstrated by the presence of endothelium: *These small hollow interspaces of the three corpora are coated with endothelium resembling that of the veins, and are consequently venous spaces* (Armocida and Natale, 2019).

As opposed to epigenesis (or neoformationism), preformationism developed in 17th century. According to this theory, as suggested by its name, living beings develop from a miniaturized preexisting form. Paradoxically, this approach became popular thanks to the first microscopic observations, when the presence of preformed organisms (*homunculi*) was believed in ova or spermatozoa. This theory was supported by important scientists of that time, such as Jan Swammerdam, Marcello Malpighi, Charles Bonnet, Albrecht von Haller and Lazzaro Spallanzani. Of course, such an approach simply admitted a pantographic growing of preformed organs and strongly limited the concept of formation of new tissues and organs from undifferentiated cells. Then, it is not surprising if the microscopist Antonie van Leeuwenhoek (1632-1723) observed *all manner of great and small vessels, so various and so numerous that I do not doubt that they be nerves, arteries and veins... And when I saw them, I felt convinced that, in no full grown body, are there any vessels which may not be found likewise in semen* (Friedman, 2008).

It should be remarked that a large part of the above-mentioned discoveries described blood vessels as static anatomical structures and said nothing about their formation and development, at least in the modern sense. Finally, in his fundamental *Theoria generationis* (Theory of Generations), a doctoral dissertation published in 1759, Cas-

par Friedrich Wolff (1734-1794), one of the founders of modern embryology, definitively affirmed the theory of epigenesis by demolishing the bases of preformationism, and showed that the organs in the embryo are formed successively from organized primitive tissues. He described the formation of veins (*De formatione venarum*) and arteries (*De formatione arteriarum*) and vessel branches (*Ramificatio venarum* and *Ramificatio arteriarum*). According to Wolff's model, the development of plants and animals was based on two main factors: the ability of organic fluids to solidify, and a mysterious organizing force named *vis essentialis* (essential force). At the moment of solidification, the movements of fluids into the new part lead to the formation of vesicles and vessels. More in depth, vesicles develop at an early step, when fluids move into the initially homogeneous secreted material, forming stationary pockets. Similarly, blood vessels are formed from the action of fluids moving through the homogeneous substance. Unlike plants, where vessels form and develop in parallel, in animals the fundamental substance is not rigid, allowing the development of branching blood vessels, which finally refer to the heart (Roe, 1979; Van Speybroeck et al., 2002). Wolff confirmed his ideas also in another work: *De formatione intestinorum* (On the Formation of the Bowel).

An important step in the history of the cardiovascular system is represented by the first *in vivo* description of blood vessel growth, which is attributed to the Scottish surgeon John Hunter (1728-1793), who showed that vascularization is an active process in tissues. In particular, in his book *A treatise on the blood, inflammation, and gunshot wounds*, published in 1794, he described the process of growth of new blood vessels, anticipating the modern concept of angiogenesis. Hunter observed an increased vascularization not only during the growth of young animals, but also in disease conditions and healing processes: *As a further proof that this is a general principle, we find that all growing parts are much more vascular than those that are come to their full growth; because growth is an operation beyond the simple support of the part: this is the reason why young animals are more vascular, than those that are full grown. This is not peculiar to the natural operation of growth, but applies also to disease, and restoration. Parts become vascular in inflammation; the callus, granulations, and new formed cutis, are much more vascular in the growing state, or when just formed, than afterwards; for we see them crowded with blood-vessels when growing, but when full grown, they begin to lose their visible vessels, and become not even so vascular as in the other neighbouring original parts, only retaining a sufficient number of vessels to carry on the simple oeconomy of the part; which would now seem to be less than in an original part. This is known by injections, when parts are in the growing state, or are just grown, and for some time after* (Stephenson et al., 2013; Lenzi et al., 2016; Natale et al., 2017; Bikfalvi, 2017; 2018).

Other important descriptions of vessel sprouting from pre-existing vessels, especially in inflammation and cancer tissues, were provided by different authors: in 1826 by Jacobus Ludovicus Conradus Schroeder van der Kolk (1797-1862) in *Observationes Anatomico-Pathologici et Practici Argumenti* (Anatomo-Pathological Observations and Practical Arguments), where new vessels in newly formed parts and in parasitical diseases were reported, and in what respect they differ from the natural structure; in 1844 by E.A. Platner in *Einige Beobachtungen über die Entwicklung der Kapillargefässe* (Some observations on the development of capillaries); in 1853 by J. Meyer in *Über die Neubildung von Blutgef*ässen (On the Formation of New Blood Vessels); in 1856 by Christian Albert Theodor Billroth (1829-1894) in *Untersuchungen über die Entwicklung der Blutgefässe* (Studies on the Development of Blood Vessels) (Natale et al., 2017).

Angiogenesis in the 20th and 21st century

Angiogenesis is a term created to indicate the process by which the vascular tree grows by sprouting, cell division, migration, and assembly of endothelial cells derived from pre-existing vessels. Angiogenesis is not characterized by additional differentiation of endothelial cells, but rather by the reorganization of an existing vascular network in response to some angiogenic factors (Ribatti, 2014; Bautch and Caron, 2015; Ribatti et al. 2015). The research on angiogenesis has been usually tightly linked with the cancer field because of the importance of this process for the development of tumor masses. Thus, it is not a surprise that the main scientific achievements on neovascularization have been made looking at the cancer angiogenesis.

The beginning of angiogenesis era

As stated before, already in John Hunter's works the concept of angiogenesis was described, but not the term "angiogenesis" to indicate this process (Natale et al. 2017). Indeed, the debut of the term "angiogenesis" was due to Flint in 1900, who described the vascularization, and its development, of the adrenal gland referring to the work of previous scientists, such as Billroth, Thoma and Arnold (Flint, 1900) who traced the new formation of capillaries from those which already existed. Moreover, three years later Flint (1903) studied the vascularization and the blood vessel development of the submaxillary gland. Tumor vascularization started to be studied systematically by Goldman (1908). He used intra-arterial injections of bismuth diluted in oil to visualize the vasoproliferative reaction of an organ where a tumor is developing. Indeed, he described a marked capillary budding and new vessel formation particularly at the border of the neoplasm, also citing the work of other colleagues such as Hunter, Schroeder van der Kolk, and Broca. In the decade, Florence Sabin (1917) (Fig. 3) focused her research on the origin of blood vessels from endothelial cells that are already integrated into the primary vascular plexus of the embryo and subsequently proposed that in the early phase of embryonic angiogenesis endothelial cells are derived from precursor cells, the angioblasts (Sabin, 1920). A year later, Clark (1918) described the capillary sprouting in tadpole tails from capillaries with high flow.

However, the angiogenic process and the vascularization of tumors had the attention of various anatomists through the 20th century. As reported by Ribatti (2009) in his book on the history of tumor angiogenesis, during 1927, Lewis (1927) described the neovascularization of several rat tumors and observed that the vascular architecture of each tumor was different, leading to the conclusions that tumor environment greatly influence the morphological characteristics of the blood vessels, and that a common pattern could not be recognized. A great increase in the knowledge and description of angiogenesis was reached with the introduction by Sandison (1928) of the experimental use of a transparent chamber that could be inserted into the ear of rabbits. This experimental device allowed the microscopic observation of living tissues underneath a glass coverslip. Successively, Clark and colleagues, thank to this experimental tool, described the morphological characteristics of blood (Clark et al., 1931) and lymphatic vessels (Clark and Clark, 1932), using also contrast media, and the changes of the newly grown vessels over a period of months (Clark et al., 1931).

Figure 3. A photograph of Florence Sabin (from the Profiles in Science of the US National Library of Medicine).

Moreover, he left detailed observations on the growth of blood capillaries in living animals, showing that capillary sprouts had adventitial cells (Clark and Clark, 1939), opening the field to the subsequent studies of Ide et al. (1939) who used the transparent chambers to investigate the relationship between the growth of rabbit epithelioma and its vascular supply. These scientists observed that the tumor mass increased with a rapid and extensive formation of new vessels that were necessary to its development. Moreover, they firstly suggested that tumors might release factors capable of stimulating the blood neovascularization growth. In 1941, Green (1941) demonstrated that the vascularization was necessary to the growth of a transplanted tumor, whereas few years later, Algire and Chalkley (1945) firstly described that the progression of malignancies could continuously elicit new capillaries from the host. Moreover, they also quantified the number of blood vessels with daily counts, comparing them to the changes in tumor size and concluding that the growth of a tumor is closely connected with the development of an intrinsic vascular network. This feature was emphasized by Rondoni (1946), an Italian pathologist, who described that a tumor acts both angioplastically and angiotactically, promoting both the formation of new vessels and the attraction of vascular capillaries.

The evolution of angiogenesis concept

In 1948, Michaelson (1948a) described the vascular morphogenesis of the retina and hypothesized that a diffusible "factor X" produced by the retina was responsible for retina neovascularization in proliferative diabetic retinopathy [Michaelson, 1948b]. Interestingly, in 1956, Merwin and Algire (1956) found out that the vasoproliferative response to normal or neoplastic tissues transplanted into muscles was not different in terms of the time of onset of new blood vessels but was significantly divergent in terms of intensity and influenced by the distance between the implant and host's vessels: tumors had a longer activity range. Another fundamental step to the comprehension of the presence of a diffusible factor stimulating the new capillaries was brought by Greenblatt and Shubik (1968) using a Millipore chamber into a hamster cheek pouch. Indeed, because the pores of the chamber were permeable to the tumor interstitial fluid but not to tumor cells, the new blood vessels from the host were formed in any case, without any contact with cancer cells. Based on this evidence, the authors hypothesized the presence of a diffusible factor responsible for the neovascularization. Moreover, Ehrmann and Knoth (1968) in the same year confirmed these data with tumor fragments laid on Millipore filters planted on a Chick Chorioallantoic membrane (CAM). In the 1970s, Gimbrone and Gullino (1976), using the rodent mammary gland, demonstrated that a resting gland had not any angiogenic capacity, whereas the presence of a neoplastic transformation induced angiogenesis.

The perspective in the field of angiogenesis changed radically with the pivotal article published in the New England Journal of Medicine (Folkman, 1971) by the surgeon Judah Folkman who reported several ideas that drastically modified the perception of angiogenic process in the scientific community, such as the essential role played by angiogenesis in cancer growth, the secretion by tumour cells of diffusible angiogenic molecules, the possibility of tumour dormancy due to the blocked angiogenesis, the development of the concept of "antiangiogenesis", the prediction of the future discovery of angiogenesis inhibitors, and finally the concept that an antibody targeting a tumour angiogenic factor (TAF) could be an anticancer drug (Fig. 4). This last idea inspired a completely new field in anticancer therapy that is still pursued by numerous scientists and oncologists (Jayson et al., 2016) with drugs such as bevacizumab, an anti-vascular endothelial growth factor (VEGF) antibody, conceived in the fundamental work by Napoleone Ferrara (Ferrara et al., 2004). In the subsequent years, Folkman provided numerous evidences supporting his initial hypothesis, also developing fundamental assays to study the angiogenic process. In 1972, his team demonstrated that *in vivo* tumour dormancy was obtained by prevention of neovascularisation (Gimbrone et al. 1972) and, a year later, he was the first, in collaboration with his group, to successfully grow and passage vascular endothelial cells *in vitro* (Gimbrone et al., 1973), an experimental technique that permitted the future development of all the antiangiogenic drugs in the next four decades. Moreover, angiogenesis was firstly observed *in vitro* by Folkman and Haudenschild (1980). After long-term culture of capillary endothelial cells, they observed the spontaneous organization of these cells into capillary-like structures with the presence of a lumen. *In vitro* three-dimensional models of endothelial cells grown in collagen gels have provided great steps in the knowledge of angiogenesis. As an example, Montesano et al. (1986) observed that fibroblast growth factor induced endothelial cells to form
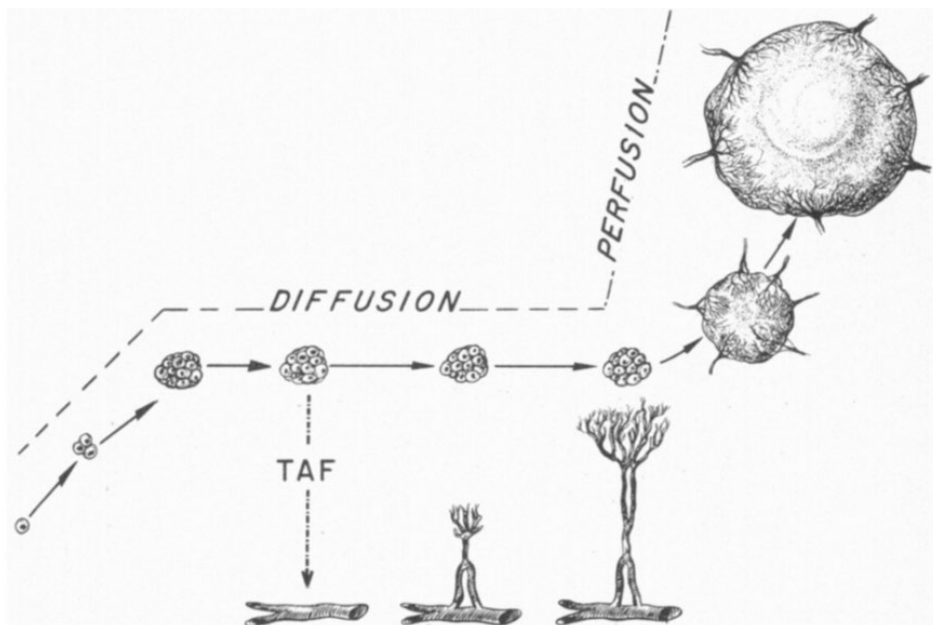
Figure 4. Original figure n. 2 of the pivotal article published by Folkman (1971). The figure describes the concept that most solid tumors require vascularization for their growth and that tumor angiogenesis factor (TAF) may be the mediator of neovascularization.

capillary-like structures in collagen gels, showing the *in vitro* angiogenic activity of this cytokine.

The exciting era of pro- and anti-angiogenic factor discoveries

Despite the work by Greenblatt and Shubik (1968), until the '70s it was largely accepted that tumors did not secrete specific angiogenic proteins. The conventional thinking was that tumor vasculature derived from the inflammatory reaction of necrotic cancer cells (Ribatti, 2009). Folkman (1971), as described above, hypothesized the presence of a soluble factor and in the same year he isolated a tumor fraction responsible for the angiogenesis process (Folkman et al., 1971). Indeed, the homogenate of a murine breast cancer was fractioned by gel-filtration and found out that a fraction of about 10,000 KDa had the strongest angiogenic activity. This active fraction was subsequently named "tumor angiogenesis factor" (TAF). This fraction induced vasoproliferative responses in different *in vivo* models such as CAM or rabbit cornea, and *in vitro* on cultured endothelial cells (Weiss et al., 1979).

Gospodarowicz (1975) found that the pituitary gland contains a potent agent for cell growth, although he did not identify the factor. However, he demonstrated that this putative factor induced fibroblast cell growth and hence he called it fibroblast growth factor (FGF) (Gospodarowicz and Moran, 1975). In 1978, he also found out that the activity of the FGF was not restricted only to fibroblasts but also to other

cell types, including endothelial cells (Gospodarowicz et al., 1978). Later, Shing et al. (1984) reported the isolation and the purification of FGF, initially identified by Gospodarowicz, the first factor that specifically stimulated the growth of endothelial cells. Moreover, the same group demonstrated that this factor was able to stimulate new vessel growth *in vivo* in the CAM assay (Shing et al., 1985).

Another important step forward to the knowledge of pro-angiogenic factors was the work of Dvorak and colleagues at the beginning of the '80s. Indeed, he demonstrated that vascular hyperpermeability to fibrinogen and other plasma protein was a common feature of many animal and human tumors (Dvorak et al., 1981; 1983; 1984). Dvorak et al. (1979) found out that supernatants from tumor cells generated blue spot to extravasated Evans blue, whereas normal cells did not. Dvorak named this tumor supernatant permeabilizing activity as vascular permeability factor (VPF) (Senger et al., 1983). Moreover, the team of Dvorak showed that VPF was a macromolecule and inactivated by the heat and proteases whereas the inhibition of protein synthesis declined its secretion (Senger et al., 1983). Senger et al. (1983) purified VPF, demonstrating that it was a 34-43kDa dimeric protein. Subsequently, Connolly et al. (1989) of the Monsanto Company showed that VPF was also an endothelial mitogen *in vitro* and an angiogenic factor *in vivo*.

In the same year, Ferrara and Henzel (1989) reported the isolation, of a diffusible endothelial cell-specific mitogen from a medium conditioned by bovine pituitary follicular cells, which they called "vascular endothelial growth factor" (VEGF). Later, they reported the isolation of cDNA clones of different isoforms of the protein with clear angiogenic characteristics (Leung et al., 1989). In 1992, the Ferrara's laboratory in collaboration with the University of California at San Francisco discovered the VEGF receptor-1 (de Vries et al., 1992) whose expression was regulated by hypoxia (Gerber et al., 1997). Moreover, in 1996 both Ferrara et al. (1996) and Carmeliet et al. (1996) demonstrated the essential role of VEGF in embryonic vasculogenesis and angiogenesis in the mouse. Indeed, the inactivation of just a single allele of VEGF resulted in the embryonic lethality with a number of developmental anomalies of the cardiovascular system.

Over the years, five VEGF-related genes have been identified, as well as five different related receptor tyrosine kinases (Uccelli et al., 2019), becoming the main known pro-angiogenic factor. The VEGF was then recognized to be the same factor discovered, but not sequenced, by Dvorak and colleagues.

In 1996, a novel family of angiogenic factors, called as Angiopoietins (Ang), has been identified by the group of Yancopoulous (Davis et al., 1996; Maisonpierre et al., 1997). Ang1 is a potent angiogenic growth factor signalling through its receptor Tie2, whereas Ang2 was initially identified as a vascular disruptive agent with antagonistic activity through the same receptor. Recent data, instead, demonstrate that Ang2 has context-dependent agonist activities (Akwii et al., 2019).

Later, the scientists discovered that the factors able to activate and regulate angiogenesis were far more than just the few hypothesized by Folkman and other scientists, including for example platelet-derived growth factors, placenta growth factor, insulin-like growth factors, hepatocyte growth factor, hypoxia-inducible factor-1 α and β, transforming growth factor α and β, tumor necrosis factor α, interleukins -1 β, -3, -6, -8, neuropilin 1 and 2, angiogenin, adrenomedullin, and stromal cell-derived factor-1 (Natale and Bocci, 2018).

Besides the pro-angiogenic factors, during the years the scientists discovered also numerous endogenous inhibitors of angiogenesis and their list continues to grow with new discovered molecules (Rao et al.. 2015). Many proteins have been identified as endogenous angiogenesis inhibitors including thrombospondins (TSP)-1 and −2, pigment epithelial derived factor, platelet factor-4, and various interleukins and interferons. Collagen and plasminogen fragments have been also identified as angiogenesis inhibitors such as angiostatin (fragment of plasminogen), endostatin (fragment of collagen XVIII) and tumstatin (fragment of collagen IV) (Natale and Bocci, 2018). Among these inhibitors, at least eleven endogenous angiogenesis inhibitors were identified or discovered in the Folkman's laboratory in almost 25 years (Folkman, 2008). In 1982 Folkman and Taylor (1982) recognized that protamine and platelet factor 4 inhibited angiogenesis and in 1985 he reported a new class of corticosteroids, called "angiostatic" steroids (Crum et al., 1985). Moreover, O'Reilly and colleagues discovered in 1994 the antiangiogenic and antitumor activity of angiostatin (O'Reilly et al., 1994) and later of endostatin (O'Reilly et al., 1997).

TSP-1 was the first protein to be identified as an endogenous inhibitor of angiogenesis by Good et al. (1990). In the same year, Taraboletti et al. (1990) demonstrated that this heparin-binding protein stored in the extracellular matrix was able to inhibit endothelial cell proliferation of different tissues. Moreover, Jack Lawler (2002) obtained TSP-1 null mice and showed that tumors grew significantly faster in these mice. Bocci et al. (2003) displayed the role of TSP-1 in the antitumor effect of metronomic chemotherapy, a therapeutic approach able to inhibit angiogenesis.

The last developments in angiogenesis field of research

However, not only solid cancers depend on angiogenesis for their growth. In 1994, for the first time, Vacca et al. (1994) demonstrated the angiogenesis involvement in haematological malignancies. These authors described the presence of bone marrow angiogenesis in multiple myeloma with a high correlation between the extent of neovascularization and plasma cell proliferation. A year later, Klein et al. (1995) confirmed these data. Moreover, Ribatti et al. (1996) firstly showed the bone marrow angiogenesis also in B cell non-Hodgkin's lymphomas, whereas Perez-Atayde et al. (1997) brought the first evidence of increased bone marrow microvessel density in acute lymphocytic leukemia.

In 1996, Zimrin et al. (1996) suggested for the first time that Jagged-Notch signaling was able to regulate FGF-induced endothelial cell migration *in vitro*, an early and key event during the process of angiogenesis. Five years later, Mailhos et al. (2001) reported the expression of Delta4 in arterial endothelium during mouse embryogenesis and in the endothelium of tumor blood vessels. The authors of this study concluded that Delta4 and the Notch signalling pathway could have a primary role in angiogenesis and suggested them as possible new targets for antiangiogenic tumor therapy. Shawber and Kitajewski (2004) stated that Notch genes were highly expressed in the vasculature suggesting an important role for Notch in guiding endothelial cells to form the vasculature. Indeed, studies in zebrafish, mice and humans indicated that Notch works in conjunction with other angiogenic pathways to pattern and stabilize the vasculature. Recently, Pan et al. (2019) revealed the inhibitory role of TSP-2 on cell invasion, migration and angiogenesis in the development of medulloblastoma *via*

blockade of the Notch signaling pathway, suggesting its potential as a new treatment target for this brain tumor.

In 1997, Asahara et al. (1997) reported the isolation of putative endothelial progenitor cells from human peripheral blood, on the basis of cell-surface expression of CD34 and other endothelial markers. These authors showed that hematopoietic cells differentiate into endothelial cells *in vitro* and *in vivo*. The importance of endothelial progenitor cells in the process of angiogenesis, and in particular of tumor angiogenesis, has been discussed during the years but, in 2008, Gao et al. (2008) demonstrated that also a low percentage of incorporated endothelial progenitors in the vasculature of tumors is sufficient and necessary for the conversion of avascular micrometastases to progressive metastatic tumors.

In 1999, Betsholtz's group described the mechanisms of pericyte recruitment to newly formed blood vessels with the pre-eminent role of PDGF-B and PDGFR-beta (Hellstrom et al., 1999), and subsequently discovered that specific cells atop the nascent vessel guide the growth of the vascular tubes (TIP cells) with the VEGF stimulus (Gerhardt et al., 2003). Few years later, different authors described that the vessel lumen formation is an active process which requires at least one endothelial cell (Kamei et al., 2006; Blum et al., 2008; Strilic et al., 2009). More recently, Carmeliet's team discovered that the vessel sprouting requires a specific metabolism and in particular the PFKFB3-driven glycolysis (De Bock et al., 2013).

In 1999 Maniotis et al. (1999) coined the term vasculogenic mimicry (VM) when they reported that human melanoma cells were able to form vascular channels observing sections from aggressive human intraocular and metastatic melanomas. The word vasculogenic was referred to the formation of blood supply system by tumor cells rather than endothelial cells, which is independent on typical modes of angiogenesis. Although the data by Maniotis and collaborators were initially harshly disputed by Mc Donald et al. (2000), later on VM has been shown and deeply described in various cancers including melanoma, breast and lung cancer, ovarian cancer, osteosarcoma, gastric cancer, bladder cancer, hepatocellular cancer, and colorectal cancer (Azad et al., 2019). Indeed, high tumor VM is associated with a high tumor grade, shorter survival, invasion, metastasis and poor prognosis (Delgado-Bellido et al., 2017).

Another important concept that has acquired recent interest in the field of neovascularization is the vessel co-option (or vascular co-option): "*a mechanism by which tumors obtain a blood supply by hijacking the existing vasculature and tumor cells migrate along the vessels of the host organ*" (Donnem et al., 2013). Pezzella et al. (1997) were the first to report a non-small cell lung cancer growing with no morphological evidence of neoangiogenesis but only exploiting normal tissue vessels already present. Indeed, many studies have confirmed that the microcirculation of some human tumors may be provided by nonsprouting vessels and that a variety of tumors can grow and metastasize without angiogenesis (Krishna Priya et al., 2016). Vessel co-option may be found in many tumors but especially in highly vascularized tissues such as brain, lung, and liver (Donnem et al., 2013). Recently, vessel co-option has been involved into the potential explanation of antiangiogenic drug resistance and it has been suggested the tumor progression can only be stopped by combination therapies that block both angiogenesis and cooption (Voutouri et al., 2019).

Recently, a new important direction of the research in this field is the study of the relation between the vascular system with immunology. Indeed, the work by two

laboratories focused on the importance of specialized vessels called high endothelial venules (HEV) in tumors to trigger anti-cancer immunity (Martinet et al., 2011; Allen et al., 2017). The tumor vasculature-immune interdependency, in the perspective of an anti-tumor response, could be an important step into a new approach to antiangiogenic therapy with the immunotherapy combination using anti-PDL1 because it is able to stimulate the number of HEV vessels in tumors (Allen et al., 2017).

In conclusion, the research on angiogenesis in the last fifty years has been tightly linked with cancer research, and more recently with anti-angiogenic drug development. Thus, in a recent review Bikfalvi (2017) placed the important question about the future of the field and which will be the landscape of angiogenesis research in the next 20 years. Indeed, industry seems not investing any additional efforts in the development of anti-angiogenic compounds in cancer and this may delay future discoveries in this fundamental field for different areas of biology and medicine.

References

Aird W.C. (2011) Discovery of the cardiovascular system: from Galen to William Harvey. J. Thromb. Haemost. 9 (Suppl 1): 118-129.

Akwii R.G., Sajib M.S., Zahra F.T., Mikelis C.M. (2019) Role of Angiopoietin-2 in Vascular Physiology and Pathophysiology. Cells 8(5). pii: E471.

Algire G.H, Chakley H.W. (1945) Vascular reactions of normal and malignant tissue in vivo. J. Natl. Cancer Inst. 6: 73-85.

Allen E., Jabouille A., Rivera L.B., Lodewijckx I., Missiaen R., Steri V., Feyen K., Tawney J., Hanahan D., Michael I.P., Bergers G. (2017) Combined antiangiogenic and anti-PD-L1 therapy stimulates tumor immunity through HEV formation. Sci. Transl. Med. 9 (385).

Armocida E., Natale G. (2019) Paolo Mascagni and Alessandro Moreschi: who discovered the vascular structure of urethra? Anatomy of an intellectual property dispute. Med. Histor. 3: 170-180.

Asahara T., Murohara T., Sullivan A., Silver M., van der Zee R., Li T., Witzenbichler B., Schatteman G., Isner J.M. (1997) Isolation of putative progenitor endothelial cells for angiogenesis. Science 275: 964-967.

Azad T., Ghahremani M., Yang X. (2019) The Role of YAP and TAZ in Angiogenesis and Vascular Mimicry. Cells 8: 407.

Azizi M.H., Nayernouri T., Azizi F. (2008) A brief history of the discovery of the circulation of blood in the human body. Arch. Iran. Med. 11: 345-350.

Bautch V.L., Caron K.M. (2015) Blood and lymphatic vessel formation. Cold Spring Harb. Perspect. Biol. 7: a008268.

Bikfalvi A. (2017) History and conceptual developments in vascular biology and angiogenesis research: a personal view. Angiogenesis 20: 463-478.

Bikfalvi A. (2018) A Brief History of Blood and Lymphatic Vessels. Springer.

Blum Y., Belting H.G., Ellertsdottir E., Herwig L., Lüders F., Affolter M. (2008) Complex cell rearrangements during intersegmental vessel sprouting and vessel fusion in the zebrafish embryo. Dev. Biol. 316: 312-322.

Bocci G., Francia G., Man S., Lawler J., Kerbel R.S. (2003) Thrombospondin 1, a mediator of the antiangiogenic effects of low-dose metronomic chemotherapy. Proc.

Natl. Acad. Sci. USA. 100: 12917-12922.

Carmeliet P., Ferreira V., Breier G., Pollefeyt S., Kieckens L., Gertsenstein M., Fahrig M., Vandenhoeck A., Harpal K., Eberhardt C., Declercq C., Pawling J., Moons L., Collen D., Risau W., Nagy A. (1996) Abnormal blood vessel development and lethality in embryos lacking a single VEGF allele. Nature 380: 435-439.

Clark E.R. (1918) Studies on the growth of blood vessels in tail of frog larvae. Am. J. Anat. 23: 37-88.

Clark E.R., Clark E.I. (1932) Observations on the new growth of lymphatic vessels as seen in trasparent chambers introduced into the rabbit's ear. Am. J. Anat. 51: 49-87.

Clark E.R., Clark E.I. (1939) Microscopic observations on the growth of blood capillaries in the living mammals. Am. J. Anat. 64: 251-301.

Clark E.R., Hitschler W.J., Kirby-Smith H.T., Rex R.O., Smith J.H. (1931) General observations of the ingrowth of new blood vessels into standardized chambers in the rabbit's ear, and the subsequent changes in the newly grown vessels over a period of months. Anat. Rec. 50: 129-167.

Connolly D.T., Heuvelman D.M., Nelson R., Olander J.V., Eppley B.L., Delfino J.J., Siegel N.R., Leimgruber R.M., Feder J. (1989) Tumor vascular permeability factor stimulates endothelial cell growth and angiogenesis. J. Clin. Invest. 84: 1470-1478.

Crivellato E., Nico B., Ribatti D. (2007) Contribution of endothelial cells to organogenesis: a modern reappraisal of an old Aristotelian concept. J. Anat. 211: 415-427.

Crivellato E., Ribatti D. (2006) Aristotle: the first student of angiogenesis. Leukemia 20: 1209-1210.

Crivellato E., Ribatti D. (2007) Soul, mind, brain: Greek philosophy and the birth of neuroscience. Brain Res. Bull. 71: 327-336.

Crum R., Szabo S., Folkman J. (1985) A new class of steroids inhibits angiogenesis in the presence of heparin or a heparin fragment. Science 230: 1375-1378.

Davis S., Aldrich T.H., Jones P.F., Acheson A., Compton D.L., Jain V., Ryan T.E., Bruno J., Radziejewski C., Maisonpierre P.C., Yancopoulos G.D. (1996) Isolation of angiopoietin-1, a ligand for the TIE2 receptor, by secretion-trap expression cloning. Cell 87: 1161-1169.

De Bock K., Georgiadou M., Schoors S., Kuchnio A., Wong B.W., Cantelmo A.R., Quaegebeur A., Ghesquière B., Cauwenberghs S., Eelen G., Phng L.K., Betz I., Tembuyser B., Brepoels K., Welti J., Geudens I., Segura I., Cruys B., Bifari F., Decimo I., Blanco R., Wyns S., Vangindertael J., Rocha S., Collins R.T., Munck S., Daelemans D., Imamura H., Devlieger R., Rider M., Van Veldhoven P.P., Schuit F., Bartrons R., Hofkens J., Fraisl P., Telang S., Deberardinis R.J., Schoonjans L., Vinckier S., Chesney J., Gerhardt H., Dewerchin M., Carmeliet P. (2013) Role of PFKFB3-driven glycolysis in vessel sprouting. Cell 154: 651-663.

de Vries C., Escobedo J.A., Ueno H., Houck K., Ferrara N., Williams L.T. (1992) The fms-like tyrosine kinase, a receptor for vascular endothelial growth factor. Science 255: 989-991.

Delgado-Bellido D., Serrano-Saenz S., Fernández-Cortés M., Oliver F.J. (2017) Vasculogenic mimicry signaling revisited: Focus on non-vascular VE-cadherin. Mol. Cancer 16: 65.

Donnem T., Hu J., Ferguson M., Adighibe O., Snell C., Harris A.L., Gatter K.C., Pezzella F. (2013) Vessel co-option in primary human tumors and metastases: an obstacle to effective anti-angiogenic treatment? Cancer Med. 2: 427-436.

Dvorak H.F., Dickersin G.R., Dvorak A.M., Manseau E.J., Pyne K. (1981) Human breast carcinoma: fibrin deposits and desmoplasia. Inflammatory cell type and distribution. Microvasculature and infarction. J. Natl. Cancer Inst. 67: 335-345.

Dvorak H.F., Harvey V.S., McDonagh J. (1984) Quantitation of fibrinogen influx and fibrin deposition and turnover in line 1 and line 10 guinea pig carcinomas. Cancer Res. 44: 3348-3354.

Dvorak H.F., Orenstein N.S., Carvalho A.C., Churchill W.H., Dvorak A.M., Galli S.J., Feder J., Bitzer A.M., Rypysc J., Giovinco P. (1979) Induction of a fibrin-gel investment: an early event in line 10 hepatocarcinoma growth mediated by tumor-secreted products. J. Immunol. 122: 166-174.

Dvorak H.F., Senger D.R., Dvorak A.M. (1983) Fibrin as a component of the tumor stroma: origins and biological significance. Cancer Metastasis Rev. 2: 41-73.

Ehrmann R.L., Knoth M. (1968) Choriocarcinoma. Transfilter stimulation of vasoproliferation in the hamster cheek pouch. Studied by light and electron microscopy. J. Natl. Cancer Inst. 41: 1329-1341.

Ferrara N., Carver-Moore K., Chen H., Dowd M., Lu L., O'Shea K.S., Powell-Braxton L., Hillan K.J., Moore M.W. (1996) Heterozygous embryonic lethality induced by targeted inactivation of the VEGF gene. Nature 380: 439-442.

Ferrara N., Henzel W.J. (1989) Pituitary follicular cells secrete a novel heparin-binding growth factor specific for vascular endothelial cells. Biochem. Biophys. Res. Commun. 161: 851-858.

Ferrara N., Hillan K.J., Gerber H.P., Novotny W. (2004) Discovery and development of bevacizumab, an anti-VEGF antibody for treating cancer. Nat. Rev. Drug Discov. 3: 391-400.

Flint J.M. (1900) The blood supply, angiogenesis, organogenesis, reticulum and histology of the adrenal. Johns Hopkins Hosp. Rep. 4: 154-229.

Flint J.M. (1903) The angiology, angiogenesis, and organogenesis of the submaxillary gland. Am. J. Anat. 2: 417-444.

Folkman J. (1971) Tumor angiogenesis: therapeutic implication. N. Engl. J. Med. 285: 1182-1186.

Folkman J. (2008) History of Angiogenesis. In: Figg W.D., Folkman J. (eds) Angiogenesis. An Integrative Approach From Science To Medicine, Spinger, New York. Pp. 1-14.

Folkman J., Haudenschild C. (1980) Angiogenesis in vitro. Nature 288: 551-556.

Folkman J., Merler E., Abernathy C., Williams G. (1971) Isolation of a tumor factor responsible for angiogenesis. J. Exp. Med. 133: 275-288.

Friedman D.M. (2001) A Mind of Its Own: A Cultural History of the Penis. The Free Press, New York.

Gao D., Nolan D.J., Mellick A.S., Bambino K., McDonnell K., Mittal V. (2008) Endothelial progenitor cells control the angiogenic switch in mouse lung metastasis. Science 319: 195-198.

Gerber H.P., Condorelli F., Park J., Ferrara N. (1997) Differential transcriptional regulation of the two vascular endothelial growth factor receptor genes. Flt-1, but not Flk-1/KDR, is up-regulated by hypoxia. J. Biol. Chem. 272: 23659-23667.

Gerhardt H., Golding M., Fruttiger M., Ruhrberg C., Lundkvist A., Abramsson A., Jeltsch M., Mitchell C., Alitalo K., Shima D., Betsholtz C. (2003) VEGF guides angiogenic sprouting utilizing endothelial tip cell filopodia. J. Cell. Biol. 161: 1163-1177.

Gimbrone M.A. Jr, Cotran R.S., Folkman J. (1973) Endothelial regeneration: studies with human endothelial cells in culture. Ser. Haematol. 6: 453-455.

Gimbrone M.A. Jr, Gullino P.M. (1976) Angiogenic capacity of preneoplastic lesions of the murine mammary gland as a marker of neoplastic transformation. Cancer Res. 36 (7 PT 2): 2611-2620.

Gimbrone M.A. Jr, Leapman S.B., Cotran R.S., Folkman J. (1972) Tumor dormancy in vivo by prevention of neovascularization. J. Exp. Med. 136: 261-276.

Goldmann E. (1908) The Growth of Malignant Disease in Man and the Lower Animals, with special reference to the Vascular System. Proc. R. Soc. Med. (Surg. Sect.) 1: 1-13.

Good D.J., Polverini P.J., Rastinejad F., Le Beau M.M., Lemons R.S., Frazier W.A., Bouck N.P. (1990) A tumor suppressor-dependent inhibitor of angiogenesis is immunologically and functionally indistinguishable from a fragment of thrombospondin. Proc. Natl. Acad. Sci. USA. 87: 6624-6628.

Gospodarowicz D. (1975) Purification of a fibroblast growth factor from bovine pituitary. J. Biol. Chem. 250: 2515-2520.

Gospodarowicz D., Brown K.D., Birdwell C.R., Zetter B.R. (1978) Control of proliferation of human vascular endothelial cells. Characterization of the response of human umbilical vein endothelial cells to fibroblast growth factor, epidermal growth factor, and thrombin. J. Cell. Biol. 77: 774-788.

Gospodarowicz D., Moran J.S. (1975) Mitogenic effect of fibroblast growth factor on early passage cultures of human and murine fibroblasts. J. Cell. Biol. 66: 451-457.

Green H.S.N. (1941) Heterologous transplantation of mammalian tumors: I. The transfer of rabbit tumors to alien species. J. Exp. Med. 73: 461-474.

Guidolin D., Crivellato E., Ribatti D. (2011) The "self-similarity logic" applied to the development of the vascular system. Dev. Biol. 351: 156-162.

Heitsch D. (2016) Descartes, Cardiac Heat, and Alchemy. Ambix 63: 285-303.

Hellström M., Kalén M., Lindahl P., Abramsson A., Betsholtz C. (1999) Role of PDGF-B and PDGFR-beta in recruitment of vascular smooth muscle cells and pericytes during embryonic blood vessel formation in the mouse. Development 126: 3047-3055.

Ide A.G., Baker N.H., Warren S.L. (1939) Vascularization of the Brown-Pearce rabbit epithelioma transplant as seen in the transparent ear chambers. Am. J. Roentg. 32: 891-899.

Jayson G.C., Kerbel R., Ellis L.M., Harris A.L. (2016) Antiangiogenic therapy in oncology: current status and future directions. Lancet 388: 518-529.

Kamei M., Saunders W.B., Bayless K.J., Dye L., Davis G.E., Weinstein B.M. (2006) Endothelial tubes assemble from intracellular vacuoles in vivo. Nature 442: 453-456.

Kemp M. (2019) Leonardo's philosophical anatomies. Lancet 393 (10179): 1404-1408.

Klein B., Zhang X.G., Lu Z.Y., Bataille R. (1995) Interleukin-6 in human multiple myeloma. Blood 85: 863-872.

Krishna Priya S., Nagare R.P., Sneha V.S., Sidhanth C., Bindhya S., Manasa P., Ganesan T.S. (2016) Tumour angiogenesis-Origin of blood vessels. Int. J. Cancer. 139: 729-735.

Latronico N. (1955) Il cuore nella storia della medicina. Recordati, Milano.

Laurenza D. (2019) Leonardo's contributions to human anatomy. Lancet 393 (10179): 1473-1476.

Lawler J. (2002) Thrombospondin-1 as an endogenous inhibitor of angiogenesis and tumor growth. J. Cell. Mol. Med. 6: 1-12.

Lenzi P., Bocci G., Natale G. (2016) John Hunter and the origin of the term "angiogenesis". Angiogenesis 19: 255-256.

Leung D.W., Cachianes G., Kuang W.J., Goeddel D.V., Ferrara N. (1989) Vascular endothelial growth factor is a secreted angiogenic mitogen. Science 246: 1306-1309.

Lewis W. (1927) The vascular patterns of tumors, Bull. Johns Hopkins Hosp. 41: 156-162.

Limet R. (2010) From Hippocrates to Harvey: twenty centuries of research on circulation. Rev. Med. Liege. 65: 562-568.

Loukas M., Youssef P., Gielecki J., Walocha J., Natsis K., Tubbs R.S. (2016) History of cardiac anatomy: a comprehensive review from the Egyptians to today. Clin. Anat. 29: 270-284.

Mailhos C., Modlich U., Lewis J., Harris A., Bicknell R., Ish-Horowicz D. (2001) Delta4, an endothelial specific notch ligand expressed at sites of physiological andtumor angiogenesis. Differentiation 69: 135-144.

Maisonpierre P.C., Suri C., Jones P.F., Bartunkova S., Wiegand S.J., Radziejewski C., Compton D., McClain J., Aldrich T.H., Papadopoulos N., Daly T.J., Davis S., Sato T.N., Yancopoulos G.D. (1997) Angiopoietin-2, a natural antagonist for Tie2 that disrupts in vivo angiogenesis. Science 277: 55-60.

Maniotis A.J., Folberg R., Hess A., Seftor E.A., Gardner L.M., Pe'er J., Trent J.M., Meltzer P.S., Hendrix M.J. (1999) Vascular channel formation by human melanoma cells in vivo and in vitro: Vasculogenic mimicry. Am. J. Pathol. 155: 739-752.

Manzoni T. (1998) The cerebral ventricles, the animal spirits and the dawn of brain localization of function. Arch. Ital. Biol. 136: 103-152.

Marinković S., Lazić D., Kanjuh V., Valjarević S., Tomić I., Aksić M., Starčević A. (2014) Heart in anatomy history, radiology, anthropology and art. Folia Morphol. (Warsz.) 73: 103-112.

Martinet L., Garrido I., Filleron T., Le Guellec S., Bellard E., Fournie J.J., Rochaix P., Girard J.P. (2011) Human solid tumors contain high endothelial venules: association with T- and B-lymphocyte infiltration and favorable prognosis in breast cancer. Cancer Res. 71: 5678-5687.

Mc Donald D.M., Munn L., Jain R.K. (2000) Vasculogenic mimicry: how convincing, how novel, and how significant. Am. J. Pathol. 156: 383-388.

Merwin R.M., Algire G.H. (1956) The role of graft and host vessels in the vascularization of grafts of normal and neoplastic tissue. J. Natl. Cancer. Inst. 17: 23-33.

Michaelson I.C. (1948a) Vascular morphogenesis in the retina of the cat. J. Anat. 82: 167-174.

Michaelson IC. (1948b) The mode of development of the vascular system of the retina with some observations on its significance for certain retinal disorders. Trans. Ophthalmol. Soc. UK 68: 137-180.

Montesano R., Orci L., Vassalli J.D. (1986) In vitro rapid organization of endothelial cells into capillary-like networks is promoted by collagen matrices. J. Cell. Biol. 97: 1648-1652.

Natale G., Bocci G. (2018) Does metronomic chemotherapy induce tumor angiogenic dormancy? A review of available preclinical and clinical data. Cancer Lett. 432: 28-37.

Natale G., Bocci G., Lenzi P. (2017) Looking for the Word "Angiogenesis" in the History of Health Sciences: From Ancient Times to the First Decades of the Twentieth

Century. World. J. Surg. 41: 1625-1634.

O'Reilly M.S., Boehm T., Shing Y., Fukai N., Vasios G., Lane W.S., Flynn E., Birkhead J.R., Olsen B.R., Folkman J. (1997) Endostatin: an endogenous inhibitor of angiogenesis and tumor growth. Cell 88: 277-285.

O'Reilly M.S., Holmgren L., Shing Y., Chen C., Rosenthal R.A., Moses M., Lane W.S., Cao Y., Sage E.H., Folkman J. (1994) Angiostatin: a novel angiogenesis inhibitor that mediates the suppression of metastases by a Lewis lung carcinoma. Cell 79: 315-328.

Pan W., Song X.Y., Hu Q.B., Zhang M., Xu X.H. (2019) TSP2 acts as a suppresser of cell invasion, migration and angiogenesis in medulloblastoma by inhibiting the Notch signaling pathway. Brain Res. 1718: 223-230.

Perez-Atayde A.R., Sallan S.E., Tedrow U., Connors S., Allred E., Folkman J. (1997) Spectrum of tumor angiogenesis in the bone marrow of children with acute lymphoblastic leukemia. Am. J. Pathol. 150: 815-821.

Pezzella F., Pastorino U., Tagliabue E., Andreola S., Sozzi G., Gasparini G., Menard S., Gatter K.C., Harris A.L., Fox S., Buyse M., Pilotti S., Pierotti M., Rilke F. (1997) Non-small-cell lung carcinoma tumor growth without morphological evidence of neo-angiogenesis. Am. J. Pathol. 151: 1417-1423.

Rao N., Lee Y., Ge R. (2015) Novel endogenous angiogenesis inhibitors and their therapeutic potential, Acta Pharmacol. Sin. 36: 1177-1190.

Ribatti D. (2009) History of Research on Tumor Angiogenesis. Springer Science+Business Media B.V.

Ribatti D. (2014) History of research on angiogenesis. Chem. Immunol. Allergy 99: 1-14.

Ribatti D., Nico B., Crivellato E. (2015) The development of the vascular system: a historical overview. Methods Mol. Biol. 1214: 1-14.

Ribatti D., Vacca A., Nico B., Fanelli M., Roncali L., Dammacco F. (1996) Angiogenesis spectrum in the stroma of B-cell non-Hodgkin's lymphomas. An immunohistochemical and ultrastructural study. Eur. J. Haematol. 56: 45-53.

Rijhsinghani K., Greenblatt M., Shubik P. (1968) Vascular abnormalities induced by benzo[a]pyrene: an in vivo study in the hamster cheek pouch. J. Natl. Cancer Inst. 41: 205-216.

Roe S.A. (1979) Rationalism and embryology: Caspar Friedrich Wolff's theory of epigenesis. J. Hist. Biol. 12: 1-43.

Rondoni P. (1946) Il cancro. Istituzioni di patologia generale dei tumori. Ambrosiana, Milano.

Sabin F.R. (1917) Origin and development of the primitive vessels of the chick and of the pig. Contrib. Embryol. Carnegie Inst. 6: 61-124.

Sabin F.R. (1920) Studies on the origin of blood vessels and of red blood corpuscles as seen in the living blastoderm of chicks during the second day of incubation. Contrib. Embryol. Carnegie Inst. Publ. (Washington) 9: 213-259.

Sandison J.C. (1928) Observations on growth of blood vessels as seen in trasparent chamber introduced into rabbit's ear. Am. J. Anat. 41: 475-496.

Santoro G., Wood M.D., Merlo L., Anastasi G.P., Tomasello F., Germanò A. (2009) The anatomic location of the soul from the heart, through the brain, to the whole body, and beyond: a journey through Western history, science, and philosophy. Neurosurgery 65: 633-643.

Scianna M., Bell C.G., Preziosi L. (2013) A review of mathematical models for the formation of vascular networks. J. Theor. Biol. 333: 174-209.

Senger D.R., Galli S.J., Dvorak A.M., Perruzzi C.A., Harvey V.S., Dvorak H.F. (1983) Tumor cells secrete a vascular permeability factor that promotes accumulation of ascites fluid. Science 219: 983-985.

Shawber C.J., Kitajewski J. (2004) Notch function in the vasculature: insights from zebrafish, mouse and man. Bioessays 26: 225-234.

Shing Y., Folkman J., Haudenschild C., Lund D., Crum R., Klagsbrun M. (1985) Angiogenesis is stimulated by a tumor-derived endothelial cell growth factor. J. Cell. Biochem. 29: 275-287.

Shing Y., Folkman J., Sullivan R., Butterfield C., Murray J., Klagsbrun M. (1984) Heparin affinity: purification of a tumor-derived capillary endothelial cell growth factor. Science 223: 1296-1299.

Shoja M.M., Agutter P.S., Loukas M., Benninger B., Shokouhi G., Namdar H., Ghabili K., Khalili M., Tubbs R.S. (2013) Leonardo da Vinci's studies of the heart. Int. J. Cardiol. 167: 1126-1133.

Stephenson J.A., Goddard J.C., Al-Taan O., Dennison A.R., Morgan B. Tumour Angiogenesis: A Growth Area – From John Hunter to Judah Folkman and Beyond. J. Cancer Res. 2013. Article ID 895019.

Strilić B., Kucera T., Eglinger J., Hughes M.R., McNagny K.M., Tsukita S., Dejana E., Ferrara N., Lammert E. (2009) The molecular basis of vascular lumen formation in the developing mouse aorta. Dev. Cell 17: 505-515.

Taraboletti G., Roberts D., Liotta L.A., Giavazzi R. (1990) Platelet thrombospondin modulates endothelial cell adhesion, motility, and growth: a potential angiogenesis regulatory factor. J. Cell. Biol. 111: 765-772.

Taylor S., Folkman J. (1982) Protamine is an inhibitor of angiogenesis. Nature 297: 307-312.

Uccelli A., Wolff T., Valente P., Di Maggio N., Pellegrino M., Gürke L., Banfi A., Gianni-Barrera R. (2019) Vascular endothelial growth factor biology for regenerative angiogenesis. Swiss Med. Wkly. 149: w20011.

Vacca A., Ribatti D., Roncali L., Ranieri G., Serio G., Silvestris F., Dammacco F. (1994) Bone marrow angiogenesis and progression in multiple myeloma. Br. J. Haematol. 87: 503-508.

Van Speybroeck L., De Waele D., Van de Vijver G. (2002) Theories in early embryology: close connections between epigenesis, preformationism, and self-organization. Ann. NY Acad. Sci. 981: 7-49.

Vangensten O.C.L., Fonahn A., Hopstock H. (1911-1916) Leonardo da Vinci. Quaderni d'anatomia. Six volumes. Con traduzione inglese e tedesca. Casa Editrice Jacob Dybwad, Christiania.

Voutouri C., Kirkpatrick N.D., Chung E., Mpekris F., Baish J.W., Munn L.L., Fukumura D., Stylianopoulos T., Jain R.K. (2019) Experimental and computational analyses reveal dynamics of tumor vessel cooption and optimal treatment strategies. Proc. Natl. Acad. Sci. USA 116: 2662-2671.

Weiss J.B., Brown R.A., Kumar S., Phillips P. (1979) An angiogenic factor isolated from tumours: a potent low-molecular-weight compound. Br. J. Cancer. 40: 493-496.

Zimrin A.B., Pepper M.S., McMahon G.A., Nguyen F., Montesano R., Maciag T. (1996) An antisense oligonucleotide to the notch ligand jagged enhances fibroblast growth factor-induced angiogenesis in vitro. J. Biol. Chem. 271: 32499-32502.

Mast cells, an evolutionary approach

Paola Saccheri[1], Luciana Travan[1], Domenico Ribatti[2] and Enrico Crivellato[1],*

[1] Department of Medicine, Section of Anatomy, Piazzale Kolbe 3, 33100 Udine, Italy
[2] Department of Basic Medical Sciences, Neurosciences and Sensory Organs, Section of Human Anatomy and Histology, Piazza Giulio Cesare 11, Policlinico, 70124 Bari, Italy

Abstract

Mast cells are tissue-based immune cells that participate to both innate and adaptive immunity as well as to tissue-remodelling processes. Their phylogenetic development can be only guessed and partly reconstructed according to present trace evidence. This kind of cells have been found in all vertebrate classes and a cell population largely with the qualities of higher vertebrate mast cells is identifiable in the most evolutionarily sophisticated fish species. In invertebrates, cells correlated with vertebrate mast cells have been documented in ascidians, a class of urochordates which made its appearance about 500 million years ago. These include the granular haemocyte with transitional features between basophils and mast cells, and the test cell. Both cells store histamine and heparin, and supply protective tasks. The test cell discharges tryptase after stimulus with compound 48/80. A leukocyte progenitor effective in primitive confined innate immunity possibly represents the mast cell ancestor. This cell was likely concerned with phagocytic and killing actions against pathogens, and functioned as a broad-spectrum activator of phlogistic processes. This defensive precursor cell was possibly engaged in associated local reparative functions. With the initiation of recombinase activating genes (RAG)-mediated adaptive immunity in the Cambrian era, about 550 million years ago, and the appearance of early vertebrates, mast cell progenitors developed towards a multifaceted cellular type. As a distinguished cell category mast cells probably emerged in the last common ancestor we shared with hagfish, lamprey and sharks about 450-500 million years ago.

1. Introduction

Mast cells (MCs) are derived from committed precursors that leave the hematopoietic tissue, migrate in the blood, and colonize peripheral tissues where they terminally differentiate under microenvironment stimuli (Frossi et al., 2018). They express adaptable and flexible activities in a great variety of immunological and non-immunological sceneries. These cells are recognized to provide important effector functions in both innate and adaptive immunity and may also exert relevant activities in tissue homeostasis, remodelling, repair, fibrosis and angiogenesis.

Comparative studies have identified granulated cells which share general characteristics of MCs in all vertebrate classes (Baccari et al., 2011). The cytoplasm of these cells is packed with metachromatic granules containing a vast array of secre-

* Corresponding author. E-mail: enrico.crivellato@uniud.it

tory compounds. Same of these compounds, as tryptase and histamine, have also been identified in MCs of teleost fish (Mulero et al., 2007; Dobson et al., 2008). Upon activation, mammalian MCs discharge a great assortment of either pre-formed or *de novo* synthesized cytokines, growth factors and other mediators. Mammalian MCs expose on their plasma membrane the stem cell factor (SCF) receptor KIT and the tetrameric $\alpha\beta\gamma_2$ form of the high-affinity receptor (FcεRI) for IgE (Frossi et al., 2018). Both surface molecules are essential in MC functional activity and, remarkably, KIT-like and FcεRI-like receptors have been recognized even in fish MCs (Dobson et al., 2008; , Da'as et al., 2011). A population of granulated cells with the general features of higher vertebrate MCs is therefore identifiable in the most evolutionarily advanced fish species. FcεRI was the firstly recognized receptor for MC activation (Blank and Rivera, 2004). It is the most important triggering receptor but mammalian MCs may also be stimulated by "alternative", IgE-independent pathways, which involve a series of mediators such as cytokines, hormones, immunoglobulins, neuropeptides, complement components, and microbes, as well as their products (Prodeus et al., 1997; Gommerman et al., 2000; Marshall, 2004; Bulfone-Paus et al., 2017; Redegeld et al., 2018).

Past studies led investigators to outline the notion of "MC heterogeneity" (Enerbäck, 1966 a-b; Bienenstock et al., 1983; Galli, 1990). This implies that MC population may differ significantly in granule number, dimension, chemical content and unique substructural pattern according to the species inspected (Dvorak, 2005). MC subtypes may also be identified at distinct structural sites even in the same species. They may react upon different inducers and express fairly distinct functional profiles. Historically, MCs were classified into two or three subtypes, according to tryptic enzymes expression. However, MCs display a striking heterogeneity that reflects a complex interplay between different microenvironmental signals delivered by various tissues, and a differentiation program that decides their identity. In rodents, MCs have been distinguished in two subtypes, i.e. connective tissue MCs and mucosal MCs (Enerbäck, 1986). In man, three MC subtypes has been identified according to their protease storage: (i) tryptase-containing MCs, (ii) MCs that contain both tryptase and chymase, along with other proteases such as carboxypeptidase A and cathepsin G, and (iii) MCs which express chymase without tryptase (Irani et al., 1986). In avian, reptile and amphibian MCs, difference in histamine content as well as chymotrypsin-like and trypsin-like activity has also been recognized (Chiu and Lagunoff, 1971; Izzo Vitiello et al., 1997; Chieffi Baccari et al., 1998; Baccari et al., 2000).

Recognition of MC phenotype throughout vertebrate classes points to a strong selective evolutionary strain in support of its maintenance and outlines the concept that these cells may be implicated in significant advantageous roles. Skin, gut, and airways location places MCs in favourable sites to come in first contact and react to pathogens. In this perspective, MCs express a range of pattern recognition receptors, including Toll-like receptors (TLRs) (Sanding and Bulfone-Paus, 2012). MCs respond to TLR ligands by secreting cytokines, chemokines, and lipid mediators, and some studies have found that TLR ligands can also cause degranulation, although this finding is contentious. It is reasonable to regard MCs as one of the first inflammatory cells which may counteract infective microorganisms and begin immune responses (Metz et al., 2008). We may envisage that since ancient times MCs

have probably been participant to defensive system. Thus, a local leukocyte progenitor effective in the operative network of primordial innate immunity, and concerned in phagocytic and killing functions against pathogens likely embodies the profile of MC phylogenetic ancestor. Its primary role was exert to be recognized in parasite and bacterial protection, and as a not specific activator of inflammation. This first type of exquisitely defensive cell underwent differentiation towards a multifaceted cell type, which was integrated into the frameworks of recombinase activating genes (RAG)-mediated adaptive immunity in the Cambrian era, some 550 million years ago. It evolved with time into a tissue-homing regulatory cell implicated in different biological functions, such as tuning of immune response, wound healing, tissue regeneration and remodelling after injury, fibrosis, angiogenesis and possibly other activities.

2. Mast cells in fish

Studies on MC equivalents in fish have contributed to elucidate some aspects of MC phylogenesis and have increased our understanding of MC functional profile in lower vertebrates. In the most advanced teleost fish, MCs comprise a cell population with the overall characteristics of higher vertebrate MCs. Thus, comparative studies in fish MCs are of great value in an attempt to reconstruct the evolutionary process accomplished by these immune and tissue-remodelling cells. In general terms, fish MCs represent a heterogeneous entity. They express different morphology, variable granule content, erratic sensitivity to fixatives, and unequal response to drugs. In salmonidis, cyprinids, and erythrinids – all teleostean fish – plentiful granular cells have been identified in the mucosa lining the intestinal tract, the dermis and the gills. It must be noted that gill, like the intestinal tract and the skin, is one of the tissues first exposed to pathogenic and environmental challenges. Cells with the overall structural and histochemical features of MCs have been identified even in primitive jawless fish (Agnatha: hagfish, lamprey) and cartilaginous fish (Chondrichthyes: sharks). However, granular cells have not been identified in all examined fish species. Remarkably, secretory granules in fish MCs show different staining properties. In many species, they appear as either basophilic or eosinophilic. For this reason, MC equivalents in fish have frequently been referred to as basophilic granular cells, or acidophilic/ eosinophilic granule cells (EGCs) (Reite and Evensen, 2006). The nomenclature MC/ EGCs has persisted in the literature in reference of these cells due probably to a failure of certain fixation techniques to consistently demonstrate metachromatic staining in a subpopulation of these cells stained with toluidine blue (Reite and Evensen, 2006). Interestingly, erratic staining responsiveness has been recognized also in some amphibian and reptile MCs (Sottovia-Filho, 1974).

The functional properties of fish MCs have recently been investigated by several authors. The picture that emerges is that of a cell involved in defensive mechanisms against parasite and bacteria infections. This cell may act directly killing pathogen microorganisms but the bulk of evidence suggests a more complex defensive function. Zebrafish (*Danio rerio* H.) MCs, for instance, participate in innate and adaptive immune responses (Da'as et al., 2011). In the gill and intestine of this teleost, cells regarded as analogous to mammalian MCs contain an ovoid eccentric nucleus and

toluidine blue-positive metachromatic granules. Under electron microscopy, they closely approximate the appearance of murine MCs (Dobson et al., 2004). Intraperitoneal injection of compound 48/80 – a well known MC secretagogue in mammals – or live *Aeromonas salmonicida* results in a rapid and significant degranulation of intestinal MCs, which is recognizable histologically and by increased plasma tryptase levels (Da'as et al., 2011). This response is abrogated by the H_1 histamine antagonist and MC stabilizing agent ketotifen. In addition, whole mount *in situ* hybridization procedures indicate that *myd88*, a Toll-like receptor adaptor, is expressed in a subset of mature MC equivalents, suggesting conservation of innate immune responses mediated through TLRs (Da'as et al., 2011). Notably, zebrafish MCs possess an analogous FcεRI which results in reproducible systemic anaphylactic responses after stimulation (Da'as et al., 2011). Histochemically, these cells demonstrate a positive reaction to polyclonal anti-human KIT and monoclonal anti-human MC tryptase antibodies (Dobson et al., 2004). A carboxypeptidase A (CPA) 5 protein, which shares 38% identity with CPA3 expressed in human MCs, has been identified in zebrafish MCs. The *cpa5*-expressing MCs represent a unique myeloid subpopulation arising from a cell with both granulocyte and monocyte potential (Dobson et al., 2004). MCs belonging to the Perciformes, the largest and most evolutionarily advanced order of teleosts, have been found to contain histamine (Mulero et al., 2007). Remarkably, histamine is biologically active in these fish and is able to regulate the inflammatory response by acting on professional phagocytic granulocytes. Thus, in the most phylogenetically developed teleostean species, a cell type with the basic structure-function profile of mammalian MC counterpart is recognizable. In addition, many studies have shown that fish MC equivalents contain serotonin instead of histamine.

In general terms, fish MCs undergo cell degranulation after inoculation of certain substances, such as *Aeromonas salmonicida* and *Vibrio anguillarum* toxins, compound 48/80, substance P and capsaicin. In addition, their number has been shown to increase after parasitic infection. Of note, migration and accumulation of neutrophils has often been observed at the site of MC degranulation (Matsuyama and Iida, 1999), suggesting that MC secretion may have a role in attracting other types of cells involved in the inflammatory process, especially during initial pathogenic challenge. Thus, fish MCs are supposed to contain or generate a variety of mediators that induce neutrophil chemotaxis, as observed in mammals.

Fish MCs store in their granules different components which are common to mammalian counterparts: alkaline and acid phosphatases, leucine aminopeptidase, arylsulphatase and 5'-nucleotidase, lysozyme and met-enkephalin. Notably, the granules of MCs in teleosts contain piscidins, a class of 22-aminoacid antimicrobial peptides that have potent, broad-spectrum antibacterial activity against fish pathogens (Silphaduang and Noga, 2001; Silphaduang et al., 2006). Piscidins are thought to inhibit the synthesis of the cell wall, nucleic acids, and proteins or even inhibit enzymatic activity (Campagna et al., 2007). Piscidin-immunoreactive MCs are most common at sites of pathogen entry, including the skin, gill and gastrointestinal tract. Remarkably, not all fish MCs are piscidin-positive. Piscidins 3 and 4, for instance, have been identified only in MCs of fish belonging to the orders of Perciformes and Gadiformes. A related family of antimicrobial peptides, called pleurocidins, are synthesized in MCs of the Atlantic halibut (*Pseudopleuronectes americanus*), a flatfish belonging to the order Pleuronectiformes (Murray et al., 2003).

3. Mast cell-like cells in invertebrates

Potential MC progenitors have been identified in ascidians, marine invertebrates commonly known as sea squirts. Ascidians belong to the subphyla of invertebrate chordates Urochordates which appeared approximately 500 million years ago. The haemolymph of ascidians contains different types of circulating cells. Some of these cells migrate from haemolymph to tissues, where they carry out several immunologic actions, such as phagocytosis of self and non-self molecules, expression of cytotoxic agents, encapsulation of foreign antigens, and also reparation of damaged tissues. In 2007, de Barros et al. reported that circulating granular haemocytes in the haemolymph of the ascidia *Styela plicata* expressed intermediate characteristics of basophils and MCs (De Barros et al., 2007). Viewed by transmission electron microscopy, these cells appeared as mononuclear cells of 3.5-6 μm diameter, characterized by a cytoplasm filled with spherical granules of uniform size and variable density. The general morphology was closely related to that of mammalian MCs and basophils. Unlike the haemocytes of any other invertebrate species, the granules of these cells contained both heparin and histamine. These molecules are major components of MC granules in mammals. Heparin is a highly sulphated glycosaminoglycan (GAG) made up of a mixture of polymers with a similar backbone of repeating hexuronic acid linked to 1,4 to α-D-glucosamine units. It represents the dominant GAG in human MCs and constitutes some 75% of the total, with a mixture of chondroitin sulfates making up the remainder (Church and Levi-Schaffer, 1997). In man, the heparin content in tryptase- and tryptase/chymase-containing MCs is roughly the same. In the mouse, the proteoglycan content of MC granules varies in the different MC subtypes. Connective tissue MCs contain heparin that lacks in mucosal MCs. Heparin proteoglycan is thought to form the granule matrix that binds histamine, neutral proteases, and carboxypeptidases primarily by ionic interactions and, therefore, it contributes to the packaging and storage of these molecules in the granules. Mice that lack the enzyme N-deacetylase/N-sulphotransferase-2 (NDST-2), which are unable to produce fully sulphated heparin, exhibit severe defects in the granule structure of MCs, with impaired storage of certain proteases and reduced content of histamine (Humphries et al., 1999; Forsberg et al., 1999). Histamine was the first discovered mediator in MCs. In human MCs, histamine is present at a concentration of 1 to 4 pg/cell (Church and Levi-Schaffer, 1997). Mammalian and avian MCs contain high concentrations of histamine in their secretory granules (Reite, 1965; Takaya, 1969). In poikilothermic vertebrates, reports of MC histamine content are contradictory. Various amounts of this biogenic amine were found in reptilian MCs using the o-phthalaldehyde fluorescence method (Reite, 1965; Takaya et al., 1967; Takaya, 1969). In the granules of frog (*Rana catesbiana*) MCs, the presence of very low amounts of histamine was revealed using a double fluorometric and ultrastructural approach (Chieffi Baccari et al., 1998). The histamine content per frog MC (about 0.1 pg/cell) was approximately 30 times lower than that of human MCs isolated from various tissues. Histamine has also been recognized in MCs belonging to the Perciformes (Mulero et al., 2007). Remarkably, histamine is biologically active in these fish and is able to regulate the inflammatory response by acting on professional phagocytic granulocytes. The presence of histamine has been reported in several classes of invertebrates, such as Cnidaria, Mollusca, Arthropoda and Equinodermata. In invertebrates, histamine is

involved in defence mechanisms. It is present in the venom of the jumper ant (*Myrmecia pilosula*), in the tentacles of anemones (Actiniaria) and in the toxin of the sea urchin (Echinoida, Diadematoida). In this perspective, the identification of histamine in the granules of the haemocyte found in the haemolymph of *Styela plicata* further supports the notion that it may represent an ancient effector cell of the innate immunity (Cavalcante et al., 2002).

Being the positions of ascidians at the top of the invertebrate phylogenetic tree, close to vertebrate chordates, these granular haemocytes might well represent the primitive counterparts of mammalian MCs. They provide defensive functions and are involved in different immunological actions, such as migration from the blood vessels to perform activities like phagocytosis, liberation of antimicrobial peptides, triggering of the complement system, encapsulation of foreign organisms and regeneration of tissues.

Another cell type in *Styela plicata*, the test cell, shares some structural and functional characteristics with vertebrate MCs (Cavalcante et al., 1999). Similarly to the granular haemocyte, this type of cell contains histamine and heparin in cytoplasmic granules and appears metachromatic under light microscopy. Test cells are accessory cells that reside in the periviteline space of oocytes (Cavalcante et al., 2002). Their origin is controversial. It has been proposed that they can derive from amoeboid cells migrating to the surface of young oocytes. Therefore, they may represent ancient effector cells of the innate immunity involved in protection of the oocyte, which in this species is in contact with the external environment, against invasion of microorganisms (Gianguzza and Dolcemascolo, 1978; Cavalcante et al., 2000). Viewed under transmission electron microscopy, these cells appear as mononuclear cells endowed with circular, membrane-bound granules composed by electron-dense filaments (Cavalcante et al., 2000). Remarkably, these cells contain heparin and histamine, and both molecules co-localize inside granules. Most remarkably, incubation of test cell-rich preparations with the MC secretagogue compound 48/80 causes tryptase release in the supernatant accompanied by loss of metachromasia and the ultrastructural organization of granules in the test cells. Thus, these cells share some morphological, biochemical and functional characteristics with vertebrate MCs.

4. Mast cells and innate immunity

The innate immunity represents the first line of host responses to pathogen invasion. Innate immunity depends on germ line-encoded receptors that have evolved to recognize highly conserved pathogen-associated molecular patterns. These receptors are termed pattern recognition receptors (Pancer and Cooper, 2006). MCs likely evolved from an ancestral defensive cell. Mammalian MCs still retain some residual functions of this ancient MC progenitor presumably implicated in defence from parasites by pathogen seclusion and direct killing. In mammals, both human and mouse MCs are capable of eliminating bacteria *in vitro* through an intracellular killing system similar to that of professional phagocytes (Féger et al., 2002). Although the physiological significance of the phagocytic activity exerted by MCs in higher vertebrates remains undetermined, mucosal MCs in mice are known to play a role in the expulsion of the nematode *Trichinella spiralis in vivo* (Knight et al., 2000) and indirect evi-

dence of MC degranulation has been provided in the intestine and muscles of rats infected with nematodes (Terenina et al., 1997). MCs in mice can kill opsonised bacteria. *Salmonella typhimurium* coated with the C3b fragment of complement is recognized through complement receptor 3 (CR3) on the MC membrane (Sher et al., 1979). Mammalian MCs express other complement receptors: C3aR, C5aR CR2, CR4, C1qR (Marshall, 2004; Gilfillan and Tkaczyc, 2006). The CR3 was first recognized in ascidians (Miyazawa et al., 2001). It represents an essential ancestral component of the primordial complement system that functioned in an opsonic manner. Indeed, the C3 complement factor – the central component of the complement system – has also been recognized in the horseshoe crab *Carcinoscorpius rotundicauda*, a protostome considered a "living fossil" originating over 500 million years ago (Zhu et al., 2005). These animals, which lack adaptive immunity, mount an effective antimicrobial defence in response to pathogens. The C3 protein has been identified in jawless vertebrates, the lamprey and hagfish, as well as in deuterostome invertebrates, ascidians, amphioxus, and sea urchins (echinoderm). Interestingly, MC equivalents have been recognized in jawless fish and a possible MC precursor has been identified in ascidians. MCs in mice can also recognize parasites, bacteria and viruses in the absence of opsonins (Marshall, 2004). This trait is likely mediated through the cell surface pattern recognition receptors, such as the TLRs and the FimH receptor CD48 (Gilfillan and Tkaczyc, 2006). TLRs are widely distributed throughout the evolutionary scale. TLR genes are absent from non-animal phyla but are recognizable in most eumetazoans, from cnidarians to vertebrates. In humans, MCs may exert bactericidal activity *via* a recently identified extracellular phagocytosis-independent mechanism consisting of the production of extracellular structures similar to neutrophil extracellular traps (NETs) (von Köckritz-Blickwede et al., 2008). In a phylogenetic perspective, these network structures provide similarities with the process of nodule formation by invertebrate granular haemocytes. Nodules are multicellular haemocytic aggregates which may entrap a large number of bacteria in an extracellular material. Bacterial killing by MC extracellular traps might represent retention of an early ability expressed by MC phylogenetic precursors to promote pathogen seclusion and removal by nodule formation.

Several lines of evidence indicate that MCs produce antimicrobial peptides, which are host defence effector molecules. Fish MCs contain antimicrobial peptides of the class of piscidins and pleurocidins, and therefore are presumed to be directly involved in killing microbes. Piscidins are the prototype of antimicrobial peptides found in fish MCs. They have strong, broad-spectrum antibacterial, antifungal and antiparasitic activity. Studies in mammals reveal that human and murine MCs contain antimicrobial peptides as well. MCs in mice express abundant amounts of cathelin-related antimicrobial peptide whilst human skin MCs have been shown to contain the cathelicidin peptide LL-37 (Di Nardo et al., 2003). Thus mammalian MCs, like fish MCs, are endowed with the defensive machinery provided by the class of antimicrobial peptides.

Besides their possible participation in direct killing of invading pathogens, MCs are regarded as sentinels of innate immunity due to their capacity to orchestrate efficient antibacterial responses by recruiting other inflammatory cells at the site of pathogen entry. This mechanism is sufficiently known in the MC-deficient mice model. Here, MCs have been shown to protect against bacteria, fungi and protozoa through

the release of proinflammatory and chemotactic mediators (Féger et al., 2002). Upon contact with invading microorganisms, MCs release a variety of molecules – including tumour necrosis factor (TNF)-α, interleukin (IL)-4, IL-8 and leukotriene B$_4$ (LTB$_4$) – which are crucial effectors in promoting the influx of neutrophils and other inflammatory cells. Although the relevant molecular machinery remains unidentified, stimulation of neutrophil recruitment has also been recognized at the site of MC degranulation in fish. Here, migration and accumulation of neutrophils have often been observed which suggests that fish MCs may contain or generate mediators capable to induce neutrophil chemotaxis, as observed in mammals (Matsuyama and Iida, 1999). Histamine has been identified in MCs of perciform fish, the largest and most evolutionarily advanced order of teleosts. Functional studies indicate that fish professional phagocyte function may be regulated by the release of histamine from MCs upon H$_1$ and H$_2$ receptor engagement (Mulero et al., 2007). Interestingly, the cathelicidin antimicrobial peptide LL-37 recognized in human MCs is active as a leukocyte chemoattractant through binding of human formyl peptide receptor like-1/lipoxin-A receptor (De et al., 2000). In addition, human LL-37 influences the expression of chemokines, such as IL-8, and chemokine receptors, such as CCR2 and IL8RB, in macrophages (Scott et al., 2002). Thus, cathelicidin antimicrobial peptides may contribute to attract neutrophils and expand the inflammatory response at the site of pathogen entry. In a similar way, antimicrobial peptides released by fish MCs might be partly responsible for the accumulation of neutrophils at sites of MC degranulation.

5. Mast cells and adaptive immunity

This is perhaps the most difficult aspect of MC function to be analyzed and interpreted in an evolutionary perspective because virtually nothing is known about MC participation to adaptive immunity in non-mammalian species. Thus, its reconstruction is absolutely conjectural.

Experimental evidence in mammals indicates that MCs are crucially involved in adaptive immunity. These cells have been more and more implicated in different aspects of immune regulation, influencing the outcome of both physiological and pathological T cell responses (Galli et al., 2005, 2008a; Sayed and Brown, 2007; Frossi et al., 2010). MCs involvement in adaptive immunity is broad. They coordinate responses to pathogens, by orchestrating migration, maturation and function of dendritic cells, T cells and B cells (Ritter et al., 2003; Merluzzi et al., 2010; Hershko and Rivera, 2010). They interact with T cells, being capable to express major histocompatibility complex (MHC) class II moieties and co-stimulatory molecules, travelling from the activation site to regional lymph nodes like dendritic cells and thereby becoming potential antigen presenting cells for T cells (Nakae et al., 2006; Kambayashi et al., 2009). They contribute to the initiation of the primary immune responses to allergens and amplify exacerbations of allergic diseases (Galli et al., 2008b). They exert important role in generating immune tolerance and primarily affect certain autoimmune diseases (Nakae et al., 2005).

When did these MC functions emerge during evolution? We have too limited information about MC participation to adaptive immunity in non-mammalian species to provide plausible answer to such question. In addition to innate defence mecha-

nisms, jawed vertebrates (gnathostomes) have evolved an adaptive immune system mediated primarily by lymphocytes. Adaptive immunity made its appearance some 550 million years ago during the Cambrian era with the emergence of the Ig-based RAG-mediated immune system that coincided with the coming out of early vertebrates (Laird et al., 2000; Pancer and Cooper, 2006). By rearrangement of IgV, D, and J gene segments – the Ig domains are an ancient protein superfamily involved in pathogen recognition or self/non self discrimination in invertebrates – the jawed vertebrates generated a lymphocyte receptor repertoire of sufficient diversity to recognize the antigenic component of any potential pathogen or toxin (Pancer and Cooper, 2006). At the down of vertebrate evolution, cartilaginous fish first rearranged their V(D)J gene segments to assemble complete genes for the cell surface antigen receptors expressed by T and B lymphocytes, whose triggering initiates specific cell mediated or humoral immune responses. This Ig-based recombinatorial system generated anticipatory receptors in T and B lymphocytes that enabled these cells to work together and with other cells to mediate effective adaptive immunity. The appearance of RAG-mediated immunity within a relatively short evolutionary period of about 40 million years represents a stunning enigma for immunologists. In this evolutionary scenario, it might be speculated that phylogenetic progenitors of MCs were transmitted from invertebrates to their vertebrate descendents and incorporated into the networks of the new defensive system. Vertebrate MCs acquired key elements of adaptive immunity, such as MHC class I and II molecules, becoming involved in co-stimulatory activity (Bachelet and Levi-Schaffer, 2007). Interestingly, even in vertebrates innate immunity provides the first line of defence against pathogens because it takes at least several days to orchestrate an efficient adaptive immune response. In this way, the modern MC may represent the pivotal cell that links primitive schemes of surveillance to more evolved and versatile defensive strategies.

Clonal B cell activation and production of specific antibodies represent a crucial aspect of adaptive immunity. The IgE molecule, and its interaction with the FcεRI, is the critical MC triggering factor of anaphylaxis in mammalian MCs (Galli et al., 2008b). IgE and its receptors are believed to have evolved as a mechanism for protection against parasites (Rihet et al., 1991; King et al., 1997). In vertebrates other than mammals, IgE molecules are not recognizable and the low-molecular weight isotype characteristic of birds, reptiles and amphibians is the IgY molecule (Warr et al., 1995). In an evolutionary scale, it is believed that IgY is the precursor of both mammalian IgE and IgG classes. Some indirect proof is available for the expression of receptors for IgY on MCs in birds (Caldwell et al., 2004) which suggests a functional relevance of IgE-like molecules in avian MC activation as well. Teleost fish produce both IgM-like and IgD-like molecules but not IgE molecules (Bengtén et al., 2006). In general terms, the FcεRI appears to be a relatively recent acquisition in MC evolution if IgE originated first with the emergence of mammalian species. Thus, it is of great interest the discovery that a polyclonal antibody directed to the γ subunit of the human FcεRI recognizes a specific determinant on the surface of zebrafish intestinal MCs and that reproducible passive systemic anaphylactic responses can be elicited in this fish species, likely as a result of the stimulation of such FcεRI analogous (Da'as et al., 2011). This finding provides evidence for a conserved IgE-like receptor throughout vertebrate evolution.

6. Linking defensive and tissue-remodelling activities

Modern MCs are tissue-based immune cells involved in innate and adaptive immunity as well as the preservation of tissue homeostasis. Probably, the key structures which provided an effective connection between protective and reparative functions in the hypothetical MC ancestor were enzymes belonging to the class of serine proteases. Tryptase and chymase are the major types of serine proteases stored in MC granules and seemingly well conserved among vertebrate species (McNeil et al., 2007). Serine proteases are important effector molecules in the immune system of mammals and have been found not only in MC granules but also in the granules of neutrophils, T cells and NK cells (Woodbury and Neurath, 1980). MC tryptase and chymase are phylogenetically related to neutrophil cathepsin G and T cell granzymes. These proteases show a large distribution through the evolutionary scale. Serine proteases related to the mammalian haematopoietic serine protease family have been identified in teleost fish (Wernersson et al., 2006). Tryptase has also been recognized in zebrafish MCs (Dobson et al., 2008). This protease is designed for exocytosis as compound 48/80-mediated degranulation of zebrafish MCs leads to elevation of plasma tryptase level. Interestingly, test cells from the urochordate *Styela plicata*, a potential MC phylogenetic progenitor, also release tryptases after incubation with compound 48/80 (Cavalcante et al., 2000).

MC proteases play an important role in innate host defence. In the mouse, at least five different granule-associated chymases (mMCP-1, mMCP-2, MMCP-3, MMCP-4, MMCP-5) and three different granule-associated tryptases (mMCP-6, mMCP-7, mMMP-11/transmembrane tryptase [mTMT]) have been described at the protein level (Huang et al., 1998). There appear to be multiple forms of human tryptases as well (tryptases αI, αII, βI, βII, βIII, γI, γII and transmembrane tryptase) (Miller et al., 1989; Vanderslice et al., 1990; Miller et al., 1990). In mice, MC-stored proteases are endowed with the capacity to generate important defensive as well as tissue-remodelling responses. MC tryptase mMCP-6, for instance, has a critical protective function in bacterial and parasite infection. mMCP-6-deficient mice are less able to clear *Klebsiella pneumoniae* injected into their peritoneal cavities, probably because of less recruitment of neutrophils (Thakurdas et al., 2007). mMCP-6 is also important for the clearance of the chronic *Trichinella spiralis* infection (Shin et al., 2008). MC chymase mMCP-1 as well is important for expulsion of the adult helminth and the larvae of *Trichinella spiralis* in infected mice (Knight et al., 2000). MC chymase mMCP-2 contributes to neutrophil recruitment and host survival in the "cecal ligation and puncture" model (Orinska et al., 2007). The human trypatse βI, the predominant form stored in secretory granules of all human MCs, is also capable to stimulate the influx of neutrophils at site of pathogen entry (Féger et al., 2002).

Serine proteases, in addition, provide fundamental role in various aspects of tissue homeostasis and tissue remodelling after injury. Tryptases are potent activators of fibroblast migration and proliferation (Ruoss et al., 1991), and can stimulate the synthesis and release of type collagen I from fibroblasts in culture, as well as provoke secretion of collagenase (Cairns and Walls, 1997). Tryptases cleave fibronectin and type VI collagen. They activate the pre-enzyme forms of some metalloproteases (MMPs) and urinary plasminogen activators (uPA) which are implicated in tissue degradation. Tryptases cleave various bronchial and intestinal neuropeptides

and may also have a role in tissue repair processes as a growth factor for epithelial and muscle cells (Gruber et al., 1997). A number of studies have demonstrated the angiogenic potential of tryptase and its important role in neovascularisation, stimulating endothelial cell activation, proliferation, migration and tube formation (Blair et al., 1997). Chymases may contribute to tissue remodelling by cleaving type IV collagen and by splitting the dermal-epidermal junction. They may also express a proangiogenic activity Chymases degrade some neuropeptides and cleave angiotensin I to angiotensin II more effectively than the angiotensin-converting enzyme (Church and Levi-Schaffer, 1997).

Genetic analysis of tryptases in different species suggests that these proteases proliferated and changed rapidly during mammalian evolution, arising from ancestral membrane-anchored peptidases, which are present in a variety of vertebrate genomes such as reptiles, amphibians and fish (Triverdi et al., 2007). We have seen that two potential MC ancestors have been identified in ascidians, namely the granular haemocyte and the test cell. Both cell types are supposed to be involved in defensive functions and provide tissue-reparative activity. Interestingly, a third type of ascidia cell called the large-granule tunic cell has been found to contain granules with tessellated substructures (Hirose et al., 2003). This cell too seems have originated from granulocytes that migrate in the tunic from the haemolymph. Granulated tunic cells have been found to infiltrate the integumentary matrix, the inner layer of the tunic – a protective envelop wholly covering the outside of the epidermis – during tissue reconstitution taking place after experimentally induced wounds of the integumentum, suggesting a direct or indirect participation of these cells in the process of tunic healing (Hirose et al., 1997). In addition, some tissue manipulations can be accomplished by granular cells in insects during metamorphosis. Thus, cells possibly belonging (or close) to MC phylogenetic lineage appear as blood-derived, tissue-homing elements involved in both protective actions and restoration of damaged structures. Since primordial times, these two aspects of tissue homeostasis – namely defence and reparation – seem to be closely related. It is most likely that a repair function would have been acquired well before the development of an adaptive immune response. During evolution, vertebrate MCs have retained and further exploited such fundamental properties, growing into highly versatile tissue sentinels capable to sense the microenvironment and to coordinate sophisticated defensive strategies as well as multifaceted tissue-remodelling actions.

7. Conclusions

In evolutionary terms, MCs appear as ancient cells. They have been identified in all classes of vertebrates and comparative analysis has suggested possible MC analogues in invertebrates. Current MCs may derive from a leukocyte ancestor, which probably displayed functional features similar to those expressed by present invertebrate granular haemocytes. This archaic cell was probably an effector cell, chiefly providing tissue defence in the context of a primitive local innate immunity. It was involved in protective functions, such as phagocytosis of self and non-self molecules, expression of cytotoxic agents, nodule formation, and encapsulation of microorganisms. Besides immunity actions, the MC ancestor probably engaged in restoration of

damaged structures. Thus, MC phylogenetic progenitors were probably involved in both aspects of tissue homeostasis – namely defence and reparation – since primordial times. In invertebrates, two types of possible MC progenitor cells have been recognized, namely the basophil/MC-like cell and the test cell. They have been identified in ascidians, chordates which appeared approximately 500 million years ago. Both cell types contain histamine and heparin in their secretory granules. Test cells also contain tryptase and are induced to degranulate by the well-known mast cell secretagogue compound 48/80.

In the Cambrian period, some 550 million years ago, an Ig-based RAG-mediated immune system appeared together with the coming out of early vertebrates. During the transition from invertebrates to vertebrates, the ancient MC precursor evolved into a novel cell type. It continued to perform innate immune and protective functions concomitantly with the stepwise acquisition of acquired immune functions. Vertebrate MCs added new molecular strategies to their functional arsenal without losing many of the properties accumulated during million years of invertebrate evolution. Archaic MCs were integrated into the complex networks of adaptive immune responses, and current MCs probably appeared in the last common ancestor we shared with hagfish, lamprey and shark about 450-500 million years ago.

Acknowledgements

References

Baccari G.C., Chieffi G., Di Matteo L., Dafnis D., De Rienzo G., Minucci S. (2000) Morphology of the Harderian gland of the Gecko, *Tarentola mauritanica*. J. Morphol. 244: 137-142.

Baccari G.C., Pinelli C., Santillo A., Minucci S., Rastogi R.K. (2011) Mast cells in non-mammalian vertebrates: an overview. Int. Rev. Cell. Mol. Biol. 290: 1-53.

Bachelet I., Levi-Schaffer, F. (2007) Mast cells as effector cells: a costimulating question. Trends Immunol. 28: 360-365.

Bengtén E., Clem L.W., Miller N.W., Warr G.W., Wilson M. (2006) Channel catfish immunoglobulins: repertoire and expression. Dev. Comp. Immunol. 30: 77-92.

Bienenstock J., Befus A.D., Denburg J., Goodacre R., Pearce F., Shanahan F. (1983) Mast cell heterogeneity. Monogr. Allergy 18: 124-128.

Blair R.J., Meng H., Marchese M.J., Ren S., Schwartz L.B., Tonnesen M.G., Gruber B.L. (1997) Tryptase is a novel, potent angiogenic factor. J. Clin. Invest. 99: 2691-2700.

Blank U., Rivera J (2004) The ins and outs of IgE-dependent mast-cell exocytosis. Trends Immunol. 25: 266-273.

Bulfone-Paus S., Nilsson G., Draber P., Blank U., Levi-Schaffer F. (2017) Positive and negative signals in mast cell activation. Trends Immunol. 38: 657-667.

Cairns J.A., Walls, A.F. (1997) Mast cell tryptase stimulate the synthesis of type I collagen in human lung fibroblasts. J. Clin. Invest. 99: 1313-1321.

Caldwell D.J., Danforth H.D., Morris B.C., Ameiss K.A., McElroy A.P. (2004) Participation of the intestinal epithelium and mast cells in local mucosal immune responses in commercial poultry. Poultry Sci. 83: 591-599.

Campagna S., Saint N., Molle G., Aumelas A. (2007) Structure and mechanism of action of the antimicrobial peptide piscidin. Biochemistry 46: 1771-1778.

Cavalcante M.C.M., Allodi S., Valente A.P., Straus A.H., Takahashi H.K., Mourão P.A.S., Pavão M.S.G. (2000) Occurrence of heparin in the invertebrate *Styela plicata* (Tunicata) is restricted to cell layers facing the outside environment. J. Biol. Chem. 275: 36189-36196.

Cavalcante M.C.M., De Aandrade L.R., Du Bocage Santos-Pinto C., Straus A.H., Takahashi H.K., Allodi S., Pavão M.S.G. (2002) Colocalization of heparin and histamine in the intracellular granules of test cells from the invertebrate *Styela plicata* (chordata-tunicata). J. Struct. Biol. 137: 313-321.

Cavalcante M.C.M., Mourãom P.A., Pavão M.S. (1999) Isolation and characterization of a highly sulfated heparin sulfate from ascidian test cells. Biochim. Biophys. Acta 1428: 77-87.

Chieffi Baccari G., De Paulis A., Di Matteo L., Gentile M., Marone G., Minacci S. (1998) *In situ* characterization of mast cells in the frog *Rana esculenta*. Cell Tissue Res. 292: 151-162.

Chiu H., Lagunoff D. (1971) Histochemical comparison of frog and rat mast cells. J. Histochem. Cytochem. 19: 369-375.

Church M., Levi-Schaffer F. (1997) The human mast cell. J. Allergy Clin. Immunol. 99: 155-160.

Da'as S., The E.M., Dobson J.T., Nasrallah G.K., McBride E.R., Wang H., Neuberg D.S., Marshall, J.S., Lin T.-J., Berman J.N. (2011) Zebrafish mast cells possess an FcεRI-like receptor and participate in innate and adaptive immune responses. Dev. Comp. Immunol. 35: 125-134.

De Y., Chen Q., Schmidt A.P., Anderson G.M., Wang J.M., Wooters J., Oppenheim J.J., Chertov O. (2000) LL-37, the neutrophil granule- and epithelia cell-derived cathelicidin, utilizes formyl peptide receptor-like 1 (FPRL1) as a receptor to chemoattract human peripheral blood neutrophils, monocytes, and T cells. J Exp Med 192: 1069.

De Barros C.M., Andrade L.R., Allodi S., Viskov C., Mourier P.A., Cavalcante M.C.M., Straus A.H., Tahahashi H.K., Pomin V.H., Carvalho V.F., Martins M.A., Pavão M.S.G. (2007) The hemolymph of the ascidian *Styela plicata* (Chordata-Tunicata) contains heparin inside basophil-like cells and a unique sulfated galactoglucan in the plasma. J. Biol. Chem. 282: 1615-1626.

Di Nardo A., Vitiello A., Gallo R.L. (2003) Cutting edge: mast cell antimicrobial activity is mediated by expression of cathelicidin antimicrobial peptide. J. Immunol. 170: 2274-2278.

Dobson J.T., Seibert J., The E.M., Da'as S., Fraser R.B., Paw B.H., Lin T.J., Berman J.N. (2008) Carboxypeptidase A5 identified a novel mast cell lineage in the zebrafish providing new insight into mast cell fate determination. Blood 112: 2969-2972.

Dvorak A.M. (2005) Ultrastructural studies of human basophils and mast cells. J. Histochem. Cytochem. 53: 1043-1070.

Enerbäck L. (1966a) Mast cells in rat gastrointestinal mucosa. 1. Effects of fixation. Acta Pathol. Microbiol. Scand. 66: 289-302.

Enerbäck L. (1966b) Mast cells in rat gastrointestinal mucosa. 2. Dye-binding and metachromatic properties. Acta Pathol. Microbiol. Scand. 66: 303-312.

Enerbäck L. (1986) Mast cell heterogeneity: The evolution of the concept of a specific mucosal mast cell. In: Befus A.D., Bienenstock J., Denburg J.A. Mast cell differentiation and heterogeneity, Raven Press, New York. Pp. 1-26.

Féger F., Varadaradjalou S., Gao Z., Abraham S.N., Arock M. (2002) The role of mast cells in host defense and their subversion by bacterial pathogens. Trends Immunol. 23: 151-157.

Forsberg E., Pejler G., Ringvall M., Lunderius C., Tomasini-Johansson B., Kusche-Gullberg M., Eriksson I., Ledin J., Hellman L., Kjellen L. (1999) Abnormal mast cells in mice deficient in a heparin-synthesizing enzyme. Nature 400: 773-776.

Frossi B., Gri G., Tripodo C., Pucillo C. (2010) Exploring a regulatory role for mast cells: 'MCregs'? Trends Immunol. 31: 97-102.

Frossi B., Mion F., Sibilano R., Danelli L., Pucillo C.E.M. (2018) I sit time for a new classification of mast cells? What do we know about mast cell heterogeneity? Immunological Reviews 282: 35-46.

Galli S.J. (1990) Biology of disease. New insights into "the riddle of mast cells": microenvironmental regulation of mast cell development and phenotypic heterogeneity. Lab. Invest. 62: 5-33.

Galli S.J., Grimbaldeston M., Tsai M. (2008a) Immunomodulatory mast cells: negative, as well as positive, regulators of immunity. Nat. Rev. Immunol. 8: 445-454.

Galli S.J., Nakae S., Tsai M. (2005) Mast cells in the development of adaptive immune responses. Nat. Immunol. 6: 135-142.

Galli S.J., Tsai M., Piliponski A.M. (2008b) The development of allergic inflammation. Nature 454: 445-454.

Gianguzza M., Dolcemascolo G. (1978) On the ultrastructure of the follicle cells of *Ascidia malaca* during oogenesis. Acta Embryol. Exp. 2: 197-211.

Gilfillan, A.M., Tkaczyc, C. (2006) Integrated signalling pathways for mast-cell activation. Nat. Rev. Immunol. 6: 218-230.

Gommerman J.L., Oh D.Y., Zhou X., Tedder T.F., Maurer M., Galli S.J., Carroll M.C. (2000) A role for CD21/CD35 and CD19 in responses to acute septic peritonitis: a potential mechanism for mast cell activation. J. Immunol. 165: 6915-6921.

Gruber B.L., Kew R.R., Jelaska A., Marchese M.J., Garlick J., Ren S., Schwartz W.B., Korn J.H. (1997) Human mast cells activate fibroblasts. J. Immunol. 158: 2310-2317.

Irani A.M., Schechter N.M., Craig S.S., De Blois G., Schwartz L.B. (1986) Two types of human mast cells that have distinct neutral protease composition. Proc. Natl. Acad. Sci. USA 83: 4464-4468.

Izzo Vitiello I., Chieffi Baccari G., Di Matteo L., Rusciani A., Chieffi P., Minucci S. (1997) Number of mast cells in the Harderian gland of the lizard *Podarcis sicula sicula* (Raf): the annual cycle and its relation to environmental factors and estradiol administration. Gen. Comp. Endocrinol. 107: 394-400.

Hershko A.Y., Rivera J. (2010) Mast cell and T cell communication; amplification and control of adaptive immunity. Immunol. Lett. 128: 98-104.

Hirose E., Shirae M., Saito Y. (2003) Ultrastructures and classification of circulating hemocytes in 9 botryllid ascidians (Chordata: Ascidiacea). Zool. Sci. 20: 647-656.

Hirose E., Taneda Y., Ishii T. (1997) Two modes of tunic cuticle formation in a colonial ascidian *Aplidium yamazii*, responding to wounding. Dev. Comp. Immunol. 21: 25-34.

Huang C., Sali A., Stevens R.L. (1998) Regulation and function of mast cell proteases in inflammation. J. Clin. Immunol. 18: 169-183.

Humphries D.E., Wong G.W., Friend D.S., Gurish M.F., Qiu W.T., Huang C., Sharpe A.H., Stevens R.L. (1999) Heparin is essential for the storage of specific granule proteases in mast cells. Nature 400: 769-772.

Kambayashi T., Allenspach E.J., Chang J.T., Zou T., Shoag J.E., Reiner S.L., Caton A.J., Koretzky G.A. (2009) Inducible MHC class II expression by mast cells supports effector and regulatory T cell activation. J. Immunol. 182: 4686-4695.

King C.L., Xianli J., Malthotra I., Liu S., Mahmoud A.A., Oettgen H.C. (1997) Mice with a targeted deletion of the IgE gene have increased worm burdens and reduced granulomatous inflammation following primary infection with *Schistosoma mansoni*. J. Immunol. 158: 294-300.

Knight P.A., Wright S.H., Lawrence C.E., Paterson Y.Y., Miller H.R. (2000) Delayed expulsion of the nematode *Trichinella spiralis* in mice lacking the mucosal mast cell-specific granule chymase, mouse mast cell protease-1. J. Exp. Med. 192: 1849-1856.

Laird D.J., De Tomaso A.W., Cooper M.D., Weissman I.L. (2000) 50 million years of chrordate evolution: seeking the origins of adaptive immunity. Proc. Natl. Acad. Sci. USA 97: 6924-6926.

Marshall J.S. (2004) Mast-cell responses to pathogens. Nat. Rev. Immunol. 4: 787-799.

Matsuyama T., Iida T. (1999) Degranulation of eosinophilic granular cells with possible involvement in neutrophil migration to site of inflammation in tilapia. Dev. Comp. Immunol. 23: 451-457.

McNeil H.P., Adachi R., Stevens R.I. (2007) Mast cell-restricted tryptase: structure and function in inflammation and pathogen disease. J. Biol. Chem. 282: 20785-20789.

Merluzzi S., Frossi B., Gri G., Parusso S., Tripodo C., Pucillo C. (2010) Mast cells enhance proliferation of B lymphocytes and drive their differentiation toward IgA-secreting plasma cells. Blood 115: 2810-2817.

Metz M., Siebenhaar F., Maurer M. (2008) Mast cell functions in the innate skin immune system. Immunobiology 213: 251-269.

Miller J.S., Moxley G., Schwartz L.B. (1990) Cloning and characterization of a second complementary DNA for human tryptase. J. Clin. Invest. 86: 864-870.

Miller J.S., Westin E.H., Schwartz L.B. (1989) Cloning and characterization of complementary DNA for human tryptase. J. Clin. Invest. 84: 1188-1195.

Miyazawa S., Azumi K., onaka M. (2001) Cloning and characterization of integrin alpha subunits from the solitary ascidian, *Halocynthia roretzi*. J. Immunol. 166: 1710-1715.

Mulero I., Sepulcre M.P., Meseguer J., Garcia-Ayala A., Mulero V. (2007) Histamine is stored in mast cells of most evolutionarily advanced fish and regulates the fish inflammatory response. Proc. Natl. Acad. Sci. *USA* 104: 19434-10439.

Murray H.M., Gallant J.W., Douglas S.E. (2003) Cellular localization of pleurocidin gene expression and synthesis in winter flounder gill using immunohistochemistry and *in situ* hybridization. Cell Tissue Res. 312: 197-202.

Nakae S., Suto H., Iikura M., Kakurai M., Sedgwick J.D., Tsai M., Galli S.J. (2006) Mast cells enhance T cell activation: importance of mast cell costimulatory molecules and secreted TNF. J. Immunol. 176: 2238-2248.

Nakae S., Suto H., Hakurai M., Sedgwick J.D., Tsai M., Galli S.J. (2005) Mast cells enhance T cell activation: importance of mast cell-derived TNF. Proc. Natl. Acad. Sci. USA 102: 6467-6472.

Orinska Z., Maurer M., Mirghomizadeh F., Bulanova E., Metz M., Nashkevich N., Schiemann F., Schulmistrat J., Budagian V., Giron-Michel V., Brandt E., Paus R., Bulfone-Paus S. (2007) IL-15 constrains mast cell-dependent antibacterial defences by suppressing chymase activities. Nat. Med. 13: 927-934.

Pancer Z., Cooper, M.D. (2006) The evolution of adaptive immunity. Annu. Rev. Immunol. 24: 497-518.

Prodeus A.P., Zhou X., Maurer M., Galli S.J., Carroll M.C. (1997) Impaired mast cell-dependent natural immunity in complement C3-deficient mice. Nature 390: 172-175.

Redegeld F.A., Yu Y., Kumari S., Charles N., Blank U. (2018) Non-IgE mediated mast cell activation. Immunological Reviews 282: 87-113.

Reite O.B. (1965) A phylogenic approach to the functional significance of tissue mast cell histamine. Nature 206: 1034-1035.

Reite O.B., Evensen O. (2006) Inflammatory cells of teleostean fish: A review focusing on mast cells/eosinophilic granule cells and rodlet cells. Fish Shellfish Immunol. 20: 192-208.

Rihet P., Demeure C.E., Bourgois A., Prata A., Dessein A.J. (1991) Evidence for an association between human resistance to *Schistosoma mansoni* and high anti-larval IgE levels. Eur. J. Immunol. 21: 2679-2686.

Ritter U., Meissner A., Ott J., Kömer H. (2003) Analysis of the maturation process of dendritic cells deficient for TNF and lymphotoxin-α reveals an essential role for TNF. J. Luekoc. Biol. 74: 216-222.

Ruoss S.J., Hartmann T., Caughey G.H. (1991) Mast cell tryptase is a mitogen for cultured fibroblasts. J. Clin. Invest. 88: 493-499.

Sanding H., Bulfone-Paus S. (2012) TLR Signaling in mast cells: common and unique features. Frontiers in Immunology 3: 185

Sayed B.A., Brown M.A. (2007) Mast cells as modulators of T-cell responses. Immunol. Rev. 217: 53-64.

Scott M.G., Davidson D.J., Gold M.R., Bowdish D., Hancock R.E. (2002) The human antimicrobial peptide LL-37 is a multifunctional modulator of innate immune responses. J. Immunol. 169: 3883-3891.

Silphaduang U., Noga E.J. (2001) Antimicrobials: peptide antibiotics in mast cells of fish. Nature 414: 268-269.

Silphaduang U., Colorni A., Noga E.J. (2006) Evidence for widespread distribution of piscidin antimicrobial peptides in teleost fish. Dis. Aq. Org. 72: 241-252.

Sher A., Hein A., Moser G., Caulfield J.P. (1979) Complement receptors promote the phagocytosis of bacteria by rat peritoneal mast cells. Lab. Invest. 41: 490-499.

Shin K., Watts G.F., Oettgen H.C., Friends D.S., Pemberton A.D., Gurish M.F., Lee D.M. (2008) Mouse mast cell tryptase mMCP-6 is a critical link between adaptive and innate immunity in the chronic phase of Trichinella spiralis infection. J. Immunol. 180: 4885-4891.

Sottovia-Filho D. (1974) Morphology and histochemistry of the mast cells of snakes. J. Morphol. 142: 109-116.

Takaya K. (1969) The relationship between mast cells and histamine in phylogeny with special reference to reptiles and birds. Arch. Hist. Jap. 30: 401-420.

Takaya K., Fujito T., Endo K. (1967) Mast cells free of histamine in *Rana catesbiana*. Nature 215: 776-777.

Terenina N.B., Asatrian A.M., Movsessian S.O. (1997) Neurochemical changes in rats infected with *Trichinella spiralis* and *T. pseudospiralis*. Dokl. Biol. Sci. 355: 412-413.

Thakurdas S.M., Melicoff E., Sansores-Garcia L., Moreira D.C., Petrova Y., Stevens R.L., Adachi R. (2007) The mast cell-restricted tryptase mMCP-6 has a critical immunoprotective role in bacterial infections. J. Biol. Chem. 282: 20809-20815.

Triverdi N.N., Tong Q., Raman K., Bhagwandin V.J., Caughey G.H. (2007) Mast cell α and β tryptases changed rapidly during primate speciation and evolved from γ-like transmembrane peptidases in ancestral vertebrates. J. Immunol. 179: 6072-6079.

Vanderslice P., Ballinger S.M., Tam E.K., Glodstein S.M., Crail C.S., Caughey G.M. (1990) Human mast cell tryptase: multiple cDNAs and genes reveal a multigene serine protease family. Proc. Natl. Acad. Sci. USA 87: 3811-3815.

von Köckritz-Blickwede M., Goldmann O., Thulin P., Heinemann K., Norrby-Teglund A., Rohde M., Medina E. (2008) Phagocytosis-independent antimicrobial activity of mast cells by means of extracellular trap formation. Blood 111: 3070-3080.

Warr G.W., Magon K.E., Higgins D.A. (1995) IgY: clues to the origins of modern antibodies. Immunol. Today 16: 392-398.

Wernersson S., Reimer J.M., Poorafshar M., Karlson U., Wermenstam N., Bengten E., Wilson M., Pilström, L., Hellman L. (2006) Granzyme-like sequences in bony fish shed light on the emergence of hematopoietic serine proteases during vertebrate evolution. Dev. Comp. Immunol. 30: 901-918.

Woodbury R.G., Neurath H. (1980) Structure, specificity and localization of the serine proteases of connective tissues. FEBS Lett. 114: 189-196.

Zhu Y., Thangamani S., Ho B., Ding J.L. (2005) The ancient origin of the complement system. EMBO J. 24: 382-394.

Camillo Golgi: the conservative revolutionary

Paolo Mazzarello[1]

Department of Brain and Behavioral Sciences and University Museum System, University of Pavia, Italy

Abstract

This article outlines the fundamental phases of the scientific life of Camillo Golgi, the first Italian to win a Nobel Prize and one of the protagonists of European biomedical research between the 19th and 20th centuries.

In August 1873 a thirty-year-old Lombard medical doctor, Camillo Golgi, published in the journal *Gazzetta Medica Italiana – Lombardia* a brief note from the modest title *Sulla struttura della sostanza grigia del cervello* ("On the structure of the grey substance of the brain"). The paper gave a hasty description of a new histological procedure for the study of the microscopic morphological structure of the central nervous system. It also provided a quick account of some substantial scientific novelties that the method had allowed to obtain. Making the silver nitrate act on pieces of brain previously hardened with potassium dichromate in succession, Golgi had succeeded in realizing the dream of all the histologists who had previously posed the problem of clarifying the spatial disposition and the remote projections of the cellular elements of which the central nervous system is composed. The miraculous and mysterious contact between the potassium dichromate and the silver nitrate, in fact, determined the precipitation of a brown salt (the silver chromate) that, in a completely unexpected and unpredictable way, occupied the body of the cell and all its extensions, up to the most remote distances. But what most impressed was the randomness of the reaction: only a minority of the cellular elements, present in the microscopic field, were stained in black. At first sight what could have been considered a partiality (and therefore a defect) of the method, was instead his great strength. The cells, and their projections, clearly emerged with respect to the surrounding structures, thus creating almost a "microdissection" of the single elements that were like "extracted" from the tangled neurocytological interweaving within which they were

---

[1] This work collects the results of many researches on Camillo Golgi and his school that I published in the last thirty years. In particular I refer to Mazzarello 2002; 2010; 2011; 2018; 2019; Mazzarello and Bentivoglio 1998; Mazzarello et al. 2001; Mazzarello et al. 2003; Mazzarello et al. 2004; Mazzarello et al. 2006; Mazzarello et al. 2009; Galliano et al. 2010; Raviola and Mazzarello 2011; Shepherd et al. 2011; Bentivoglio et al. 2019.

Corresponding author. E-mail: paolo.mazzarello@unipv.it

imprisoned. It was as if one had succeeded in removing an entire, intact tree, with all its branches and roots, from an inextricable forest. The reaction began to be known as a "chrome-silver reaction" or the "black reaction" or even the "Golgi method". It was a significant scientific contribution destined to change forever the microscopic neuroanatomy but also the professional perspectives of the doctor who had created it. It was not the first time that Golgi's fate had changed compared to the rigid tracks that seemed to constrain the early course of his life.

1. From clinical medicine to basic research

Camillo Golgi was born in Corteno (now Corteno Golgi), a small mountain village in upper Valcamonica in the extreme north of Austrian Lombardy. He was the third of four children of the local doctor, Alessandro, of Pavia origins. After his primary and high school studies, he enrolled at the University of Pavia with the "sole aspiration to regularly obtain the [...] professional degree" to practice medicine as his father had done so many years before. On August 7th 1865 Golgi became medical doctor but could not immediately find his way. He had had the good fortune of being reformed by the military service due to frailty, he then began to operate as a civilian doctor for military health services and was employed in the fight against cholera with an operational base in Zavattarello (a small village in the province of Pavia); for a short period he worked in the Novara Hospital as a surgeon, and in the end he managed to get a modest job as "secondary" doctor (in essence, a low-paid doctor employed both for welfare activities and, occasionally, also for research) at the ancient Hospital of San Matteo in Pavia. Depending on the sanitary requirements, he was also employed in the surgical department, in the small psychiatric ward and in the "syphilocomy" (the dermatological ward where syphilis patients were admitted). An experiment that Golgi did on himself at the time, indicative of the degree of positivist scientific fanaticism, was aimed at finding the solution to the problem of transmissibility of syphilis from mother to child, through mother's milk. According to a testimony, Golgi went so far as to self-inoculate the milk of an infected woman. A singular experiment of which, unfortunately, no known scientific report exists.

Meanwhile, Golgi entered the scientific orbit of Cesare Lombroso, a professor at the University of Pavia and head of the psychiatric department, who was to become internationally known for his anthropological theories on genius, madness and criminality. The meeting with Lombroso certainly constituted a turning point in Golgi's scientific life. The psychiatrist was a man of marked originality, known since he published an essay *On the madness of Cardano* at the age of twenty, in which he already outlined some themes that will make him become, in a few years, one of the leading figures in psychiatric and forensic Italian medical culture. The passion for the scientific research of the brilliant professor had to have a contagious effect because it opened on boundless horizons. After so much speculation it seemed then to be at hand a work program that promised enormous developments in the knowledge of the encephalon, the most fascinating organ of the entire biological domain. Neuropsychiatric illnesses freed themselves of the ballast of "metaphysics"; the brain ceased to be "the organ of the soul" to become, more modestly, "the organ of the psyche". Thus the structural element, the anatomical and anthropometric data, became

Figure 1. Cesare Lombroso, around 1860, in military uniform (Historical Museum, University of Pavia).

the way through which to explore the biology of "mental alienations". Interests that soon caught Golgi still uncertain of the way to follow.

Lombroso often referred to Golgi around 1867-68, mentioned in the publications as a zealous collaborator and sometimes as "the friend Golgi", who took on much of the routine work of the psychiatric ward. However, Lombroso's star then began to set from the horizon of the young doctor; the psychiatrist stated one thing and did another, declaring himself firmly adherent to the experimental method, but his way of proceeding was without methodological rigor. Everything was used to confirm his theories. Instead of proceeding on an inductivistic basis, "gathering the facts", and then constructing interpretations, as the positivistic epistemology of the time wanted, Lombroso was struck by brilliant intuitions, but often outlandish, which became the "filter" through which to select the experimental data. Golgi, who had the practical sense, or we could say common sense, of the mountaineers, could certainly not approve these methods, indeed this lack of method. The sunset of Lombroso was accompanied by the rise of a new scientific star in the Pavia of the time: Giulio Bizzozero.

Born in Varese, three years younger than Golgi, Bizzozero graduated in medicine in 1866, at the age of twenty, passing quickly from the student bench to the professorship of general pathology to replace the professor Paolo Mantegazza, who had

been elected deputy in the national parliament. Bizzozero had the magnetic ability to attract anyone interested in scientific research into the orbit of his powerful personality. Everything in him impressed: the speech, the quick gestures, the fascinating way to teach lessons by presenting the topics as a knowledge in progress, in this aspect extraordinarily different from an academic environment where science was still taught as a truth *ex cathedra.* The meeting with Bizzozero was certainly the decisive event for the development of the future scientific personality of Camillo Golgi. From the very young lecturer, soul and guide of the Laboratory of Experimental Pathology (later General Pathology) located in the Palace of the Botanical Garden, he acquired the knowledge of the histological techniques he will adopt and will not abandon for the rest of his life.

If it was Lombroso who ignited in Golgi a passion for the nervous system, it was nevertheless Bizzozero who catalysed his scientific personality, endowing it with a working method and making him discover the *histological path* to neurobiology. From that moment, and for several years, the nervous system became a favoured destination of his studies, just as histological techniques were a privileged (though not exclusive) means of his way of doing research.

In the time that Golgi was free from his hospital clinical commitment, he began to attend the Laboratory of Experimental Pathology under the guidance of Bizzozero. Thus the first scientific publications appeared including the essay written under the influence of the new Lombrosian anthropological doctrines *Sull'eziologia delle alienazioni mentali* ("On the etiology of mental alienations"). However, the relationship with Bizzozero became increasingly narrow; the two also lived in the same building (Lombroso also lived there for a while) and it is likely that those candlelight evenings would pass quickly with the young scholars discussing science at a time when Charles Darwin had upset the world cultural environments important with his theory of evolution. Under the guidance of Bizzozero, Golgi published histological works: a remarkable study on the glia, which represents his first relevant contribution to histology and neurobiology, and a work on the lymphatic of the brain in which he used, in addition to potassium dichromate, silver nitrate for the study of brain membranes. They are the two reagents that, used in succession, would have allowed him to set up the "black reaction" his most precious methodological invention.

Having enrolled at the university with the "sole aspiration to regularly obtain the [...] professional degree" to practice medicine as his father Alessandro had done so many years before, Golgi had by now profoundly changed his life interests and scientific research was become a deeply felt vocation. Unfortunately, there were no important job opportunities in the academic environment of Pavia. The medical faculty, it is true, gave him a teaching assignment in "Clinical Microscopy" and scientific satisfactions were not lacking; his first works had been cited and summarized in German and English literature, the "Rivista Clinica" of Bologna included him in the editorial committee since 1870. But what was missing, above all in the consideration of his father Alessandro, was a properly paid job. So at the age of twenty-eight, pressed by that worried parent, Camillo Golgi felt forced to find a safe and well-paid place to stay, even at the cost of abandoning the University's mirage and betraying his passion for scientific research.

2. Make the invisible visible

In January 1872 a competition was published for a post of primary doctor at the "Pia Casa degli Incurabili", an old hospice for the chronically ill, of Abbiategrasso, a town twenty-five kilometres from Pavia. Alessandro Golgi had also worked in the same hospital about fifteen years earlier, always keeping a good memory of his activity in this hospital.

It was therefore natural for that father to push the son Camillo, who earned little and, moreover, spent money in order to publish his works, to participate in the Abbiategrasso competition. Thus, reluctantly, Golgi took part in it and, naturally, obtained the position of primary doctor, starting the activity on 10 June 1872. He had reached a point in his life where everything gave the premonition of the total and permanent abandonment of the research. The institute did not possess scientific instruments and no costs were foreseen for an experimental activity. Immediately after his arrival in Abbiategrasso, Golgi then experienced a first period of uncertainty in which he accused "slight disturbances" which caused him "intellectual dullness so great" as to "completely inhibit the possibilities of work".

The link with the vast world of research was however maintained, albeit at a distance, by the letters of his friends Bizzozero and those of the ophthalmologist Nicolò Manfredi. By the end of 1872 he had recovered and organized a tiny histological laboratory in the kitchen of the small apartment that had been assigned to him in the Pia Casa.

Many years later, remembering that period, he will write:

Educated in working with the minimum of means, rich in the sacred fire of scientific work, even if I find myself in a kind of isolation, I had no difficulty in continuing to still occupy
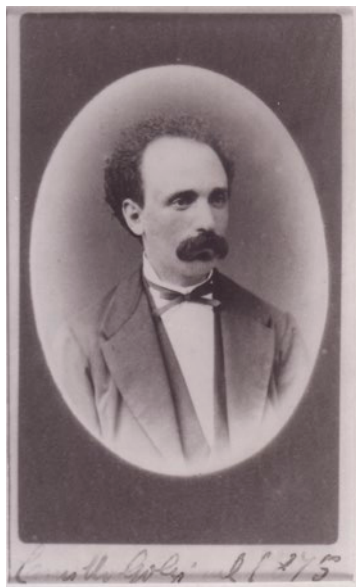

Figure 2. Camillo Golgi in 1875 (Historical Museum, University of Pavia).

myself with microscopic research in the rudimentary laboratory I organized in the kitchen of the small apartment that I had been assigned in the Pio Luogo.

The "sacred fire of scientific work" had taken over again.

On February 16, 1872, a letter from Golgi sent to Manfredi contained this communication:

Now I have regained the energy that for a few months I had completely lost. I spend long hours at the microscope. I am happy to have found a new reaction to demonstrate even to the blinds the structures of the interstitial stroma of the cerebral cortex. I let the silver nitrate act on the pieces of brain hardened in potassium dichromate I have already achieved very good results and I hope to get more.

This is the first announcement known to us, of the discovery (or invention) of the "black reaction" which, as it is easy to imagine, had an electrifying effect on the young Camillo. It had come at the right moment, just when the part-time researcher needed an intellectual medicine to fight the sense of abandonment from the wider world of scientific research, the intellectual horizon to which to hold on.

The black reaction consists of a first phase of "fixation" of the nervous tissue in potassium dichromate (2.5%), for a period varying from 1 to 45 days (and sometimes even more), followed by a second phase of immersion in a solution of silver nitrate. The result obtained is the selective precipitation of a salt, the silver chromate that goes to occupy every part of the neuron and glia including all their extensions. But the singularity of this intracellular reaction is given by its partiality: only a few nerve cells among those included in the microscopic field (in a percentage between 1 and 5%) are stained in black and stand out clearly compared to all the others. A bit like if you could extract a single tree, with all its extensions, from an inextricable forest. It is therefore precisely the partiality of the precipitation of silver chromate that provides the incredible cognitive power of this method that became the fundamental means for studying the structure of the nervous system. To date, the chemical-biological principle underlying this selective precipitation is still unknown. According to some histologists it would depend on the functional state of the cell when the precipitate develops. With regard to the black reaction, one can therefore speak of both discovery (because it is a new biological chemical phenomenon) and the invention of a research method.

An aspect that should be emphasized is the "biotechnological" character of the method developed by Golgi, which realizes a sort of morphological amplification of the histological structures caused by the deposition of an insoluble compound around or in structures so fine that they are not otherwise appreciated. A technique that, appropriately varied and refined, has found application in many areas of biological research allowing, among other things, the discovery of the internal reticular apparatus (Golgi apparatus), the discovery of the system of intracellular canalicular secretion of parietal cells (delomorph) of the gastric glands producing hydrochloric acid (Müller-Golgi canaliculi), the discovery of the pericellular nerve network (Golgi-Netz) and the discovery of the T system linked to the functions of the sarcoplasmic reticulum (by Golgi's pupils Romeo Fusari and Emilio Veratti). But the applications of silver methods related to the "black reaction" have extended to research fields as distant as the highlighting of the hepatic network of the intralobular bile canaliculi, or the identification and analysis of the diffuse endocrine system in the pre-electron microscopy and pre-immunohistochemical era, or the study of biological structures with the electron microscope.
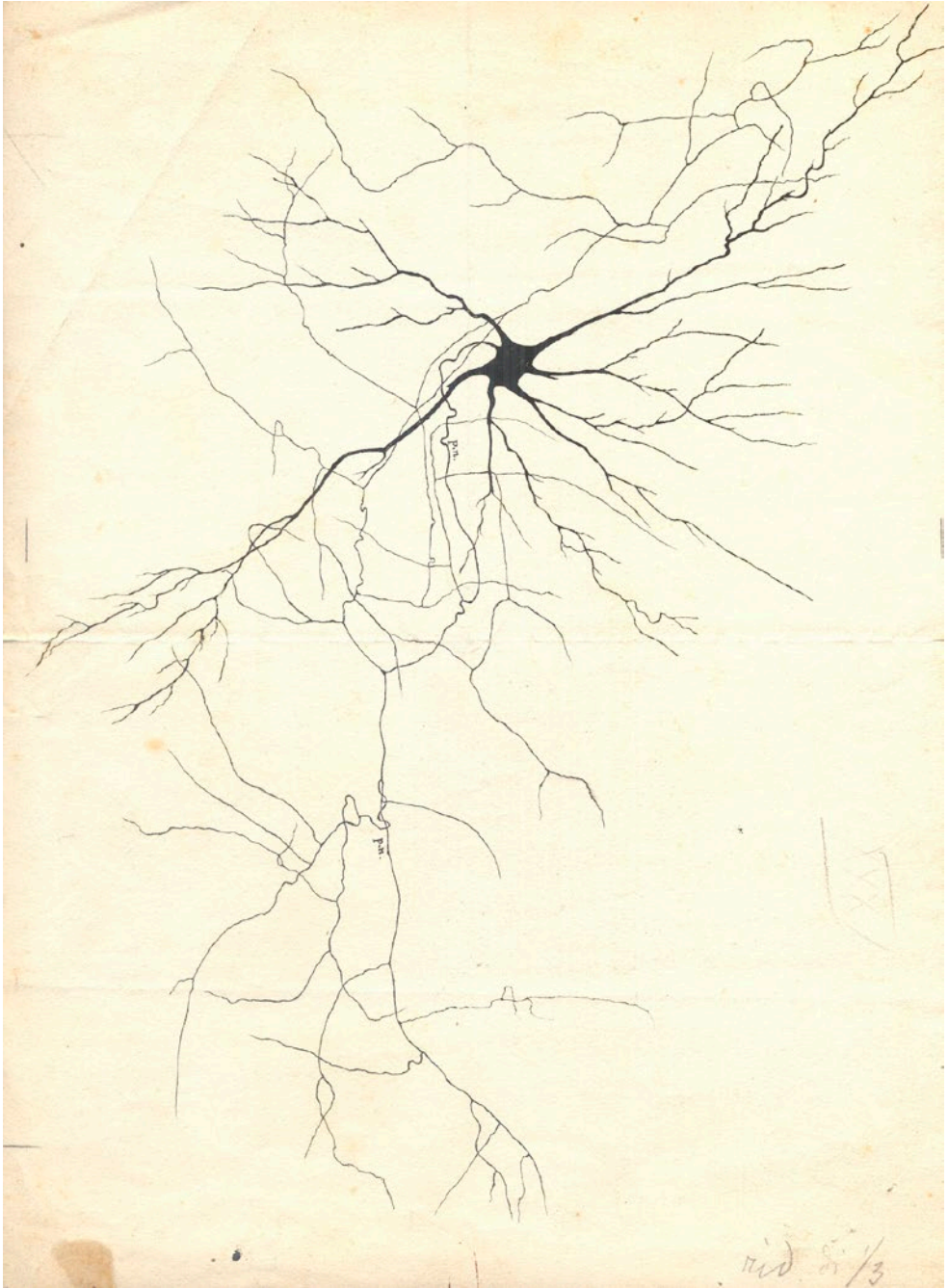
Figure 3. A nerve cell drawn by Golgi (Historical Museum, University of Pavia).

Golgi immediately understood the importance of the extraordinary instrument he had created. In due proportion, someone argued that as Galileo had discovered new stars in any celestial region explored with his telescope, so Golgi saw new nerve architectures in any brain region studied with the black reaction. The young researcher was thus in one of those positions that rarely occur in the history of science, that of the privileged explorer of a new continent. In the isolation of Abbiategrasso his research activity became so hectic. A few months later he had the first scientific communication ready based on the new method: *Sulla struttura della sostanza grigia del cervello*, a work that marks a watershed compared to the previous neurobiological tradition. Immediately afterwards, works appeared on the neuropathological alterations in the nervous system in a case of chorea (in which Golgi described some lesions in the striatum and the frontal cortex), on the structure of the cerebellum (where, among other things, he described the cells bearing his name) and on the morphology of the olfactory bulbs.

Each of these was a seminal work destined to open new perspectives to neuroanatomical and neuropathological research. The work on chorea, in particular, was a pioneering research on the presence of structural alterations in the brain of a patient with a neurodegenerative disease.

3. From neurocytological discoveries to the "diffuse nervous network"

Golgi's neurocytological discoveries were fundamental, reversing the concepts of nerve cell physiology of the time. According to the dominant model of Joseph von Gerlach, a well-known German histologist who introduced new methods of staining tissues with carmine and, subsequently, with gold chloride, the nerve cells were anastomosed in a labyrinthine syncytia, through the fusion of their dendrites, called at that time protoplasmic extensions (Gerlach protoplasmic network). This gigantic interdendritic reticulum would have created an anatomical connection system between the different nervous elements, through an intercellular continuum. Myelinated nerve fibres could originate in two ways: either directly from the interdendritic reticulum, or directly from the axon (called at the time "cylinder axis" or "nervous extension") emerging from the cellular body. It was a model that placed itself in explicit contrast with the cellular theory: the nervous system was not the result of the assembly of so many elementary "bricks" juxtaposed like pieces of a mosaic, but it had the appearance of a gigantic frame of "wires" that encompassed many cell bodies.

Thus the anatomists of the time began to think that at the base of the nervous functions there was a reticular structure, and this idea was well suited to the metaphor of the telegraphic network referred to the nervous physiology, suggested by Hermann von Helmholtz, Emil du Bois-Reymond and other explorers of the border area between physics and biology.

Golgi showed that dendrites did not merge into a network and discovered that the axon was an element *constantly* present in nerve cells. The fundamental neurocytological discovery, only vaguely intuited previously, was however the branching of the axons. These observations undermined Gerlach's reticularism. It was therefore the axon, according to Golgi, the way through which the transmission of the nerve impulse occurred at a distance, and not the dendrite to which he tentatively assigned trophic

Figure 4. The first drawing of a nervous territory observed under a microscope with the black reaction: the olfactory bulbs (1875) (Historical Museum, University of Pavia).

functions. However, the inventor of the black reaction did not abandon the reticularist "paradigm". Around 1870, the "holistic" or "globalistic" neurophysiological vision, supported by Marie Jean Pierre Flourens from the first half of the century, was still influential, according to which the cerebral cortex, in exercising its functions, would have carried out a "unitary" action. This hypothesis was in tune with a cellular model with "communicating vessels" where each element was in diffuse relationship with all the others through a syncytial network. When Golgi observed the slides obtained with the black reaction he had to think that if the net did not exist among the dendrites – to account for the complex relationships inside the nervous system - it must certainly exist between the branches of the newly discovered axons. And the observations that highlighted the tangle of nerve extensions seemed to confirm this assumption. Thus was born the theory of the *diffuse nervous network* within which nerve transmission was not "isolated" along very specific and extremely selective routes, but propagated to the whole nervous system. At the base of this nervous network there had to be either the fusion of the axons or their intimate weaving; the fundamental physiological factor of the model was constituted by the diffused transmission of the nervous impulses. However, these propagations would not have been isotropic, without any order, but able to ensure "prevalent or elective pathways of transmission". Thus, according to Golgi, in the nervous system, there had to be regions "not rigorously delimited, which, as they are prevalently or selectively excited, predominantly responding in a direction corresponding to the actual excitation". In some ways Golgi conceived *fields* of elective or prevalent propagations. A gigantic frame would therefore have served as a support for communication between the various parts of the nervous system. The novelty of Golgi's "reticularist" model, however, was - in addition to the role assigned to axons as a substrate in communication within the nervous system - the functional connotation of the network, conceivable as a true *physiological organ* capable of accounting for the complexity of brain properties. And perhaps for the first time, in the history of science, this concept was *explicitly* related to a complex function. What escaped Golgi was that the only concept of network was insufficient to account for neurological functions; in fact, without a node destined to compartmentalize the nervous energy through a valve mechanism present between cell and cell, able to channel and make the impulses unidirectional, thus preventing their dispersion and decay, the system could not have ensured the division of labour and the order of succession of neuropsychic functions. For Golgi, these functions, were perhaps assured by the differential density of the network between zone and zone, the fact that in certain regions it was richer or more lax. Perhaps, in his view, this idea could have justified the articulated functional differentiation from province to province, within the nervous system.

Golgi maintained this view of cellular relationships within the nervous system that developed in his mind in the 1870s and early 1880s throughout his life. When in 1886-87 he had almost completely abandoned neuroanatomical studies, devoting himself to other subjects of study, the idea emerged that even the nervous tissue was composed of single cells isolated and not fused into a network: the *theory of neuron* was born. First proposed explicitly in 1886-87 by two Swiss scientists, the embryologist Wilhelm His and the psychiatrist Auguste Henri Forel, and also hinted by the Norwegian biologist (and subsequently polar explorer and diplomat) Fridtjof Nansen, was officially baptized by the German anatomist Wilhelm Waldeyer in 1891 and fully developed by the great Spanish histologist and neurobiologist Santiago Ramón y Cajal.
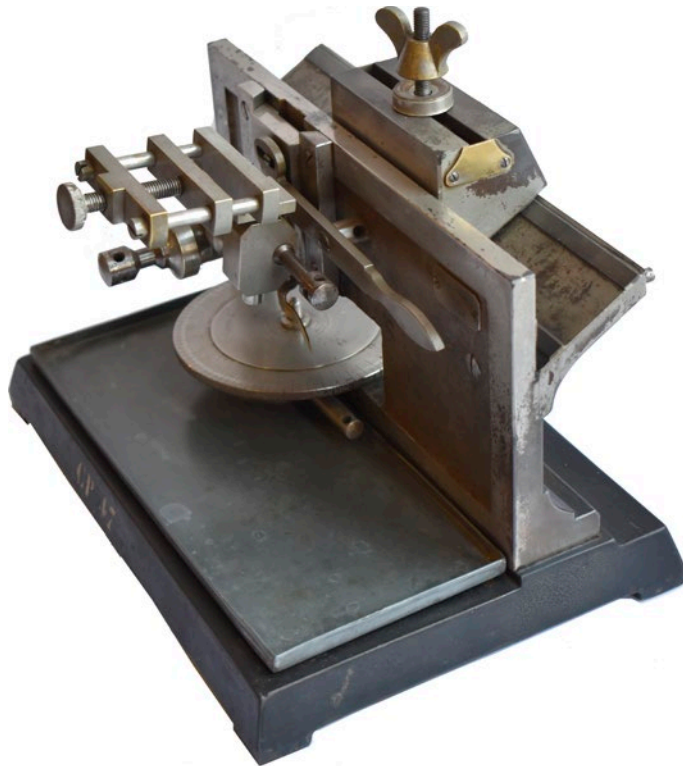
Figure 5. Schanze microtome purchased in 1905 from the Golgi laboratory (Golgi Museum, University of Pavia).

4. Discoveries

With the discovery of the black reaction, Golgi's talent was recognized. At the beginning of 1876 he became professor "straordinario" of histology in Pavia, in May he was promoted to the highest rank of an academic career that of professor "ordinario" (full professor) of anatomy in Siena but after a few months he preferred to return to Pavia on the chair of histology (and starting from 1881 of general pathology).

In Pavia Golgi organized a laboratory that quickly became a reference point for Italian biological research. Here worked, among others, Adelchi Negri whose name is linked to the characteristic lesions of the brain infected with the rabies virus, Antonio Carini who identified in Brasil the fungus *Pneumocystis carinii*, Emilio Veratti, who discovered the T system linked to the sarcoplasmic reticulum functions, Giovanni Battista Grassi who, at the end of the nineteenth century, identified in Rome the vector of human malaria, Carlo Martinotti, whose name is linked to the ascending axon cells of the cerebral cortex, Vittorio Marchi, the inventor of an important myelin staining method that was used in studies on nerve pathways, Aldo Perroncito whose

Figure 6. Laboratory scissors and small tools used by Camillo Golgi (Golgi Museum, University of Pavia).

name has remained linked to studies on peripheral nerve regeneration, after experimental injury.

Golgi himself developed important research in the laboratory, identifying two sensory corpuscles in the thickness of the tendons, the Golgi muscle tendon organs (muscle tension transducers) and the Golgi-Mazzoni corpuscles (sensitive to pressure stimuli), defining new details in the structure of the nerve fibres (horny funnels of Golgi-Rezzonico), discovering that the distal tubule of the kidney enters into relation with the vascular pole of the Malpighian corpuscle (thus clarifying the anatomical basis of what physiologists consider the site of important mechanisms for regulating the arterial pressure), accurately describing the evolutionary phases of the nephron and renal corpuscles.

Furthermore, until the First World War, Golgi maintained the direction of a small clinical department in the San Matteo Hospital of Pavia (as an honorary primary doctor), a circumstance that allowed him to perform important medical observations. An excellent clinician who always refused the practice of private activity, he published papers on intestinal worm infestation, peritoneal transfusions, and the regenerative capacity of renal tissue. Above all, starting from the end of 1885, he developed fundamental clinical-laboratory researches on the evolution of the malarial microbe, the plasmodium, of the quartan and of the tertian form of the disease in the erythrocyte, describing the subsequent morphological modifications (*Golgi cycle*) and establishing the relationship existing between the periodic febrile bouts of patients and the "sporulation" (that is the reproduction) of the protozoan (*Golgi law*). Between 1892 and 1893 he also observed, independently from the Swedish histologist Erik Müller, the canaliculi of the parietal cells of the gastric glands, often called Müller-Golgi tubules.

Naturally this great number of discoveries and the evident international reputation emphasized by acknowledgments and quotations on prestigious publications reverberated also in the Pavia university environment. Thus Golgi was first appoint-

ed rector of the University of Pavia in the years 1893-96. During this period it slowed down considerably with scientific research. But between 1897 and 1898 the time came for another revolutionary discovery that would change the structural concepts of the cell.

5. A brick of the cell

In the course of 1897, studying the spinal ganglia with a variant of the classic chromium-silver method, Golgi discovered, in some cells, a convoluted filamentous apparatus arranged in such a way as to form a cytoplasmic network clearly separated from the nucleus and the cell membrane. However the observation was not easily reproducible. So he decided to wait before publishing these preliminary results. When between the end of 1897 and the first months of 1898 his pupil Emilio Veratti succeeded in demonstrating the endocellular formation by studying the cells of origin of the fourth cranial nerve, Golgi decided to make his discovery known. In the meantime he had succeeded in reproducing the reticular structure also in the Purkinje cells of the cerebellum. Thus in April 1898 he communicated the discovery of the internal reticular apparatus to the Pavia Medical-Surgical Society. It was, to use his words, "represented by a fine and elegant reticulum hidden within the cell body and of so
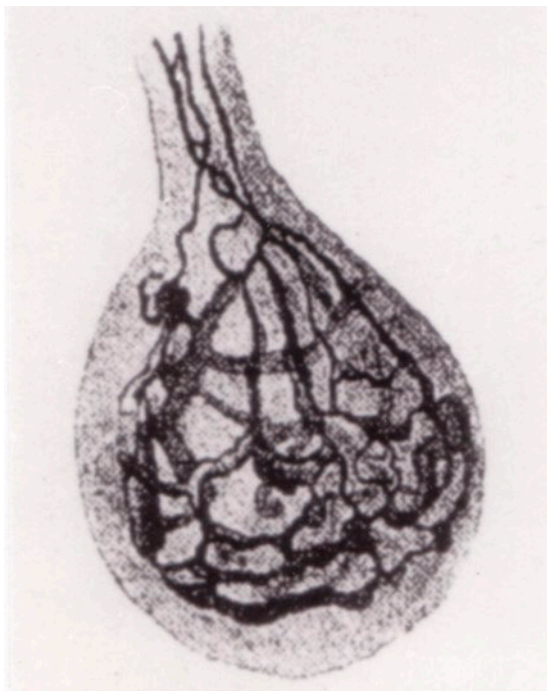

Figure 7. First published illustration (1898) of the Golgi apparatus (Historical Museum, University of Pavia).

characteristic appearance that even small fragments of it, given that the reaction is partial, can safely be recognized as belonging to the same endocellular apparatus [...] But the most characteristic note of the apparatus results from its physiognomy – that is, while it is clearly limited towards the outside, so that [...] the zone of cellular substance comprised between the limit itself and the surface of the cell appears perfectly free and in the form of a regular clear edge, towards the inside, instead, the filaments of the reticulum deepen in different planes".

Shortly after the discovery, Golgi's students Antonio Pensa, Adelchi Negri and Edoardo Gemelli showed their presence also in non-nervous tissues. However for many years the discovery of the internal reticular apparatus was not fully accepted by the international scientific community and in fact did not enter into the official motivation of the conferment of the Nobel Prize to Golgi in 1906. On one hand it was believed that the organelle constituted a part of a wider "lymphatic" canal system extended among several cells, the "Trophospongium", whose existence had been hypothesized by the Swedish histologist Emil Algot Holmgren and who believed himself involved in trophic functions. But in the early decades of the century it was shown that the Trophospongium had nothing to do with the internal reticular apparatus (as Golgi had always claimed) and finally came to consider it an artefact. Others denied the same in vivo existence of the reticular apparatus considering it a fictitious structure secondary to chemical-physical processes of cytoplasm precipitation. The intrinsic uncertainty of the chromo-silver reaction and the difficulty encountered by the researchers in reproducing the results of the Golgian school, had also led to hypothesize (more or less seriously) that some chemical peculiarities of the water of Pavia were the determining factor. The controversy over the existence of the structure discovered by Golgi continued for many years and was definitively resolved in 1954 by Marie Felix and Albert Dalton with the electron microscope.

When, on the basis of his reticular aspect and of its intracellular distribution, Golgi had proposed to call it "internal reticular apparatus", he certainly would not have imagined that it would remain associated with his name making him one the most mentioned biologist in the international scientific literature. Perhaps the first who began to speak of "the Golgi apparatus" was Carlo Besta in 1910. However, the eponymous became internationally known only starting from 1913 after the publication of a seminal work of Jòsef Nusbaum, professor at the University of Lemberg (Lwòw), and the subsequent penetration in the English scientific literature. From the fifties we talk about the "Golgi complex" and in the last forty years we speak of "Golgi" *tout court*. Then there was a clonal terminological amplification of Golgian eponyms: Golgi vesicles, Golgi recycling, Golgi budding, Golgi saccules, Golgi stack, Golgi network, Golgi enzymes etc. The name Golgi, like the fixed part of family surname, is thus always present for any structure or function that refers to the organelle. Thus it has become a mere label without any link to the histologist of Pavia.

Equally variable were the functions attributed to this organelle from the moment when Golgi timidly alluded to a cellular secretory or nutritional functions. In recent years, research developed in laboratories around the world is clarifying its fundamental physiological importance in many cellular processes; the multifunctional role of the Golgi apparatus is increasingly emerging in processes such as the modification, transport and sorting of proteins to the secretory cell surface and the biosynthesis of oligosaccharides and lipids. The communication in which Golgi announced the observa-

tion of the internal reticular apparatus contained the description of a second important discovery. The scientist from Pavia in fact observed on the surface of the nerve cells a "very delicate special covering made of a substance clearly differentiable from that of the cell body". This perineuronal reticulum is now recognized as a specific neurocytological entity that has become increasingly important in neurohistological studies.

6. The last years of an experimental genius

With the new century the scientific creativity of Camillo Golgi faded. He continued to publish some work but had to divide himself with the new commitments to the direction of the University of Pavia of which he was dean of the medical faculty (1899-1901), rector again for a second period from 1901 to 1909. He also assumed a political role both locally in the municipality of Pavia and nationally as a senator of the Kingdom of which he became a member since 1900.

In 1906 he reached the apex of his international fame with the awarding of the Nobel Prize for Medicine, ironically won also by his scientific antagonist Ramón y

Figure 8. The 1906 Nobels seen by the Swedish magazine Aftonbladet.

Figure 9. The Nobel gold medal conferred to Golgi. Historical Museum, University of Pavia.

Cajal, in the same year in which the Italian poet Giosuè Carducci was also recognized for literature.

In addition to the Nobel Prize he obtained other international awards: in 1893-94 the Rinecker prize and medal of the University of Würzburg, in 1894 the Riberi Prize of the Turin Academy of Medicine and in 1907 the Mary Kingsley Prize of the Liverpool School of Tropical Medicine; he also received honorary degrees in Cambridge (1898), Geneva (1909), Kristiania (Oslo, 1911), Athens (1912) and Paris (Sorbonne, 1923).

In the last twenty years of his life, Golgi conducted a tenacious and stubborn battle against the institution of the University of Milan that he considered a threat to Pavia, fearing that it might swallow up the university, sooner or later. During the First World War he headed the Collegio Borromeo military hospital in Pavia and gave impetus to the rehabilitative treatment of war wounded; after the conflict he continued to work in the laboratory, publishing scientific papers until 1923.

But when he died in Pavia on January 21, 1926 this man so full of glory was apparently a loser. He had lost the battle against Ramón y Cajal and the theory of the neuron that was triumphing; he had been defeated in his long war against the institution of the University of Milan whose foundation he bitterly saw.

However after so many years we can say that Golgi was, in reality, one of the most successful researchers in the history of biology: his formidable black reaction had provided the key to opening up the mysterious brain black box, constituting the stele of Rosetta for deciphering the nervous cryptogram and thus helping to found modern neuroscience. The organelle he discovered is one of the building blocks of the cell and a protagonist of cytological research. His malaria studies have inspired generations of researchers.

But it was Golgi's entire scientific work that opened up new fundamental frontiers for biomedical research.

References

Bentivoglio M., Cotrufo T., Ferrari S., Tesoriero C., Mariotto S., Bertini G., Berzero A., Mazzarello P. (2019) The original histological slides of Camillo Golgi and his discoveries on neuronal structure. Front. Neuroanat. 13: (3) 1-13.

Galliano E., Mazzarello P., D'Angelo E. (2010) Discovery and rediscoveries of Golgi cells. J. Physiol. 588: 3639-3655.

Mazzarello P. (2002) Emilio Veratti and the first application of the "black reaction" to muscle research: a historical account. Rend. Fis. Acc. Lincei 13 (s.9): 273-288.

Mazzarello P. (2010) Golgi. Oxford University Press, New York.

Mazzarello P. (2011) The rise and fall of Golgi's school. Brain Res. Rev. 66: 54-67.

Mazzarello P. (2018) From images to physiology: a strange paradox at the origin of modern neuroscience. Progr. Brain Res. 243: 233-256.

Mazzarello P. (2019) Il Nobel dimenticato. La vita e la scienza di Camillo Golgi (Third edition revised). Bollati Boringhieri. Turin.

Mazzarello P., Bentivoglio M. (1998) The centenarian Golgi apparatus. Nature 392:543-544.

Mazzarello P., Calligaro A.L., Calligaro A. (2001) Giulio Bizzozero: a pioneer of cell biology. Nature Rev. Mol. Cell. Biol. 2: 776-781.

Mazzarello P., Calligaro A., Vannini V., Muscatello U. (2003) Nature Rev. Mol. Cell. Biol. 4: 69-74.

Mazzarello P., Calligaro A., Patrini C., Vannini V. (2004) La rigenerazione del nervo periferico: il contributo della scuola pavese. Neurol. Sci. 25: S423-S425.

Mazzarello P., Calligaro A., Garbarino C., Vannini V. (2006) Golgi architetto del cervello. Skira, Milan.

Mazzarello P., Garbarino C., Calligaro A. (2009) How Camillo Golgi became "the Golgi". Febs Letters 583: 3732-3737.

Raviola E., Mazzarello P. (2011) The diffuse nervous network of Camillo Golgi: facts and fiction. Brain Res Rev. 66: 75-82.

Shepherd G.M., Greer C.A., Mazzarello P., Sassoè-Pognetto M. (2011) The first images of nerve cells: Golgi on the olfactory bulb 1875. Brain Res. Rev. 66: 92-105.

Structure, morphology and signalling development mechanisms of human salivary glands

Margherita Sisto*, Domenico Ribatti and Sabrina Lisi

Department of Basic Medical Sciences, Neurosciences and Sensory Organs (SMBNOS), Section of Human Anatomy and Histology, University of Bari "Aldo Moro", Bari, Italy

Abstract

The human salivary gland (SGs) develops as a highly branched structure designed to produce and secrete saliva indispensable to maintain the health of the oral cavity and for carry out physiological functions like mastication, taste perception and speech. Here we review the anatomy and cytoarchitecture of SGs and the most recent literature that has enabled a better understanding of the molecular signalling pathways of SGs development to translate this basic research towards therapy for patients suffering from salivary hypo function.

Introduction

The salivary glands (SGs) are multicellular exocrine glands that synthesize and secrete saliva into the mouth, maintaining several physiological functions ranging from the protection of teeth and surrounding soft tissues to the lubrication of the oral cavity, crucial for speech and perception of taste sensitivity (Carpenter, 2013; Feller et al., 2013). The SGs are divided into the major paired and minor SGs. Humans have three paired major SGs [parotid (PG), submandibular (SMG), and sublingual (SLG)] as well as hundreds of minor SGs. (Edgar et al., 2012). SGs can be affected by infection, inflammation, autoimmune disease, and tumorigenesis. Indeed, advances in routine imaging have played an important role in visualization of morphology and function and have led to improved sensitivity in the diagnosis of several diseases that involve the major and minor SGs. Here we aim to provide a perspective on what is currently known about the anatomical findings on SGs, as well as the recent progresses in the identification of the signalling pathways involved in SGs morphogenesis. Understanding the molecular mechanisms involved in gland biogenesis provides a template for regenerating, repairing or reengineering SGs which will hopefully one day restore SGs function in patients who suffer from xerostomia.

* Corresponding author. E-mail: margherita.sisto@uniba.it

Anatomical structure of the major SGs

The largest of the three major SGs is the PG. It is located superficially, below the external acoustic meatus between the sternocleidomastoid muscle and the masseter extending from the mastoid tip to just below the angle of the mandible. The gland is enveloped by the superficial layer of the deep cervical fascia that splits to constitutes the parotid space delimited anteriorly by the masticator space. The PG is divided into a superficial and deep lobe by the facial nerve, which passes through the gland (Chaurasia's, 2006; Som & Brandwin-Gensler, 2011).

The secretions of the PG are transported to the oral cavity by the Stensen's duct. It arises from the anterior border of the gland traversing ventrally the superficial surface of the masseter muscle. The duct that perforates the buccinators muscle, moving medially, and it opens out into the oral cavity in the buccal mucosa near the second maxillary molar. It is important to note that a relevant number of individuals have an accessory duct that drains directly into the main parotid duct (Carpenter, 2013; Kessler & Bhatt, 2018).

The SMG is the second largest of the three major SGs. It is positioned deeply and inferiorly to the mandible, precisely in the posterior part of the submandibular triangle, which borders are anterior and posterior bellies of the digastric muscle and the lower border of the mandibular body; SMG overlies both bellies of the digastric muscle. A line drawn through the SMG at the level of the posterior margin of the mylohyoid muscle can be used to separate the submandibular (superficial) portion of the SMG from the sublingual (deep) portion of the SMG (Carlson, 2000). The excretory Wharton's duct, extends from the anterior aspect of the SMG deep to mylohyoid on the lateral surfaces of the hyoglossus muscle and genioglossus muscle, which are lateral to the hypoglossal nerve (Johns, 1977; Carlson, 2000). Laterally to the Wharton's duct lies the SLG, the smallest of the three major SGs. It is situated submucosally in the floor of the mouth and deeply to the body of the mandible, precisely in the sublingual space. The sublingual space, bounded between the mylohyoid muscle and the geniohyoid and genioglossus muscles, contains the lingual artery and nerve, the hypoglossal nerve, the glossopharyngeal nerve, Wharton's duct, and the SLG, which drains into the oral cavity through several small excretory ducts in the floor of the mouth and a major duct known as Bartholin's duct. (Johns, 1977; Carlson, 2000).

Anatomical structure of the minor SGs

The mucosa of the upper aerodigestive tract is lined by hundred small, minor SGs spread throughout the submucosa of the sinonasal cavity, oral cavity, pharynx, larynx, trachea, lungs, and middle ear cavity. However, the minor SGs are ubiquitous but most concentrated along the buccal mucosa, labial mucosa, lingual mucosa, soft/hard palate, and floor of mouth. They lack a distinct capsule, instead mixing with the connective tissue of the submucosa or muscle fibres of the tongue or cheeks (Nanci, 2013; Kessler, 2018). Minor SGs also are formed from a complex ductal network similar to those of the major glands although constitute from small ducts. Minor salivary glands contribute substantially to the amount of secreted saliva within the oral cav-

ity that usually occurs through several short ducts, instead of being collected by a single large duct as the major SGs (Ferraris & Muñoz, 2006; Nanci, 2013). Therefore, paradoxically, the minor SGs have an efficient system of salivary production that is considered the most important for the mucosal protective and lubricant functions for the oral cavity (Edgar, 1990).

Cytoarchitecture of SGs

Acini

Saliva is secreted by the SGs end-pieces, the acinar lobules, which are composed by acinar cells (Figure 1). There are three main types of acini: serous, mucinous and seromucous, (Berkovitz et al., 1992; Tandler & Phillips, 1998). Serous acini have a spherical morphology and produce a watery secretion containing proteins that are modified and stored in secretory, or zymogen, granules abundant at the apex of the cell. In contrast, mucinous acini store a glycoprotein mixture (mucous, like mucins), which becomes hydrated upon exocytosis to form mucus. Lastly, seromucous acini contain secretions of both types (Tandler & Phillips, 1998).

Serous and mucinous acini are characterized by a distinct cellular architecture; the serous cells are pyramidal or triangular in shape, are distinguished by basophilic basal cytoplasm, a centrally-located nucleus, and variously-staining secretory vesicles (zymogen granules) in apical cytoplasm. These cells, arranged in a spherical structure with a narrow apex that forms a central lumen, secrete pre-packaged secretory granules located in the apical cytoplasm that contain salivary molecular components (Berkovitz et al., 1992; Carpenter, 2013). The mucous saliva provides oral lubrication and form a relevant glycan barrier in mucosal protection (Munger, 1964; Carpenter, 2013). Serous acini secrete protein and glycoprotein and high levels of amylase, ions and water. (Ligtenberg et al., 2015).

Ductal system

The ductal system modifies the composition of the primary hypotonic saliva into an isotonic fluid through ionic changes between saliva and ductal cells (Figure 1). These events occur into three different types of ducts known as intercalated, striated and excretory ducts (Carlson, 2000). The intercalated ducts, connecting directly to the acini, are the first to receive the primary hypotonic saliva since that the lumen of the secretory acini is contiguous with the lumen of the intercalated ducts. These ducts are constituted by simple cuboidal epithelial cells, partially covered by contractile myoepithelial cells that contribute to the salivary flow. Intercalated ductal cells present microvilli pointing towards the lumen space and in the apical region, contain granules of lysozyme and lactoferrin that are secreted in the saliva (Berkovitz et al., 1992; Carpenter, 2013; Ellis & Auclair, 2008).

Striated ducts, considered as intralobular ducts, are specialized in promoting the essential salivary modification from isotonic to hypotonic saliva trough the secretion and reabsorption of electrolytes in a bidirectional way between the lumen and the extracellular space. In the striated duct cells are present a large amount of mitochon-
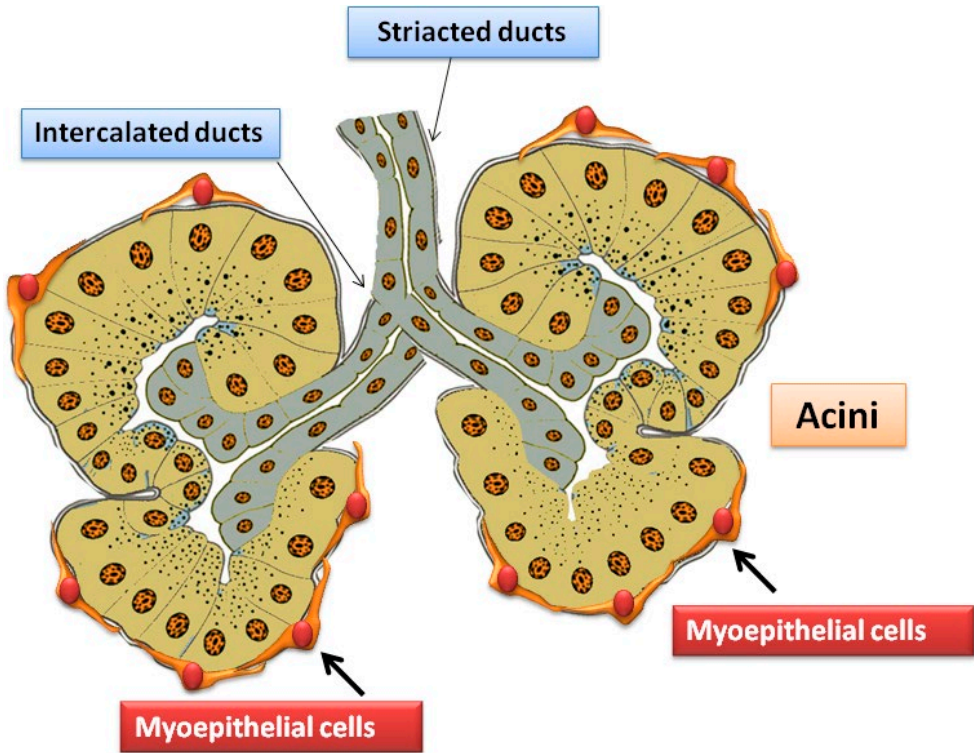
Figure 1. Schematic representation of the structural features of major salivary glands.

dria along their basolateral membrane that characterizes the striated aspect by their multiple folding (Berkovitz et al., 1992; Carpenter, 2013).

The final collecting ducts, interlobular excretory ducts, are formed by pseudostratified epithelium and insert between the glandular lobules. These ducts reabsorb the sodium and potassium secretions in a continuous way, and subsequently are responsible to drive the final saliva production versus oral cavity (Ligtenberg & Veerman, 2014).

Myoepithelial cells

Myoepithelial cells have dual epithelial and contractile properties and play an essential role in acinar salivary secretion (Figure 1). These cells present in their cytoplasm keratin filaments and contractile proteins such as actin, caldesmon, calponin and smooth muscle actin (Redman, 1994; Ianez et al., 2010; Chitturi et al., 2015). They have variable distribution between types of glands and also even within the same gland during the development (Redman, 1994; Hardy & Kramer, 1998; Ogawa, 2003; Chitturi et al., 2015). The myoepithelial cells are stellate or spiderlike, with a flattened nucleus scanty, perinuclear cytoplasm and numerous branching processes that

embrace the secretory and duct cells. These cells rhythmically contract to squeeze saliva from the acinar units upon stimulation by nerves, through the duct system, and into the oral cavity (Shah et al., 2016). Furthermore, it has been suggested that myoepithelial cells play a role in propagation neural stimuli transport of metabolites and in inflammatory state of SGs (Caselitz et al, 1986; Redman., 1994; Ogawa, 2003; Ianez et al., 2010; Chitturi et al., 2015; Shah et al., 2016; Sisto et al. 2018).

Salivary gland innervation and vascularization

   The composition and volume of secreted saliva depends on neural stimulation, and the normal secretion is associated with the autonomic nerve supply, that is important to understand autonomic effects on not only salivation, but also biogenesis (Proctor & Carpenter 2007; Ferreira & Hoffman, 2013). Parasympathetic stimulation results in secretion of serous, or watery, salivary secretion and ions, whereas sympathetic stimulation increases the secretion of proteins. In the central nervous system, the salivatory nuclei are the pontine superior salivatory nucleus responsible for the innervation of SMG and SLG, and the pontine inferior salivatory nucleus that innervate PG. From the superior salivatory nucleus preganglionic parasympathetic fibers are distributed via the chorda tympani and lingual nerves to the submandibular and sublingual ganglia, which are within the glands. The SMG and SLG are innervated by post-ganglionic fibres that stimulate saliva secretion and innervate myoepithelial cells (Ishizuka et al. 2010). From the inferior salivatory nucleus, the preganglionic parasympathetic fibres originate in the glossopharyngeal nerve. They leave the glossopharyngeal nerve by its tympanic branch and then pass via the tympanic plexus and the lesser petrosal nerve to the otic ganglion. Here, the fibres synapse, and the postganglionic fibres pass by communicating branches to the auriculotemporal nerve, a branch of the mandibular nerve (Tosios et al., 2010), which conveys them to the parotid gland. For the sympathetic innervation, the cell bodies of the are located in the superior cervical ganglion in the neck and post-ganglionic fibres innervate the SGs through the blood vessels of the carotid plexus (Kahle & Frotscher, 2003).
   Regards the vascularization, for the PG the blood is supplied by the posterior auricular and superficial temporal arteries, both branches of the external carotid artery, which arise within the parotid gland itself (Ten cate, 1998) Venous drainage is achieved via the retromandibular vein. It is formed by unification of the superficial temporal and maxillary veins. For SMG, blood supply is via the submental arteries which arise from the facial artery; a branch of the external carotid artery. Venous drainage is through the submental veins which drain into the facial vein and then the internal jugular vein (Fehrenbach MJ, Herring SW, 2012). For SLG, blood supply is via the sublingual and submental arteries which arise from the lingual and facial arteries respectively; both of the external carotid artery. Venous drainage is through the sublingual and submental veins which drain into the lingual and facial veins respectively; both then draining into the internal jugular vein. (Nanci, 2013) The lymphatic system of the parotid gland differs from that of SMG and SLG, because in that there is a high density of lymphnodes in and around it. PG contains two nodal layers, draining into both the superficial and deep cervical lymph systems (Garatea-Crelgo J, 1993).

Development of human SGs

Morphogenesis of SGs requires the cooperation of signalling pathways that coordinately direct cell proliferation, cell quiescence, apoptosis, and histological differentiation (Melnick and Jaskoll, 2000; Melnick et al., 2001 a, b, c, d; Davidson et al., 2002; Gardner et al., 2003). The development of the major SGs in humans begins the sixth to eighth embryonic week. The SMG of the mouse shows a classic organogenetic and branching morphogenesis process and is commonly used as a model to study human organogenesis (Borghese, 1950). The highly branched structure of SGs development is regulated by multiple stage-specific growth factors, cytokines, and transcription factors which are expressed at specific time points to trigger the organogenesis process (Kashimata and Gresik, 1997; Jaskoll and Melnick, 1999; Melnick et al., 2001 a, b, c, d; Jaskoll et al., 2002). SGs organogenesis involves epithelial, mesenchymal, neuronal, lymphatic, and endothelial cells, together with their corresponding stem and progenitor cells. These cell types and their extracellular matrix microenvironment interact spatiotemporally to induce a program of genetic and epigenetic tissue patterning and cellular differentiation, ultimately resulting in functional SGs. There is some controversy within the literature about the developmental origin of the epithelium of the major SGs; while it is accepted that major SGs are primarily derived from the oral epithelium, it is unclear which part of the oral epithelium they arise from and where this is in comparison to the junction of the oral ectoderm with the foregut endoderm (Avery, 2002; Hisatomi et al., 2004). During oral cavity development, a transient formation begins, that initially defines the boundaries of the ectoderm and endoderm and furthermore it separates the oral cavity from the cavity of the primordial pharynx (Patel and Hoffman, 2014), but the exact position of this formation as compared to sites of SGs initiation remains to be clarified. Using the genetic Cre-loxP system, in which expression of Cre-recombinase in neural crest cells genetically enables the expression of a Cre-reporter allele, to permanently mark neural crest-derived cells, the fate of neural crest cells has been determined (Debbache et al., 2018), demonstrating that the mesenchyme and nerves in the SGs are neural crest in origin as shown by lineage tracing with Wnt1-cre (Jaskoll et al., 2002). However, many authors agree that the parotid is ectodermal, whereas the SMG and sublingual are endodermal (Avery, 2002). The endoderm origin was supported by data showing that adult SGs progenitors can differentiate into pancreatic β-cells and hepatocytes when transplanted into hepatectomized liver (Hisatomi et al., 2004), even if there is no evidence to prove that *in vivo* the salivary epithelium is derived from the endoderm. Recent genetic lineage tracing experiments using the Sox17-2A-iCre/R26R mouse, which marks endodermal cells, showed that the epithelia of all three major SGs are not of endoderm origin, suggesting an ectodermal lineage (Rothova et al., 2012). In addition, animal models and human mutations that cause ectodermal dysplasia, developmental syndromes that specifically affect ectodermal organs, suggest that the major SGs arise from common multipotent precursors residing in the embryonic ectoderm (Jaskoll et al., 2003; Thesleff and Mikkola, 2002).

The SMG placode is visible as a localized thickening of the oral epithelium adjacent to the tongue around at embryonic day (ED) 11,5 of development, known as the. prebud stage (Tucker, 2007). Migrating neural crest cells coalesce adjacent to the salivary placode. These neural crest-derived mesenchymal cells contain Schwann

cell precursors that migrate along nerves, differentiate into neurons, and coalesce within their target tissue to form parasympathetic ganglia (Knosp et al., 2015). By ED12, the salivary proof enlarges and invaginates into the underlying mesenchyme which begins to condense leading to the formation of a primary bud; a duct secures the link to the oral surface and this duct will become the major secretory duct. By ED13, known as the pseudoglandular stage, the final part of the bud grows in size and undergoes a process of cluster formations resulting in ramification of the SMG. At this point, the epithelium is characterized by a high level of proliferation unlike the mesenchyme which shows a relatively low grade of proliferation in all stages of gland development (Tucker, 2007). At ED13.5 the epithelium begins a process termed branching morphogenesis. These buds continue branching producing a multi-lobed gland by ED14.5. Lumen formation of the primary duct occurs by ED13.5, while lumenization of the secondary and tertiary ducts starts after ED14, and end bud lumenization occurs by ED15. The majority of the ducts develop lumen at the canalicular stage, from about ED15.5. After ED15.5, the polarized end buds begin secretory cytodifferentiation, while the cells locate around at the lumens are undergoing apoptosis. Around ED17.5, the branches and terminal buds are delved to form the ductal and acinar system and at this point, the terminal bud stage is completed and exhibits distinct lumina and presumptive ducts (Melnick and Jaskoll, 2000). SGs development carry on after birth with the final differentiation of the granular convoluted tubules until at puberty (Gresik et al., 2009). By 13-16 weeks in humans, the SMG appears well differentiated, and continue to develop up to 28 weeks, at which stage secretory products can be seen in acini. At birth the glands are functional to secrete saliva (Holmberg and Hoffman, 2014), (Figure 2).

Signalling mechanisms controlling SGs morphogenesis

The SGs development is a progressive process involving complex multiple reciprocal interactions between epithelial and its surrounding mesenchyme. The recent literature reports that a series of cross talk between mesenchyme and epithelium drive the migrating neural crest cells to control placode initiation in mice SGs. Multiple molecules, including components of the extracellular matrix, cell adhesion receptors, proteases, and growth factors, mediate these instructive interactions crucial to govern organ branching by providing structural integrity and regulating cell shape, cell motility and cell growth (Jaskoll & Melnick, 1999). Different experimental studies conducted on SMG, demonstrated that SMGs, as well as lung and the mammary glands, are formed during embryonic development by epithelial branching, which establishes the architecture of these organs (Patel et al. 2006). Branching involves repetitive formation of epithelial clefts and buds that invade surrounding embryonic ECM, which changes in composition and distribution over time. In these sequential events, the mesenchyme and mesenchyme-secreted factors control the glandular pattern formation and the branching of the glands (Patel et al. 2006). The extracellular matrix, through integrin engagement, collaborates with growth factors in cell signaling and, as clearly demonstrated, the EGF system acts as key regulator of development of mouse SMG and α6 integrin expression is coordinated by the level of EGF, which in turn control the interactions between epithelial cells and the extracellular
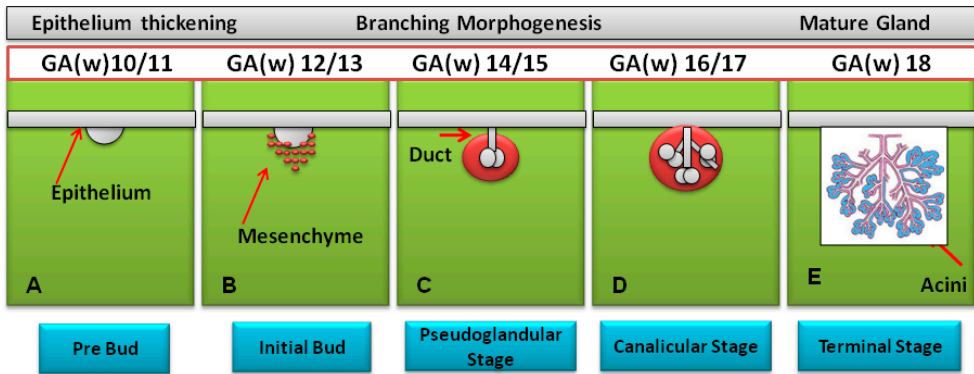
Figure 2. Embryonic branching morphogenesis of human salivary glands (GA: gestional age; W: week).

matrix (Kashimata & Gresik, 1997). The EGFR is strongly expressed in developing ducts and EGF can act as ligand (Gresik, 1997). In the EGFR mutant mice, the SGs have a substantial reduction of number of terminal buds indicating that the EGF-EGFR ligand-receptor system is fundamental for physiological SMG development (Jaskoll & Melnick, 1999). Advanced genetic studies have demonstrated that branching morphogenesis appears to be controlled by molecular conserved regulators, including FGF family. Indeed, the FGF/FGFR system has an essential key role for the development processes branching morphogenesis of the SGs (Hoffman et al., 2002), as demonstrated, for example, from the evidence that FGF/FGFR transgenic mice display altered MSG phenotype (De Moerlooze et al., 2000; Ohuchi et al., 2000; Ornitz and Itoh, 2001; Jaskoll et al., 2004).Therefore, FGFR cleavage seems to be increased by MMPs activity allowing localized spread of the epithelium at sites where proliferation occurs (Simian et al., 2001). These interesting results suggest that FGFR pathway involves a regulatory network that triggers bud formation and duct elongation during branching morphogenesis (Steinberg et al., 2005). In human patients, mutations in FGF/FGFR pathway are linked with aplasia of the SGs demonstrating that the normal development of the glands depends on balance of signalling triggered by this system (Shams et al., 2007). The critical role of BMPs (2, 4, 7) to control initial stages of embryonic SMG branching morphogenesis was also reported by innovative studies. In particular, BMP7 mutant mice exhibit an altered phenotype, the mesenchymal tissue of the SGs is disorganized with reduced branching and lumen formation (Jaskoll et al., 2002). The TNF/TNF-R1 signal transduction represents another widely studied pathway playing a critical role in balancing pro- and anti-apoptotic factors during SMG ducts and acini formation (Melnick et al., 2001c). Results obtained derived from the study of a genetic disease known as hypohidrotic ectodermal dysplasia caused by mutations in ectodysplasin (EDA) gene (Kere et al., 1996; Mikkola, 2008). EDA and its receptor EDAR are members of the TNF superfamily critically involved during teeth, hair and sweat glands development (Srivastawa et al., 1997; Monreal et al., 1998) and in the EDA knockout gene mice, a loss or reduction in lumen formation is evident (Kere et al., 1996; Mikkola, 2008). Indeed, EDA and EDAR mutant mice have hypoplastic and dysplastic glands
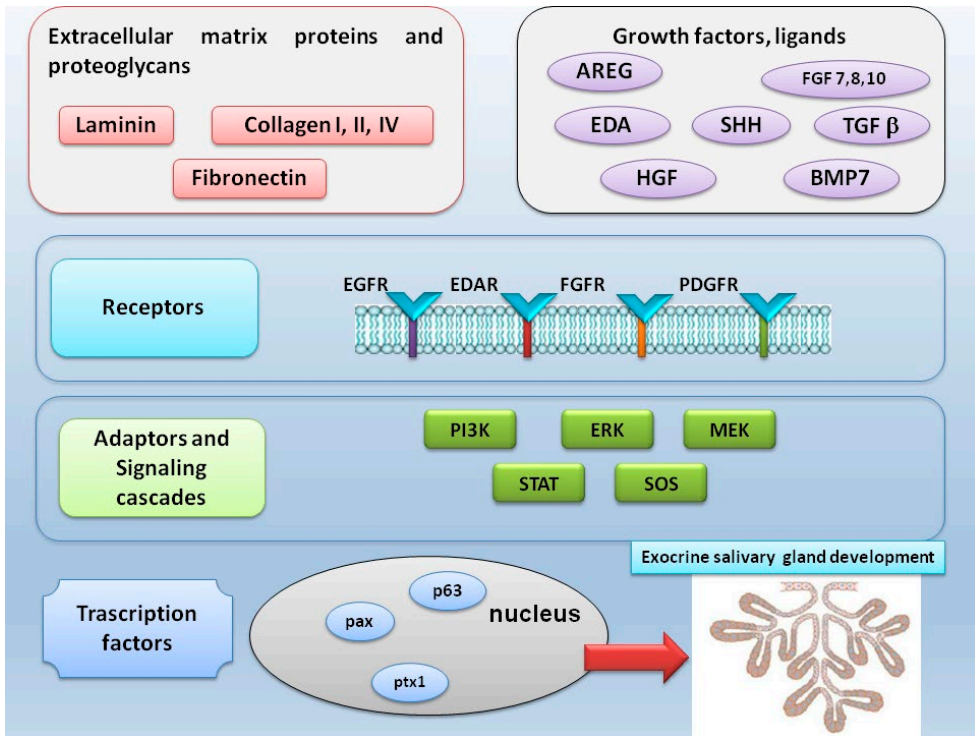
Figure 3. Representation of the best known molecular regulatory mechanisms of branching morphogenesis in human salivary glands.

like as lack lumens and acini (Melnick et al., 2009); in addition, when EDA recombinant is added to SMG organotypic cultures branching is increased, while soluble form of EDAR supplemented in embryonic SMG cultures abrogates EDA/EDAR signalling resulting in a significant decrease in branching morphogenesis (Mikkola, 2008; Melnick et al., 2009). Further studies focusing on the effects of signals through EGFR on *in vitro* differentiation recognize EGFR as a critical regulator during the final stages of the SMG development, when the EGF/TGFα/EGFR pathway was activated that controls the rate of branching and histodifferentiation and progression from the canalicular stage to the terminal bud stage. The increased expression of TGFα and EGFR suggests the importance of this signalling pathway during the development of the terminal bud stage (Melnick et al., 2000). It is clear that, while many details regarding cell physiology of adult acinar and ductal SGs cells have been identified, further studies are required to investigate new aspects of the SGs human developmental process providing new methods to interpret glandular health and disease A scheme of signalling pathways involved in SGs development is represented in Figure 3.

Conclusion

SGs development requires the interaction of multiple cell types including epithelial, mesenchymal, endothelial and neuronal cells and the coordination of many signalling pathways to direct the cell shape changes, cell movements, and cell-cell interactions. Although much progress has been made in the past several years, we remain in the early stages of the understanding of the specific molecular pathways that mediate the development of the SGs. This review is not exhaustive and there is still much to learn but our hope is that a better understanding of molecular development pathways will inform efforts to provides a template for regenerating, repairing or reengineering diseased or damaged adult human SGs.

Acknowledgement

Disclosure

The authors declare that they have no conflict of interests.

References

Avery J.K. (2002). Oral development and histology. New York: Thieme. 1-435

Berkovitz B.K.B., Holland G.R., Moxham B.J. (1992). A colour atlas and textbook of oral anatomy histology and embryology, 2nd ed. London: Wolfe Publishing Ltd. 1-148

Borghese E. (1950) The development in vitro of the submandibular and sublingual glands of Mus musculus. J. Anat. 84: 287-302.

Carlson G.W. (2000) The salivary glands. Embryology, anatomy, and surgical applications. Surg. Clin. North Am. 80: 261-273.

Carpenter G.H. (2013) The secretion, components, and properties of saliva. Annu. Rev. Food Sci. Technol 4: 267-276.

Caselitz J., Walther B., Wustrow J., Seifert G., Weber K., Osborn M. (1986) A monoclonal antibody that detects myoepithelial cells inexocrine glands, basal cells in other epithelia and basal and suprabasal cells in certain hyperplastic tissues. Virchows Arch. Pathol. Anat. Histopathol .409:725-738.

Chaurasia's B.D. (2006) Human Anatomy Regional and Applied Dissection and Clinical: Head, Neck and Brain. 4th ed. Satish Kumar Jain; 133-138.

Chitturi R.T., Veeravarmal V., Nirmal R.M., Reddy V.R.B. (2015) Myoepi-thelial cells (MEC) of the salivary glands in health and tumours. J. Clin. Diagn. Res. 9: ZE14–ZE18.

Davidson E.H., Rast J.P., Oliveri P. Ransick A., Calestani C., Yuh C.H., Minokawa T., Amore G., Hinman V., Arenas-Mena C., Otim O., Brown C.T., Livi C.B., Lee P.Y.,

Revilla R., Rust A.G., Pan Z.j., Schilstra M.J., Clarke P.J., Arnone M.I., Rowen L., Cameron R.A., McClay D.R., Hood L., Bolouri H. (2002) A genomic regulatory network for development. Science 295:1669-1678.

De Moerlooze L., Spencer-Dene B., Revest J.M., Hajihosseini M., Rosewell I., Dickson C. (2000) An important role for the III b isoform of fibroblast growth factor receptor 2 (FGFR2) in mesenchymal-epithelial signaling during mouse organogenesis. Development 127:483-492.

Debbache J., Parfejevs V., Sommer, L. (2018) Cre-driver lines used for genetic fate mapping of neural crest cells in the mouse: an overview. Genesis 56, e23105.

Edgar W.M. (1990). Saliva and dental health. Clinical implications of saliva: Report of a consensus meeting. Br. Dent. J. 169: 96-98.

Edgar M., Dawes C., O'Mullane D., eds. (2012). Saliva and oral health (4th ed.). Little Steine, Hill Farm Lane, Duns Tew, OX25 6JH: Stephen Hancocks Limited. p. 1.

Ellis G.L., Auclair P.L. (2008) AFIP atlas of tumor pathology: The normal salivary glands, 4th ed. Maryland: ARP Press

Fehrenbach M.J., Herring S.W. (2012) Illustrated anatomy of the head and neck (4th ed.). St. Louis, Mo.: Elsevier/Saunders. p. 154.

Feller L., Altini M., Khammissa R.A., Chandran R., Bouckaert M., Lemmer J. (2013) Oral mucosal immunity. Oral Surg. Oral Med. Oral Pathol. Oral Radiol. 116: 576 - 583.

Ferraris M.E.G., Munõz A.C. (2006) Histologia e Embriologia Bucodental: Bases Estruturais da Patologia, diagnóstico, tratamento e prevenção odontológica, 2°edição. Rio de Janeiro: Guanabara Koogan.

Ferreira J.N., Hoffman M.P. (2013) Interactions between developing nerves and salivary glands. Organogenesis 9: 199-205.

Garatea-Crelgo J., Gay-Escoda C., Bermejo B., Buenechea-Imaz R. (1993) Morphological study of the parotid lymph nodes. J. Craniomaxillofac. Surg. 21: 207-9.

Gardner T.S., Bernardo D.D., Lorenz D., Collins J.J. (2003) Inferring genetic networks and identifying compound mode of action via expression profiling. Science 301: 102-105.

Gresik E.W., Koyama N., Hayashi T., Kashimata M. (2009) Branching morphogenesis in the fetal mouse submandibular gland is codependent on growth factors and extracellular matrix. J. Med. Invest. 56: 228-233.

Hardy G., Kramer B. (1998) The myoepithelium of human major salivary glands revisited. SADJ 53:371–375.

Hisatomi Y., Okumura K., Nakamura K., Matsumoto S., Satoh A., Nagano K., Yamamoto T., Endo F. (2004). Flow cytometric isolation of endodermal progenitors from mouse salivary gland differentiate into hepatic and pancreatic lineages. Hepatology 39: 667–675.

Holmberg K.V., Hoffman M.P. (2014). Anatomy, biogenesis and regeneration of salivary glands. Monogr Oral Sci. 24: 1-13.

Ianez R.F., Buim M.E., Coutinho-Camillo C.M., Schultz R., Soares F.A.,.Lourenc¸o S.V. (2010) Human salivary gland morphogenesis: Myoe-pithelial cell maturation assessed by immunohistochemicalmarkers. Histopathology 57: 410-417.

Ishizuka K., Oskutyte D., Satoh Y., Murakami T. (2010) Multi-source inputs converge on the superior salivatory nucleus neurons in anaesthetized rats. Auton. Neurosci. 156: 104–110.

Jaskoll T., Melnick M. (1999) Submandibular gland morphogenesis: Stage-specific expression of TGF-alpha, EGF, IGF, TGF-beta, TNF and IL-6 signal transduction in normal mice and the phenotypic effects of TGF-beta2, TGF-beta3, and EGF-R null mutations. Anat. Rec. 256: 252-268.

Jaskoll T., Witcher D., Toreno L., Bringas P., Moon A.M., Melnick M. (2004) FGF8 dose-dependent regulation of embryonic submandibular salivary gland morphogenesis. Dev. Biol. 268: 457-469.

Jaskoll T., Zhou Y.M., Chai Y., Makarenkova H.P., Collinson J.M., West J.D., Hajihosseini M.K., Lee J., Melnick M. (2002) Embryonic submandibular gland morphogenesis: Stage-specific protein localization of FGFs, BMPs, Pax 6 and Pax 9 and abnormal SMG phenotypes in Fgf/ R2-IIIc+/Δ, BMP7-/- and Pax6-/- mice. Cells Tiss. Org. 270: 83-98.

Jaskoll T., Zhou Y.M., Trump G., Melnick M. (2003) Ectodysplasin receptor-mediated signaling is essential for embryonic submandibular salivary gland development. Anat. Rec. A Discov Mol. Cell Evol. Biol. 271:322-31.

Johns M.E. (1977) The salivary glands: anatomy and embryology. Otolaryngol. Clin. North Am. 10: 261-71.

Kahle W., Frotscher M. (2003) Color atlas of human anatomy - nervous system and sensory organs. 1. Stuttgart-New York: Thieme Publisher. 1-484.

Kashimata M., Gresik E.W. (1997) Epidermal growth factor system is a physiological regulator of development of the mouse fetal submandibular gland and regulates expression of the alpha6- integrin subunit. Dev. Dyn. 208: 149-161.

Kere J., Srivastava A.K., Montonen O., Zonana J., Thomas N., Ferguson B., Munoz F., Morgan D., Clarke A., Baybayan P., Chen E.Y., Ezer S., Saarialho-Kere U., de la Chapelle A., Schlessinger D. (1996). X-linked anhidrotic (hypohidrotic) ectodermal dysplasia is caused by mutation in a novel transmembrane protein. Nat. Genet. 13: 409-416.

Kessler A.T., Bhatt A.A. (2018) Review of the Major and Minor Salivary Glands, Part 1: Anatomy, Infectious, and Inflammatory Processes. J. Clin. Imaging Sci. 8: 47.

Knosp W.M., Knox S.M., Lombaert I.M., Haddox C.L., Patel V.N., Hoffman M.P. (2015) Submandibular parasympathetic gangliogenesis requires sprouty-dependent wnt signals from epithelial progenitors. Dev. Cell. 32: 667-677.

Ligtenberg A.J., Brand H.S., van den Keijbus P.A., Veerman E.C. (2015) The effect of physical exercise on salivary secretion of MUC5B, amylase and lysozyme. Arch. Oral Biol. 60: 1639-1644.

Ligtenberg A.J.M., Veerman E.C.I. (eds) (2014) Saliva: Secretion and Functions. Monogr. Oral Sci. Basel, Karger, 24: 1-13.

Melnick M., Chen H., Min Zhou Y., Jaskoll T. (2001a) The functional genomic response of developing embryonic submandibular glands to NF-kappa B inhibition. BMC Dev. Biol. 1:15.

Melnick M., Chen H., Zhou Y., Jaskoll T. (2001b) An alternatively spliced Muc10 glycoprotein ligand for putative L-selectin binding during mouse embryonic submandibular gland morphogenesis. Arch. Oral Biol. 46: 745-747.

Melnick M., Chen H., Zhou Y., Jaskoll T. (2001c) Embryonic mouse submandibular salivary gland morphogenesis and the TNF/TNF-R1 signal transduction pathway. Anat. Rec. 262: 318-330.

Melnick M., Chen H., Zhou Y., Jaskoll T. (2001d) Interleukin-6 signaling and embryonic mouse submandibular salivary gland morphogenesis. Cells Tiss. Org.168: 233-245.

Melnick M., Jaskoll T. (2000) Mouse submandibular gland morphogenesis: a paradigm for embryonic signal processing. Crit. Rev. Oral Biol. Med. 11: 199-215.

Melnick M., Phair R.D., Lapidot S.A., Jaskoll T. (2009) Salivary gland branching morphogenesis: a quantitative systems analysis of the Eda/Edar/NFkappaB paradigm. BMC Dev. Biol. 9: 32.

Mikkola M.L. (2008) TNF superfamily in skin appendage development. Cytokine Growth Factor Rev. 19: 219-230.

Monreal A.W., Zonana J., Ferguson B. (1998) Identification of a new splice form of the EDA1 gene permits detection of nearly all X-linked hypohidrotic ectodermal dysplasia mutations. Am. J. Hum. Genet.63: 380–389.

Munger B.L. (1964) Histochemical studies on seromucous- andmucous-secreting cells of human salivary glands. Am. J. Anat. 115: 411-429.

Nanci A. (2013). Ten Cate's Oral Histology: Development, Structure, and Function (8th ed.). St. Louis, Mo.: Elsevier Publisher.

Ogawa Y. (2003) Immunocytochemistry of myoepithelial cells in the salivary glands. Prog. Histochem. Cytochem. 38: 343-426.

Ohuchi H, Hori Y, Yamasaki M., Harada H., Sekine K., Kato S., Itoh N. (2000) FGF10 acts as a major ligand for FGF receptor 2 IIIb in mouse multi-organ development. Biochem. Biophys. Res. Commun. 277: 643–649.

Ornitz D.M., Itoh N. (2001) Fibroblast growth factors. Genome Biol 2: REVIEWS 3005

Patel V.N., Hoffman M.P. (2014) Salivary gland development: a template for regeneration. Semin. Cell Dev. Biol. 25-26: 52-60.

Patel V.N., Rebustini I.T., Hoffman M.P. (2006) Salivary gland branching morphogenesis. Differentiation 74: 349-364.

Proctor G.B., Carpenter G.H. (2007) Regulation of salivary gland function by autonomic nerves. Auton. Neurosci. 133: 3-18.

Redman R.S. (1994) Myoepithelium of salivary glands. Microsc. Res. Tech. 27: 25-45.

Rothova M., Thompson H., Lickert H., Tucker A.S. (2012) Lineage tracing of the endoderm during oral development. Dev. Dyn. 241: 1183–1191.

Shah A.A., Mulla A.F., Mayank M. (2016) Pathophysiology of myoepithelial cells in salivary glands. J. Oral Maxillo fac. Pathol. 20: 480–490.

Shams I., Rohmann E., Eswarakumar V.P., Lew E.D., Yuzawa S., Wollnik B., Schlessinger J., Lax I. (2007) Lacrimoauriculo-dento-digital syndrome is caused by reduced activity of the fibroblast growth factor 10 (FGF10)-FGF receptor 2 signaling pathway. Mol. Cell. Biol. 27:.6903–6912

Simian M., Hirai Y., Navre M., Werb Z., Lochter A., Bissell M.J. (2001) The interplay of matrix metalloproteinases, morphogens and growth factors is necessary for branching of mammary epithelial cells. Development 128: 3117-3131.

Sisto M., Lorusso L., Ingravallo G., Tamma R., Nico B., Ribatti D., Ruggieri S., Lisi S. (2018) Reduced myofilament component in primary Sjögren's syndrome salivary gland myoepithelial cells. J. Mol. Histol. 49: 111-121.

Som P.M., Brandwin-Gensler M.S. (2011) Anatomy and pathology of the salivary glands. In: Som PM, Curtin HD, editors. Head and Neck Imaging. 5th ed. St. Louis: Mosby p. 2449-602.

Srivastava A.K., Pispa J., Hartung A.J., Du Y., Ezer S., Jenks T., Shimada T., Pekkanen M., Mikkola M.L., Ko M.S., Thesleff I., Kere J., Schlessinger D. (1997) The Tabby phenotype is caused by mutation in a mouse homologue of the EDA gene that reveals novel mouse and human exons and encodes a protein (ectodysplasin-A) with collagenous domains. Proc. Natl. Acad. Sci. USA 94: 13069-13074.

Steinberg Z., Myers C., Heim V.M., Lathrop C.A., Rebustini I.T., Stewart J.S., Larsen M., Hoffman M.P. (2005) FGFR2b signaling regulates ex vivo submandibular gland epithelial cell proliferation and branching morphogenesis. Development 132:.1223-1234.

Tandler B., Phillips C.J. (1998) Microstructure of salivary glands andits relationship to diet. In: Garrett JR, Ekstr€om J, Anderson LC,.editors. Glandular mechanisms of salivary secretion, Vol. 1. Basel:Karger. p 21–35.

Ten Cate A.R. (1998) Oral histology: Development, structure, and function. 5. St. Louis: Mosby

Thesleff I., Mikkola M.L. (2002) Death receptor signaling giving life to ectodermal organs. Sci STKE. pe22.

Tosios K.I., Nikolakis M., Prigkos A.C., Diamanti S., Sklavounou A. (2010) Nerve cell bodies and small ganglia in the connective tissue stroma of human submandibular glands. Neuroscience Letters 475: 53-55.

Tucker A.S. (2007) Salivary gland development. Semin. Cell. Dev. Biol. 18: 237-244.

Research Article - Basic and Applied Anatomy

Position of mandibular foramen and its clinical implications

Abebe Muche[1,*], Arthur Saniotis[2,3,4]

[1] Department of Human Anatomy, School of Medicine, College of Medicine and Health Sciences, University of Gondar, Gondar, Ethiopia
[2] College of Medicine, Hawler Medical University. Erbil, Iraq
[3] Biological and Comparative Anatomy Research Unit. Adelaide Medical School, University of Adelaide, Adelaide, SA 5005
[4] Institute of Evolutionary Medicine, University of Zürich, Zürich, Switzerland

Abstract

Mandibular foramen is an irregular foramen located above the center on the medial surface of the ramus, containing the inferior alveolar nerve. This study aimed at determining the position of the mandibular foramen in adult Ethiopian populations. A cross-sectional study was conducted at the Department of Human Anatomy, College of Medicine and Health Sciences, University of Gondar, Ethiopia, on 130 human dry adult human mandibles of unknown gender and age. The position of right and left mandibular foramina was determined in reference to the distance of different landmarks with the help of sliding digital vernier caliper. The data were analyzed using SPSS version-20. The data were compared using Student's t-test. $P<0.05$ was considered as statistically significant. The average distance of mandibular foramen from the anterior border of mandibular ramus was 23.81 ± 0.332 mm (right side) and 24.73 ± 0.456 mm (left side); from the posterior border of the ramus was 16.99 ± 0.273 mm (right side) and 16.23 ± 0.252 mm (left side), $P<0.05$. The mandibular foramen was located 20.19 ± 0.379 mm and 19.32 ± 0.346 mm away from the gonion of right and left sides, respectively. Furthermore, on average the mandibular foramen was away from the mandibular notch at a distance of 21.82 ± 0.356 mm (right side) and 21.65 ± 0.329 mm (left side). Conclusion: Anatomical knowledge of the average distance of mandibular foramen from various anatomical landmarks is useful for surgeons to safeguard from neurovascular complication.

Introduction

Mandibular foramen (MF) is an irregular foramen located above the center on the medial surface of the ramus. The mandibular canal descends into the body of the mandible and opens into the mental foramen. It contains the inferior alveolar branch of the mandibular division of the trigeminal nerve, which in turn emerges as the mental nerve supplying the mandibular teeth (Beale and Robinson, 2008).

The position of the MF is an important anatomical landmark for effective anesthesia in the field of dentistry procedures that include dental extraction from the lower jaw and placing mandibular implants. The uncertainty in the location of the MF has

* Corresponding author. E-mail: abemuche@yahoo.com

---

been claimed to be the main factor for the high failure rate of anesthesia and complications of orthodontic procedures (Sandhya et al., 2015).

Usually, dentists implement inferior alveolar nerve blocking techniques; however, failure of anesthesia presumably happens due to variation in the position of the MF, as well as to the presence of an accessory mandibular foramen (Cvetko, 2014). Additionally, the absence of a specific anatomic bony landmark, as well as variation in width and height of the mandibular ramus may play an important role in the failure of anesthesia. The failure rate was estimated between 20-25% (Kanan et al., 2013). Thus, clear and precise information on the variations in the position of MF are important for an effective and a successful anesthesia during nerve block prior to the surgical intervention (Kanan et al., 2013).

Several studies have reported differences in the anatomy of the mandible among different ethnic groups throughout the globe. However, to the best of our knowledge, no study was conducted in Ethiopia. Hence, in the present study, an attempt was made to determine the position of the MF in adult dried Ethiopian mandibles with respect to the surgically encountered anatomical landmarks. Therefore, this study may provide necessary information to dentists and maxillofacial surgeons in Ethiopia.

Material and methods

A cross-sectional study was conducted at the Department of Human Anatomy, College of Medicine and Health Sciences, University of Gondar, Ethiopia, from the 1st to the 20th of October 2016, to investigate the position of MF.

A total of 130 dry adult human mandibles collected in the Department of Human Anatomy for the purpose of teaching were used for the present study. The gender and exact age of each mandible was unknown. Mandibles which had sockets for third molars were selected; mandibles with gross pathological deformities were excluded from the present study.

As it is presented in Figure 1, the position of MF was determined using the distances of the mandibular foramen to the (a) base of mandible (MF-MB), (b) mandibular notch (MF-MN), (c) anterior border of the ramus (MF-AB) (d) posterior border of the ramus (MF- PB), (e) head of the mandible (MF- MH), (f) posterior edge of third molar socket (MF- TMS), (g) gonion (MF-G) and (h) midpoint on symphysis menti (MF- SM), which were measured on both sides with the help of a sliding vernier caliper. In order to maximize the accuracy of the results, the distances from the MF of various reference points were calculated as a mean of three measurements recorded independently by three data collectors. Measurements were recorded in millimeter (mm). A comparison of the mean values between the sides was performed using the t-test for independent samples and p-value < 0.05 was considered as statistically significant.

Results

In our study, 130 mandible bones were used. The position of MF was evaluated on the basis of various reference points, including the mandibular notch and symphysis
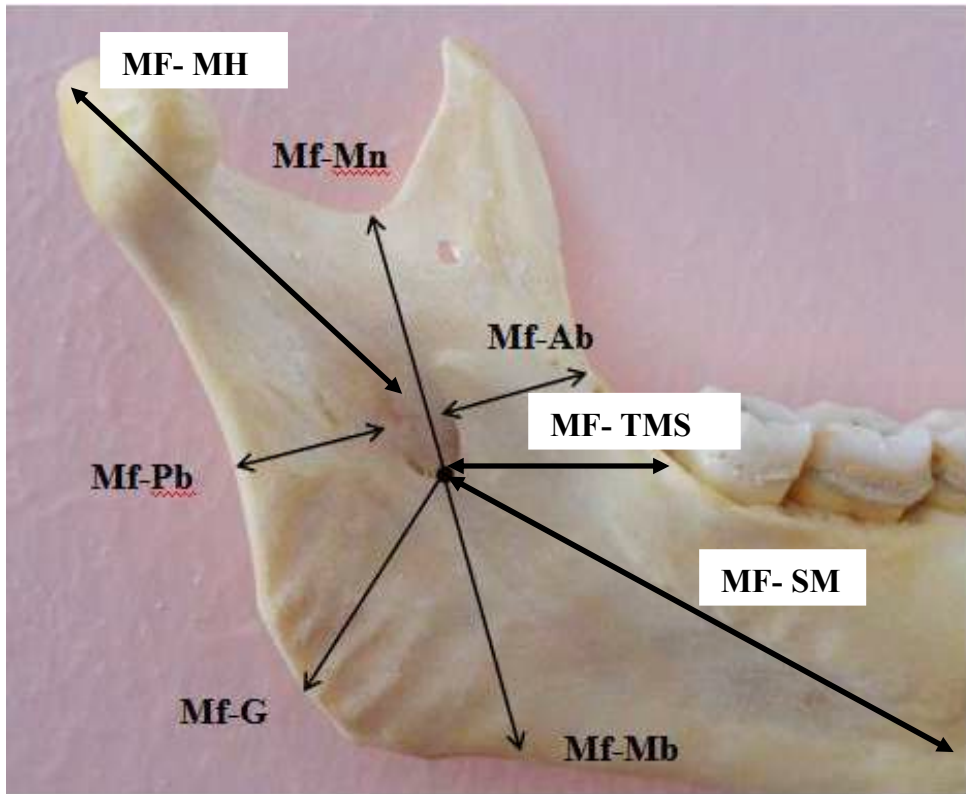
Figure 1. Representative example of the medial surface of mandible used to locate the position of mandibular foramen in relation to different reference points including mandibular notch. MF, Mf: mandibular foramen; MH: mandible head; Pb: posterior border of ramus; G: gonion; Mb: mandible base; SM: mid-point of symphysis menti; TMS: posterior edge of third molar socket; Ab: anterior border of ramus.

menti situated on the medial surface of the mandible. The mean distance for each reference point measurement of the right and left mandible is presented in Table 1.

The MF was located at an average distance of 29.98 ± 0.532 mm (right side) and 29.52 ± 0.554 mm (left side) from the base of the mandible, without significant difference (Table 1 and Figure 2a, b).

The MF was situated at an average distance of 21.82 ± 0.356 mm and 21.65 ± 0.329 mm away from the mandibular notch of right and left sides, respectively. The difference was not significant (Table 1 and Figure 3a, b).

Related to the anterior border of ramus of mandible, the MF was located on average at a distance of 23.81 ± 0.332 mm on the right side and 24.73 ± 0.456 mm on the left side (Table 1 and Figure 4a, b). The difference was not statistically significant.

The mean distance of MF from the posterior border of the ramus of the mandible was 16.99 ± 0.273 mm and 16.23 ± 0.252 mm on the right and left sides, respectively; the difference was significant ($p<0.05$; Table 1 and Figure 5a, b).

Table 1. Reference points used to indicate the mandibular foramen on the medial surface of mandible.

Reference points	Sides	N	Mean distance (mm)	Standard error of the mean	P (2-tailed)	95% CI
MF-MB	Right	130	29.98	0.532	not significant	(-1.058, 1.965)
	Left	130	29.52	0.554		
MF-MN	Right	130	21.82	0.356	not significant	(-0.793, 1.116)
	Left	130	21.65	0.329		
MF-AB	Right	130	23.81	0.332	not significant	(-2.035, 0.189)
	Left	130	24.73	0.456		
MF-PB	Right	130	16.99	0.273	<0.05	(0.029, 1.494)
	Left	130	16.23	0.252		
MF-MH	Right	130	39.35	0.475	not significant	(-0.607, 1.946)
	Left	130	38.68	0.441		
MF-TMS	Right	130	25.72	0.470	not significant	(-0.949, 1.765)
	Left	130	25.31	0.504		
MF-G	Right	130	20.19	0.379	not significant	(-0.141, 1.880)
	Left	130	19.32	0.346		
MF-SM	Right	130	74.09	0.706	not significant	(-2.120, 1.720)
	Left	130	73.29	0.673		

MF-MB: mandibular foramen to base of mandible; **MF-MN**: mandibular foramen to mandibular notch; **MF-AB**: mandibular foramen to anterior border of ramus; **MF-PB**: mandibular foramen to posterior border of ramus; **MF-MH**: mandibular foramen to the head of the mandible; **MF-TMS**: mandibular foramen to the posterior edge of third molar socket; **MF-G**: mandibular foramen to the gonion; **MF-SM**: mandibular foramen to the mid-point on symphysis menti.
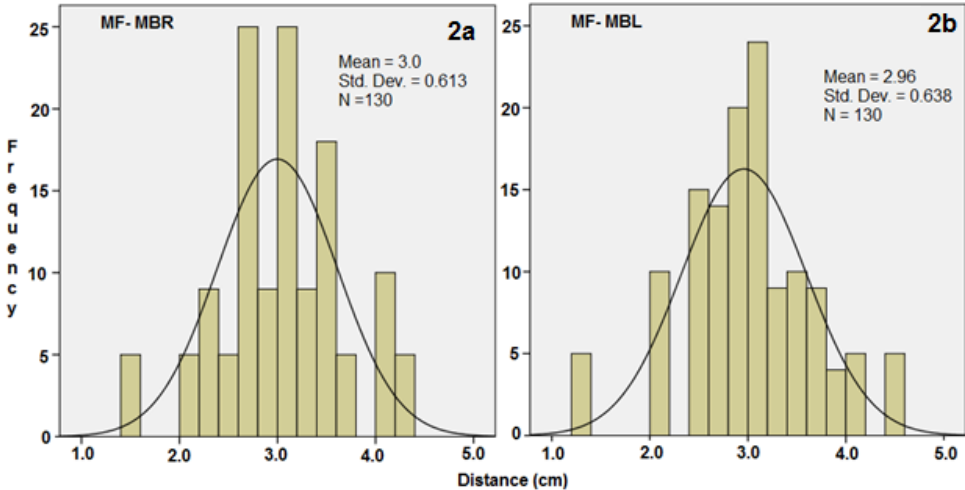

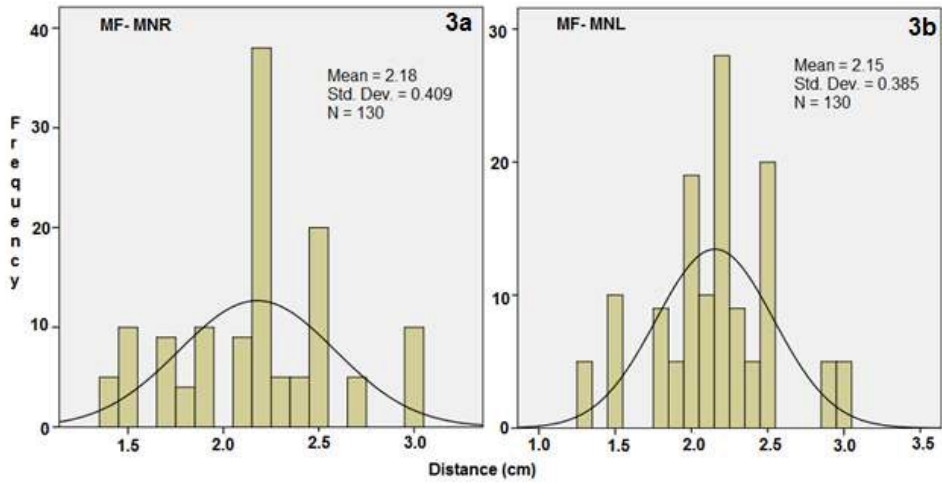**Figure 2.** Distance of mandibular foramen from base of mandible; a) right side; b) left side.

Figure 3. Distance of mandibular foramen from mandibular notch; a) the right side; b) left side.
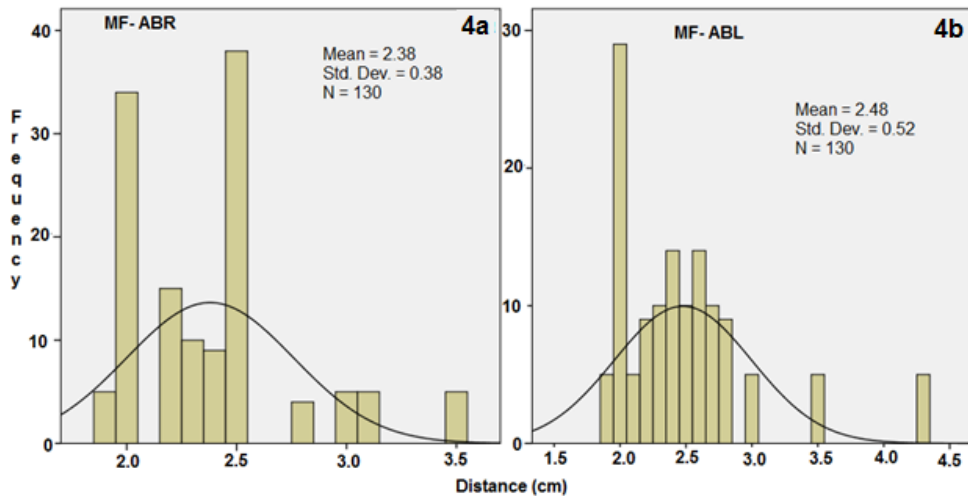

Figure 4. Distance of mandibular foramen from anterior border of ramus; a) right side; b) left side.

The MF was positioned from the mandibular head at an average distance of 39.35 ± 0.475 mm on the right side and 38.68 ± 0.441 mm on the left side (Table 1 and Figure 6a, b). The difference was not significant.

In our study, the distance from the posterior edge of the third molar socket to the MF was also taken as a reference point. The mean distance measurement was 25.72 ± 0.470 mm and 25.31 ± 0.504 mm on the right and left sides, respectively (Table 1 and Figure 7a, b). The difference was not significant.
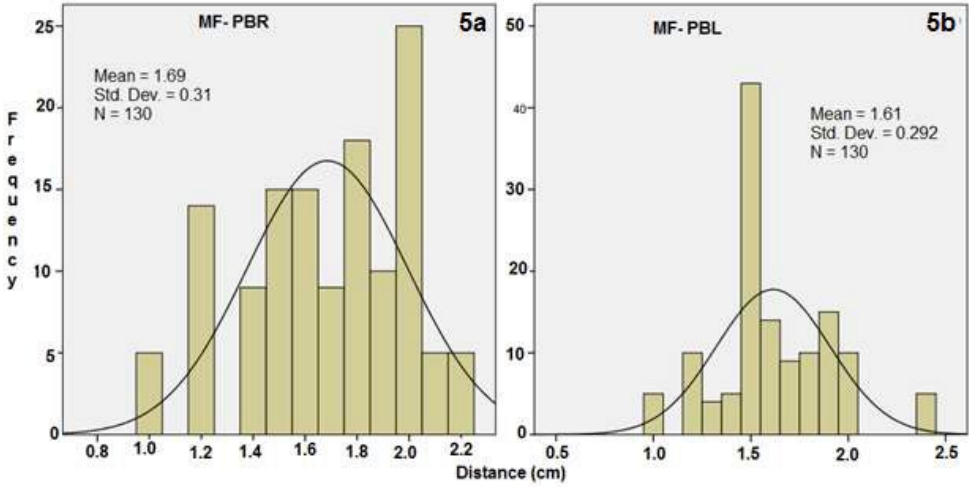
Figure 5. Distance of mandibular foramen from posterior border of ramus; a) right side; b) left side.
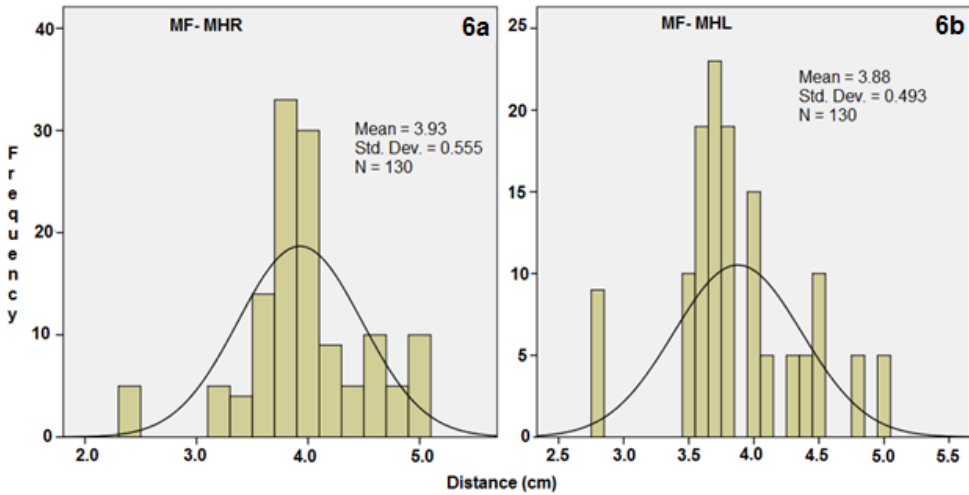

Figure 6. Measured distance of mandibular foramen from mandibular head; a) right side; b) left side.

The mean and distribution of the distance of the MF from the gonion is presented in Table 1 and Figure 8a, b. The mean distance of MF from the right and left sides of the gonion, respectively was 20.19 ± 0.379 mm and 19.32 ± 0.346 mm; the difference was not significant.

The MF was positioned at an average distance from the symphysis menti of 74.09 ± 0.706 mm and 74.29 ± 0.673 mm on the right side and left side, respectively (Table 1 and Figure 9a, b); the difference was not significant.
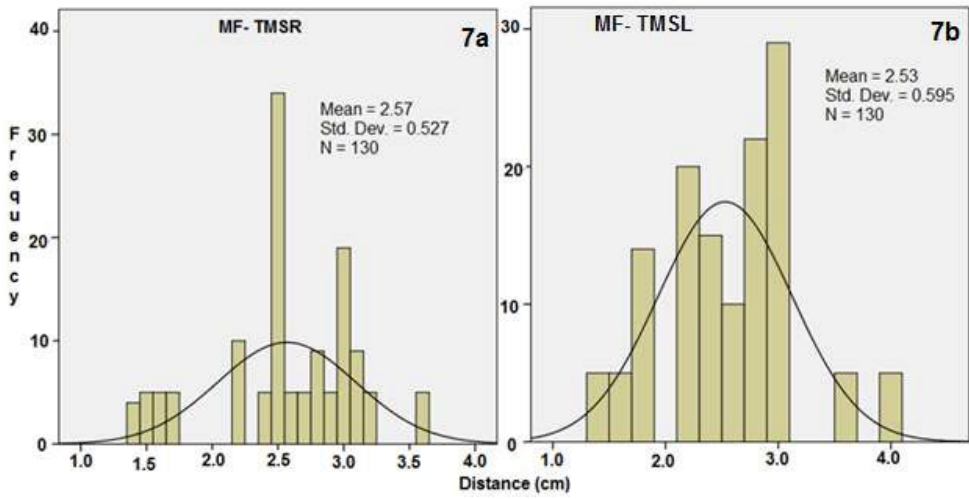
Figure 7. Distance of mandibular foramen from posterior edge of third molar socket; a) right side; b) left side.

Figure 8. Distance of the mandibular foramen from gonion; a) right side; left side.

Discussion

Various anatomists have attempted to instigate morphometric methods to ascertain the location of the MF as a landmark for applying inferior alveolar nerve anesthesia. Unfortunately, locating the MF is difficult since there is no specific bony mandibular landmark for its position (Khan and Ansari, 2016). These authors have also
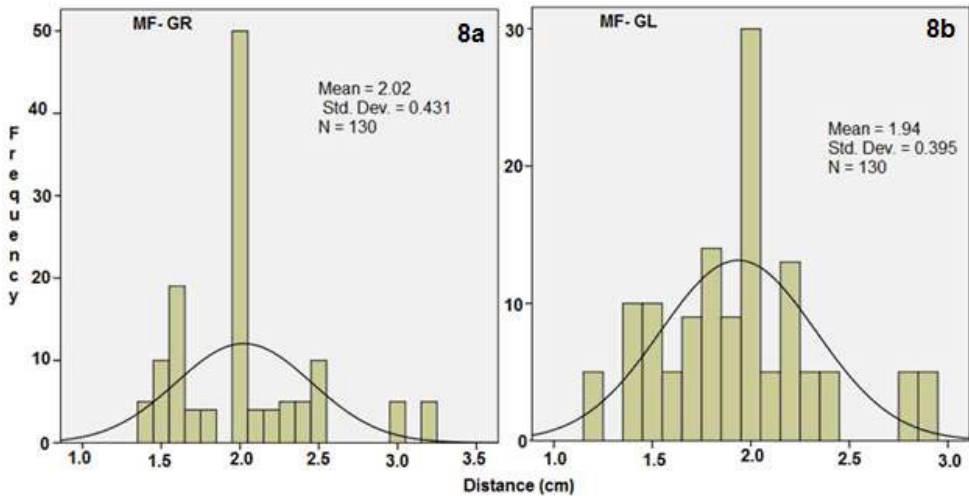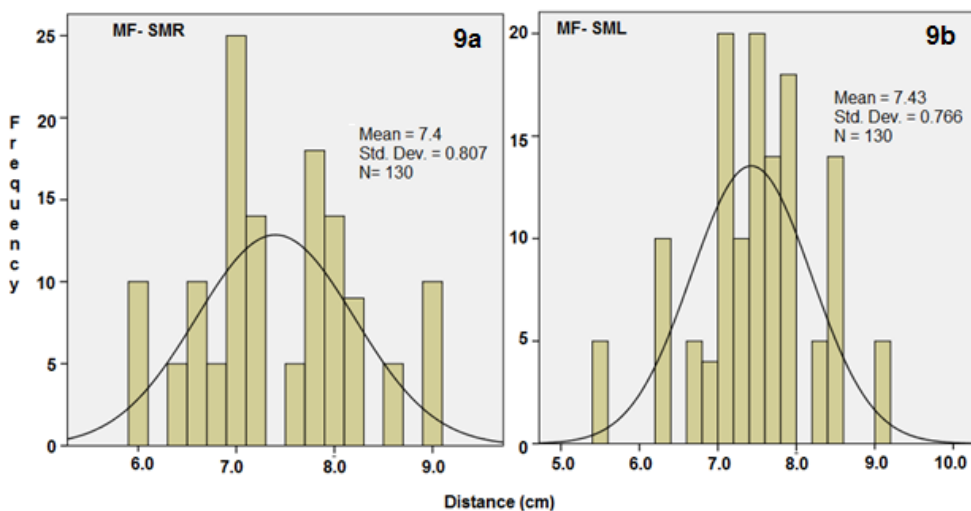
Figure 9. Measured distance of mandibular foramen from symphysis menti; a) right side; b) left side.

revealed that the absence of reliable bony landmarks as well as anatomical variation and age related mandibular changes may cause the high failure rate of anesthesia. Consequently, this has led to the development of various methods for locating the MF, which have yet to be proven to achieve a high success rate. Operator caused error when attempting to perform inferior alveolar nerve anesthesia should also be viewed as an additional cause of failure.

While there has been considerable research on the MF in various ethnic groups, there have been few morphometric studies on the MF in African groups. A recent Tanzanian study assessed 44 cadaveric mandibles of adult black male Tanzanians (30-45 years) found bilateral concurrence of the MF superior to the occlusal plane of the first molar and second premolars in all the mandibles. The study also claimed that the inferior alveolar nerve block can be successfully accomplished by locating the MF at 10.4 mm and 13.9 mm superior to the occlusal plane of the first molar or second premolar, and 20 mm from the anterior border of the ramus (Russa and Fabian, 2014)

In contrast, another African study on 38 dry mandibles from adult black Zimbabweans revealed significant differences in the location of the MF. The average MF was 20.8 mm (left) and 25.6 mm (right) posterior to the midpoint of the ramus width bilaterally (Mbajiorgu, 2000).

A study done on 79 mandibles of adult Kenyan Bantus indicated that 64.6% MF were located inferior to the posterior extension of the occlusal plane, while 30.7% were located alongside of the occlusal plane. Additionally, 56.1% MF were located inferior to the second premolar while 31.1% were found between the first molar and the second premolar. Moreover, the opening of the MF was posterosuperior in 72.5% of the mandibular surfaces. The study also found 4.5% of mandibular samples with multiple MF (Mwaniki and Hassanali, 1992). In the present study various morpho-

metric measurements were not significantly different between sides. Thus, it is proposed that failure to locate the MF for inferior alveolar nerve anesthesia is probably due to human inability to find the nerve and not due to anatomical variation. At this time, there is a lack of consensus on how to evaluate the correct position of MF (Barker and Davies, 1972; Hayward et al., 1977; Hetson et al., 1988; Murphy and Grundy, 1969; Nicholson, 1985) and despite the abundance of these ways there is still a considerable failure rate. Various authors have estimated inferior alveolar nerve anesthesia failure rates between 20% and 25% (Qudusia et al., 2016), and 29% and 35% of the patients (Levy, 1981; Robertson, 1979).

Other authors have reported that human error in inferior alveolar nerve anesthesia is a likely cause for incorrect needle placement (Qudusia et al., 2016). At present, the principal landmarks used for needle insertion for inferior alveolar nerve anesthesia are between the pterygomandibular raphe and the coronoid notch, superior to the occlusal plane of the lower teeth (Khalil, 2014). There are eight alternative methods to access the inferior alveolar nerve; however, the success rate of these methods has not received rigorous evaluation (Khalil, 2014).

In summary, the position of MF is crucial for correct performance of inferior alveolar nerve anesthesia. During the surgical procedure, the failure of the anesthesia is probably due more to operator error than to anatomical variation.

In conclusion, in the present study the MF was found situated at the same distance from the anatomical landmarks on the right and left sides, thus indicating bilateral symmetry. Our findings may be useful for maxillofacial surgeons and radiologists during surgical procedures and X-ray film interpretations.

Acknowledgements

References

Barker B.C., Davies P.L. (1972) The applied anatomy of the pterygomandibular space. Br. J. Oral Surg. 10: 43-55.

Beale T.J., Robinson P.D. (2008) Infratemporal and pterygopalatine fossae and temporomandibular joint, in: S. Standring (Ed.), Gray's Anatomy: The Anatomical Basis of Clinical Practice, Elsevier Churchill Livingstone. Pp. 530-533.

Cvetko E. (2014) Bilateral anomalous high position of the mandibular foramen: a case report. Surg. Radiol. Anat. 36: 613-616.

Hayward J., Richardson E.R., Malhotra S.K. (1977) The mandibular foramen: its anteroposterior position. Oral Surg. Oral Med. Oral Pathol. 44: 837-843.

Hetson G., Share J., Fommer J., Kronman J.H. (1988) Statistical evaluation of the position of the mandibular foramen. Oral Surg. Oral Med. Oral Pathol. 65: 32-34.

Kanan S., Pratik S., Ajay P. (2013) Study of the location of the mandibular foramina in Indian dry mandibles. Global J. Res. Anal. (GJRA) 2: 128-130.

Khalil H. (2014) A basic review on the inferior alveolar nerve block techniques. Anesth. Essays Res. 8: 3-8.

Khan I.A., Ansari M.A. (2016) An anatomical study and clinical correlations of mandibular foramen in dry adult human mandibles of north Indian origin. Ann. Intern. Med. Dent. Res. (AIMDR) 2: 161-164.

Levy T.B. (1981) An assessment of the Gow-Gates mandibular block for third molar surgery. J. Am. Dent. Assoc. 103: 37-41.

Mbajiorgu E.F. (2000) A study of the position of the mandibular foramen in adult black Zimbabwean mandibles. Centr. Afr. J. Med. 46: 184-190.

Murphy T.R., Grundy E.M. (1969) The inferior alveolar neurovascular bundle at the mandibular foramen. Dent. Pract. Dent. Rec. 20: 41-48.

Mwaniki D.L., Hassanali J. (1992) The position of mandibular and mental foramina in Kenyan African mandibles. East Afr. Med. J. 69:2 10-213

Nicholson M.L. (1985) A study of the position of the mandibular foramen in the adult human mandible. Anat. Rec. 212: 110-112.

Qudusia S., Shariff M.H., Ramakrishna A. (2016) Study of surgical landmarks of mandibular foramen for inferior alveolar nerve block: An osteological study. Indian J. Clin. Anat. Physiol. 3: 37-40.

Robertson W.D. (1979) Clinical evaluation of mandibular conduction anesthesia. Gen. Dent. 27: 49-51.

Russa A.D., Fabian F.M. (2014) Position of the mandibular foramen in adult male Tanzania mandibles. Ital. J. Anat. Embryol. 119: 163-168.

Sandhya K., Singh B., Lugun N., Prasad R. (2015) Localization of mandibular foramen relative to landmarks in East Indian mandibles. Indian J. Dent. Res. 26: 571-575.

Research Article - History of Anatomy and Embryology

Erasistratus of Chios: a pioneer of human anatomy and physiology

Theodoros Mariolis-Sapsakos[1], Maria Zarokosta[1,*], Menelaos Zoulamoglou[1], Theodoros Piperos[1], Euthumios Nikou[1], Anastasios Katsourakis[2], George Noussios[2]

[1] Anatomy and Histology Laboratory, Nursing School, University of Athens, Greece
[2] Department of Anatomy, School of Physical Education and Sport Sciences, Serres, Aristotles University of Thessaloniki, Greece

Abstract

Erasistratus of Chios (310-250 BC) was one of the great Greek physicians of antiquity. Historical investigation reveals that he was an innovative anatomist, neuroanatomist and a pioneer of human physiology. His accurate discoveries formed the basis of positive sciences and ameliorated medicine.

Introduction

Erasistratus of Chios (310-250 BC) was one of the great Greek scientists whose prominent discoveries concerning the human body composed the basis of positive sciences and medicine (Wiltse and Pait, 1998; Acar et al., 2005). Indeed, Erasistratus in addition to Herophilus of Chalcedon (335-280 BC) were pioneers of scientific anatomy, since deploying for the first time the method of human body dissection (Dobson, 1927; Bay and Bay, 2010). Hence, it is quite reasonable that Erasistratus is considered as a great anatomist and a master of experimental physiology (Acar et al., 2005). Unfortunately though, the studies of Erasistratus have been lost entirely and only a few details of his marvelous work may be recovered from the writings of Galen (Rocca, 1997, 2003). The present manuscript aims to underline the impact of ancient Greek heritage in current medicine and emphasizes to the remarkable discoveries of Erasistratus referring to human anatomy and physiology.

Background

Erasistratus was a Greek physician, born in the island of Chios (310-250 BC) that has been taught by Theophrastus (Mavrodi and Paraskevas, 2014). As well as Herophilus, who is considered as the "father" of scientific anatomy (Wiltse and Pait, 1998; Acar et al., 2005; Bay and Bay, 2010) Erasistratus belonged in the scientific Alexan-

drian mileu and worked at the Herophilean Medical School in Egypt during the Hellenistic period (Durant, 1934; Wiltse and Pait, 1998; Crivellato and Ribatti, 2007). Through this period, Ptolemies achieved to transform Alexandria to the intellectual and scientific center of the Western World (Persaud, 1984). In fact, it was Ptolemy I who permitted for the first time, in approximately 300 BC, the human body cadaveric dissection in medicine (Wiltse and Pait, 1998).

Both Herophilus and his younger contemporary Erasistratus dissected an abundance of human cadavers and subsequently provided astonishing descriptions of the brain, the nerves and the cardiovascular system in addition to descriptions of physiological mechanisms (Castiglioni, 1958; Wiltse and Pait, 1998; Crivellato and Ribatti, 2007). That was a great moment in medicine that actually formed the basis of scientific and clinical anatomy plus physiology (Wiltse and Pait, 1998) and almost eliminated the improbabilities into which Aristotle has fallen due to the religious "fear of the corpse" (Durant, 1934; Gordon, 1949).

This sole opportunity to dissect, although short-lived, accounts for marvelous advances in the knowledge of human anatomy and physiology (Potter, 1976; Wiltse and Pait, 1998).

Erasistratus' eminent contributions

a. Nervous System

Erasistratus in addition to Herophilus is also credited with one of the first detailful descriptions of the cerebrum and cerebellum (Wiltse and Pait, 1998). Erasistratus was the first to describe the nerves as anatomical structures originating from the substance of the human brain (Crivellato and Ribatti, 2007). He and Herophilus suggested that there are two kind of nerves: a) the sensory nerves (αἰσθητικά νεύρα) and the b) motor nerves (κινητικά νεύρα) and that the nerves "that make voluntary motion" originate from the cerebrum and the spinal marrow (Garofalo, 1988; Crivellato and Ribatti, 2007).

Furthermore, he emphasized to dura mater (παχεῖα μῆνινξ) (Galen, edited 1962), which he long considered as the command seat of cognitive, motor and sensory functions of the human (Crivellato and Ribatti, 2007; Bhogal et al.2015). As so, he used to claim that the cause of delirium was a disorder of the meninx activity and that lethargy arose from a malfunction of the psychic faculty in the meninx as well (Garofalo, 1997).

b. Cardiovascular System

Erasistratus was the first physician who recognized the heart's activity as a "pump" contracting perpetually, due to its "intrinsic force" (Bestetti et al., 2014). The heart's construction and activity may be compared with the ingenious mechanism known as the Ctesibius pump. That pump was invented by Ctesibius of Alexandria in approximately 250 BC. The pump consists of two identical cylinders, just like the two heart chambers, each with a piston, that converge in a chamber with valves that open and close alternately in order the water to pass through without interruption, just like the blood in the heart (Shapiro, 1964).

Another great innovation of Erasistratus, was the meticulous description of all four heart valves. In particular, he observed the presence of two and three cusps respectively in the bicuspid and tricuspid valve, in addition to the sigmoid shape of the valves of the pulmonary artery and the aorta (Mavrodi and Paraskevas, 2014).

Additionally, Erasistratus approached the anatomical description of blood movement, considering the heart as the common origin of both arteries and veins (French, 1978; Mavrodi and Paraskevas, 2014). Although Erasistratus recognized that arteries connected with the left ventricle and veins with the right one, he wrongly believed that arteries transported the pneuma, since they remained empty at dissection (Cockle, 1860) and consequently he could not observe the functional continuity between veins and arteries (Bestetti et al., 2014).

Nevertheless, regarding the vascular system he discovered the progressive subdivision of vessels till the point that, due to their minor diameter, it was no longer efficient to make the distinction between arteries and veins. (Androutsos et al. 2013) Erasistratus observed that such small vessels were always filled with blood and named them "synanastomoses". After a long period, they were denominated as "capillaries" (Dobson, 1928).

c. Other contributions

Erasistratus is the first physician that may be credited with abandoning the ancient humoral theory of Hippocratis. Unfortunately though, Galen returned to that ancient theory four centuries later (Wiltse and Pait, 1998).

Moreover, Erasistratus and Herophilus opposed to the theory of Aristotle who suggested that the human heart is the center of both intellect and emotions. In fact, Herophilus claimed that Aristotle's theory is an error (Peck, 1965) and in addition to Erasistratus attemped to prove that the brain is the center of consciousness (Wiltse and Pait, 1998). However, due to the great influence of Aristotle it has been extremely difficult to break utterly with the idea that the human heart is the command seat of emotions.

In collaboration with Herophilus, Erasistratus also improved on the understanding of respiration. In particular, he was the first who recognized an essential relation between the respiratory and vascular system (Von Staden, 1989. 1992). Finally, both of them improved our knowledge concerning the heart beat (Wiltse and Pait, 1998).

Conclusion

Conclusively, a meticulous historical investigation reveals that Erasistratus was an eminent, skilled anatomist, neuroanatomist (Wiltse and Pait, 1998; Crivellato and Ribatti, 2007) and an innovator in human physiology (Acar et al. 2005). Without his astonishing, accurate observations medical knowledge would not have progressed that rapidly.

References

Acar F., Naderi S., Guvencer M., Ture U., Arda M.N. (2005) Herophilus of Chalcedon: a pioneer in neuroscience. Neurosurgery 56: 861-867.

Androutsos G., Karamanou M., Stefanadis C. (2013) The contribution of Alexandrian physicians to cardiology. Hellenic J. Cardiol. 54: 15-17.

Bay Noel S.-Y., Bay B.-H. (2010) Greek anatomist Herophilus: the father of anatomy. Anat. Cell Biol. 43: 280-283.

Bestetti R.B., Restini C.B.A., Couto L.B. (2014) Development of anatamophysiologic knowledge regarding the cardiovascular system: From Egyptians to Harvey. Arq. Bras. Cardiol. 103: 538-545.

Bhogal P., Makalanda H.L., Brouwer P.A., Gontu V., Rodesch G., Mercier P., Söderman M. (2015) Normal pio-dural arterial connections. Interv. Neuroradiol. 21: 750-758.

Castiglioni A. (1958) A History of Medicine. Krumbhaar E.B., Ed. 2nd edn. New York, Alfred A. Knopf.

Cockle, J. (1860) Lectures on the historic literature of the pathology of the heart and great vessels. Br. Med. J. 1: 81-84.

Crivellato E., Ribatti D. (2007) Soul, mind, brain: Greek philosophy and the birth of neuroscience. Brain Res. Bull. 71: 327-336.

Dobson J.F. (1927) Erasistratus. Proc. R. Soc. Med. 20: 825-832.

Durant W. (1939) The Life of Greece. Vol 2. The Story of Civilization. New York, Simon and Schuster. Pp. 337-671.

French R.K. (1978) The thorax in history 2. Hellenistic experiment and human dissection. Thorax 33: 153-166.

Galen in: Duckworth W.L.H. (Transl.) (1962) Anatomical Procedures the Later Books. London, The Syndics of the Cambridge University Press.

Garofalo I. (1988) Erasistrati Fragmenta. Collegit et Digessit. Pisa: Giardini.

Garofalo I. (1997) Anonimi Medici. De morbis Acutis et Chronicis. Leiden, E.J. Brill.

Gordon G.L. (1949) Medicine throughout antiquity. Philadelphia, F.A. Davis Publishers. Pp. 589-608.

Mavrodi A., Paraskevas G. (2014) Morphology of the heart associated with its function as conceived by ancient Greeks. Int. J. Cardiol. 172: 23-28.

Peck A.L. (1965) Historia Animalium by Aristotle. Cambridge, Harvard University Press.

Persaud T. (1984) Early History of Human Anatomy. Springfield. C.C. Thomas. Pp. 44-49.

Potter P. (1976) Herophilus of Chalcedon: An assessment of his place in the history of anatomy. Bull. Hist. Med. 50: 45-60.

Rocca J. (1997) Galen and the ventricular system. J. Hist. Neurosci. 6: 227-239.

Rocca J. (2003) Galen on the brain. Anatomical knowledge and physiological speculation in the 2nd century AD. Stud. Anc. Med. 26: 1-313.

Shapiro S. (1964) The origin of the suction pump. Technology and Culture 5: 566-574.

Von Staden H. (1989) Herophilus: the Art of Medicine in Alexandria. 1st ed. Cambridge, Cambridge University Press. Pp. 1-666.

Von Staden H. (1992) The discovery of the body. Human dissection and its cultural contexts in Ancient Greece. Yale J. Biol. Med. 65: 223-241.

Wiltse L., Pait T.G. (1998) Herophilus of Alexandria (325-255 BC): The father of anatomy. Spine 23: 1904-1914.

Research Article - Human Anatomy Case Report

An accessory tendon of flexor digitorum superficialis to the fifth digit

Logan S. Bale[1,2, *], Sean O. Herrin[1]

[1] Department of Basic Sciences, University of Western States, Portland, Oregon, USA 97230
[2] Department of Biomedical and Molecular Sciences, Queen's University, Kingston, Ontario, Canada K7L 3N6

Abstract

Variations of the muscle belly and tendon of flexor digitorum superficialis to the fifth digit are common. We encountered an unusual variant during routine educational dissection; an accessory tendon of flexor digitorum superficialis that united with the tendon of flexor digitorum profundus to the fifth digit. This variant is not documented in the literature. Known variations of flexor digitorum superficialis to the fifth digit are discussed to allow for comparison with the variant identified in this report. The potential clinical significance of the variant is speculated upon.

Introduction

Flexor digitorum superficialis (FDS) is the sole muscle of the intermediate layer of the anterior forearm. It arises as two distinct heads (humeroulnar and radial), inserts via four tendons onto the middle phalanges of digits 2-5, is innervated by the median nerve, and is supplied blood by the ulnar artery. Variations associated with the muscle belly and tendon of flexor digitorum superficialis to the fifth digit (FDS-V) have been discussed at great length in dedicated reviews and in case reports. To our knowledge, a tendon of FDS that 1) is found in addition to the muscle's four typical tendons, and 2) unites with the tendon of flexor digitorum profundus to the fifth digit (FDP-V) has not been reported in the literature. This variant may be of clinical interest because of its possible role in compression of the median nerve or because it may be encountered unexpectedly during surgical procedures.

Case report

Bilateral variations of the FDS muscles were identified during routine educational dissection of a 77-year-old female cadaver. On each side, FDS featured an accessory tendon that arose from the muscle's humeroulnar head. The accessory tendon did not replace any of the typical tendons of FDS, thus each muscle featured five tendons instead of the usual four.

* Corresponding author. E-mail: bl46@queensu.ca

Figure 1. Left upper extremity (1: flexor digitorum profundus muscle, 2: accessory tendon of flexor digitorum superficialis, 3: flexor digitorum superficialis muscle).

On the left side, the accessory tendon of FDS was 18 cm long and 0.3 cm wide (Fig. 1). The most proximal portion of the tendon was located approximately 8 cm superior to the musculotendinous junction of the FDS muscle belly and the typical tendons of FDS. The accessory tendon was located between the muscle bellies of FDS and FDP. Upon entering the hand, the accessory tendon of FDS united with the tendon of FDP-V (Fig. 2). The point of union of the two tendons was approximately 1.5 cm proximal to the decussation of the tendon of FDS-V. The united FDP-V/accessory tendon of FDS coursed through the FDS bifurcation and inserted onto the base of the distal phalanx in the manner that is typical for the tendon of FDP-V.

On the right side, the accessory tendon of FDS measured 13.5 cm in length and 0.3 cm in width. It traveled between the intermediate and deep layers of the anterior forearm and was associated with a small slip of muscle from the humeroulnar head of FDS. The accessory tendon merged with the tendon of FDP-V at the level of the wrist (proximal compared to the point of union on the left side).

Discussion

While variants of FDS-V are common, to the best of our understanding the specific variant documented presently is not reported in the literature. Developmentally, this variant may represent abnormal splitting of the common premuscle mass that gives rise to elements of the intermediate and deep layers of the anterior forearm (Jones, 1966). A brief review of variants of FDS-V is provided for comparison to the present case.

Wood (1867) identified a separate muscle for the little finger which took origin from the medial condyle of the humerus. A connection between the tendons of FDS-V and FDP-V was reported by Macalister (1875), however that case did not involve a long accessory tendon as documented here. An accessory muscle, the flexor digiti minimi longus, was reported by Greiner (2008) and is somewhat similar to the abnor-
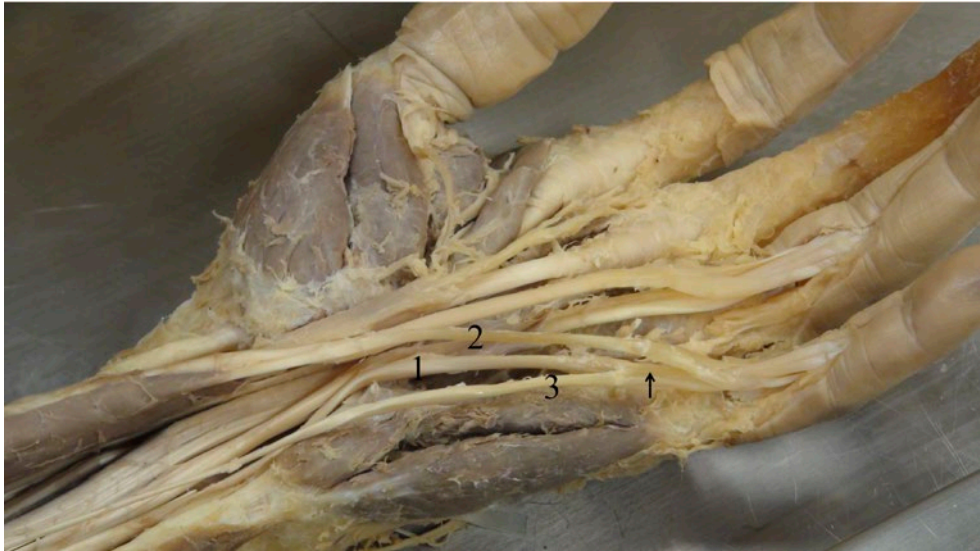
Figure 2. Left wrist and palm (1: FDP-V tendon, 2: FDS-V tendon, 3: accessory tendon of FDS, arrow: united FDP-V and accessory tendons).

mal musculotendinous slip identified in the present case report. As flexor digiti minimi longus featured an origin that was independent of flexor digitorum superficialis, we feel that the variant identified here is not an example of flexor digiti minimi longus. The FDS-V muscle belly may have a digastric appearance, whereby an accessory belly is located in the palm (Gonzalez et al., 1997). The tendon of FDS-V is often absent; the prevalence of this relatively common variation has been determined for a range of ethnicities (see Guler et al., 2013 for a comprehensive summary). If absent, FDS-V may be replaced by a belly that can arise from several locations, such as the medial collateral ligament of the ulna, the palmar aponeurosis, and the fourth lumbrical (Tubbs et al., 2016). There is no link between absence of FDS-V and absence of palmaris longus (Thompson et al., 2002).

Anomalous muscles can cause compression of the median and ulnar nerves (De Smet, 2002). Normal side to side movement of the median nerve has been shown to occur during flexion of the index finger or thumb (Van Doesburg et al., 2010). It is unknown how the actions of FDS and/or FDP would be affected by the accessory tendon described in this case report and whether altered biomechanics, if any, could lead to a peripheral neuropathy. The accessory tendon of FDS-V may cause issues during tendon transfer surgery or other operative procedures of the forearm, wrist, and hand.

Acknowledgements

References

De Smet L. (2002) Median and ulnar nerve compression at the wrist caused by anomalous muscles. Acta. Orthop. Belg. 68: 431-438.

Gonzalez M.H., Whittum J., Kogan M., Weinzweig N. (1997) Variations of the flexor digitorum superficialis tendon of the little finger. J. Hand Surg. Br. Eur. 22: 277-280.

Greiner T.M. (2008) An additional flexor of the fifth digit: Flexor digiti minimi longus. Clin. Anat. 21: 792-793.

Guler F., Kose O., Turan A., Baz A.B., Akalin S. (2013) The prevalence of functional absence of flexor digitorum superficialis to the little finger: A study in a Turkish population. J. Plast. Surg. Hand Surg. 47: 224-227.

Jones E.G. (1966) Some unusual muscular anomalies explained embryologically. Acta. Anat. (Basel) 64: 516-530.

Macalister A. (1875) Additional observations on muscular anamolies in the human anatomy (third series) with a catalouge of the principal muscular variations hitherto published. Trans. Roy. Irish Acad. 25: 1-130.

Thompson N.W., Mockford B.J., Rasheed T., Herbert K.J. (2002) Functional absence of flexor digitorum superficialis to the little finger and absence of palmaris longus – is there a link? J. Hand Surg. Am. 27: 433-434.

Tubbs R.S., Shoja M.M., Loukas M. (2016) Bergman's comprehensive encyclopedia of human anatomic variation. Wiley-Blackwell, Hoboken.

Van Doesburg M.H.M., Yoshii Y., Villarraga H.R., Henderson J., Cha S.S., An K.N., Amadio P.C. (2010) Median nerve deformation and displacement in the carpal tunnel during index finger and thumb motion. J. Orthop Res. 28: 1387-1390.

Wood J. (1867) On human muscular variations and their relation to comparative anatomy. J. Anat. Physiol. 1: 44-59.

Review - Histology and Cell Biology

Anatomy of the hippocampus and its emerging roles in modulating emotion-dependent autonomic activities

Itopa E. Ajayi

Department of Veterinary Anatomy, University of Abuja, Main campus, Nigeria, and School of Biomedical Sciences, The University of Queensland, St. Lucia campus, Queensland, Australia

Abstract

The hippocampus is popularly known to be involved in learning and memory. However, emerging evidence indicates that the hippocampus also mediates emotions in a process that involves modulating motor and autonomic outflow. The parts of the hippocampus involved in modulating autonomic activities are distinct and thus support the argument of inherent structural and functional segregation. It is suggested that the ability to modulate emotion-dependent autonomic rhythm results from descending synaptic interactions with nuclei in the hypothalamus and brainstem where the rhythm of motor and autonomic activities is generated and maintained. However, there is little knowledge of the anatomical pathways and circuit physiology that support the modulation of such autonomic activities. Also, in coordinating physiologic responses, forebrain structures operate through functional networks, but the neural pathways and mechanisms involved in such complex interactions are not clear. Thus, the current review aims at elucidating the anatomy of the hippocampus with emphasis on the intra and inter structural circuits responsible for modulating emotion-dependent autonomic activities.

Introduction

Emotional behaviours are processed, formed and expressed by a complex network of brain structures known as the limbic system, which relies upon sensory perception of the external environment. During the expression of emotions, autonomic responses are responsible for maintaining homeostasis and meeting metabolic demands. Early studies also suggested that autonomic activities can be used to distinguish between emotions (Ekman et al., 1983). However, there is limited understanding of the forebrain areas that modulate autonomic activities, and the mechanisms/neural pathways involved.

Studies have identified the hippocampus as a potential mediator in the processing of emotions (Kjelstrup et al., 2002; Maren and Holt, 2004; Ballesteros et al., 2014). More recent studies have examined certain autonomic concepts that are relevant to the expression of emotions and identified significant roles played by the ventral hippocampus (Ajayi and Mills, 2017; Ajayi et al., 2018). For instance, stimulation of the

* Corresponding author. E-mail: mailitopa@gmail.com, i.ajayi@uq.edu.au

ventral hippocampus completely suppressed the motor expression of augmented breaths (Ajayi and Mills, 2017). The same region of the ventral hippocampus was implicated in regulating the expression of fear and anxiety (Kjelstrup et al., 2002; Maren and Holt, 2004; Ballesteros et al., 2014). Juxtaposing these two findings suggests that during the emotional processing of fear and anxiety, the motor expression of augmented breaths is modulated. Empirical studies in rats have buttressed this inference by showing that the expectation of the termination of an aversive stimulus increases the incidence of augmented breaths by about 20 times (Soltysik and Jelen, 2005). Similarly, the physiological changes demonstrated in anesthetized animals during a neurochemical mapping study (Ajayi et al., 2018) are consistent with those that accompany the behavioural expressions of emotions thought to be regulated by the ventral hippocampus. These pieces of evidence indicate a need for further research into the hippocampus in the light of descending autonomic control.

Against the backdrop of the emerging evidence about the roles of the hippocampus in processing emotions, the current review aims at elucidating the anatomy of the hippocampus with emphasis on the intra and inter structural substrates responsible for modulating emotion-dependent autonomic activities.

Anatomy of the hippocampus

The hippocampus is a paired forebrain structure that is relatively conserved both functionally and phenotypically across the animal kingdom. In the rat, the structure extends from the septum all the way to the medial portion of the temporal lobe (Bregma; -1.72 to -6.84 mm). As it extends caudally, it assumes different shapes, with specific portions appearing in different sections (Figure 1). Hence, in a midsagittal brain section, the hippocampus is only partially visible in an area immediately ventral to the posterior half of the corpus callosum and lying at an oblique angle (septal area, Figure 1A). The hippocampus in approximately full extent is only visible in serial coronal sections between 4.36 - 5.88 mm caudal to Bregma, where the ventral hippocampus lies adjacent to the amygdaloid complex. In this region, the outline of the hippocampus assumes a C-shape (Figure 1) (Tombol et al., 2000; Cappaert et al., 2015; Striedter, 2016).

Histologically, based on the presence of three cortical layers and distinct unidirectional connections, the hippocampal region is composed of two sets of cortical structures: 1) the hippocampal formation and 2) the parahippocampal region. The hippocampal formation is divided into three distinct regions: a dentate gyrus, Ammon's horn also known as *Cornu Ammonis* and a subiculum. The parahippocampal region consists of areas that surround the ventral and caudal portions of the hippocampal formation. These areas include the entorhinal, perirhinal and postrhinal cortices, presubiculum and parasubiculum, all of which possess more than three lamina layers and reciprocally connects with the hippocampus (Witter and Amaral, 2004). However, the two sets of structures, hippocampal and parahippocampal, are interconnected and function together in a unidirectional circuit to produce physiological changes.

On the basis of cell types and laminar organization, the Ammon's horn is further divided into subfields: CA1, CA2 and CA3 according to the terminology of Lorente de Nó from 1934 (El-Falougy and Benuska, 2006). Each subfield is identified based
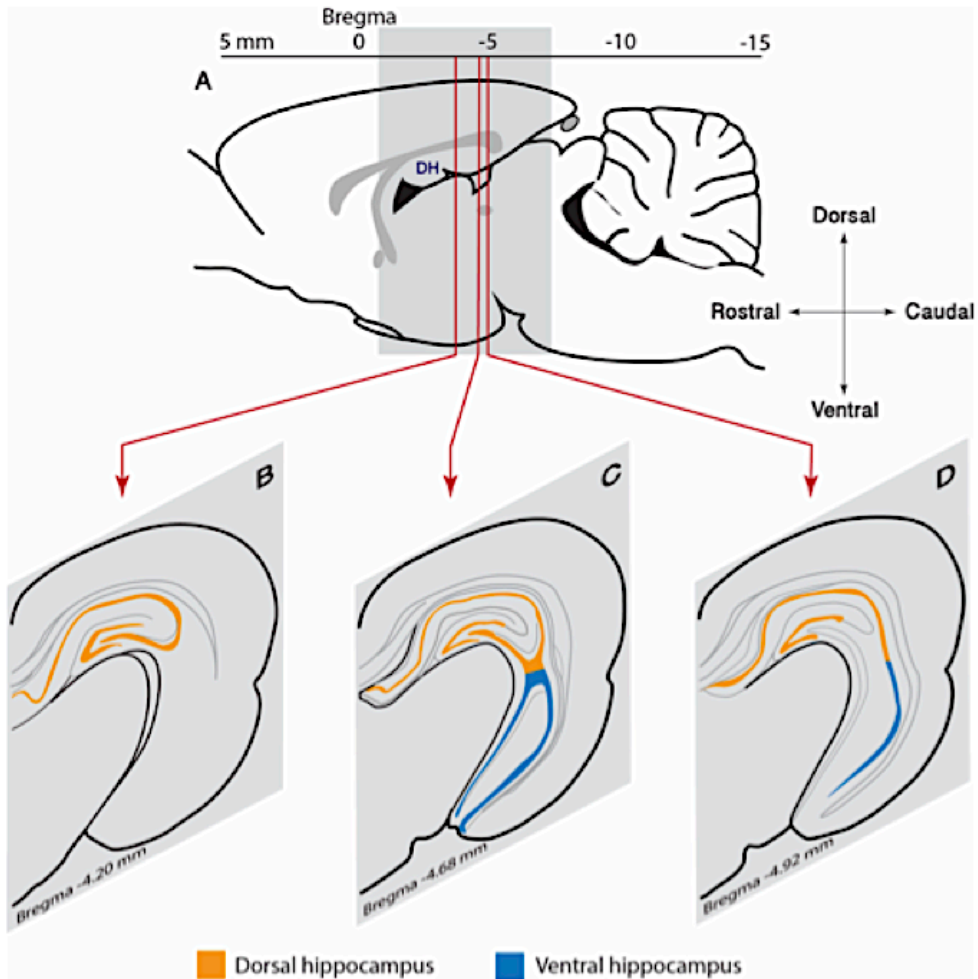
Figure 1. Schematic representations showing the organization of the dorsal and ventral hippocampal region in the rat brain. A) A midsagittal section of the whole rat brain. The shaded portion represents the area of the brain that contains the hippocampus. Only the dorsal hippocampus (DH) is visible in this plane. B - D) Illustrations showing the progressive change and organization in shape of the hippocampus rostrocaudally.

on the features of individual neuron structure and cytoarchitectural organization of neuron clusters (Ishizuka et al., 1995; Altemus et al., 2005). These subtle variations in structure also suggest possible differences in function and information processing.

Each subfield of cells is further organized into distinct layers. *Stratum pyramidale* (also known as the Pyramidal layer or Cell body layer) is the main cellular layer containing approximately 300,000 – 400,000 cells in the rat (Miettinen et al., 2012). Neurons from the pyramidal layer project to different cortical and subcortical structures except in a few instances where one neuron simultaneously projects to two differ-

ent regions (Ishikawa and Nakamura, 2006). However, the implication of the diverse projections are still subjects of debate. A recent study that perturbed the ventral hippocampus, physiologically and anatomically, suggested that anatomic projections from the ventral hippocampus to the medial nucleus of the amygdala were responsible for modulating bulbar cardiorespiratory control circuits (Ajayi et al., 2018). Other studies have also indicated the presence of multisynaptic connections originating from the ventral hippocampus, and with a capacity to modulate the sympathetic nervous system (Westerhaus and Loewy, 2001). Although the study by Westerhaus and Loewy (2001) did not show the structures that constitute the descending pathway, Ajayi et al. (2018) identified the medial nucleus of the aamydala as one relay structure. Further studies would be required to highlight details of the structures that complete the pathway for descending autonomic modulation.

Other cell layers include the following. The *Stratum oriens* is relatively cell-free and deep to the pyramidal layer. The *Stratum lucidum,* is a layer found only in the CA3 field. The layer is also cell-free and located above the pyramidal layer. In CA1 and CA2 subfields, the *stratum lucidum* is immediately superficial to the pyramidal cell layer and contains the apical dendrites of the cells in the pyramidal cell layer. Also, mossy fibres that project from the dentate gyrus to the CA3 subfield predominantly occupy this layer. *Stratum radiatum* is located superficial to the *stratum lucidium*. The *stratum radiatum* contains intrinsic fiber connections such as CA3 to CA3 connections and CA3 to CA1 connections. Finally, there is a *Stratum lacunosum-moleculare,* which is the most superficial layer of the hippocampal region. It is the area that receives terminal projections from the entorhinal cortex, thalamus and other cortical areas (Cappaert et al., 2015). Since the CA1 plays a significant role as an output relay for the hippocampus, emphasis will be placed on this region as literature is reviewed.

Differences between the CA1 and other CA subfields

The CA1 field has been distinguished from CA2 and CA3 fields based on morphological (Figure 2) and electrophysiological properties. The morphological differences include soma size of pyramidal cells: CA1 pyramidal cells are significantly smaller than those of CA2 and CA3 (Altemus et al., 2005; Mercer et al., 2007; Luszczewska-Sierakowska et al., 2015). Furthermore, the pyramidal cells of CA1 subfield give off apical dendrites that enter the *stratum lacunosum-moleculare*. This feature has been observed with both Golgi-Cox and intracellular labelling techniques in monkeys (Altemus et al., 2005). Electrophysiologically, the average spiking rate of CA1 cells is significantly higher than CA2 neurons but less than CA3 neurons (Mizuseki et al., 2012; San Antonio, 2014). These distinguishing features indicate differences in function and direct synaptic connections with nerve terminals from extrinsic sources.

Neuronal connections of the hippocampus

The hippocampus possesses unique intrinsic and extrinsic connectivity patterns recruited to regulate other regions, including autonomic functions (Ajayi et al., 2018; Ajayi and Mills, 2017). Nevertheless, understanding the functions of the hippocampus can be enhanced by analyzing the neuronal projections to and from this region.
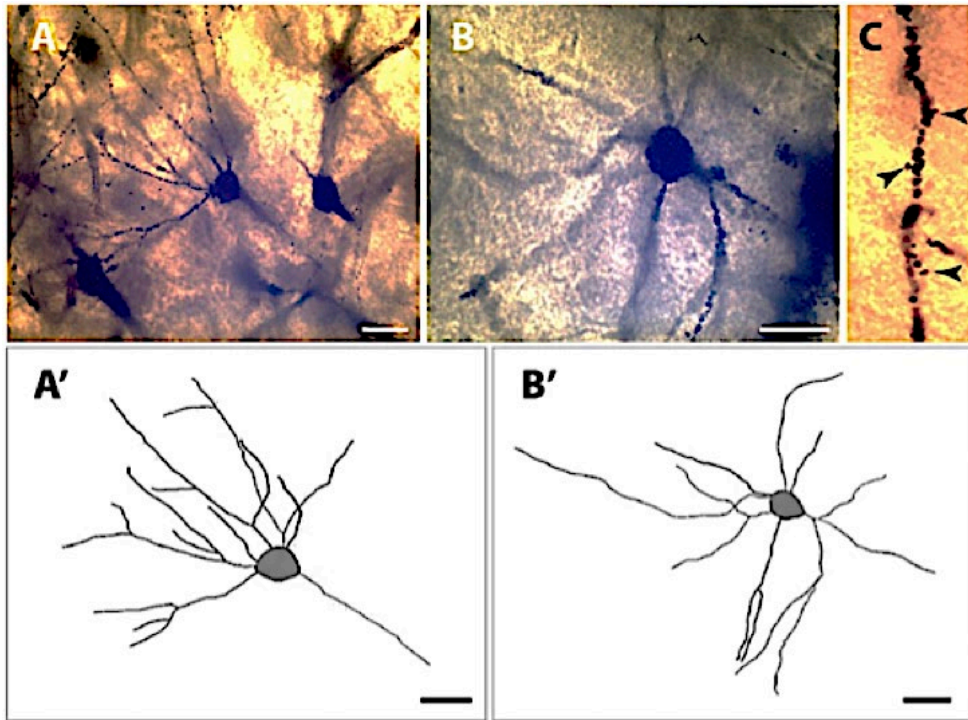
Figure 2. Neurons in the ventral hippocampus with the ability to modulate the autonomic nervous system are typically pyramidal. Light photomicrograph showing two distinct geometries of pyramidal cells, including the distribution of their dendritic trees, in the stimulated areas of the dorsal (A) and ventral (B) hippocampus as reported by Ajayi (2016). A modified Golgi-Cox technique was used to stain the neurons. The black arrows in (C) point at dendritic spines. Note: The neuron of the ventral hippocampus was selected from the CA1 field because the region was by far the most responsive area of the ventral hippocampus. Within the dorsal hippocampus, the representative neuron was also selected from the CA1 region. A′ and B′ are camera lucida reconstructions of the micrographs in A and B, respectively. Scale bar: 20 μm. Adapted from Ajayi (2016).

Intrinsic circuits of the hippocampus

The intrinsic connections of the hippocampus have a unique glutaminergic unidirectional organization (Andersen et al., 1971), although some studies have reported a colocalization of both glutamate and GABA within the same terminals (Munster-Wandowski et al., 2013). The intrinsic circuit is thought to begin in the entorhinal cortex, which is a region believed to link projections from other cortical areas with the hippocampus proper. The entorhinal cortex then sends excitatory signals to the dentate gyrus through a fiber bundle called the perforant pathway. Neurons of the dentate gyrus project to the hilus of CA3 field through mossy fibers. The CA3 neurons, in turn, project to the CA1 area through the Schaffer collaterals. The CA1 neurons project to the subiculum, which sends projections back to the entorhinal cortex and other cortical structures (Witter et al., 2000). A simplified illustration of the unidirectional circuit within the hippocampus is presented in Figure 3. Although details of
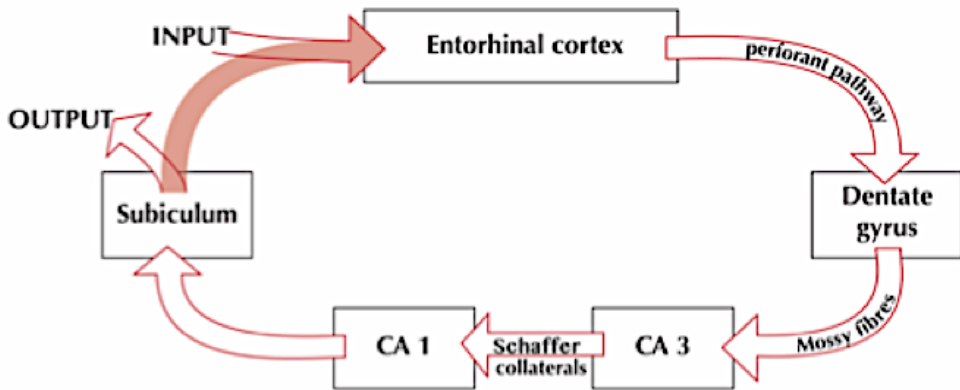
Figure 3. Diagram of the unique unidirectional intrinsic circuit of the hippocampus. The figure is a representation of the parahippocampal-hippocampal neuronal circuitry, illustrating the unique unidirectional connectivity loop within the hippocampus. Note that while the subiculum is the major output structure in the loop, it also projects back to the entorhinal cortex. This projection is represented by the red shaded arrow from the subiculum to the entorhinal cortex. It is also important to note that recent advancements in science have reported output projections from the CA1 region to other limbic structures involved in emotion processing.

the contribution of each area in this circuit is still being investigated, signals reaching the hippocampus are processed through this intrinsic loop before being transmitted downstream.

Output pathway of the hippocampus to cortical/subcortical structures

The subiculum, which is located in both dorsal and ventral hippocampal fields, has been reported as the principal output structure of the hippocampus. The subiculum receives major projections from the CA1 region and, in turn, targets various cortical and subcortical structures such as the infralimbic, entorhinal and perirhinal cortices, *nucleus accumbens*, thalamus and amygdala (Witter and Groenewegen, 1990; Witter et al., 1990). Subicular fibers that target these regions are thought to travel through three principal routes: the fornix, angular bundle and amygdalohippocampal area (Agster and Burwell, 2013). While the dorsal subiculum utilizes the first two routes, the ventral subiculum utilizes the amygdalohippocampal area. It is through the amygdalohippocampal area that ventral subicular projections connect to structures such as the ventral hypothalamus and amygdala (Witter, 1986).

However, there is evidence that the subiculum is not the only output structure of the hippocampus. Classical anatomical studies show that the ventral CA1 region also sends direct projections to cortical and subcortical structures (Cenquizca and Swanson, 2006, 2007; Ishikawa and Nakamura, 2006; Kishi et al., 2006; Ajayi et al., 2018). Perhaps there are different synaptic mechanisms in the connections between the subiculum and the ventral CA1, which have not been tested. It is also unknown if each pathway serves a different behavioral function.
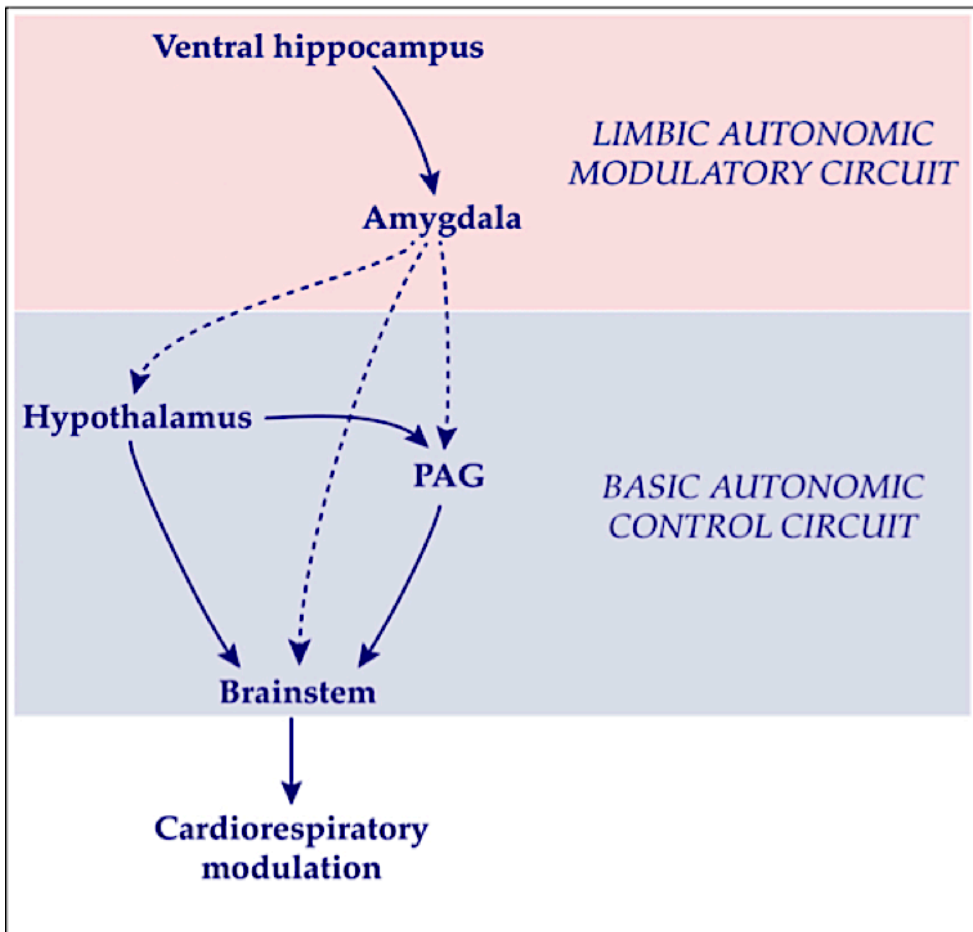
Figure 4. Proposed descending circuit diagram of the pathways for ventral hippocampus modulation of autonomic functions. The solid lines represent circuits that have been established using anatomic tract tracing techniques and confirmed by physiological manipulations. The broken lines represent identified anatomical projections but without confirmatory physiological evidence. The current thesis represents both anatomical and physiological evidence of pathways for autonomic modulation between the ventral hippocampus and the amygdala. PAG: periaqueductal gray.

Extrinsic connections with the potential to influence autonomic activities (Figure 4) include connections with the medial prefrontal cortex, specifically the infralimbic (Swanson, 1981; Cenquizca and Swanson, 2007) and prelimbic areas (Verwer et al., 1997; Cenquizca and Swanson, 2007), hypothalamus (Cenquizca and Swanson, 2006) and amygdala (Kishi et al., 2006; Ajayi et al., 2018). These projections are reported to be GABAergic following *in vivo* electrophysiological cell recording, labeling and neuron tracing (Jinno et al., 2007; Miyashita and Rockland, 2007), but most of the studies were limited to the dorsal hippocampus with the exception of ventral hippocampal

projections to the amygdala (Kishi et al., 2006; Ajayi et al., 2018). Thus, the functions and synaptic mechanisms of cells in the ventral hippocampus, particularly regarding emotional behavior, are uncertain.

Structural and functional segregation of the hippocampus

In the past decade, evidence argued in favor of anatomical and functional differences between the dorsal and ventral hippocampal fields (Bannerman et al., 2004a; Trivedi and Coover, 2004; Strange et al., 2014). The dorsal field of the hippocampus is the area adjacent to the septum and corresponds with the posterior hippocampus in humans while the ventral field is the distal half of the hippocampus located medial to the amygdala in the temporal lobe, and it corresponds with the anterior hippocampus in humans (Witter and Amaral, 2004). Although both fields possess similar cytoarchitectural configuration, less attention was given to the ventral hippocampus. This may be due to focus on elucidating and expanding on the breakthroughs that emerged from the dorsal field of the hippocampus, i.e. the discovery of place cells (O'Keefe and Dostrovsky, 1971; O'Keefe, 1976). However, today, the differentiation into dorsal and ventral fields is becoming significant as physiological, lesion and molecular studies uncover major differences (Bannerman et al., 2004b,c; Trivedi and Coover, 2004).

While the dorsal hippocampus is implicated in spatial navigation, episodic memory and associative learning, the ventral hippocampus is implicated in modulating stress responses and emotional behaviors such as fear and anxiety (Strange et al., 2014). This functional difference has been studied using a range of approaches among which include behavioral assays and separate lesioning (McHugh et al., 2004; Pentkowski et al., 2006), chemical stimulating and inhibition of various neuron populations within the ventral and dorsal hippocampus (Bertoglio et al., 2006; McHugh et al., 2008a; Zhang et al., 2014). The studies implicate the ventral hippocampus in anxiogenesis without much emotional effect from the dorsal hippocampus. On the other hand, lesioning and inactivation of the dorsal hippocampus have resulted in spatial memory impairment (Morris et al., 1982) and learning deficits in rats (Moser et al., 1995; McHugh et al., 2008a,b).

Interestingly, using a combined approach of optogenetics and electrophysiology, Ciocchi et al. (2015) demonstrated that the ventral hippocampus is capable of sending information of emotional content to specific neuron populations in the amygdala, *nucleus accumbens* and medial prefrontal cortex. In a combined experimental approach of multi-site neural recording and optogenetics, Padilla-Coreano et al. (2016) showed that inhibition of ventral hippocampus projections to the medial prefrontal cortex disrupted the behavioral expression of anxiety. However, studies of this association have given less attention to the involvement of the ventral hippocampus in modulating basic physiological parameters such as respiratory and cardiovascular function. Rather more attention has been given to holistic behaviors.

Motor and autonomic functions are amenable to modulation by the ventral hippocampus through direct and multisynaptic connections to the hypothalamus (Herman et al., 2005) and perhaps the periaqueductal gray (PAG). Such modulations are less likely influenced by the dorsal hippocampus (Ajayi and Mills, 2017; Ajayi et al.,

2018). Ballesteros et al. (2014) demonstrated that lesions in the ventral hippocampus affected the ability of the periaqueductal gray to produce the defensive freezing posture normal observed upon stimulating the dorsal region (Carrive and Morgan, 2012). Their study reported that neither the dorsal nor ventral hippocampal lesion completely disrupted periaqueductal gray activity. However, ventral hippocampal lesions significantly reduced defensive freezing behavior (Ballesteros et al., 2014). A similar report by Rogers et al. (2006) emphasized a greater involvement of the ventral hippocampus in fear conditioning. Thus, in addition to ventral hippocampal connections to the hypothalamus, these findings suggest possible connections of the ventral hippocampus to the periaqueductal gray.

Functions of the hippocampus

The hippocampus plays a crucial role in the limbic network because of its involvement in memory and cognition. These functions were first identified and described in 1953 following bilateral removal of the medial temporal lobe structures to ameliorate refractory epilepsy (Scoville and Milner, 1957). The frequency of seizures decreased, but the patient suffered from amnesia, suggesting that the hippocampus played crucial roles in storing memory (Scoville and Milner, 1957). The role of the hippocampus in memory and learning was further established by the discovery of the so-called "place cells", which fire bursts of action potentials in specific places ('place fields') as an animal worked through a maze (O'Keefe, 1976).

The seminal discovery of place cells over four decades ago (O'Keefe and Dostrovsky, 1971) has significantly shaped the functional knowledge of cells in the hippocampus. The correlation of neuron firing activities with particular locations of an animal in a defined space suggested that hippocampal cells could provide an accurate representation of the animal's location. This discovery was termed "the biological global positioning system", and it lead to a Nobel Prize in Medicine and Physiology in 2014. Since the discovery of place cells, several studies have attempted to further characterize the morphological features and physiological properties of the cells as well as define their precise distribution in the hippocampus. To this end, studies have suggested that there is a high density of place cells in the dorsal parts of the CA1 region (Henriksen et al., 2010). This observation implies that cells in the ventral hippocampus serve other functions.

Researchers have reported that the ventral hippocampus plays crucial roles in the expression of emotions, such as anxiety and stress (Bannerman et al., 2004c; Trivedi and Coover, 2004; Bertoglio et al., 2006; Fanselow and Dong, 2010; Femenia et al., 2012; Ballesteros et al., 2014; Padilla-Coreano et al., 2016), as well as the development of associated disorders, including post-traumatic stress disorder and major depressive disorder (Bonne et al., 2008; Femenia et al., 2012). A common feature in the expression of these emotions is an alteration of basic physiological parameters and it is becoming clear that the hippocampus is involved in autonomic regulation by modulating various aspects of cardiorespiratory rhythm, including the motor expression of augmented breaths (Ajayi and Mills, 2017; Ajayi et al., 2018). However, the mechanisms through which these behaviors are expressed are yet to be clarified.

Emotion processing and the hippocampus

Emotions are physical behaviors that reflect the mental state of an individual. These behaviors, which are expressed as joy, sadness, pleasure, fear, etc., are subjective, and in experimental conditions, mostly non-reproducible. Thus, most of the studies that attempt to describe the mechanisms of emotions are questionable. However, the Pavlovian fear-conditioning paradigm has been very useful in defining objective principles for the study of emotions. The Pavlovian paradigm involves the pairing of two stimuli: a conditioned stimulus (non-aversive) usually a light or a sound, and an unconditioned stimulus (aversive) often a foot shock. Following repeated pairing, the conditioned stimulus can produce the effect of the unconditioned stimulus (fear reaction). The paradigm has been used to objectively reproduce fear, a primary emotion that is conserved across species. Based on this paradigm, the amygdala is identified and extensively researched as a crucial structure in expressing the objective emotion of fear (LeDoux, 2003, 2007, 2012). However, the amygdala does not function as an entity in producing a fear reaction. Rather it is part of a circuit. Evolving evidence suggests that either by direct modulation of sensory inputs of an environmental challenge or by modifying neural mechanisms in the amygdala through synaptic transmission, other brain areas play crucial roles in forming and expressing emotions. One of such brain areas is the ventral hippocampus. Studies have demonstrated that lesion pf the hippocampus completely abolishes the Pavlovian reflex (Anagnostaras et al., 2002) but it is uncertain if this effect results from loss of the memory component of the conditioning stimulus or direct involvement in expressing the behavior. Studies also showed that the limbic system recruits the medial nucleus of the amygdala to produce autonomic changes (Ajayi et al., 2018). These studies are indications that emotional behaviors are processed through functional networks rather than individual brain regions.

In expressing an emotional behavior, changes in underlying physiologic parameters are expected as a homeostatic mechanism of adaptation to altered metabolic demands. Studies have shown that lesions to the ventral hippocampus create a fundamental homeostatic imbalance that could result in gastric ulcers (Henke, 1990a,b) although other autonomic parameters were not measured. Owing to established anatomical projections of the ventral hippocampus to the amygdala (Kishi et al., 2006; Ajayi et al., 2018), and the involvement of the amygdala in stress (Ressler, 2010), there is an interaction between the ventral hippocampus and amygdala that supports the physiological changes during emotional behaviors. Moreover, Henke (1990b) showed that high-frequency stimulation of the ventral CA1 region evoked potentials in the amygdala, and animals that received such stimulations were less vulnerable to stress-induced gastric ulcers.

In a more behavior-focused research in rats, Bannerman et al. (2003) demonstrated deficits in the expression of fear following lesions that encompassed 50 % of the ventral hippocampus. The lesions led to significant reduction in freezing following a foot shock stimulus. Furthermore, there were clear indications of increased anxiety demonstrated by observing various physical indices. All these effects were restricted to the ventral hippocampus (Bannerman et al., 2003).

Various physiological investigations (Ballesteros et al., 2014; Zhang et al., 2014) have also provided evidence underpinning the ventral hippocampus in emotions

using the principles of chemical inhibition and fear conditioning, respectively. Inhibition of the ventral hippocampus using optogenetics has also been shown to alter aspects of contextual fear (Goshen et al., 2011). All the reports mentioned above are in addition to human data where significant changes have been observed in people with post-traumatic stress disorder (Bonne et al., 2008) and bipolar disorders (Frey et al., 2007). However, the specific role(s) of the ventral hippocampus regarding inter-structural neuronal interactions require more investigations as only a few studies (Ajayi and Mills, 2017; Ajayi et al., 2018) have provided insight in the context of motor and autonomic functions underlying these behavioral changes.

The mechanisms involved in expressing emotions and stress include a collection of smaller motor and autonomic processes. For example, during the expression of an emotion such as anxiety, depression or fear, an organized and simultaneous recruitment of multiple motor and autonomic components is expected: the phrenic nerve and vago-sympathetic systems would be recruited as final motor tracts to modulate the respiratory and cardiovascular systems, respectively, so that homeostasis is maintained while adapting to the situation. At the same time, nerve supplies to specific skeletal muscles associated with emotional expression will be recruited to relax or tense such muscles. The simultaneous occurrence of these events suggests that circumscribed higher brain areas, known to control emotional behaviors, exert their effects by modulating, resetting and recruiting motor and autonomic drivers in the brainstem.

However, it is important to note that there are no known direct projections of the ventral hippocampus to brainstem autonomic centers but indirect connections could exist. Studies have shown that one relay structure between the ventral hippocampus and the brainstem is the amygdala (Ajayi et al., 2018). The role of the amygdala does not rule out the involvement of other critical relays such as the hypothalamus and periaqueductal gray. In fact, it is possible that the amygdala, in turn, recruits both hypothalamus and periaqueductal gray for motor and autonomic control.

Concluding remarks

The hippocampus and amygdala are principal components of the limbic system due to their roles in expressing emotions and processing memory. However, in appropriating emotional behaviors, the hippocampus and amygdala rely on complex linkages, known as functional networks, between other brain regions to process information and express distinct behaviors. For example, the hippocampus is known to be involved in memory, learning (Bannerman et al., 2014) and limbic modulation autonomic activities (Ajayi and Mills, 2017; Ajayi et al., 2018) while fear is principally regulated by the amygdala (LeDoux, 2003, 2007; Phelps and LeDoux, 2005). However, these regions must interact with other structures that directly control autonomic and endocrine functions to produce homeostatic changes, necessitating that the limbic structures provide a modulatory hierarchical level in autonomic control. It is through such interactions that integrated respiratory and autonomic changes accompany emotional behaviors (Ajayi et al., 2018). However, the interactions are complex and involve mechanisms and pathways many of which have not been fully elucidated. The studies to date have focused on the medial prefrontal cortex because of its established roles in processing emotions. However, more recently, other parts of the limbic system such as the ventral hippocampus

have been shown to affect emotion processing, and also modulate motor and autonomic function (Ajayi and Mills, 2017; Ajayi et al., 2018). A likely pathway maybe through the periaqueductal gray. The periaqueductal gray directly regulates autonomic function and it is believed to be essential to the integration of various autonomic responses, such as respiration, vocalization, cardiovascular function and micturition for the expression of emotions during a survival challenge (Bandler et al., 1991; Zhang et al., 1994). Investigations into the anatomic organization of inputs into the periaqueductal gray, the synaptic mechanisms driving such inputs and the manner in which the inputs shape the output of the periaqueductal gray would be relevant in broadening current knowledge of descending modulation of emotion-dependent autonomic activities.

Conflict of interest

The author declares no competing financial interests.

References

Agster K.L., Burwell R.D. (2013) Hippocampal and subicular efferents and afferents of the perirhinal, postrhinal, and entorhinal cortices of the rat. Behav. Brain Res. 254: 50-64.

Ajayi I.E. (2016) Limbic modulation of the autonomic nervous system. PhD Thesis, School of Veterinary Science, The University of Queensland, Australia. doi: 10.14264/uql.2017.31.

Ajayi I.E., Mills P.C. (2017) Effects of the hippocampus on the motor expression of augmented breaths. PLoS One 12: e0183619.

Ajayi I.E., McGovern A.E., Driessen A.K., Kerr N.F., Mills P.C., Mazzone S.B. (2018) Hippocampal modulation of cardiorespiratory function. Respir. Physiol. Neurobiol.; doi: 10.1016/j.resp.2018.03.004.

Altemus K.L., Lavenex P., Ishizuka N., Amaral D.G. (2005) Morphological characteristics and electrophysiological properties of CA1 pyramidal neurons in macaque monkeys. Neuroscience 136: 741-756.

Anagnostaras S.G., Gale G.D., Fanselow M.S. (2002) The hippocampus and Pavlovian fear conditioning: reply to Bast et al. Hippocampus 12: 561-565.

Andersen P., Bliss T.V., Skrede K.K. (1971) Lamellar organization of hippocampal pathways. Exp. Brain Res. 13: 222-238.

Ballesteros C.I., de Oliveira Galvao B., Maisonette S., Landeira-Fernandez J. (2014) Effect of dorsal and ventral hippocampal lesions on contextual fear conditioning and unconditioned defensive behavior induced by electrical stimulation of the dorsal periaqueductal gray. PLoS One 9: e83342.

Bandler R., Carrive P., Zhang S.P. (1991) Integration of somatic and autonomic reactions within the midbrain periaqueductal grey: viscerotopic, somatotopic and functional organization. Progr. Brain Res. 87: 269-305.

Bannerman D.M., Grubb M., Deacon R.M., Yee B.K., Feldon J., Rawlins J.N. (2003) Ventral hippocampal lesions affect anxiety but not spatial learning. Behav. Brain Res. 139: 197-213.

Bannerman D.M., Deacon R.M., Brady S., Bruce A., Sprengel R., Seeburg P.H., Rawlins J.N. (2004a) A comparison of GluR-A-deficient and wild-type mice on a test battery assessing sensorimotor, affective, and cognitive behaviors. Behav. Neurosci. 118: 643-647.

Bannerman D.M., Matthews,P., Deacon R.M., Rawlins J.N. (2004b) Medial septal lesions mimic effects of both selective dorsal and ventral hippocampal lesions. Behav. Neurosci. 118: 1033-1041.

Bannerman D.M., Rawlins J.N., McHugh S.B., Deacon R.M., Yee B.K., Bast T., Zhang W.N., Pothuizen H.H., Feldon J. (2004c) Regional dissociations within the hippocampus--memory and anxiety. Neurosci. Biobehav. Rev. 28: 273-283.

Bannerman D.M., Sprengel R., Sanderson D.J., McHugh S.B., Rawlins J.N., Monyer H., Seeburg P.H. (2014) Hippocampal synaptic plasticity, spatial memory and anxiety. Nature Rev. Neurosci. 15: 181-192.

Bertoglio L.J., Joca S.R., Guimaraes F.S. (2006) Further evidence that anxiety and memory are regionally dissociated within the hippocampus. Behav. Brain Res. 175: 183-188.

Bonne O., Vythilingam M., Inagaki M., Wood S., Neumeister A., Nugent A.C., Snow J., Luckenbaugh D.A., Bain E.E., Drevets W.C., Charney D.S. (2008) Reduced posterior hippocampal volume in posttraumatic stress disorder. J. Clin. Psychiatry 69: 1087-1091.

Cappaert N.L.M., Van Strien N.M., Witter M.P. (2015) Chapter 20 - Hippocampal Formation, in: Paxinos G. (Ed.), The Rat Nervous System (Fourth Edition). Academic Press, San Diego. Pp. 511-573.

Carrive P., Morgan M.M. (2012) Chapter 10 - Periaqueductal Gray, in: Paxinos J.K.M. (Ed.), The Human Nervous System (Third Edition). Academic Press, San Diego. Pp. 367-400.

Cenquizca L.A., Swanson L.W. (2006) Analysis of direct hippocampal cortical field CA1 axonal projections to diencephalon in the rat. J. Comp. Neurol. 497: 101-114.

Cenquizca L.A., Swanson L.W. (2007) Spatial organization of direct hippocampal field CA1 axonal projections to the rest of the cerebral cortex. Brain Rese. Rev. 56: 1-26.

Ciocchi S., Passecker J., Malagon-Vina H., Mikus N., Klausberger T. (2015) Brain computation. Selective information routing by ventral hippocampal CA1 projection neurons. Science 348: 560-563.

Ekman P., Levenson R.W., Friesen W. (1983) Autonomic nervous system activity distinguishes among emotions. Science 221: 1208-1210.

El-Falougy H., Benuska J. (2006) History, anatomical nomenclature, comparative anatomy and functions of the hippocampal formation. Bratisl. Lek. Listy 107: 103-106.

Fanselow M.S., Dong H.W. (2010) Are the dorsal and ventral hippocampus functionally distinct structures? Neuron 65: 7-19.

Femenia T., Gomez-Galan M., Lindskog M., Magara S. (2012). Dysfunctional hippocampal activity affects emotion and cognition in mood disorders. Brain Res. 1476: 58-70.

Frey B.N., Andreazza A.C., Nery F.G., Martins M.R., Quevedo J., Soares J.C., Kapczinski F. (2007) The role of hippocampus in the pathophysiology of bipolar disorder. Behav. Pharmacol. 18: 419-430.

Goshen I., Brodsky M., Prakash R., Wallace J., Gradinaru V., Ramakrishnan C., Deisseroth K. (2011) Dynamics of retrieval strategies for remote memories. Cell 147: 678-689.

Henke P.G. (1990a). Hippocampal pathway to the amygdala and stress ulcer development. Brain Res. Bull. 25: 691-695.

Henke P.G. (1990b) Limbic system modulation of stress ulcer development. Ann. N.Y. Acad. Sci. 597: 201-206.

Henriksen E.J., Colgin L.L., Barnes C.A., Witter M.P., Moser M.B., Moser E.I. (2010) Spatial representation along the proximodistal axis of CA1. Neuron 68: 127-137.

Herman J.P., Ostrander M.M., Mueller N.K., Figueiredo H. (2005) Limbic system mechanisms of stress regulation: hypothalamo-pituitary-adrenocortical axis. Progr. Neuropsychopharmacol. Biol. Psychiatry 29: 1201-1213.

Ishikawa A., Nakamura S. (2006) Ventral hippocampal neurons project axons simultaneously to the medial prefrontal cortex and amygdala in the rat. J. Neurophysiol. 96: 2134-2138.

Ishizuka N., Cowan W.M., Amaral D.G. (1995) A quantitative analysis of the dendritic organization of pyramidal cells in the rat hippocampus. J. Comp. Neurol. 362: 17-45.

Jinno S., Klausberger T., Marton L.F., Dalezios Y., Roberts J.D., Fuentealba P., Bushong E.A., Henze D., Buzsaki G., Somogyi P. (2007) Neuronal diversity in GABAergic long-range projections from the hippocampus. J. Neurosci. 27: 8790-8804.

Kishi T., Tsumori T., Yokota S., Yasui,Y. (2006) Topographical projection from the hippocampal formation to the amygdala: a combined anterograde and retrograde tracing study in the rat. J. Comp. Neurol. 496: 349-368.

Kjelstrup K.G., Tuvnes F.A., Steffenach H.A., Murison R., Moser E.I., Moser M.B. (2002) Reduced fear expression after lesions of the ventral hippocampus. Proc. Natl. Acad. Sci. U.S.A. 99: 10825-10830.

LeDoux J. (2003) The emotional brain, fear, and the amygdala. Cell. Mol. Neurobiol. 23: 727-738.

LeDoux J. (2007) The amygdala. Curr. Biology 17: R868-R874.

LeDoux J.E. (2012) Evolution of human emotion: A view through fear. Prog. Brain Res. 195: 431-442.

Luszczewska-Sierakowska I., Wawrzyniak-Gacek A., Guz T., Tatara M.R., Charuta A. (2015) Morphometric parameters of pyramidal cells in CA1-CA4 fields in the hippocampus of arctic fox (Vulpes lagopus). Folia Biol. (Krakow) 63: 263-267.

Maren S., Holt W.G. (2004) Hippocampus and Pavlovian fear conditioning in rats: muscimol infusions into the ventral, but not dorsal, hippocampus impair the acquisition of conditional freezing to an auditory conditional stimulus. Behav. Neurosci. 118: 97-110.

McHugh S.B., Deacon R.M., Rawlins J.N., Bannerman D.M. (2004) Amygdala and ventral hippocampus contribute differentially to mechanisms of fear and anxiety. Behav. Neurosci. 118: 63-78.

McHugh S.B., Campbell T.G., Taylor A.M., Rawlins J.N., Bannerman D.M. (2008a) A role for dorsal and ventral hippocampus in inter-temporal choice cost-benefit decision making. Behav. Neurosci. 122: 1-8.

McHugh S.B., Niewoehner B., Rawlins J.N., Bannerman D.M. (2008b) Dorsal hippocampal N-methyl-D-aspartate receptors underlie spatial working memory performance during non-matching to place testing on the T-maze. Behav. Brain Res. 186: 41-47.

Mercer A., Trigg H.L., Thomson A.M. (2007) Characterization of neurons in the CA2 subfield of the adult rat hippocampus. J. Neurosci. 27: 7329-7338.

Miettinen R., Hajszan T., Riedel A., Szigeti-Buck K., Leranth C. (2012) Estimation of the total number of hippocampal CA1 pyramidal neurons: new methodology applied to helpless rats. J. Neurosci. Methods 205: 130-138.

Miyashita T., Rockland K.S. (2007) GABAergic projections from the hippocampus to the retrosplenial cortex in the rat. Eur. J. Neurosci. 26: 1193-1204.

Mizuseki K., Royer S., Diba K., Buzsaki G. (2012) Activity dynamics and behavioral correlates of CA3 and CA1 hippocampal pyramidal neurons. Hippocampus 22: 1659-1680.

Morris R.G., Garrud P., Rawlins J.N., O'Keefe J. (1982) Place navigation impaired in rats with hippocampal lesions. Nature 297: 681-683.

Moser M.B., Moser E.I., Forrest E., Andersen P., Morris R.G. (1995) Spatial learning with a minislab in the dorsal hippocampus. Proc. Natl. Acad. Sci. U.S.A. 92: 9697-9701.

Munster-Wandowski A., Gomez-Lira G., Gutierrez R. (2013) Mixed neurotransmission in the hippocampal mossy fibers. Front. Cell. Neurosci. 7: 210.

O'Keefe J. (1976) Place units in the hippocampus of the freely moving rat. Exp. Neurol. 51: 78-109.

O'Keefe J., Dostrovsky J.O. (1971) The hippocampus as a spatial map. Preliminary evidence from unit activity in the freely-moving rat. Brain Res. 34: 171-175.

Padilla-Coreano N., Bolkan S.S., Pierce G.M., Blackman D.R., Hardin W.D., Garcia-Garcia A.L., Spellman T.J., Gordon J.A. (2016) Direct ventral hippocampal-prefrontal input is required for anxiety-related neural activity and behavior. Neuron 89: 857-866.

Pentkowski N.S., Blanchard D.C., Lever C., Litvin Y., Blanchard R.J. (2006) Effects of lesions to the dorsal and ventral hippocampus on defensive behaviors in rats. Eur. J. Neurosci. 23: 2185-2196.

Phelps E.A., LeDoux J.E. (2005) Contributions of the amygdala to emotion processing: From animal models to human behavior. Neuron 48: 175-187.

Ressler K.J. (2010) Amygdala activity, fear, and anxiety: modulation by stress. Biol. Psychiatry 67: 1117-1119.

Rogers J.L., Hunsaker M.R., Kesner R.P. (2006) Effects of ventral and dorsal CA1 subregional lesions on trace fear conditioning. Neurobiol. Learn. Mem. 86: 72-81.

San Antonio A.A. (2014) Distinct physiological and developmental properties of hippocampal CA2 subfield revealed by using anti-Purkinje cell protein 4 (PCP4) immunostaining. J. Comp. Neurol. 522: 1333-1354.

Scoville W.B., Milne, B. (1957) Loss of recent memory after bilateral hippocampal lesions. J. Neurol. Neurosurg. Psychiatry 20: 11-21.

Soltysik S., Jelen P. (2005) In rats, sighs correlate with relief. Physiol. Behav. 85: 598-602.

Strange B.A., Witter M.P., Lein E.S., Moser E.I. (2014) Functional organization of the hippocampal longitudinal axis. Nat. Rev. Neurosci. 15: 655-669.

Striedter G.F. (2016) Evolution of the hippocampus in reptiles and birds. J. Comp. Neurol. 524: 496-517.

Swanson L.W. (1981) A direct projection from Ammon's horn to prefrontal cortex in the rat. Brain Res. 217: 150-154.

Tombol T., Davies D.C., Nemeth A., Sebesteny T., Alpar A. (2000) A comparative Golgi study of chicken (Gallus domesticus) and homing pigeon (Columba livia) hippocampus. Anat. Embryol. 201: 85-101.

Trivedi M.A., Coover G.D. (2004) Lesions of the ventral hippocampus, but not the dorsal hippocampus, impair conditioned fear expression and inhibitory avoidance on the elevated T-maze. Neurobiol. Learn. Mem. 81: 172-184.

Verwer R.W., Meijer R.J., Van Uum H.F., Witter M.P. (1997) Collateral projections from the rat hippocampal formation to the lateral and medial prefrontal cortex. Hippocampus 7: 397-402.

Westerhaus M.J., Loewy A.D. (2001) Central representation of the sympathetic nervous system in the cerebral cortex. Brain Res. 903: 117-127.

Witter M.P. (1986) A survey of the anatomy of the hippocampal formation, with emphasis on the septotemporal organization of its intrinsic and extrinsic connections. Adv. Exp. Med. Biol. 203: 67-82.

Witter M.P., Amaral D.G. (2004) Chapter 21 - Hippocampal formation, in: Paxinos G. (Ed.) The Rat Nervous System (Third Edition). Academic Press, Burlington. Pp. 635-704.

Witter M.P., Groenewegen H.J. (1990) The subiculum: cytoarchitectonically a simple structure, but hodologically complex. Progr. Brain Res. 83: 47-58.

Witter M.P., Ostendorf R.H., Groenewegen H.J. (1990) Heterogeneity in the dorsal subiculum of the rat. Distinct neuronal zones project to different cortical and subcortical targets. Eur. J. Neurosci. 2: 718-725.

Witter M.P., Wouterlood F.G., Naber P.A., Van Haeften T. (2000) Anatomical organization of the parahippocampal-hippocampal network. Ann. N.Y. Acad. Sci. 911: 1-24.

Zhang S.P., Davis P.J., Bandler R., Carrive P. (1994) Brain stem integration of vocalization: role of the midbrain periaqueductal gray. J. Neurophysiol. 72: 1337-1356.

Zhang W.N., Bast T., Xu Y., Feldon J. (2014) Temporary inhibition of dorsal or ventral hippocampus by muscimol: distinct effects on measures of innate anxiety on the elevated plus maze, but similar disruption of contextual fear conditioning. Behav. Brain Res. 262: 47-56.

Research Article - Basic and Applied Anatomy

An application of the graph theory to the study of the human locomotor system

Ferdinando Paternostro[1], Ugo Santosuosso[1], Daniele Della Posta[2], Piergiorgio Francia[1,*]

[1] Department of Clinical and Experimental Medicine, University of Florence, Florence, Italy
[2] aNETomy - The Anatomical Network, Roma, Italy

Abstract

The study of the relationships between the different structures of the human locomotor system still raises great interest. In fact, the human body networks and in particular the "myofascial system network" underlie posture and movement and new knowledge could be useful and applied to many fields such as medicine and prosthetics. The hypothesis of this study was to verify the possibility of creating a structural network representing the human locomotor system as well as to study and describe the relationship between the different structures considered. The graph theory was applied to a network of 2339 body parts (nodes) and 7310 links, representing the locomotor system. The open source platform software Cytoscape was used for data entry (nodes and links) as well as for debugging. In addition, the "NetworkAnalyzer" plugin was used for the descriptive statistics of the network obtained. In order to achieve a better rendering, the results of the network parameters gained were then imported into Gephi graph platform. At the end of this procedure, we obtained an image of a human being in an orthostatic position with a precise distribution of the nodes and links. More specifically, "the shortest pathways analysis of the network" demonstrated that any two randomly selected nodes on the network were connected by pathways of 4 or at most 6-8 nodes. Moreover, the Edge Radiality Distribution analysis was carried out in order to define how a single node is functionally relevant for other nodes: the probability distribution ranged from 0.4 to 0.77. This indicates that the majority of nodes tend to be functionally relevant for the others, but none of these is predominant. As a whole, the Cluster Coefficient (0.260) demonstrates that the network is neither random nor "strongly organized".

Introduction

Although in some branches of medicine such as anatomy and kinesiology as well as osteopathy the relationship between different parts of the body and in particular of the musculoskeletal system is taken into consideration, no precise indications are yet given in this regard (Esteve-Altava et al., 2011; Swanson, 2013; Diogo et al., 2015).

The human locomotor system is a complex system that affects thousands of anatomical structures; each part with its own morpho-functional peculiarities, showing specific functions both individually and together (i.e. to support the person and allow movements, connect, protect other organs), thus creating a complicated system of relationships that characterizes the musculoskeletal system itself.

* Corresponding author. E-mail: piergiorgiofrancia@libero.it

Consequently, studies aimed at an increasing in-depth knowledge of the human body and the relationships between the different systems in static and dynamic conditions is still raising great interest (Diogo et al., 2015; Esteve-Altava et al., 2011).

Some authors have tried to answer this question by applying the principles of tensegrity to the study of the musculoskeletal system, human movement and posture and relationships between the different body segments (Levin, 2002; Swanson, 2013; Dischiavi et al., 2018).

Tensegrity refers to structures that maintain their integrity by balancing continuously braided tensile forces along the structure (Chen and Ingber, 1999; Ingber, 2008). In this sense, it is known that the forces acting in human connective tissue can be represented as a continuous network affecting all structures of the musculoskeletal system. This would allow us to overcome the limits of a segmental study and to explain more complex properties of locomotor system through a holistic approach (Chen and Ingber, 1999, Dischiavi et al., 2018).

Moreover, in recent years the human body and the relations between its different parts has been studied using the theory of networks (Bolwijn et al., 1996; Fling et al., 2014; Esteve-Altava et al., 2015). This approach has allowed the study of the human body from a different perspective.

The results achieved by the generation of a structured network representing the musculoskeletal system can be further studied and graphically represented with the use of the graph theory (Mason and Verwoerd, 2008; Murphy et al., 2018).

In this sense, graph theory in scientific literature is applied to several fields, including the medical (Bullmore and Sporns, 2009, van Wijk et al., 2010) and social one (Makagon et al., 2012; De Vico Fallani et al., 2014; Zang et al., 2018). Recently, some authors have studied the human posture by applying the graph theory to achieve a simple model, but at the same time an accurate and faithful picture of the original system (Thome et al., 2006; Tahir et al., 2007; Liu and Zhan, 2013; Boonstra et al., 2015). In particular, the graph theory can allow the objective representation of the data set of the network obtained from the anatomical examination of the human musculoskeletal system, as has been done in the present study.

An approach considering these theories, as a mathematical measure of the relationships inside the musculoskeletal system, could help to better understand the relationships between the different structures of this system and become a new way to investigate anatomical complexity, that could be widely applied.

The aim of the present study was to verify the possibility to create a network representing the human musculoskeletal system and then define a structural network applied to anatomy to study and describe the relationship between the different structures considered.

Materials and Methods

In this study, as a whole, numerous interconnected parts (nodes) of the musculoskeletal system were identified, in order to create a structural network that allows an in-depth topological analysis of the musculoskeletal system itself. In this sense, we considered a total of 2339 anatomical structures (Table 1). Specifically, all the osteomusculo-ligamentous structures of the arthrodial system, the diaphragm, the pelvic

Table 1. Body parts considered in this research: typology and number.

Anatomical structures	N°
Ligaments	1062
Bones	216
Muscles	590
Fasciae	103
Cartilages	124
Innards (eye)	2
Other	5
Tendons	237
Total	**2339**

floor muscles, the supra and subhyoid muscles and the pharyngeal muscles were considered. Bone, capsuloligamentous and joint structures of the inner ear were not considered.

Among these structures (nodes), the undirected links (the connection is not associated with a direction) have been defined according to the existing anatomical relationship. The study of the network following the analysis of such a large number of nodes, that is, the "graphic" representation, even if not univocal, of every single part of the musculoskeletal system was aimed at obtaining a graphic representation of such network (graph) and therefore of the relationships between the structures.

In this sense, the open source software platform Cytoscape (www.cytoscape.org) was used for data entry (nodes and links) as well as for their debugging. In addition, the plugin "NetworkAnalyzer" was used for the descriptive statistics of the network obtained.

The resulting network parameters were then imported into the open-source and multiplatform software Gephi (www.Gephi.org) for a better rendering, using the plugin "ForceAtlas 2" with the option "Dissuade hubs".

The structured network obtained and expressed through a graph was characterized by its own density. The formula applied to calculate the network density, that is, how many links are there in the network compared to the maximum number of links that a network with the same number of nodes N can have was the following:

$$D = \frac{2(E - N + 1)}{N(N - 3) + 2}$$

where D is the graph density, N is the number of nodes inside the network and E is the number of possible links that a network with N nodes can contain.

The diameter of a graph G it is the greatest distance between any pair of vertices and it was considered as the number of edges in the shortest path between the most distant vertices.

The clustering coefficient is the measure of the degree to which nodes in a graph tend to cluster together and results from the number n of links existing between the k_i nodes next to i and the maximum number of possible arches between them. This value was calculated as follows:

$$C_i = \frac{2e_i}{k_i(k_i - 1)}$$

where k_i is the number of neighbours of the i'th node and e_i is the number of connections between these neighbours. Closeness centrality measures the importance of a node in a network according to the notion that "An important node is typically *close to*, and can communicate quickly with, the other nodes in the network"; it was cal-

Table 2. Anatomical network parameters.

Clustering coefficient:	0.260	Number of nodes:	2339
Connected components:	1	Network density:	0.003
Network diameter:	14	Network heterogeneity:	1.397
Network centralization:	0.033	Isolated nodes:	0
Shortest paths:	5468582 (100%)	Number of self-loops:	6
Characteristic path length:	6.682	Multi-edge node pairs:	7310
Avg. Number of neighbors:	6.253	Analysis time (sec):	9.389

culated as the sum of the length of the shortest pathways between the node and all other nodes in the graph (Friedkin et al., 1981; Mason and Verwoerd, 2008; Opsahl et al., 2010).

Results

This study allowed us to create a network and thus obtain a connected graph in which self-organization shows a clear reconstruction of the human musculoskeletal system. In particular, the topological analysis defined a network of 2339 anatomical parts (nodes) and 7310 links (Tables 1, 2).

The definition of the network is the result of two consecutive steps. After the full definition of a first network (preliminary network), debugging was carried out to find imperfections and oversights. At the end of the debugging process, data entry errors (about 100) were found and were corrected, obtaining the "final" network considered in this study. From the comparison of the two networks (preliminary vs. final) it was possible to verify how the difference in the numerical results achieved was less than the fourth decimal place ($<10^{-4}$ error).

The descriptive parameters of the final network achieved by Cytoscape processing are listed in Table 2. In particular, the network density was 0.003, while the graph diameter graph resulted 14, and the clustering coefficient was 0.260.

The shortest pathway analysis of the network demonstrated that any two randomly selected nodes on the network were connected by pathways of 4 or at most 6-8 jumps and each network node was connected on average with 6.25 other nodes (Figure 1).

The results of the Edge Radiality Distribution analysis showed that the "probability" of a node to be functionally relevant for several other nearby nodes ranged from 0.4 to 0.77.

Discussion

In this study, we created an anatomical network model of the locomotor system by evaluating all its anatomical structures and, within this set, the relationships that each single structure (node) has with the others through the definition of edges.
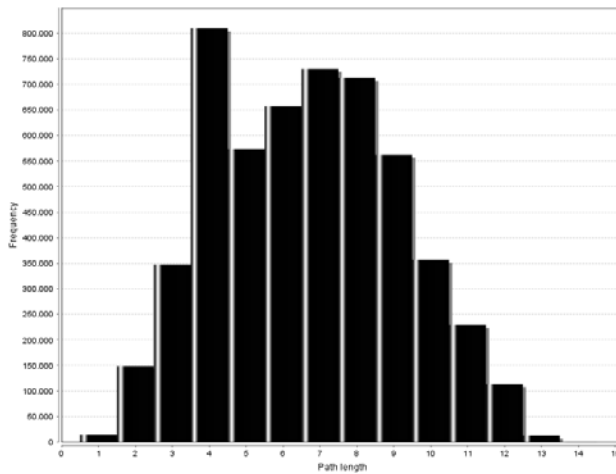
Figure 1. Shortest Path Histogram.

We carried out this study with the same approach as previous ones on the human head (Esteve-Altava et al., 2015), body (Thome et al., 2006) posture (Tahir et al., 2007) and hand grasp posture (Liu and Zhan, 2013) and analysis using the theory of data graphs has allowed a new and more detailed description of the locomotor system. This result could be an important step forward in the study of the relationship between the different structures of locomotor system and of this with other body systems and the environment in static and dynamic conditions. Contrary to other studies (Murphy et al., 2018) we defined nodes as all the structures considered, while links indicate an anatomic relationship between the nodes.

In particular, processing the network step by step (see Figures 2-5) created an image of a man in orthostatic position, that is a precise distribution of the nodes and the links resulted from the graphic representation of the outcomes.

It is worthy noting that the data histograms, screened by the plugging network analysis of Cytoskape (Network Analizer), fitted precisely with the theoretical curves without points that distinctly deviate from those curves (Figures 2).

At the same time, the density value of the generated network demonstrated that the network and its structure is very flexible and elastic, the Cluster Coefficient obtained from the analysis of the network resulting from this study is 0.260, which can be considered a intermediate value indicating that the network is neither random nor "strongly organized". In this sense it is known that the Cluster Coefficient (or transitivity) value of a randomly generated network tends to be very low while in networks resulted from "engineered" structures it is usually a higher value. The heterogeneity of a network should measure the diversity in the node degrees compared to a full homogeneous network with the same number of nodes. In this study it was 1.397 indicating that there are no structural holes in the network and its nodes, that affect the whole network (Burt, 2004; Mason and Verwoerd, 2008; Jacob et al., 2017).
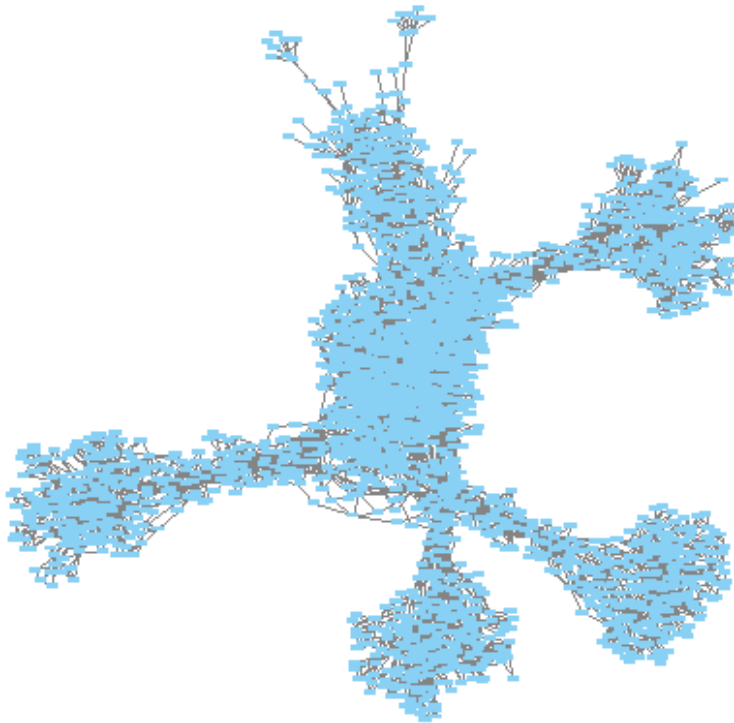
Figure 2. Anatomical Network data rendering with Cytoscape.

All this suggests that the "locomotor" network of a human being is at the same time robust, elastic, redundant. In the analysis of these results, we did not the need to consider this structure to adapt to the environment in which it lives and, therefore, the reciprocal relationship between man and the environment; this network could paradoxically appear not "perfected".

The approach to the analysis of the musculoskeletal system of this pilot study could open new perspectives and find areas of application in many disciplines interested in the study and treatment of the locomotor system. In fact, this method could lead to an integrated study of human movement and posture considering the relationships between each structure by also applying the principles of tensegrity. As previously reported, among the several fields of this approach application there are the medical and movement ones. Within these branches, there are real global health emergencies such as patients with diabetes and in particular with history of neuropathy, or greater or lesser amputation who could be studied by the approach proposed in this study for the serious and typical alterations of movement caused by this condition (Anichini et al., 2017; Francia et al., 2017, 2018). This should theoretically be useful for the definition of tailored patients treatments for impairments affecting the musculoskeletal system.
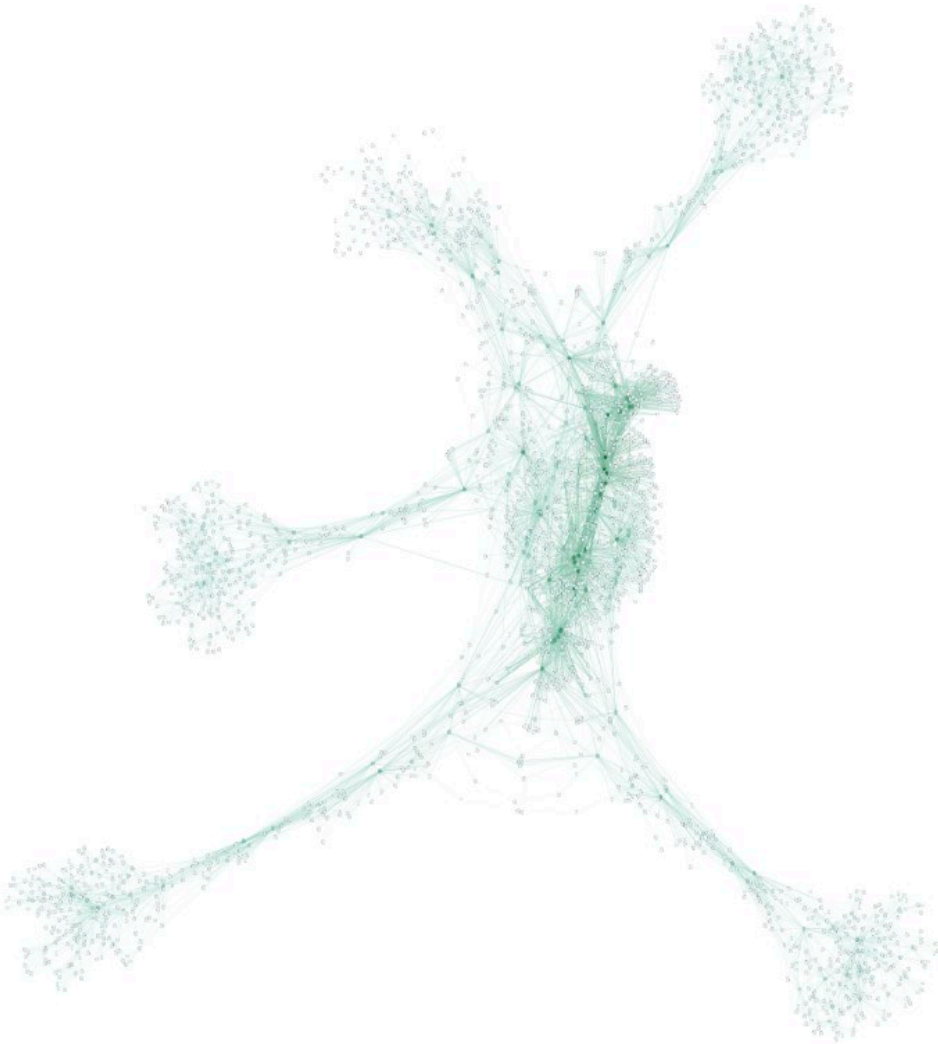
Figure 3. Cytoscape Rendering imported in Gephi.

Conclusions

By applying certain concepts of tensegrity to the human body, in this study it has been possible to develop a complete anatomical network of the locomotor system and its graphical representation. The resulting network is well representative of the different anatomical parts of the locomotor system and describes important structural characteristics of the system and of their interdependent relationships. This result can be a useful means for further understanding the musculoskeletal system and designing better targeted treatment and therapy of disease.
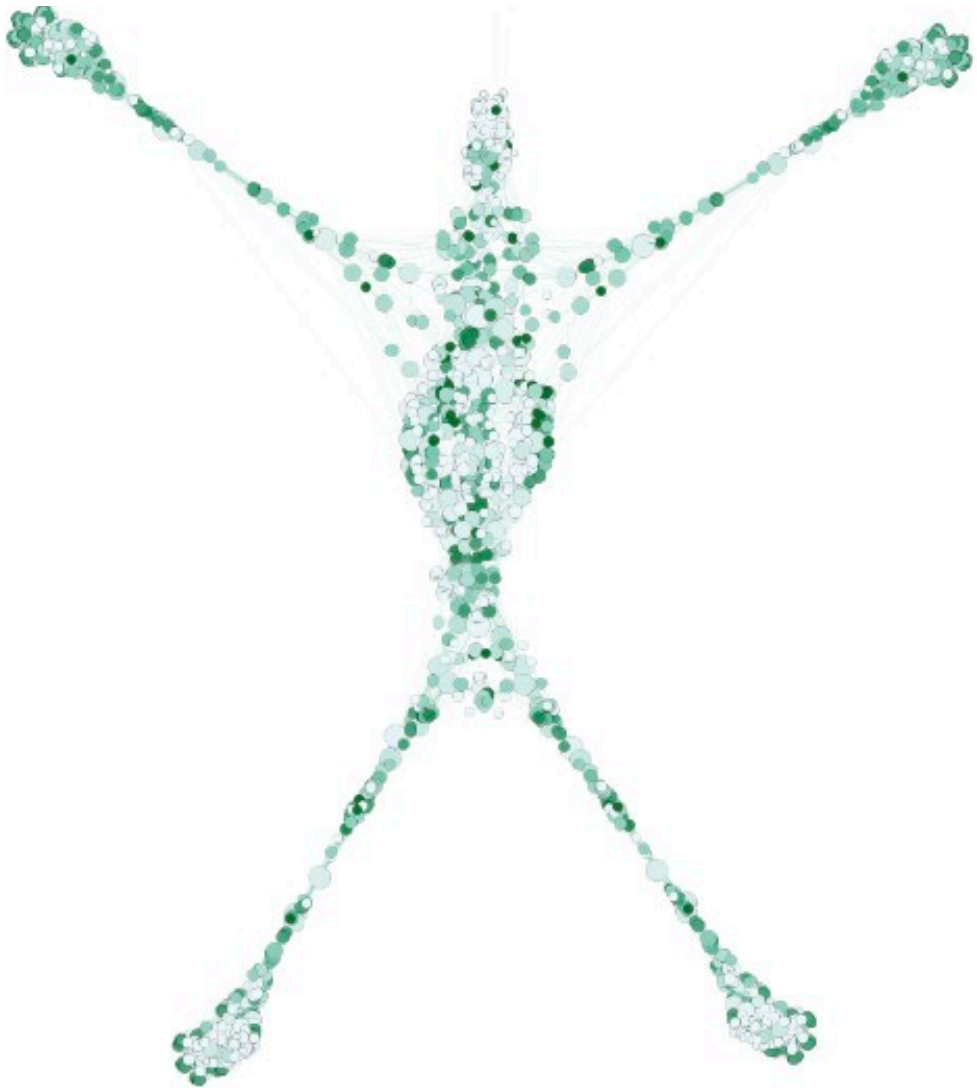
Figure 4. Anatomical network rendering with ForAtlas 2.

Acknowledgements
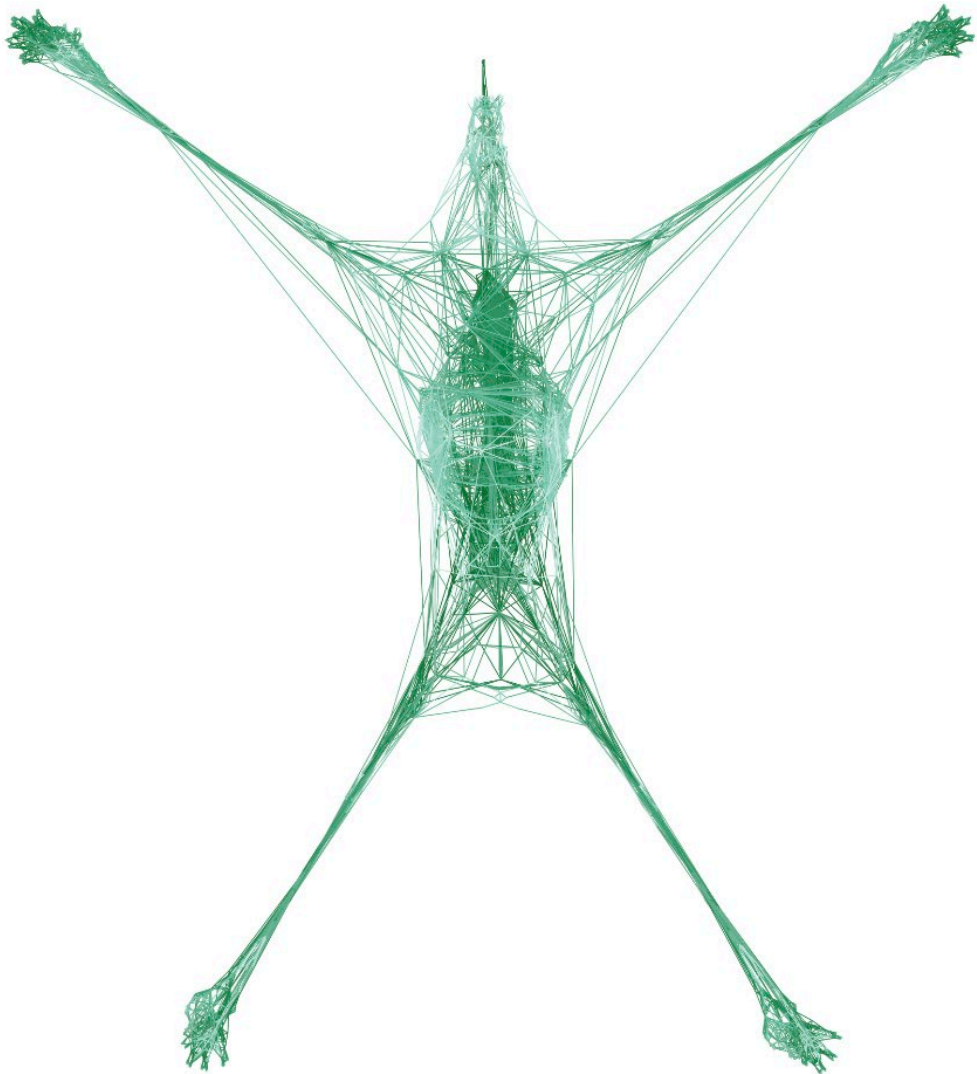
Figure 5. Final rendering of the anatomical network of human locomotor system.

References

Anichini R., Policardo L., Lombardo F.L., Salutini E., Tedeschi A., Viti S., Francia P., Brocco E., Maggini M., Seghieri G., De Bellis A. (2017) Hospitalization for Charcot neuroarthropathy in diabetes: A population study in Italy. Diabetes Res. Clin. Pract. 129: 25-31.

Bolwijn P.H., Baars H.M. J., Kaplan C.D., van Santen-Hoeufft M.H.S., van der Linden S. (1996) The social network characteristics of fibromyalgia patients compared

with healthy controls. Arthritis Care Res. 9: 18-26.

Boonstra T. W., Danna-Dos-Santos A., Xie H., Roerdink M., Stins J.F., Breakspear M. (2015) Muscle networks: Connectivity analysis of EMG activity during postural control. Sci. Rep. 5: 17830.

Bullmore E., Sporns O. (2009) Complex brain networks: graph theoretical analysis of structural and functional systems. Nat. Rev. Neurosci. 10: 186-198.

Burt R.S. (2004) Structural holes and good ideas. Am. J. Sociol. 110: 349-399.

Chen C.S., Ingber D.E. (1999) Tensegrity and mechanoregulation: from skeleton to cytoskeleton. Osteoarthritis Cartilage 7: 81-94.

De Vico Fallani F., Richiardi J., Chavez M., Achard S. (2014) Graph analysis of functional brain networks: practical issues in translational neuroscience. Philos. Trans. R. Soc. Lond. B Biol. Sci. 369: 20130521.

Dischiavi S.L., Wright A.A., Hegedus E.J., Bleakley C.M. (2018) Biotensegrity and myofascial chains: A global approach to an integrated kinetic chain. Med. Hypotheses 110: 90-96.

Diogo R., Esteve-Altava B., Smith C., Boughner J.C., Rasskin-Gutman D. (2015) Anatomical network comparison of human upper and lower, newborn and adult, and normal and abnormal limbs, with notes on development, pathology and limb serial homology vs. homoplasy. PLoS One 10: e0140030.

Esteve-Altava B., Marugán-Lobón J., Botella H., Rasskin-Gutman D. (2011) Network models in anatomical systems. J. Anthropol. Sci. 89: 175-184.

Esteve-Altava B., Diogo R., Smith C., Boughner J.C., Rasskin-Gutman D. (2015) Anatomical networks reveal the musculoskeletal modularity of the human head. Sci. Rep. 5: 8298.

Fling B.W., Cohen R.G., Mancini M., Carpenter S.D., Fair D.A., Nutt J.G., Horak F.B. (2014) Functional reorganization of the locomotor network in Parkinson patients with freezing of gait. PLoS One 9: e1002.

Francia P., Anichini R., Seghieri G., De Bellis A., Gulisano M. (2018) History, prevalence and assessment of limited joint mobility: from stiff hand syndrome to diabetic foot ulcer prevention. Curr. Diabetes Rev. 14: 411-426.

Francia P., Perella A., Sorelli M., Toni S., Piccini B., Sardina G., Gulisano M,. Bocchi L. (2017) A mathematical model of the effect of metabolic control on joint mobility in young type 1 diabetic subjects. CMBEBIH - IFMBE Proceedings; Springer, Singapore. 62:355-359. https://doi.org/10.1007/978-981-10-4166-2_54

Friedkin N.E. (1981) The development of structure in random networks: an analysis of the effects of increasing network density on five measures of structure. Social Networks 3: 41-52.

Ingber D.E. (2008) Tensegrity and mechanotransduction. J. Bodyw- Mov- Ther. 12: 198–200.

Jacob R., Harikrishnan K.P., Misra R., G. Ambika. (2017) Measure for degree heterogeneity in complex networks and its application to recurrence network analysis. R. Soc. Open Sci. 4: 160757.

Levin S.M. (2002) The tensegrity-truss as a model for spine mechanics: Biotensegrity. J. Mech. Med. Biol. 02: 375-388.

Liu X., Zhan Q. (2013) Description of the human hand grasp using graph theory. Med. Eng. Phys. 35: 1020-1027.

Makagon M.M., McCowan B., Mench J.A. (2012) How can social network analysis

contribute to social behavior research in applied ethology? Appl. Anim. Behav. Sci. 138: 152-161.

Mason O., Verwoerd M. (2007) Graph theory and networks in biology. IET Syst. Biol. 1: 89-119.

Murphy A.C., Muldoon S.F., Baker D., Lastowka A., Bennett B., Yang M., Bassett D.S. (2018) Structure, function, and control of the human musculoskeletal network. PLoS Biol. 16: e2002811.

Opsahl T., Agneessens F., Skvoretz, J. (2010). Node centrality in weighted networks: Generalizing degree and shortest paths. Social Networks 32: 245-251.

Swanson R.L. 2nd. (2013) Biotensegrity: A unifying theory of biological architecture with applications to osteopathic practice, education, and research - a review and analysis. J. Am. Osteopath. Assoc. 113: 34-52.

Tahir N., Hussain A., Samad S.A., Husain H. (2007) Shock graph for representation and modeling of posture. ETRI J. 29: 507-515.

Thome N., Mérad D., Miguet S. (2006) Human body part labeling and tracking using graph matching theory. Proc. IEEE Int. Conference on Video and Signal Based Surveillance (AVSS'06): 38-43; ; doi: 10.1109/AVSS.2006.59.

van Wijk B.C., Stam C.J., Daffertshofer A. (2010) Comparing brain networks of different size and connectivity density using graph theory. PLoS One 5: e13701.

Zhang S., de la Haye K., Ji M., An R. (2018) Applications of social network analysis to obesity: a systematic review. Obes. Rev. E19: 976-988.

Morphology of the caudate lobe of the liver in a Caribbean population

Michael T. Gardner[1], Shamir O. Cawich[2],*, Yuxue Zheng[1], Ramanand Shetty[1], Diane E. Gardner[1], Vijay Naraynsingh[2], Neil W. Pearce[3]

[1] Faculty of Medical Sciences, University of the West Indies, Mona Campus, Kingston 7, Jamaica
[2] Department of Clinical Surgical Sciences, University of the West Indies, St. Augustine Campus, St. Augustine, Trinidad & Tobago
[3] University Surgical Unit, Southampton General Hospital , Southampton, United Kingdom

Abstract

There have been no prior reports of the morphology of the caudate lobe of the liver in a Caribbean population. We sought to document the variations in caudate surface anatomy in this population. Two independent investigators observed 56 consecutive cadaveric dissections over a period of five years. Each liver was explanted using a standardized technique. The caudate lobe was observed and standardized measurements were taken using electronic calipers. There were 56 cadavers dissected over the study period. Morphologic anomalies of the caudate lobe were present in 64% of unselected persons in this Caribbean population. These included the presence of a linguiform process (64.3%), absence of a caudate process (28.6%), presence of an inferior caudate notch (21.4%), the presence of a vertical caudate fissure (19.6%) and the presence of a papillary process (10.7%). The caudate fissure co-existed with a caudate notch in 91.6% of our population. Only 36% of persons in this Caribbean population had normal caudate lobe anatomy. These variations carry clinical significance and are of importance to any clinician treating liver diseases in persons of Caribbean extract. This population has the highest prevalence of a linguiform process (64.3%) to be reported in medical literature. It is unclear why the incidence was so high in this Caribbean population, but it is tempting to think that there might be an ethnic predisposition since the majority of cadavers in our study were of Afro-Caribbean ethnicity (91.1%).

Introduction

The caudate lobe of the liver was originally assigned the name "Lobus Exiguus" by Adrien van den Spieghel in 1622 (Van den Spieghel and Casseri, 1627). It was later renamed "Spieghel's Lobe" by Glisson et al. (1654) and as then "segment I" by Couinaud (1957).

In classic anatomic descriptions, the caudate lobe is a projection from the posterior hepatic surface that is elongated vertically (Sibulesky et al., 2013). It is bounded on the left by the fissure for the ligamentum venosum, anteriorly by the porta hepatis and on the right by the groove for the inferior vena cava (IVC) (Dodds et al., 1990;

---

* Corresponding author. E-mail: socawich@hotmail.com

Sibulesky et al., 2013; Sagoo et al., 2018). Superiorly, the caudate lobe continues into the superior surface of the right upper end of the fissure for the ligamentum venosum (Dodds et al., 1990; Sibulesky et al., 2013; Sagoo et al., 2018). From the visceral surface of the liver, two parts of the normal caudate lobe are described: (1) Spieghel's lobe (Couinaud's segment I) to the left of the IVC and (2) the para-caval portion (so-called caudate process) that extends anterior to the IVC toward the right half of the liver. A thin bridge of parenchyma, known as the caudate isthmus, joins these parts. This classic anatomy is demonstrated in figures 1 and 2.

Many authors have previously described variations in the surface anatomy of the caudate lobe (Auh et al., 1984; Chang et al, 1989; Dodds et al., 1990; Sahni et al., 2000; Murakami and Hata, 2002; Sagoo and Agnihotri, 2009; Sibulesky et al., 2013; Chavan and Wabale, 2014; Sagoo et al., 2018), but to the best of our knowledge the variations have not been evaluated in a Caribbean population. This is important information for any clinical practitioners treating liver disorders in patients of Caribbean extraction.

Figure 1. Normal caudate lobe (sI) displayed on the dissection bench, as seen from the visceral surface of the liver. The boundaries of the caudate lobe are labeled as follows: porta hepatis (broken line), fissure for sinus venosum (white arrow), groove for inferior vena cava (IVC), quadrate lobe (sIVb), segment II of left liver (sII), segment VI of right liver (sVI). The normal caudate process can be seen in this image (asterix).
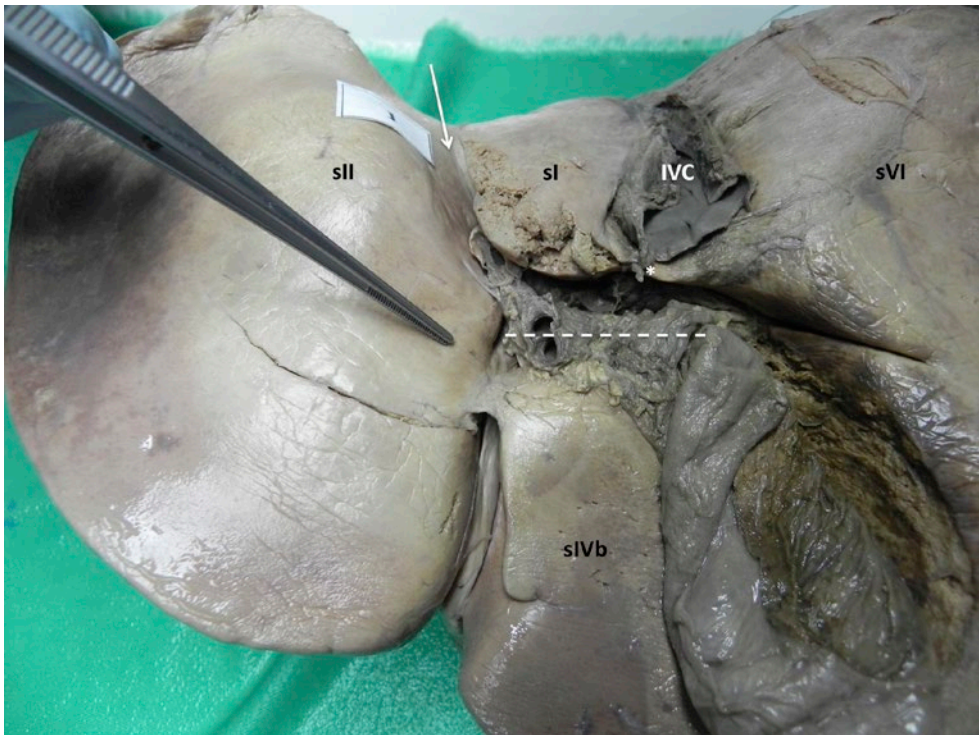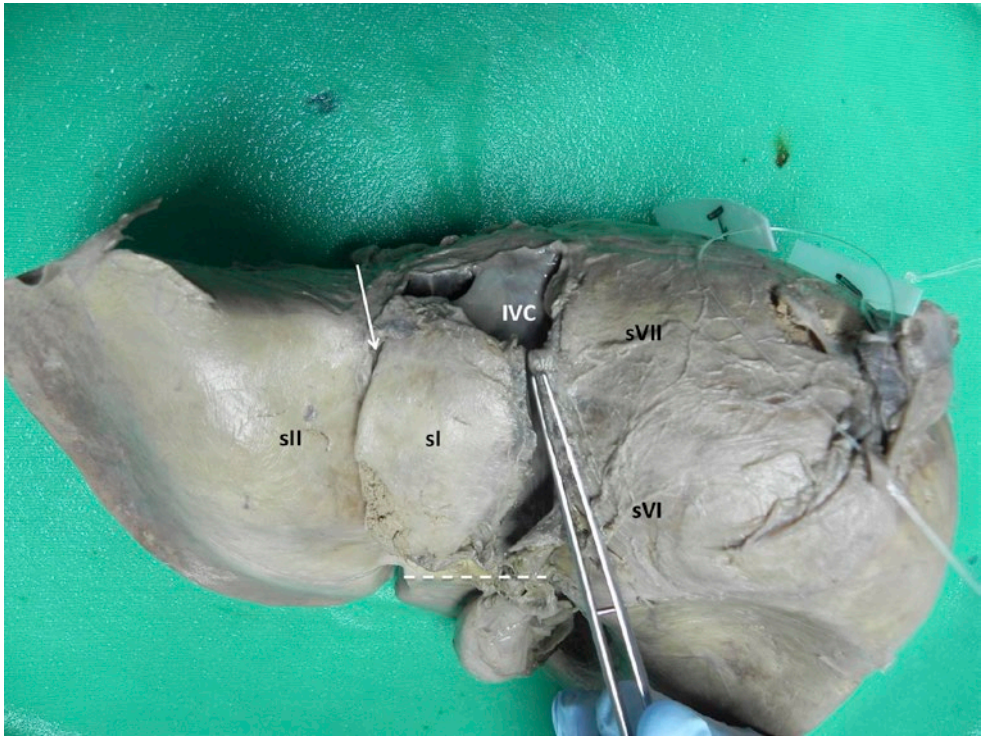
Figure 2. Normal caudate lobe (sI) displayed on the dissection bench, as seen from the retro-peritoneal bare area of the liver. The boundaries of the caudate lobe are marked: porta hepatis (broken line), fissure for sinus venosum (white arrow), groove for inferior vena cava (IVC), segment II of left liver (sII), segment VI of right liver (sVI) and segment VII of the right liver (sVII).

Material and Methods

Cadaver dissections were performed to facilitate anatomical teaching for post-graduate surgical residents at the University of the West Indies in Jamaica. Two independent investigators observed all consecutive cadaveric dissections at this facility over a period of five years. Upon opening the abdomen, the liver was inspected in situ to evaluate any deviations from classic anatomy (Sibulesky et al., 2013). The hepato-duodenal ligament was transected at the upper border of the pancreas. The IVC was transected 5 cm superior and inferior to the liver surfaces. The ligamentous attachments were then dissected to completely explant each liver.

Once the liver was explanted, gross observation of each caudate lobe was carried out on the dissection bench. When observing the caudate lobe, the classic descriptions of caudate lobe anatomy were considered. We recorded the height, width and depth of the caudate lobe using electronic calipers (General Tools, MFg Co., New York, USA). Each dimension was measured independently by one of two investigators and the average measurement was used as the final dimension.

Standardized landmarks, as defined by Chavan and Wabale (2014), were used to perform measurements. The transverse diameter of the caudate lobe was measured from a vertical plane passing through the mid-point of the intra-hepatic IVC (used to mark the right extent of the caudate lobe) and the mid-point of the fissure for sinus venosum (used to make the left extent of the caudate lobe). The distance between these points was considered the width of the caudate lobe. The depth of the caudate lobe was measured from the right lateral margin of portal vein trunk at the bifurcation to the posterior-most projection from the liver. This allowed us to calculate the transverse dimension of caudate-to-right liver (CRL) ratio that is customarily measured in studies on caudate morphology (Chavan and Wabale, 2014; Arora et al., 2016).

We used standardized terminology to describe any anatomic variations that were encountered (Chang et al., 1989; Sagoo and Agnihotri, 2009, Sagoo et al., 2018) as outlined in Table 1. These variations included: caudate agenesis (Chavan and Wabale, 2014; Arora et al., 2016), the presence of a papillary process (Sagoo et al., 2018), the presence of a linguiform process (Chang et al., 1989; Sagoo and Agnihotri, 2009, Sahni et al, 2000), the presence of a caudate fissure (Auh et al., 1984) and the presence of a caudate notch (Auh et al., 1984).

Many authors also described variations in the shape of the caudate lobe (Auh et al., 1984; Kogure et al., 2000; Sahni et al., 2000; Sagoo and Agnihotri, 2009; Chavan and Wabale, 2014; Sarala et al., 2015; Arora et al., 2016). We used these standardized descriptions, as outlined in table 2, to describe the variations encountered in our dissections.

All data were entered into a Microsoft excel worksheet and then analyzed using the Statistical Package for Social Sciences (SPSS) version 14. Descriptive analyses were generated as appropriate. Data were expressed as frequencies or means, with standard deviations as appropriate. A two-tailed P value was calculated for variables of interest in each group using Fisher's exact test. Continuous variables in each group were compared using paired T-Test. A P value <0.05 was considered statistically significant.

Results

There were 56 cadavers dissected over the study period and 20 (36%) demonstrated classic anatomy of the caudate lobe. In these cadavers, the caudate had a mean height of 52.6 mm (standard deviation +/-11.13), mean width of 32.17 mm (standard deviation ± 6.30) and mean antero-posterior diameter of 29.25 mm (standard deviation ± 9.69). The CRL ratio ranged from 0.21-0.48 (mean 0.34; standard deviation ± 0.066). When the mean CRL ratios were compared between cirrhotic and non-cirrhotic livers, we found no statistically significant difference between the groups (0.373 vs 0.330 respectively; P 0.2264; 95%CI -0.1126 to 0.0276). A caudate process was present in 40 (71.4%) cadavers.

There were variations from classic anatomy in 36 (64%) cadavers. There were no cadavers with caudate agenesis. Sixteen (28.6%) cadavers did not have a normal caudate process present.

A papillary process was present in 6 (10.7%) cadavers (figure 3). The papillary processes had a mean length of 21.4 mm (standard deviation ± 6.7) and mean thickness of 15.9 mm (standard deviation ± 5.5).
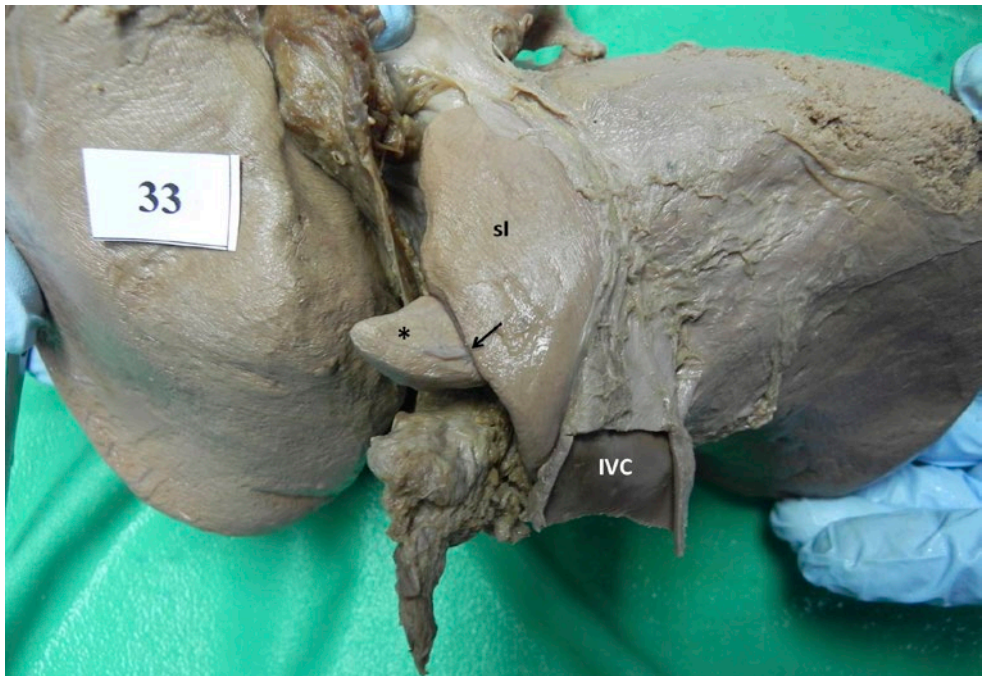
Figure 3. A well-developed papillary process (asterix) is seen extending from the infero-medial part of the caudate lobe proper (sl) and passing to the left into the region of the superior recess of the omental bursa. A caudate notch is also present in this specimen (arrow).

A linguiform process was identified in 36 (64.3%) cadaveric livers, covering the retro-hepatic IVC to varying degrees (figures 4, 5). The linguiform processes had a mean thickness of 2.75 mm (standard deviation ± 0.14).

There were 12 (21.4%) cadavers with (horizontal) caudate notches at the inferior border of the caudate (figures 3,4,6). The caudate notches had a mean depth of 10.3 mm (standard deviation ± 7.3). Eleven (19.6%) cadavers also had well-defined (vertical) caudate fissures that appeared to bisect the caudate lobe (figure 7). The vertical fissures had a mean height of 16.5 mm (standard deviation ± 1.52) and a depth of 6.52 mm (standard deviation ± 3.28).

A few caudate lobes were irregularly shaped as outlined in table 2. We encountered one shape (1.8%) for which we could not find an existing description. We could best describe it as "fish-tailed" (figure 8) and we have not seen a comparable finding in the literature.

Discussion

Although variations in the caudate surface anatomy have been described (Auh et al., 1984; Chang et al, 1989; Dodds et al., 1990; Sahni et al., 2000; Murakami and Hata,
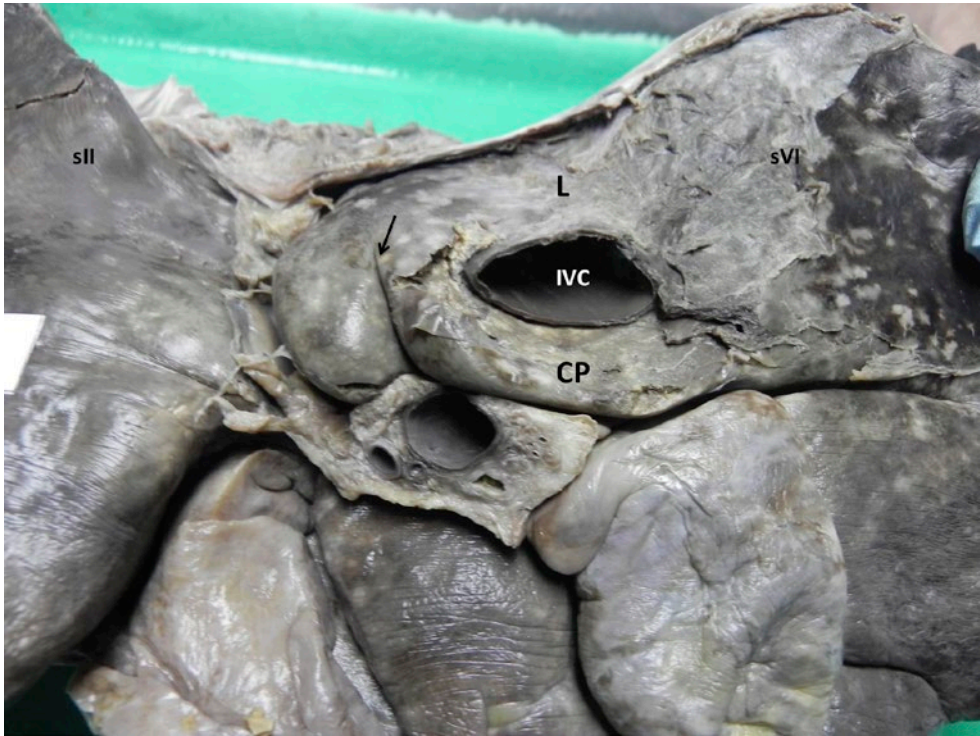
Figure 4. A well-developed linguiform process (L) that convers the groove for the inferior vena cava (IVC), completely turning it into a tunnel. A well-developed caudate process (CP) and caudate notch (arrow) are also present in this specimen.

2002; Sagoo and Agnihotri, 2009; Sibulesky et al., 2013; Chavan and Wabale, 2014, Sagoo et al., 2018), there are no existing data on variations in a Caribbean population. We found that classic anatomy of the caudate lobe was only present in 36% of unselected cadavers in this Caribbean population. The mean dimensions of the caudate lobe were generally comparable to existing literature.

An important clinical relationship is the ability to diagnose early degenerative liver conditions using the CRL ratio. Essentially, due to the independent vascular supply and biliary drainage, the caudate lobe is considered an independent part of the liver. Consequently, there will be compensatory caudate hypertrophy when the remaining liver is affected by cirrhosis. Therefore, the CRL ratio will increase to a value of greater than or equal to 0.65 in cirrhotic livers (Giorgio et al., 1986; Awaya and Mitchell, 2002; Chavan and Wabale, 2014 Arora et al., 2016). Most of the reports on caudate anatomy document the CRL ratio (Chavan and Wabale, 2014; Arora et al., 2016), but these are generally not clinically useful unless the absence / presence of cirrhotic change is noted. Chavan and Wabale (2014) documented a CRL ratio ranging between 0.28 and 0.46, Sahni et al (2000) documented a range of CRL ratios of 0.23-0.40 and Arora et al (2016) documented a CRL ratio range of 0.15-0.58 (average

Figure 5. A normal caudate lobe in which a linguiform lobe is absent. The groove for the IVC is not covered, leaving the IVC exposed. In this case, the IVC is accessible intra-operatively without dissection of linguiform parenchyma.

0.36). The range of CRL values in our study were generally comparable with previous ones. But in order for our study to be clinically relevant, we divided the livers into two groups: cirrhotic and non-cirrhotic livers. We found no statistically significant difference between the mean CRL in cirrhotic livers compared to non-cirrhotic livers.

In 64% unselected cadavers in this Caribbean population, variant anatomy of the caudate lobe was encountered. These included the following.

Papillary process

Sagoo et al (2018) proposed that a papillary process should be considered present when there was a prominent elevation, sometimes separated from the caudate lobe proper by a notch and separated by the groove for the ligamentum venosum from the left lobe of the liver and by the porta hepatis inferiorly. Using these definitions, we found the papillary process in 10.7% of our study population. The prevalence of the papillary process varies widely, from as low as 0% at Ahmednagar in west-central India (Chavan and Wabale, 2014) to 52% at London in the United Kingdom (Sagoo et al., 2018). The prevalence in this Caribbean population more closely resembled the prevalence at Bareilli in North India (Arora et al., 2016).

Figure 6. A caudate notch (arrow) is seen in this specimen. It is a groove on the visceral surface (inferior border) of the caudate lying in a horizontal plane and separating caudate proper (sl) from the para-caval / caudate process (asterix).

The presence of a papillary process has clinical significance because it could be mistaken for extra-hepatic masses or enlarged porta-hepatis nodes (Auh et al., 1984) and it may also mimic a pancreatic tumor if it extends to the left and displaces the stomach anteriorly (Auh et al., 1984). It may also interfere with the performance of a hepato-caval shunt (Heloury et al., 1988). Additionally, depending on its size, a papillary process may prevent surgeons accessing the structures in the porta hepatis when performing anatomic major liver resections. Therefore, it is important for providers treating patients with liver diseases to be aware of the presence of a papillary process in 10.7% of unselected persons with no obvious chronic liver diseases.

Linguiform process

The prevalence of a linguiform process in this population (64.3%) was greater than expected. Mamatha et al (2014) reported finding a linguiform process in 4% of persons from southwest India. Comparatively, Sagoo et al (2018) reported 40% prevalence in Caucasian populations from London. The highest prevalence was 56.7% in an observational study of 30 Parisian cadavers (Heloury et al., 1988).

It is unclear why the incidence was so high in this Caribbean population. It is tempting to think that there might be an ethnic predisposition since the major-
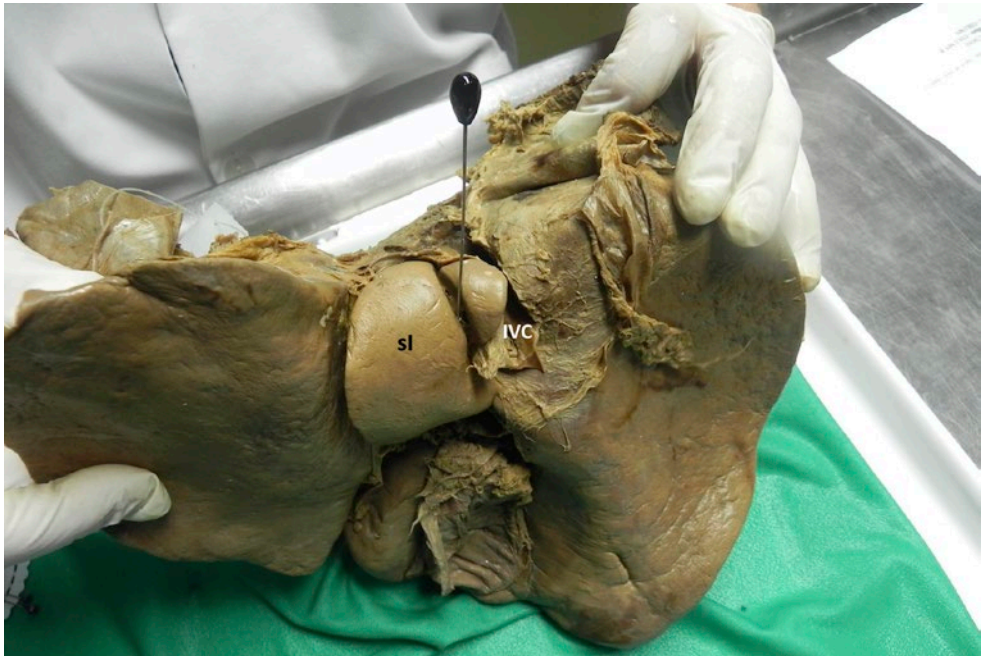
Figure 7. A caudate fissure (marked by black pin) is seen in this specimen, running in a vertical plane on the caudate proper (sl). In this image, the caudate fissure is continuous with a caudate notch inferiorly that is in a horizontal plane.

ity of cadavers in our study were of Afro-Caribbean ethnicity (91.1%). Most of the reports in print in the literature study mostly Indian (Sahni et al., 2000; Joshi et al., 2009; Sagoo et al., 2009; Chavan and Wabale, 2014; Mamatha et al., 2014; Sarala et al., 2015; Arora et al., 2016) and Caucasian populations (Heloury et al., 1988; Sagoo et al., 2018). We did not encounter any other reports that documented the prevalence of the linguiform process in predominantly black populations.

Regardless of the reason for the high prevalence, the linguiform process is an important feature because it makes access to the retro-hepatic IVC difficult during liver resections. A linguiform process is also disadvantageous during trauma operations because it makes control and repair of the IVC difficult in patients with retro-hepatic IVC injuries.

Absence of caudate process

The caudate process is a bridge of parenchyma that extends anterior to the IVC toward the right half of the liver, joined to the caudate proper by a thin bridge of parenchyma known as the caudate isthmus. Occasionally, the caudate process may be elevated and form a relatively wide roof over the porta hepatis (Sagoo et al., 2018). The caudate process is a normal anatomic feature, but it was absent in 28.6% of unselected cadavers in our study.

Figure 8. A "fish-tail" caudate lobe.

The prevalence of the caudate process varies widely, from as low as 9% in at Karnataka in south-west India (Sarala et al., 2015) to 100% at Bareilly in Northern India (Arora et al., 2016). In our population, it was present in 71.4% of unselected cadavers. It is important to be aware of the presence of the caudate process because it may also cause diagnostic confusion, being mistaken for neoplastic disease on cross sectional imaging (Auh et al., 1984). In addition, during major anatomic liver resections, the presence of a well-developed caudate process would increase the technical difficulty of performing the hanging maneuver, where a surgical instrument is passed in the potential space anterior to the retro-hepatic IVC (Cawich et al., 2015)

Inferior groove / notch of caudate

Occasionally, instead of a flat bridge of parenchyma (caudate isthmus) joining the caudate proper and the caudate process, a horizontal groove (the caudate notch) separates the caudate process from the caudate lobe proper on the visceral surface of the liver (Sagoo et al., 2018). The presence of an inferior caudate notch varies widely, with a reported prevalence ranging from 9% at Chandigarh in Northern India (Sahni et al., 2000) to 100% at Karnataka in Southwest India (Sarala et al., 2015). A caudate notch was seen in 21.4% of unselected cadavers in our population.

Kogure et al (2000) performed cast studies to study the notch at the inferior border of the caudate lobe and suggested that the notch corresponds to the presence of an underlying hepatic vein. Couinaud (1989) also reported that in 35% of cases the hepatic vein runs in this fissural plane. Therefore, the caudate notch may be used as a landmark to separate the caudate proper from the para-caval portions and to identify the presence of an underlying vein during liver resections involving the caudate lobe. Unfortunately, the notch is inconsistent and its prevalence reduces with age (Sahni et al., 2000).

Caudate fissure

The caudate fissure is a well-defined fissure in a vertical plane separating the caudate proper from the remainder of the liver (Auh et al., 1984). There are wide variations in the reported prevalence of a caudate fissure, ranging from 3.7% at Vadodara in Western India (Chaudhari et al., 2017) to 32% at Maharashtra in West-Central India (Joshi et al., 2009). The prevalence of the caudate fissure in our population was in between at 19.6%. Often, but not always, the caudate fissure co-exists with the caudate notch. We found this relationship in 91.6% of our cadavers.

Again, there is inconsistent terminology. For example, Singh et al. (2013) reported on a male cadaver in whom the caudate lobe was "*divided into two lobes by a fissure having length of 2.5 cm along with a notch on superior surface of caudate lobe and another fissure of length, 2.0 cm located in inferiorly placed caudate lobe*" Although they described this as a duplicated caudate lobe, the images in their published case report appear to show a bi-cornuate caudate with an inferior caudate notch (groove) continuous with a deep vertical fissure as described above.

Conclusions

There are morphologic anomalies of the caudate lobe in 64% of unselected persons in this Caribbean population. These included the presence of a linguiform process (64.3%), absence of a caudate process (28.6%), presence of a caudate notch (21.4%), the presence of a vertical caudate fissure (19.6%) and the presence of a papillary process (10.7%).

This population had the highest prevalence of a linguiform process (64.3%) to be reported in medical literature. It is unclear why the incidence was so high in this Caribbean population, but it is tempting to think that there might be an ethnic predisposition since the majority of cadavers in our study were of Afro-Caribbean ethnicity (91.1%).

Acknowledgements

Authors' contributions

MG, SOC, RS, NP and VN conceptualized the study. MG and RS carried out observations and collected data; MG, SOC, RS, NP, and VN checked the manuscript and endorsed the academic content.

References

Arora N.K., Srivastava S., Haque M., Khan A.Z., Singh K. (2016) Morphometric study of caudate lobe of liver. Ann. Int. Med. Dent. Res. 2: 275-79.

Auh Y.H., Rosen A., Rubenstein W.A., Englel I.A., Whalen J.P., Kazam E. (1984) CT of the papillary process of the caudate lobe of the liver. Am. J. Roentgenol. 142: 535-538.

Awaya H., Mitchell D. (2002) Cirrhosis: Modified caudate-right lobe ratio. Radiology 224: 769-774.

Cawich S.O., Thomas D., Ragoonanan V., Naraynsingh V. (2015) The hanging manoeuver to complete liver resection for a locally advanced angiosarcoma: A case report. Int. J. Surg. Case Rep. 16: 52-55.

Chang R.W.H., Sun S.Q., Yen W.W.C. (1989) An applied anatomical study of the ostia venae hepaticae and the retrohepatic segment of the inferior vena cava. J. Anat. 164: 41-47.

Chaudhari H.J., Ravat M.K., Vaniya V.H., Bhedi A.N. (2017) Morphological study of human liver and its surgical importance. J. Clin. Diagn. Res. 11: 9-12.

Chavan N.N., Wabale R.N. (2014) Morphological study of caudate lobe of liver. Indian J. Bas. Appl. Med. Res. 3: 204-211.

Couinaud C. (1957) The Liver. Anatomical and Surgical Investigations. Le Foie. Études Anatomiques et Chirurgicales. Paris, Masson.

Couinaud C. (1989) Posterior or dorsal liver. In: Couinaud C. Surgical Anatomy of the Liver Revisited. Paris, Couinaud. Pp. 123-134.

Dodds W.J., Erickson S.J., Taylor A.J., Lawson T.L., Stewart E.T. (1990) Caudate lobe of the liver: anatomy, embryology and pathology. Am. J. Roentgenol. 154: 87-93

Giorgio A., Amoroso P., Lettieri G., Fico P., de Stefano G., Finelli L., Scala V., Tarantino L., Pierri P., Pesce G. (1986) Value of caudate to right lobe ratio in diagnosis with ultrasound. Radiology 161: 443-445.

Glisson F. (1654) Anatomia Hepatis (Anatomy of the Liver). Vol. 3. Cambridge Wellcome. London,

Heloury Y., Leborgne J., Rogez J.M., Robert R., Barbin J.Y., Hureau J. (1988) The caudate lobe of the liver: Review of clinical anatomy. Surg. Radiol. Anat. 10: 83-91.

Joshi S.D., Joshi S.S., Athavale S.A. (2009) Some interesting observations on the surface features of the liver and their clinical implications. Singapore Med. J. 50: 715-719.

Kogure K., Kuwano H., Fujimaki N., Makuuchi M. (2000) Relation among portal segmentation, proper hepatic vein and external notch of the caudate lobe in the human liver. Ann. Surg. 231: 223-228.

Mamatha Y., Murthy C.K., Prakash B.A. (2014) Study on morphological surface variations in human liver. Int. J. Health Sci. Res. 4: 97-102.

Murakami G., Hata F. (2002) Human liver caudate lobe and liver segment. Anat.. Sci Int. 77: 211-224.

Sagoo M.G., Agnihotri G. (2009) The retrohepatic segment of inferior vena cava and the ostia venae hepaticae in a Northwest Indian population. Braz. J. Morphol. Sci. 26: 141-144.

Sagoo M.G., Aland R.C., Gosden E. (2018) Morphology and morphometry of the caudate lobe of the liver in two populations. Anat. Sci. Int. 93: 48-57.

Sahni D., Jit I., Sodhi L. (2000) Gross anatomy of the caudate lobe of the liver. J. Anat. Soc. India 49: 123-126.

Sarala H.S., Jyothilakshmi T.K., Shubha R. (2015) Morphological Variations Of Caudate Lobe Of The Liver And Their Clinical Implications. Int J Anat Res 3: 980-983.

Sibulesky L. (2013) Normal liver anatomy. Clin. Liver Dis. 2: 1-3.

Singh R., Singh K., Man S. (2013) Duplicate caudate lobe of liver with oblique fissure and hypoplastic left lobe of liver. J. Morphol. Sci. 30: 309-311.

van den Spieghel A., Casseri G.C. (1627) De Humani Corporis Fabrica Libri Decem. Venice, Evangelista Deuchino.

The Martin-Gruber Anastomosis in Bosnian population: an anatomical study

Renata Hodzic[1,*], Ermina Iljazovic[2], Nermina Piric[1], Sanela Zukić[1]

[1] Department of Neurology, University Clinical Centre Tuzla, Bosnia and Herzegovina
[2] Deparment of Pathology, University Clinical Centre Tuzla, Bosnia and Herzegovina

Abstract

The Martin-Gruber anastomosis (MGA) is the anastomosis in which the anastomotic branch originates proximally from the median nerve (MN) and unites distally with the ulnar nerve (UN). This is the most common form of "anomalous" innervation that have been reported in the upper part of the forearm. This study has a purpose to report the incidence, type, topography of MGA found and access the lenght and diameter of these anastomosis. For this study, 60 anterior forearms (30 right and 30 left) from adult adavers were dissected. The presence of MGA was verified in 18,33% forearms. Single MGA anastomosis was found in 90,9%, corresponding to type A in 10%, type B in 10% and type C in 80%, while double MGA was found in 9,1%, both been duplification of type C. Anastomoses were found mainly on the right side in anatomical examination (seven against four). No statistically significant difference was found between men and women regarding the frequency of the MGA. In pattern I, the course of of MGA was transveral in 90% of cases, and arched in 10%, while in pattern II, the superior connection was tranversal and the inferior was oblique. The MGA passed in front of the ulnar artery in 3 cases and behind in 9 cases. The average length of the anastomosis was 6.2 cm, while the average diameter was 1.14 mm. The anastomoses between MN and UN are clinically relevant so therefore the knowledge of the existance of the MGA in the forearm, types of presentation and topography is extremely important for the correct diagnosis of neuropathies as well as essential to diferrentiate a complete damage from a partial injuries of peripheral nerves.

Keywords

Nervus medianus, nervus ulnaris, Martin-Gruber anastomosis.

Introduction

The Martin-Gruber anastomosis (MGA) is the anastomosis in which the anastomotic branch originates proximally from the median nerve (MN) and unites distally with the ulnar nerve (UN). This is the most common form of "anomalous" innervation that have been reported in the upper part of the forearm. The MGA was first described by Martin in 1763 (8). First, he described a branch between the MN and UN that sometimes runs under the pronator teres muscle, and also a connection between MN and UN in the palm which he called the "arcus volaris nervorum". In 1870, Gruber dissected 212 forearms and found in 38 forearms that nerve branches coursed from the MN proximally to the to the UN distally (2). MGA has been reported to occur in 15-31% of subjects (7,18). Most often the anomalous axons innervate

* Corresponding author. E-mail: renata.hodzic@ukctuzla.ba

the first dorsal interosseous muscle and less often the hypothenar and thenar muscles (3).

The purpose of our research was to determine the incidence and also the characteristics of MGA anastomosis in the Bosnian population. We also compared our results to those of similar previous studies.

Material and Methods

Sixty anterior forearms of fresh frozen adult cadavers were dissected in the Department for pathology of University Clinical Centre Tuzla and the morgue of Tuzla during a time period of two years. The forearms with traumatic lession that unables dissection are not included in the study. The forearm is placed in the position of supine. An 'S' shaped incision from the lower limit od cubital fossa to the radiocarpal joint was carried out. This type of incision covered the whole anterior surface of the forearm. The superficial fascia was opened and the flexor carpi ulnaris muscle and tendon mobilised to give full exposure of the ulnar artery and UN. The branches of the UN in the forearm were dissected and all possible anastomoses between MN and UN were documented. The level at which the connections joined the MN and UN was measured using the medial epicondyle of the humerus as reference (point 0). The NM, NU and their branches were carefully dissected with the aid of magnifying glasses. The lenght and diameter of anastomosis were measured with a caliper. All anatomical parts were photographed in order to register the anatomical arrangement and the relation with adjacent structures. Statistical comparisons were performed using the chi-squared test. P < 0.05 was regarded as statistically significant.

Results

Out of sixty forearms (30 left and 30 right), 46 belonged to males and 14 to females. The age of cadavers ranged from 22 to 73 years (fig. 1). The lenght of cadavers ranged from 162 to 185 centimeters while the lenght of dissected forearms measured from cubital fossa to radiocarpal joint ranged from 24,5 to 27 centimeters. The presence of MGA was verified in 11 (18,33%) forearms which were studied. Single anastomosis was found in 10 (90,9%) forearms-pattern 1, while in one forearm we found 2 (1,67%) anastomosis in the left forearm-pattern 2 (fig. 2). It occurred in 6 of the 46 male cadavers (1 bilateral, 3 only in the right and 1 only in the left forearm) and in 5 of the 14 female cadavers (1 bilateral, 2 only in the right forearm and 1 only in the left forearm).Therefore, the MGA was found in 11 of the 60 forearms, which were dissected. These anastomoses were classified into three types depending on the level of origin of the anastomosis from the MN. Type A originates from the branch of the MN to the superficial forearm flexor muscles, type B from the MN itself and type C from the anterior interosseous nerve. Out of 10 single MGA, type A occurred in 1 case (10%), type B in 1 (10%) and type C in 8 cases (80%) while double MGA was found in 1 (9,1%) case, both being a duplification of type C. MGA was registered in 75% in one hand, and in 25% in both hands. Out of 6 unilateral MGA, 83,33% was registered in right and 16,67% in left hand what is statistically significant (p=0,01). No
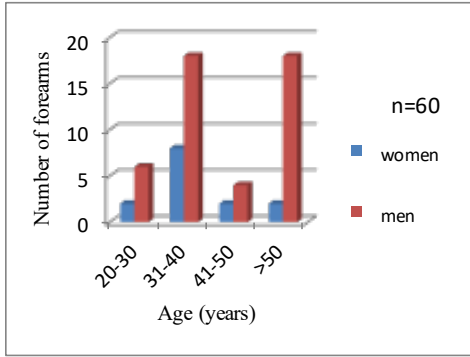
Figure 1. Dissected forearms according to age and sex.
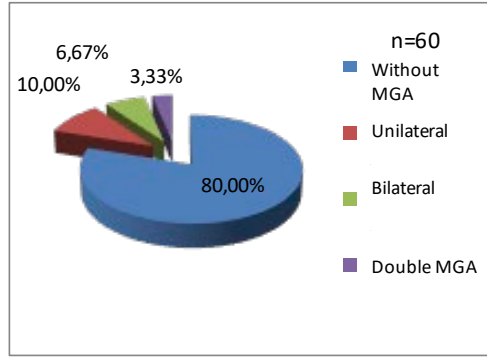
Figure 2. The incidence of Martin-Gruber anastomosis.

statistically difference was found between men and women regarding the frequency of MGA (p=0,53). In pattern I, the course of of MGA was transveral in 9 (90%) cases, and arched in 1 (10%) while in pattern II, the superior connection was tranversal and the inferior was oblique. The MGA passed in front of the ulnar artery in 3 cases and behind in 9 cases. The average length of the anastomosis was 6.2 cm while the average diameter was 1.14 mm (fig. 3). Its origin was on average 6.6 cm distal to the medial epicondyle, and its connection to the UN was on average 11.2 cm distal to the medial epicondyle.

A   B.
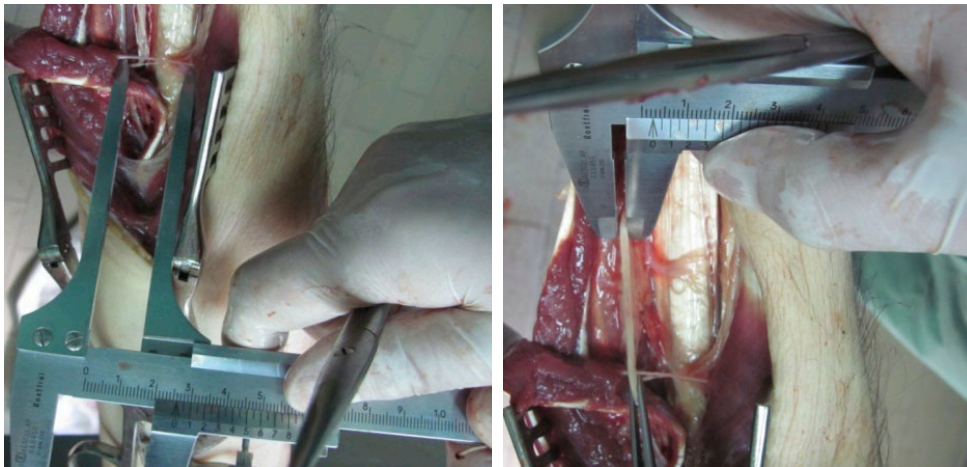
Figure 3. The lenght and diameter of Martin-Gruber anastomosis.

Discussion

Anastomoses between MN and UN occur frequently in humans so therefore they are considered aa a variation rather than an anomaly. In the forearms of 15% to 31% of individuals, motor axons descend from the MN, crossing to the UN, and ultimately innervating intrinsic hand muscles which are normally supplied by the UN (7,18). There is no consensus in the literature about the classification of anastomosis between the two nerves (5). Classifications based on anatomical dissections have been proposed by Nakashima (9), Hirasawa (4), Thomson (16), Shu et al. (13), Srinivasan and Rhodes (14) and Rodriguez-Niedenfuhr et al. (11). Uchida and Sugioka (17), Oh et al. (10) and Kimura et al. (6) proposed classifications based on electrophysiological examinations while Shu (13) proposed classification based on histological examinations (5). The incidence of anastomosis between the two nerves in earlier reports was 15.2% according to Gruber (2), 15.5% according to Thomson (16), 10.5% according to Hirasawa (4), 15.5% according to Mannerfelt (7), 23% according to Taams (24), 21.3% according to Nakashima (9), 13.1% according to Rodriguez-Niedenfuhr et al. (11). Mannerfelt (7) was the first to use electrodiagnostic techniques to detect anastomosis between the two nerves and reported a 15% incidence, while other authors, using the same technigue have reported incidences ofanastomosis ranging from 15% to 39% in normal or unselected subjects. The highest incidence of the anastomosis was found for the first dorsal interosseous muscle (FDI). Wilbourn and Lambert (18) reported that anomalous axons innervate the FDI muscle much more commonly (95%) than the hypothenar (41%) and thenar muscles (14%). We compared our results to those of previous reports. Pattern I comprises cases with one anastomotic branch, and Pattern II those with two anastomotic branches. Types A, B, and C are subdivisions depending on the level of origin of the anastomosis from the MN. Type A originates from the branch of the MN to the superficial forearm flexor muscles; type B from the MN itself and type C from the anterior interosseous nerve. In our study, the incidence of the MGA was 18,33%. Single MGA anastomosis was found in 90,9%, corresponding to type A in 10%, type B in 10% and type C in 80%, while double MGA was found in 9,1%, both been duplification of type C. Our results confirm that the anastomosis appears as single or double branch with various origins from the MN or its branches, as already described by Thomson (16), Srinivasan and Rhodes (14) and Taams(15). The unilateral MGA occurs more often on the right side than on the left (15). In our study anastomoses were also found mainly on the right side in anatomical examination (seven against four). No statistically significant difference was found between men and women regarding the frequency of these anastomoses. The course of the anastomosis has been more frequently described as transverse or oblique than arched (2,4). We found that in pattern I, the course of MGA was transversal in 9 cases and arched in 1 case, while in pattern II, the superior connection was transversal and the inferior was oblique. MGA passed in front of the ulnar artery in 3 cases and behind in 9 cases.

The anastomoses between MN and UN are clinically relevant. These connections are often suggested as causes for unusual motor losses of the muscles in the hand after peripheral nerve lesions (1,12). The knowledge of the existance of the MGA in the forearm, its types of presentation and topography is extremely important for the correct diagnosis of neuropathies, essential to differentiate a complete damage from a partial injuries and to prevent complications during surgical procedures.

References

1. Cliffton E (1948) Unusual innervation of the intrinsic muscles of the hand by median and ulnar nerve. Surgery 23:12-31.
2. Gruber W (1870) Uber die Verbindung Des Nervus medianusmit dem Nervus ulnaris am Unterarme des Menschen undder Saugethiere. Arch Anat Physiol Wissen Med 3.
3. Gutmann L (1993) AAEM minimonograph: important anomalous innervations of the extremities. Muscle Nerve 16: 339-347.
4. Hirasawa K (1931) Untersuchungen uber das periphere Nerven-system, Plexus brachialis und die Nerven der oberen Extremität. Arb Anat Inst Kaiserlichen Univ Kyoto A2: 135-136.
5. Kazakos K, Smyrnis A, Xarchas K, Dimitrakopoulou A, Verettas DA (2005) Anastomosis between the median and ulnar nerve in the forearm. An anatomical study and literature review. Acta Orthop Belg 71:29-35.
6. Kimura J, Murphy MJ, Varda DJ (1976) Electrophysiological study of anomalous innervation of intrinsic hand muscles.Arch Neurol 33: 842-844.
7. Mannerfelt L (1966) Studies on the hand in ulnar nerve paralysis. A clinical-experimental investigation in normal and anomalous innervation. Acta Orthop Scand 87(2): 19-29.
8. Martin R (1763) Tal om nervus allmanna Egenskaperi Mannisikans Kropp. Las Salvius.
9. Nakashima T (1993) An anatomic study on the Martin-Gruber anastomosis. Surg Radiol Anat 15: 193-195.
10. Oh SJ, Claussen GC, Ahmad BK (1995) Double anastomosis of median-ulnar and ulnar-median nerves: report of an electrophysiologically proven case. Muscle Nerve 18: 1332-1334.
11. Rodriguez-Niedenfuhr M, Vazquez T, Parkin I,Logan B, Sanudo JR (2002) Martin-Gruber anastomosis revisited. Clin Anat 15: 129-134.
12. Rowntree T (1949) Anomalous innervation of the hand muscles. J Bone Joint Surg 31-B: 505-510.
13. Shu H, Chantelot C, Oberlin C, Alnot JY, Shao H (1999) Anatomic study and review of the literature on the Martin-Gruber anastomosis. Morphologie 83: 71-74.
14. Srinivasan R, Rhodes J (1981) The median-ulnar anastomosis (Martin-Gruber) in normal and congenitally abnormal fetuses. Arch Neurol 38: 418-419.
15. Taams KO (1997) Martin-Gruber connections in South Africa. An anatomical study. J Hand Surg 22-B: 328-330.
16. Thomson A (1893) Third annual report of the Committee of Collective Investigations of the Anatomical Society of Great Britain and Ireland for the years 1891-1892. J Anat 27: 183-194.
17. Uchida Y, Sugioka Y (1992) Electrodiagnosis of Martin-Gruber connection and its clinical importance in peripheral nerve surgery. J Hand Surg 17-A: 54-59.
18. Wilbourn AJ, Lambert EH (1976). The forearm median to ulnarnerve communication: electrodiagnostic aspects. Neurology 26:368.

Morphometric evaluation of the infraorbital foramen in human dry skulls of South Indian population

Bhagath Kumar Potu[1,*], Gowtham Chandra Srungavarapu[2], Thejodhar Pulakunta[3]

[1] Department of Anatomy, College of Medicine and Medical Sciences, Arabian Gulf University, Bahrain
[2] Department of Oral and Maxillofacial surgery, Dental College and Hospital, RGUHS, India
[3] Department of Medical Neuroscience, Faculty of Medicine, Dalhousie University, Halifax, Nova Scotia, Canada

Abstract

The aim of this study was to determine the location of the infraorbital foramen (IOF) in relation to infraorbital margin (IOM), anterior nasal spine (ANS) and Nasion (NA), Supraorbital margin (SOM) and sockets of the maxillary teeth in adult skulls (of South Indian population). Fourteen skulls (28 sides) have been analyzed. In order to analyse the size and the relative position of the IOF with the above parameters, we have used a digital caliper for measurements with a precision of 0.01 mm. The IOF was oval in shape (85.7 %) on right side and (71.4 %) on left side while none of them were found either in semilunar or triangular shape in contrast to previous reports. In most of the cases IOF was found to be situated lateral to the plane of SOM. The vertical and transverse diameter of the IOF on both sides was found to be almost equal. The mean distance and standard deviation (mean ± SD) between right IOF and ANS, IOM and NA were 33.6 ±2.22 mm, 5.49± 1.10 mm and 41.4± 3.27 mm respectively, while the mean ± SD between left IOF and ANS, IOM and NA were 33.1 ± 2.30 mm, 5.85 ±1.06 mm and 40.3 ± 3.09 mm respectively. The results obtained from descriptive analysis are relevant and help surgeons for blocking the infraorbital nerve while performing surgeries in midface region, particularly in patients with edema of the infraorbital region when precise location of the IOF is difficult.

Introduction

Infraorbital region, particularly the infraorbital foramen is an important site for various surgical and anesthetic procedures. The infraorbital nerve, which is the continuation of the second (maxillary) division of the trigeminal nerve passes through it and is responsible for the sensory innervation of the lower eyelid, nasal ala, upper lip, the anterior, premolar teeth and associated gingiva (Standring, 2008). The classical location of the infraorbital foramen (IOF) is seen on the external anterior surface of the maxilla below the infraorbital margin. Precise localization of the foramen is the key to success in blocking this nerve and this can be challenging due to its anatomical variation in its shape and size (Zide & Swift, 1998). We have undertaken this study to determine a more precise location of the IOF in relation to the infraorbital margin (IOM), nasion (NA) and anterior nasal spine (ANS) and also to measure its

* Corresponding author. E-mail: potubk@agu.edu.bh

shape, location with reference to the plane of supraorbital margin (SOM), molar and premolar teeth respectively to derive an accurate reference point to locate the IOF and its structures in clinical situations such as surgery and anesthetic procedures. Multiple studies have been attempted to determine the position of IOF with nearby landmarks and have shown to vary among population groups. And standard text books show that the IOF is located approximately 1 cm inferior to the IOM. However, various studies reported that this range may vary between 6-12mm respectively (Hindy & Abdel-Raouf, 1993; Chung *et al.*, 1995; Canan *et al.*, 1999; Aziz *et al.*, 2000; Kazkayasi *et al.*, 2001; Karakas *et al.*, 2002; Elias *et al.*, 2004; Agthong *et al.*, 2005; Apinhasmit *et al.*, 2006; Gupta, 2008; Lopes *et al.*, 2009; Macedo *et al.*, 2009; Ilayperuma *et al.*, 2010; Boopathi *et al.*, 2010; Singh, 2011; Lokanayaki, 2013; Elsheikh *et al.*, 2013; Ukoha *et al.*, 2014; Aggarwal *et al.*, 2015; Veeramuthu *et al.*, 2016; Cisneiros de Oliveira *et al.*, 2016; Nanayakkara *et al.*, 2016; Masabni & Ahmad, 2017). Although few studies were conducted on human dry skulls of Indian region using a different set of landmarks, the information available on the dimensions and relative position of the IOF from various points of reference in the South Indian population is scarce. Thus, for an accurate surgical practice, it is very important to have knowledge of the topographical anatomy of the IOF. Hence, the present study was undertaken on the dry human skulls of southern part of India considering all the important landmarks around IOF. A comprehensive review of literature has also been conducted in this study.

Materials and Methods

This study was carried out on 14 dry skulls obtained from Farooqia Dental College & Hospital in southern India. The skulls were measured on both sides (right and left) totaling 28 sides. The sex and age of the skulls were unknown. Deformed skulls were excluded from the study. The study has been approved by the ethical committee of Farooqia Dental College & Hospital, Mysore (number: FDC/ MDS/09/2018-19).

The skulls were first placed in the anatomical position and then examined for the shape; presence of accessory foramina and the direction of the IOF. These were recorded in a tabular column before taking the measurements. Superior margin of IOF was the main reference point from which all the measurements were recorded with a digital caliper (Japan, 0.01 mm precision). The following parameters were measured on the right and left sides parallel to sagittal plane and perpendicular to Frankfurt plane.
- The vertical diameter of the IOF
- The horizontal diameter of the IOF
- The distance between the IOF and ANS (A) (Figures. 1A,B)
- The distance between the IOF and the nasion (B) (Figures. 1A,B)
- The vertical distance between the IOF and IOM (C) (Figures. 1A,B)
- The relative position of the IOF with regards to the socket of maxillary teeth (D) (Figure 1)
- The relative position of the IOF in relation to the SOM (E) (Figures. 1A,B)

The distance from the most superior border of IOF to the upper margin of the sockets of the first molar, first premolar and second premolar was measured along with the vertical axis (D). The above measurements were repeated three times to
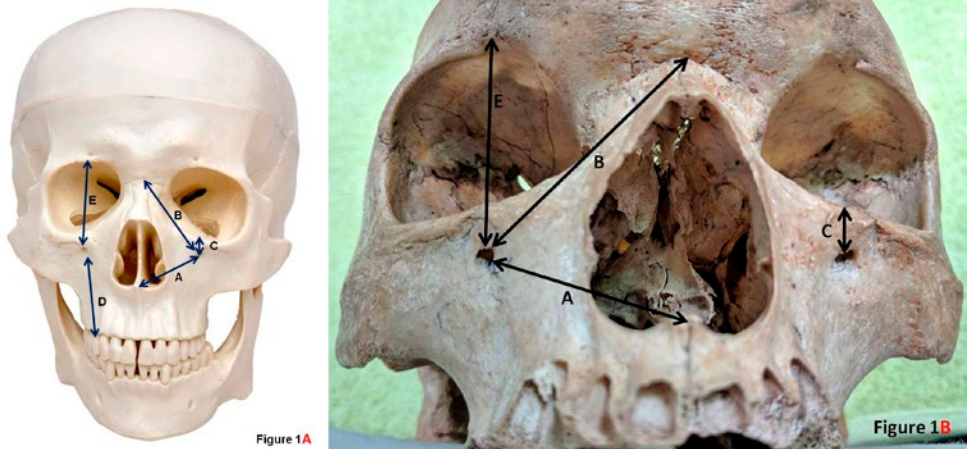
Figure 1. Showing the measurements conducted on the skulls. The distance between the IOF and ANS (A). The distance between the IOF and the nasion (B) (Figure 1A &1B);The vertical distance between the IOF and IOM (C) (Figure 1A & 1B);The relative position of the IOF with regards to the maxillary teeth (D) (Figure 1);The relative position of the IOF in relation to the SOM (E) (Figure 1A& 1B).

Figure 2. Showing the different shapes of the IOF found in the study. 2A: Oval shaped IOF; 2B: Circular shaped IOF.

avoid procedural error/bias. The mean, range, and standard deviation of all the measurements were statistically analyzed. (Figure 1A is presented from the skull model to show the landmarks clearly and Figure 1B is one of the skulls we used in the study).

Results

All skulls studied have presented an IOF on both sides. The most frequent shape of the IOF was oval (Figure 2A) (85.7% on the right side and 71.4% on the left side) followed by circular (Figure 2B) (14.2% on the right side and 28.5% on the left side) while no semilunar and triangular outlined IOF's were found (Table 1) (Figure 2). The vertical and horizontal diameters of the IOF and distance its from ANS, IOM and NA are shown in Table 2 (left side) and Table 3(right side). The differences between left and right sides were not statistically significant.

With regards to the position of IOF to SOM (Table 4), it is evident that the majority of the IOF were located lateral to SOM (57.1% on left side and 50% on right side) and medial to SOM (21.4% on left side and 14.2% on right side). The incidence of IOF

Table 1. Shape of the IOF on the right and left sides in %. IOF: infraorbital foramen.

| Shape | Right (%) | Left (%) | Accessory IOF (%) | |
			Right	Left
Ovoid	85.7	71.4	14.2%	14.2%
Circular	14.2	28.5	-	-
Semilunar	0	0	-	-
Triangular	0	0	-	-

Table 2. Measurements of the IOF on left side. IOF: infraorbital foramen, IOM: infraorbital margin, ANS: anterior nasal spine,NA: nasion.

Measurement(mm)	Minimum	Maximum	Mean ± SD
Vertical diameter	2.08	5.39	3.82± 0.83
Transverse diameter	2.11	6.91	3.86± 1.54
Distance from IOF to ANS	29.18	35.92	33.13± 2.30
Distance from IOF to IOM	4.51	8.56	5.85 ±1.06
Distance from IOF to NA	34.52	46.95	40.39 ±3.09

Table 3. Measurements of the IOF on right side. IOF: infraorbital foramen, IOM: infraorbital margin, ANS: anterior nasal spine,NA: nasion.

Measurement (mm)	Minimum	Maximum	Mean ± SD
Vertical diameter	2.23	5.02	3.95 ±0.86
Transverse diameter	0.98	5.54	3.70± 1.20
Distance from IOF to ANS	28.47	37.99	33.62 ±2.22
Distance from IOF to IOM	3.29	7.59	5.49±1.10
Distance from IOF to NA	34.07	47.10	41.45 ±3.27

Table 4. Positioning of the IOF in relation with SOM and maxillary teeth.SOM: supraorbital margin.

Position	Right	Left
Along with same plane of SOM	35.7%	21.4%
Medial to SOM	14.2%	21.4%
Lateral to SOM	50%	57.1%
With regards to teeth		
In line with 1st molar	14.2%	0%
In line with 1st premolar	7.14%	0%
In line with 2nd premolar	64.2%	85.7%
In line with junction of 2nd premolar & 1st molar	14.2%	14.2%

Table 5. Showing the comparison of mean distance from the IOF-IOM in different studies reported. IOF: infraorbital foramen, IOM: infraorbital margin.

Study & Year	Distance from IOF-IOM (mm)
Hindy & Abdel-Raouf,1993	6.10
Chung et al.,1995	8.60
Silva et al.,1998	6.80
Canan et al.,1999	Females:8.30; Males:10.90
Aziz et al.,2000	Females:7.80; Males:8.50
Kazkayasi et al.,2001	7.19
Karakas et al.,2002	6.70
Elias et al.,2004	6.77
Agthong et al. ,2005	7.9
Apinhasmit et al. ,2006	Females:8.71; Males:9.53
Gupta et al. ,2008	7.00
Lopes et al. ,2009	6.66
Macedo et al. ,2009	6.37
Ilayperuma et al.,2010	Females:9.02; Males:10.56
Boopathi et al.,2010	6.57
Singh et al.,2011	6.16
Lokanayaki et al.,2013	6.32
Elsheikh et al. ,2013	6.53
Ukoha et al.,2014	7.38
Aggarwal et al.,2015	6.32
Veeramuthu et al.,2016	7.00
Nanayakkara et al. ,2016	6.91
Masabni & Ahmad ,2017	6.60
Our study*	**5.67**

Table 6. Showing the comparison of mean distance from the IOF to the ANS in different studies reported. IOF: infraorbital foramen, ANS: anterior nasal spine.

Study & Year	Distance from IOF to the ANS (mm)
Agthong et al. ,2005	Females:32.9; Males:34.9
Lopes et al.,2009	35.0
Singh et al.,2011	36.6
Gnanagurudasan *et al.*, 2014	Females: 33.6; Males:36.1
Ukoha et al.,2014	29.0
Singh et al.,2015	36.6
Nanayakkara et al.,2016	Females:32.8; Males:34.3
Veeramuthu et al.,2016	33.0
Cisneiros de Oliveira et al., 2016	Females: 34.0; Males:36.0
Our study*	**33.3**

Table 7. Showing the comparison of mean distance from the IOF to the NA in different studies reported. IOF: infraorbital foramen, NA: nasion.

Study & Year	Distance from IOF to the Na (mm)
Przygocka et al.,2012	44.76
Gnanagurudasan *et al.*,2014	Females: 31.4; Males:38.2
Singh et al.,2015	44.95
Nanayakkara et al.,2016	42.44
Our study*	**40.90**

in the same plane as SOM was 21.4% on left side and 35.7% on right side. In relation to the sockets of the maxillary teeth, it was observed that most of the IOF's were in line with the 2nd premolar (85.7% on left side and 64.2% on right side) while few were in line with 1st premolar (0% on left side and 7.14% on right side).

Discussion

The infraorbital nerve and foramen are significant areas to discuss in dental surgeries due to the fact that the nerve is responsible for the sensory innervation of the maxillary region. Since it is supplying a large area, it is very important to know the exact location of IOF while inducing local anesthesia to block the nerve passing it. Due to its inconstant positions, a wide number of studies conducted in the past have documented the location of IOF in relation with surrounding bony landmarks. Although many studies appear in the literature from different populations, there is no detailed study on south Indian population so far. Hence, in this study, we determined the shape, diameters and location of the IOF in 28 sides of skulls obtained

from the region. Most common shape of IOF observed in our sample is oval shape (85.7% on right side and 71.4% on left side). Many other studies also found that the IOF was predominantly of oval shape followed by circular, semilunar and triangular shapes. In our study we didn't encounter any semilunar and triangular shapes. The frequency of multiple/accessory IOF has been widely reported. In the year 1875, Gruber reported that the number of accessory IOF may vary from 1 to 5 as reported by Leo et al. (Leo et al., 1995). A study by Cisneiros de Oliveira et al.(Cisneiros de Oliveira et al.,2016) reported that the multiplicity of IOF was found to be 10.7% in sample studied and most of the other studies also reported their frequency ranging from 4% to 11% (Gour et al.,2006; Singh,2011; Gnanagurudasan *et al*.,2014). Most of the studies also suggest that there is no significant difference in relation to the sex and sides. In our study, the frequency of multiple or accessory IOF was found to be 14.2%. However, higher incidences have been reported from a study on Indian population by Boopathi et al. (16.25%) (Boopathi et al., 2010) And in Mexican population by Berry (18.2%) (Berry, 1975).

In present study, the mean vertical and transverse diameters on the left and right sides were 3.82mm, 3.86mm and 3.95mm, 3.70mm respectively. These findings are compared with other studies conducted on different regions of Indian population and diameters are not exactly the same (Boopathi et al., 2010; Gour et al.,2006; Singh,2011; Lokanayaki,2013; Aggarwal et al.,2015; Veeramuthu et al.,2016). Previously published literature mentioning the distance between IOF and IOM are compared with results of our study in (Table 5). The minimum –maximum distance between IOM-IOF has been in a range from 5.7 mm to 10.9 mm respectively. Gnanagurudasan *et al*., 2015, reported that this distance was significantly greater on the right side, which is in contrast to the report of Macedo et al. (Macedo et al., 2009) wherein the distance was greater on the left side. In our study, the distance was found to be 5.85mm on left side and 5.49mm on right side with no significant difference between the sides. This is similar to a study reported by Singh et al. (Singh, 2011) but greatly varies from other studies of the Indian population (Boopathi et al., 2010; Gour et al., 2006; Lokanayaki, 2013; Aggarwal et al., 2015; Veeramuthu et al., 2016; Singh et al., 2015). This could be due to geographical and genetic/ ethnic differences.

With regards to the distance from IOF to ANS and NA, we did not find any difference between sides. These findings are inagreement with the studies originated from Nigeria (Ukoha et al., 2014), Brazil (Cisneiros de Oliveira et al., 2016) and India (Singh, 2011; Veeramuthu et al., 2016) (Table 6, 7). However, contrary to these observations, Agthong et al.; Cisneiros de Oliveira et al. reported that the distance between IOF and ANS varied significantly between the sexes and sides of the crania. The distance between IOF and NA in our study found to be 40.39mm on the left side and 41.45mm on the right side. These values are found to be lower when compared to those of other studies (Table 7). It is quite obvious that the distances from IOF-IOM, IOF-ANS, and IOF-NA are variable among different population studies, a point which emphasizes the significance of meticulous preoperative evaluation of the IOF in facial/dental surgeries.

Our study showed that the majority of the IOF were located lateral to the vertical plane passing through the SOF. The prevalence was 57% on the left side and 50% on the right side. These results agree with the findings of Thai and Korean populations. The occurrence of IOF in the same vertical plane of SOF was recorded to be

21.4% on the left side and 35.7% on the right side which goes along with the observations found in the Thai (23.4%) (Agthong et al.,2005) and Korean (38.1%) (Chung et al.,1995) populations, respectively.

With regards to the maxillary teeth, our study found that the IOF was frequently located in a vertical plane passing through the 2nd premolar teeth (85.7% on the left side and 64.2% on the right side). Our results support the findings of Thai (Agthong et al., 2005) and Egyptian (Elsheikh et al., 2013) populations. However, according to Aziz et al. the IOF was located in a vertical plane through the 1st premolar. In our study the incidence of this was found to be 0% on the left side and 7.14% on the right side.

The infraorbital nerve is the nerve of choice for regional anesthesia while performing surgeries in mid-face areas. The results of this and previous studies indicate that the IOF's location, size, shape and its distance from important landmark differs in different populations. These findings are valuable not only in orbital surgeries and Caldwell-Luc operation but also while inducing local anesthesia (Masabni &Ahmad, 2017).

Conclusion

The risk associated with surgeries in the maxillofacial area could be reduced if the surgeons are aware of these studies and this will help the surgeon to avoid injures to the neurovascular bundle of IOF. Various studies conducted on the skulls of Indian population show minor to major differences in the measurements suggesting that many more studies are to be conducted to see whether the people of India are a pool of dissimilar genes? And also it is important to mention that the sample of our study was limited, hence future studies with larger sample are needed.

Author's contributions

Dr. Bhagath Kumar Potu, Dr. Gowtham Chandra Srungavarapu **-** contributed to the study design, standardizing the methodology, data collection and statistical analysis. Dr. Thejodhar Pulakunta – contributed to literature review and in setting up the research objectives.

Disclosure of interest

Authors have "no conflict of interests" related to the study and manuscript.

Acknowledgment

References

Aggarwal A., Kaur H., Gupta T., Tubbs R. S., Sahni, D., Batra, Y. K., Sondekoppam R. V. Anatomical study of the infraorbital foramen: A basis for successful infraorbital nerve block. *Clin. Anat., 28(6)*:753- 60, 2015.

Agthong, S.; Huanmanop, T. & Chentanez, V. Anatomical variations of the supraorbital, infraorbital, and mental foramina related to gender and side. *J. Oral Maxillofac. Surg., 63(6)*:800-4, 2005.

Apinhasmit, W.; Chompoopong, S.; Methathrathip, D.; Sansuk, R. & Phetphunphiphat, W. Supraorbital Notch/Foramen, Infraorbital Fora- men and Mental Foramen in Thais: anthropometric measurements and surgical relevance. *J. Med. Assoc. Thai., 89(5)*:675-82, 2006.

Aziz, S. R.; Marchena, J. M. & Puran, A. Anatomic characteristics of the infraorbital foramen: a cadaver study. *J. Oral Maxillofac. Surg., 58(9)*:992-6, 2000.

Berry, A. C. Factors affecting the incidence of non-metrical skeletal variants. *J. Anat., 120(Pt. 3)*:519-35, 1975.

Boopathi, S.; Chakravarthy Marx, S.; Dhalapathy,S.& Anupa, S. Anthropometric analysis of the infraorbital foramen in a South Indian population. *Singapore Med. J., 51(9)*:730-5, 2010.

Canan, S.; Asim, O. M.; Okan, B.; Ozek, C. & Alper, M. Anatomic variations of the infraorbital foramen. *Ann. Plast. Surg., 43(6)*:613-7, 1999.

Chung, M. S.; Kim, H. J.; Kang, H. S. & Chung, I. H. Locational relationship of the supraorbital notch or foramen and infraorbital and mental foramina in Koreans. *Acta Anat. (Basel), 154(2)*:162-6, 1995.

Cisneiros de Oliveira, L. C. S.; Silveira, M. P. M.; de Almeida Júnior, E.; Reis, F. P. & Aragão, J. A. Morphometric study on the infraorbital fora- men in relation to sex and side of the cranium in northeastern Brazil. *Anat. Cell Biol., 49(1)*:73-7, 2016.

Elias, M. G.; Silva, R. B.; Pimentel, M. L.; Cardoso, V. T. S.; Rivello, T. & Babinski, M. A. Morphometric analysis of the infraorbital foramen and acessories foraminas in Brazilian skulls. *Int. J. Morphol., 22(4)*:273-8, 2004.

Elsheikh, E. M.; Nasr, W. F. & Ibrahim, A. A. S. Anatomical variations of infraorbital foramen in dry human adult Egyptian skulls, anthropometric measurements and surgical relevance. *Otorhinolaryngol. Clin., 5(3)*:125-9, 2013.

Gnanagurudasan, E.; Ahamed, S. R.; Deepalaxmi, S. & Gnanadesigan, E. A gender-wise study on the morphometry of infraorbital foramen and its laterality in dry adult skulls oh South Indian population. *Int. J. Med. Sci. Public Health, 3(5)*:546-8, 2014.

Gupta, T. Localization of important facial foramina encountered in maxillo- facial surgery. *Clin. Anat., 21(7)*:633-40, 2008.

Hindy, A. M. & Abdel-Raouf, F. A study of infraorbital foramen, canal and nerve in adult Egyptians. *Egypt. Dent. J., 39(4)*:573-80, 1993.

Ilayperuma, I.; Nanayakkara, G. & Palahepitiya, N. Morphometric analysis of the infraorbital foramen in adult Sri Lankan skulls. *Int. J. Morphol., 28(3)*:777-82, 2010.

Karakas¸, P.; Bozkir, M. G. & Oguz, O. Morphometric measurements from various reference points in the orbit of male Caucasians. *Surg. Radiol. Anat., 24(6)*:358-62, 2002.

Kazkayasi, M.; Ergin, A.; Ersoy, M.; Bengi, O.; Tekdemir, I & Elhan, A. Certain anatomical relations and the precise morphometry of the infraorbital foramen--canal

and groove: an anatomical and cephalometric study. *Laryngoscope, 111(4 Pt. 1)*:609-14, 2001.

Leo, J. T.; Cassell, M. D. & Bergman, R. A. Variation in human infraorbital nerve, canal and foramen. *Ann. Anat., 177(1)*:93-5, 1995.

Lokanayaki, V. Anatomic variations of infra orbital foramen. *CIBTech J. Surg., 2(2)*:30-6, 2013.

Lopes, P. T. C.; Pereira, G. A. M.; Santos, A. M. P. V.; Freitas, C. R.; Abreu, B. R. R. & Malafaia, A. C. Morphometric analysis of the infraorbital foramen related to gender and laterality in dry skulls of adult individuals in southern *Brazil. Braz. J. Morphol. Sci., 26(1)*:19-22, 2009.

Macedo, V. C.; Cabrini, P. R. & Faig-Leite, H. Infraorbital foramen location in dry human skulls. *Braz. J. Morphol. Sci., 26(1)*:35-8, 2009.

Masabni, O. & Ahmad, M. Infraorbital *Foramen and Pterygopalatine Fossa Location in Dry Skulls: Anatomical Guidelines for Local Anesthesia. Anat. Res. Int., 2017*:1403120, 2017.

Nanayakkara, D.; Peiris, R.; Mannapperuma, N. & Vadysinghe, A. Morphometric analysis of the infraorbital foramen: the clinical relevance. *Anat. Res. Int., 2016*:7917343, 2016.

Przygocka, A.; Szymanski , J; Jakubczyk, E ; Jedrzejewski, K; Topol, M & Polguj, M. Variations in the topography of the infraorbital canal/groove complex: a proposal for classification and its potential usefulness in orbital floor surgery. *Folia .Morphol.*,72:311–317,2013.

Singh, A. K.; Agarwal, P.; Singh, N. & Debberma, S. Accessory infraorbital foramen and morphometric localization of infraorbital foramen in North Indian region. *Natl. J. Integr. Res. Med., 6(5)*:28-33, 2015.

Singh, R. Morphometric analysis of infraorbital foramen in Indian dry skulls. *Anat. Cell Biol., 44(1)*:79-83, 2011.

Standring, S. *Gray's Anatomy: Anatomical Basis of Clinical Practice*. 40th ed. London, Churchill Livingstone Elsevier, 2008.

Ukoha, U. U.; Umeasalugo, K. E.; Udemezue, O. O.; Nzeako, H. C.; Ndukwe, G. U. & Nwankwo, P. C. Anthropometric measurement of infraorbital foramen in South-East And South-South Nigeria. *Natl. J. Med. Res., 4(3)*:225-7, 2014.

Veeramuthu, M.; Varman, R.; Shalini & Manoranjitham. Morphometric analysis of infraorbital foramen and incidence of accessory foramen and its clinical implications in dry adult human skull. *Int. J. Anat. Res., 4(4)*:2993-3000, 2016.

Zide, B. M. & Swift, R. How to block and tackle the face. *Plast. Reconstr. Surg., 101(3)*:840-51, 1998.

Anatomical variations in position of mandibular foramen: An East European morphometric study in dry adult human mandibles for achieving a successful inferior alveolar nerve block

Nityanand Jain[1,*] (ORCID: 0000-0002-7918-7909), Dzintra Kažoka[2] (ORCID: 0000-0003-0816-6446), Shivani Jain[3] (ORCID: 0000-0002-0648-745X), Māra Pilmane[2] (ORCID: 0000-0001-9804-4666)

[1] Faculty of Medicine, Rīga Stradiņš University, Riga, Latvia
[2] Department of Morphology, Institute of Anatomy and Anthropology, Rīga Stradiņš University, Riga, Latvia
[3] Department of Oral and Maxillofacial Surgery, Maharaja Ganga Singh Dental College and Research Center, Sriganganagar, Rajasthan, India

Abstract

In today's era of modern dentistry, the race towards developing painless and trauma-less procedures remain an important goal of all major companies and dental researchers. One such technique of focus is the Inferior Alveolar Nerve Block (IANB) which remains by far the most common anesthetic technique followed worldwide prior to any submaxillary treatment procedure. Despite of it being so popular, the failure rates remain significantly high with estimates at 15-60% among dental practitioners and dental students alike. Major reasons for failure include inaccurate determination of Mandibular foramen, variations in location of foramen, presence of accessory foramen, etc. to name a few. The present article aims to present the morpho-anatomical variations in the position of Mandibular Foramen in East European population. For this reason, the distance of the foramen was measured from 5 different bony landmarks using digital Vernier caliper on dry human adult mandibles. Analyzing the results, the foramen was found to be positioned at a mean distance of 16.88 ± 2.43 mm on the right side and 17.33 ± 2.24 mm on the left side from the anterior border of the ramus. Similarly, it was found to be 12.31 ± 2.49 mm and 11.75 ± 2.47 mm on right and left sides respectively from posterior border of ramus. It was found to be 17.41 ± 3.22 mm and 18.01 ± 3.44 mm and 19.80 ± 3.86 mm and 20.11 ± 4.08 mm on right and left sides from mandibular notch and angle of mandible respectively.

Introduction

Most of the available contemporary anatomical literature and text describes the Mandibular foramen as an irregular opening which is located on the medial surface of the ramus of the mandible (Standring, 2008). It leads into the mandibular canal, which runs obliquely downwards and forward within the ramus of the mandible and then run horizontally forward within the body of the mandible below the roots of the

* Corresponding author. E-mail: nityapkl@gmail.com

molar teeth with which it communicates with small openings. The foramen transmits the Inferior Alveolar Nerve and its vessels into the mandibular canal (Varsha S. et al., 2012). The foramen has more or less been studied for its variations in position but has never been done for Eastern European population and compared with other geographic zones to understand the evolutionary as well as environmental differences that include dietary differences, chewing habits, genetic variations etc. The foramen forms the passageway for the Inferior Alveolar Nerve. It is the branch of Mandibular Nerve which is itself the 3rd branch of Trigeminal Nerve. The nerve passes behind the pterygoid muscle before making an entrance into the foramen. Inferior Alveolar Nerve Block is one of the most common anesthetic procedure prior to various submaxillary surgeries. The success of the procedure depends upon the position of the needle tip and Mandibular Foramen at the time of anesthetic injection (Varsha S. et al., 2012). The main complications during this technique are hemorrhage, injury to the neurovascular bundle, fractures, and necrosis of *Ramus Mandibulae* (Daw Dl et al., 1999). The most recurring causes of failure include inapposite location of needle, inaccurate judgement of locus of Mandibular Foramen or by marked variability in its location (Ennes and Medeiros, 2009; Oguz and Boz, 2002; Varsha S. et al., 2012). Earlier, location of the foramen was located by palpating the lingula (Ennes and Medeiros, 2009) or by using radiographs (Hwang TJ. et al., 1990; Mbajiorgu EF, 2000).

The main goal of this study was to locate the Mandibular Foramen and determine its distance from various anatomical landmarks on medial surface of the ramus of the mandible in several adult dry human mandibles in East European populations and then compare our results with studies from other geographical zones, in a desire to add our findings to our predecessors and contribute to ever-growing field of dentistry and anesthesia research.

Materials and Methods

The present study was conducted in Department of Morphology, Institute of Anatomy and Anthropology, Rīga Stradiņš University, Riga, Latvia. The department`s personal collection included 125 dry human adult mandibles which were used for this study. The Mandibles taken had both the left and right Ramus with foramen and hence a total of 250 foramens (125 on each side) were assessed for their location. Figure 1. shows Mandibular foramen on the ramus from posterior view. Each Mandible was assigned a specific serial number starting from 1 to 125 and were observed for the presence, prevalence rate and laterality of the Mandibular Foramen.

Mandibles that were regular in shape and devoid of any irregularities and deformities only were included in this study. The damaged mandibular bones and those having pathological abnormalities were excluded from the scope of this study. Also, the mandibles that didn`t had an erupted 3rd Molar Tooth/Wisdom tooth socket in the Mandible were excluded.

Irrespective of any shape of the lingula, the center of the Foramen was taken as the reference point and marked as Point F for all measurements in the study. Magnifying glass and Digital Vernier Caliper were used for taking measurements. The Digital Vernier Caliper used had a resolution of 0.01 mm (millimeters) with range from 0-300 mm and had a zero error. The external jaws of the Caliper were brought togeth-

Figure 1. Figure showing the medial surface of right and left Mandibular Ramus from posterior view.

er until they touched each other, and zero button was pressed before taking every individual reading.

Following points were marked on the Mandible:
1) Point F: - It is the center of Foramen. The most inferior position of the Foramen was taken for vertical measurements and the most anterior position was taken for the horizontal measurements.
2) Point A: - The most anterior point on the anterior border of ramus.
3) Point B: - The most posterior extent of the line AB on the posterior border of ramus.
4) Point C: - The most inferior point of the sigmoid notch.
5) Point D: - The point on the angle (inferior border) of the mandible which makes the terminus of the line CD.
6) Point E: - It is a point at the distal surface of the mandibular third molar tooth.

The distances from the foramen to various bony landmarks were recorded by 2 authors. Each author took three independent measurements and the average of both readings from both authors were considered. This was done to eliminate and reduce the chances of human error, parallax and other external sources of errors. The Mean and Standard Deviation were calculated for the right and left sides separately and were presented in tabular form. The reference points and lines of measurements were marked with a pencil and are shown in Figure 2.

All the parameters were carefully measured and then entered in Excel Spreadsheet in Microsoft Excel, 2010 and analyzed using IBM Corp. Released 2016. IBM SPSS Statistics for Windows, Version 22.0 (Statistical Package for Social Sciences); Armonk, New York: IBM Corp. The results of the present study were compared with the results of previous studies done on various ethnic groups in various geographical locations. The minimum, maximum, mean and standard deviation for each were

Figure 2. Figure representing the reference points used in the study and lines of measurements marked with a marker as: 1) Point A - Anterior Border of Ramus; 2) Point B – Posterior Border of Ramus; 3) Point C – Mandibular Notch; 4) Point D - Angle of the Mandible; 5) Point E – Posterior Border of 3rd Molar tooth; 6) Point F – Center of the Mandibular Foramen.

calculated separately by using the respective statistical formulas on either side of the mandibles.

Results

The mean distances of the position of Mandibular Foramen, along with the standard deviation, maximum distance and minimum distance measured on both the left and right side are concluded in Table 1. Student`s t-test was used as test of significance to compare the mean values of right and left side and a P value of less than 0.05 was taken to be statistically significant. The results from the Student`s t- test are also compared in Table 1. Symmetrical measurements of localization of Foramen on right versus left sides were found in only 22% – 34% of the Mandibles. The Pearson

Table 1. Table concluding the mean, maximum and minimum distance with significance of foramen from various bony landmarks.

Sr. No.	Position of the mandibular foramen from various landmarks	Side of the Mandible	Mean Distance (in mm)	S.D*	Maximum Distance measured (in mm)	MinimumDistance measured (in mm)	P <0.05
1.	Anterior Border to Foramen (Line AF)	Right Side	16.88	2.43	21.12	11.92	0.0371*
		Left Side	17.33	2.24	22.25	13.35	
2.	Posterior Border to Foramen (Line BF)	Right Side	12.31	2.49	20.20	8.87	0.0415*
		Left Side	11.75	2.47	16.85	7.58	
3.	Mandibular Notch to Foramen (Line CF)	Right Side	17.41	3.22	24.16	12.46	0.1080
		Left Side	18.01	3.44	24.04	10.65	
4.	Angle of Mandible to Foramen (Line DF)	Right Side	19.80	3.86	28.03	11.56	0.2515
		Left Side	20.11	4.08	27.74	12.05	
5.	Posterior Border of 3rd Mandibular Molar to Foramen (Line EF)	Right Side	22.88	4.53	31.64	10.97	0.2727
		Left Side	23.22	4.61	31.59	11.12	

* Significant (P < 0.05)

Table 2. Table showing localization of the foramen in Antero-posterior axis.

Side of the Mandible	Mean (in mm)		Midpoint of Line AB	Difference Between Line AF and midpoint of Line AB	Location of Foramen in reference to Midpoint of Line AB
	Line AB	Line AF			
Right Side	29.19	16.88	14.59 mm	2.29 mm	Posterior to midpoint
Left Side	29.08	17.33	14.54 mm	2.79 mm	Posterior to midpoint

Table 3. Table showing localization of the foramen in Superio-inferior axis.

Side of the Mandible	Mean (in mm)		Midpoint ofLine CD	Difference Between Line CF and midpoint of Line CD	Location of Foramen in reference to Midpoint of Line CD
	Line CD	Line CF			
Right Side	37.21	17.41	18.60 mm	- 1.19 mm	Inferior to midpoint
Left Side	38.12	18.01	19.06 mm	- 1.05mm	Inferior to midpoint

Correlation was also used to test the correlation R of measurements of right and left side of each distance and a P value of less than 0.01 was taken to be significant statistically. Line AF on both sides showed a strong positive linear correlation while Line BF showed a moderate positive linear correlation. Line CF had a weak positive linear correlation and both Line DF and Line EF had moderate to strong positive linear correlation on both sides of the Mandibles.

The localization of foramen in anteroposterior and superio-inferior axis of the ramus of the mandible was also determined as shown in Tables 2-3. It was found out that the foramen is not localized at the midpoint of any of the two axes. Neither was it localized at the point of cross section of both axes. Rather it was about 2 – 3 mm posterior from midpoint on anteroposterior axis and about 1 mm inferior from the midpoint of superio-inferior axis. There was statistically significant difference in the location of the foramen on the right and left sides ($p < 0.05$) in the anteroposterior axis ($p = 0.014$) while in the superio-inferior axis ($p = 0.286$), no statistically significant difference found ($p > 0.05$).

Discussion

The knowledge of the position of Mandibular foramen is of great importance for many procedures in dentistry. The location of the foramen is also of great importance to Radiologists and Oncologists. It is also clinically crucial in achieving Inferior Alveolar Nerve Block which is most commonly used for administering local anesthesia for any operative procedure on the Mandible. The commonest reason for failure of the technique is the inappropriate location of the tip of the anesthetic needle due to inaccurate localization of the Foramen (Ennes and Medeiros, 2009; Palti DG. et al., 2011; Patrical and Arthur, 2003). The surgeon has to select an appropriate needle to give the Inferior Alveolar Nerve Block. The average length of the long needles used should be

23 mm long and for short needles should be 21.5 mm long in consideration to the size of the patient`s mandible especially while using the pterygomandibular technique of Inferior Alveolar Nerve Block. If a long needle is used in a patient with small mandible then there is a risk of perforating the capsule of Parotid gland thereby causing damage to the branches of the Facial Nerve. If a short needle is used in a patient with big mandible there may be chances of fracture of needle when it is completely introduced in the oral tissues (Ennes and Medeiros, 2009). Hence localization of the Foramen is very important to select the size of the anesthetic needle. In the present study, the locus of the Mandibular foramen and its distances from various bony landmarks on dry mandibles was determined and calculated. This study also compared the location of the foramen on right and left sides of the Mandible. Mbajiorgu EF. (2000) in his study on adult black Zimbabweans has reported that the Foramen lies 2.56 mm behind the midpoint of width of *Ramus Mandibulae* on the right side and 2.08 mm behind the midpoint of width of *Ramus Mandibulae* on the left side. In the present study, the foramen lied 2.30 mm behind the midpoint of the width of *Ramus Mandibulae* on right side while 2.79 mm on the left side in anteroposterior axis of mandibular ramus. The variability of the distance from anterior border to foramen was also not significant enough to produce failure of Anesthetics. If we compare our study with some other ethnic groups, then we see that the distance of foramen to Anterior Border of *Ramus Mandibulae* which were 16.88 mm and 17.33 mm on right and left side respectively, are in range with that of the other studies (Asma and Imtiaz, 2015; Hoque MM et al., 2013, Oguz and Boz, 2002; Sandhya K. et al., 2015). Oguz and Boz (2002) have tried to localize the Mandibular foramen in the Turkish population. Ennes and Medeiros (2009), Prado et al. (2010), and many others (Afdhali and Flora, 2014; Asma and Imtiaz, 2015; Gopalakrishna K. et al., 2016; Hoque MM et al., 2013; Jin Hoo et al., 2018; Mbajorgu EF, 2000; Prajna and Poonam, 2013; Sandhya K. et al., 2015; Wandee A. et al.,2015), have also studied the location of Foramen in different population. There are variations in the values obtained in each of the studies when compared with the results of the present study as seen in Table 4. Kilarkaje et al. (2005), have reported that the foramen was within 25 mm from the distal edge of third molar tooth. Varma et al. (2011), have reported that the mean distance of mandibular foramen from third molar tooth socket was 15 mm on right side and 18 mm on the left side. Ghorai et al (2016), have reported the distance to be 22.8 mm on right side while 21.7 mm on the left side. The results of the present study are similar to both Kilarkaje et al. (2005), and Ghoraj et al. (2016), as the measured mean distances were 22.88 mm on right side and 23.22 mm on the left side. Kilarkaje et al. (2005), from their study have also reported that the foramen maintains bilateral symmetry in dry mandibles in all ages. In the present study, Bilateral symmetry of the distance of the foramen from various landmarks of the Ramus Mandibulae ranged from 22% to 34% only. In the vertical dimension, the foramen was found at mean distance of 17.41 mm on right side and 18.01 mm on left side from the mandibular notch in our study. Ennes and Medeiros (2009) found that this distance from mandibular notch in Brazilian Population was 18.30 mm on right side and 17.50 mm on the left side. When it was taken in reference to the midpoint of height of ramus, Mandibular foramen was located 1.19 mm superior to midpoint on right side while 1.05 mm superior to midpoint on left side. This is in sharp contrast to our study as well as the study carried out by Nicholson (1938). According to Nicholson (1938), the foramen was predominantly located at the center of the ramus of the

Table 4. Table comparing location of foramen with other geographical regions from previous studies with the present study.

Study Conducted & the Year	Country of Study	Lines (in mm)									
		AF		BF		CF		DF		EF	
		Right Side	Left Side	Right Side	Left Side	Right Side	Left Side	Right Side	Left Side	Right Side	Left Side
Mbajiorgu EF (2000)	Zimbabwe	18.95	14.30	22.50	28.44	-	-	-	-	-	-
Oguz & Bozkir (2002)	Turkey	16.90	16.78	14.09	14.37	22.37	22.17	-	-	-	-
Ennes & Medeiros (2009)	Brazil	09.40	06.90	08.60	08.40	18.30	17.50	-	-	-	-
Prado et al. (2010)	Brazil	19.20	18.80	14.20	13.00	23.60	23.10	-	-	-	-
Prajna P. et al. (2013)	India	15.72	16.23	13.29	12.73	22.70	22.27	21.54	21.13	-	-
Hoque et al. (2013)	Bangladesh	16.34	16.27	14.14	14.04	22.29	22.18	-	-	16.70	16.72
Afadhali D. et al. (2014)	Tanzania	19.88	20.19	12.69	12.65	21.54	20.70	26.23	25.68	-	-
Kumari S. et al. (2015)	India	16.00	16.27	10.21	10.28	20.48	20.15	24.15	24.86	12.31	10.93
Wandee et al. (2015)	Thailand	-	-	12.70	17.50	-	-	-	-	-	-
Asma Saher et al. (2015)	Pakistan	17.69	17.65	12.03	11.84	20.51	21.03	-	-	-	-
Gopalkrishnan K. et al. (2016)	India	14.63	15.31	12.34	13.51	21.23	21.16	22.14	22.10	14.37	19.26
Jin Hoo Park et al. (2018)	South Korea	19.69	14.41	21.56	25.18	-	-	-	-	-	-
Present Study	Latvia	16.88	17.33	12.31	11.75	17.41	18.01	19.80	20.11	22.88	23.22

mandible. Soames RW. (1995), also concluded like Ennes and Medeiros (2009) that the foramen was located above the center of the *Ramus Mandibulae* on the medial surface. Mbajiorgu EF. (2000) reported that the foramen is located approximately 8 mm above the midpoint of Ramus Mandibulae height on both sides in the Zimbabwean population. The distance from the foramen to the inferior border of the Angle of Mandible was 19.80 mm on right and 20.11 mm on left side in this study. Again, when compared with studies on different ethnic groups we notice some differences (Afdhali and Flora, 2014; Gopalakrishna K. et al., 2016; Jin Hoo et al., 2018; Mbajorgu EF, 2000; Prajna and Poonam, 2013; Sandhya K. et al., 2015).

The reader may argue that many new diagnostic techniques are available these days in the clinics including the Intraoral Periapical (IOPA), Orthopantomograms (OPG) and Cone beam Computed Tomography (CBCT). Although these may have become a routine, still the "old-school" technique of morphometric measurements of mandibular foramen plays a crucial role in the development and application of Local Anesthesia administering techniques. Knowing the position of the foramen before-hand gives an assurance as well as confidence to the doctor. It gives the doctor a benchmark to compare to while analyzing the foramen for any deformities as well as diseases. It also is useful in patients that show extreme signs of gagging and with patients who can`t afford these diagnostic tools given the relatively high costs associated with them.

Dental Surgeons, Prosthodontists, Endodontists and practicing dental graduates can utilize this information on the locus of the foramen during administering local anesthesia involving the Inferior Alveolar Nerve for different procedures such as dental extractions, placement of mandibular implants and other therapeutic procedures involving Mandibles in the local population. Clinicians can also use internal oblique ridge as a reference point for planning different techniques of Inferior Alveolar Nerve Block.

Conclusions

The precise localization of Mandibular foramen is very important to achieve a successful Inferior Alveolar Nerve Block, prior to dental surgeries in the lower jaw. The present study concludes that the knowledge of the pinpoint position of Foramen Mandibulae with respect to its normality and laterality is important for planning and conducting dental surgeries, which will help for effective management, better clinical results and prognosis. Comparison from other studies shows that geographical, genetic and dietary variations does exist and hence knowing its position in native population is essential as it plays a crucial role in success of "pain-less" and "patient friendly" surgical procedures.

Acknowledgements

Conflicts of Interest

None of the authors declare any conflicts of interest.

References

1. Afadhali D. Russa, Flora M. Fabian (Jan 2014). Position of the Mandibular Foramen in adult male Tanzania Mandibles. Ital. J. Anat. Embryol. 119(3): 163-168.

2. Asma Saher Ansari, Imtiaz Ahmed (2015). Localization of Mandibular Foramen on the panoramic radiographs. J. Ayub. Med. Coll. Abbottabad. 27(3): 576-579.
3. Daw JL, Jr, De La Paz MG, Han H, Aitken ME, Patel PK (1999). The Mandibular Foramen: An anatomic study and its relevance to the sagittal ramus osteotomy. J. Craniofac. Surg. 10: 475-479.
4. Ennes JP, Medeiros RM (2009). Localization of the Mandibular Foramen and its clinical implications. Int. J. Morphol. 27(4): 1305-1311.
5. Ghorai S, Pal M, Jana S (2016). Distance of Mandibular Foramen from 3rd molar tooth in dry adult mandible of West Bengal population. Anat. J. Afr. 5: 640-643.
6. Gopalakrishna K, Deepalaxmi S, Somashekara SC, Rathna BS (2016). An anatomical study on the position of Mandibular foramen in 100 dry Mandibles. Int. J. Anat. Res. 4(1):1967-1971.
7. Hoque MM, Ara S, Begum S, Kamal AM, Momen MA (July 2013). Study of Morphometric Analysis of Mandibular Foramen in Bangladeshi dry adult human mandibles. Bangladesh Journal of Anatomy.11(2): 58-61.
8. Hwang TJ, Hsu SC, Huang QF, Guo MK (1990). Age changes in location of Foramen Mandibulae. Zhonghua Ya Yi Xue Hui Za Zhi. 9(3): 98-103.
9. Jin Hoo Park, Hin-Dong Jung, Young-Soo Jung (December 2018). Anatomical study of the location of Antilingula, lingula and Mandibular Foramen for vertical Ramus osteotomy. Maxillofac. Plast. Reconstr. Surg. 40(1): 15.
10. Kilarkaje N, Nayak SR, Narayan P, Prabhu LV (2005). The location of the mandibular foramen maintains absolute bilateral symmetry in mandibles of different age groups. Hong kong Dent. J. 2: 35-37.
11. Mbajiorgu EF (2000). A study of position of Foramen Mandibulae in adult black Zimbabwean Mandibulae. Cent. Afr. J. Med. 46(7): 184-190.
12. Nicholson ML (1938). A study of the position of the mandibular foramen in adult human mandible. J. Dent. Res. 17: 125-149.
13. Oguz O, Boz Kir MG (2002). Evaluation of the location of mandibular and the mental foramina in dry young adult human male dentulous mandibles. West Indian Med. J. 51: 14-16.
14. Palti DG, Akmeida CM, Rodrigues AC, Andreo JC, Lima Jeo (2011). An anesthetic technique for the inferior alveolar nerve block: a new approach. J. Appl. Oral. Sci. 19(1): 11-15.
15. Patrical LB, Arthur HJ (2003). The key to profound local anesthesia. J.A.D.A. 134: 753-760.
16. Prado FB, Groppo EC, Volpato MC and Caria P.H.F (2010). Morphological changes in the position of the Mandibular Foramen in dentate and edentate Brazilian subjects. Clin. Anat. 23: 394-399.
17. Prajna Paramita Samanta, Poonam Kharb (2013). Morphometric analysis of Mandibular foramen and incidence of accessory mandibular foramina in adult human mandibles of Indian Population. Rev. Arg. De. Anat. Clin. 5(2): 60-66.
18. Sandhya K., Bhoopendra S., Namita L., Renu P (2015). Localization of Mandibular foramen relative to landmarks in East Indian mandibles. Indian J. Dent. Res. 26: 571-575.
19. Soames RW (1995). Skeletal System. In: Williams PL, Bannister LH, Berry MM (editors). Gray`s Anatomy. New York: Churchill, Livingstone p 576-579.
20. Standring S (2008). The anatomical basis of clinical practice. In: Susan Standring

(Chief Editor). Gray`s Anatomy. 40th ED. Churchill, Livingstone. Elsiever. Chapter 31, p 530-533, 595-614.

21. Varma CL, Haq I, Rajeshwari T (2011). Position of Mandibular Foramen in South Indian Mandibles. Anatomica Karnataka. 5: 53-56.

22. Varsha S., S. Vijayalaxmi, P Saraswathi (May (supplement 2) 2012). Osteometric Analysis of the Mandibular foramen in dry Mandibles. J.C.D.R. 6(4): 557-560.

23. Wandee A, Supin C, Pornchai J (2015). Alternative Landmarks of the mandibular foramen to prevent nerve injury during ramus surgery. J. Med. Assoc. Thai. 98(6): 574-581.

Root canal anatomy and morphology of permanent maxillary canine teeth in an Iranian population

Maryam Kuzekanani*, Alireza Mahdavi Jafari

Endodontology Research Center, Department of Endodontics, Kerman Dental School, Kerman University of Medical Sciences, Kerman, Iran

Abstract

Thorough knowledge from anatomical characteristics of different teeth is a must, to achieve successful root canal, Orthodontic, surgical and other dental treatments on them. This cross- sectional study aimed to study the anatomy and morphology of permanent maxillary canine teeth in Kerman, a province in the southeast Islamic Republic of Iran. One hundred extracted permanent maxillary canines with intact apices were collected from five different dental centers within five different city districts in Kerman. The number of roots, the root curve direction and the length of each tooth was assigned by macroscopic observation and length measurement of each sample. Also, after staining, decalcification and clearing of each selected tooth the existence of lateral canals and their location was carefully evaluated under magnification. The results showed that all maxillary canine teeth had 1 root and one root canal in this study. The average length for this tooth was 27.31mms. The curve direction of the roots, in 32% of the cases was; distally, in 8%; buccally, in 4%; mesially and in 3%; palatally. 53% of the teeth had straight roots and root canals and, 25%, had lateral canals that in all of the cases were located in the apical third of the roots and were never observed in the middle and coronal thirds. As a conclusion, in this population, roots of maxillary canine teeth have straight roots in 53% of the cases, and in 25%, they have lateral canals that are usually located in the apical thirds.

Introduction

The canine teeth, also called cuspids, fangs, dog or eye teeth (in the maxillary jaws), are long pointed and in some cases, more flattened teeth which cause them to be similar to incisors and to be named, incisiforms.Their corner position, complements their major function in the mastication which is tearing of the food. Canines are the longest teeth in the mouth and also the only anterior teeth with one cusp. (Wikipedia. *Accessed* 2/05/2019).

The root canal space of this tooth is wider in the Labio-lingual than in the mesiodistal, in contrast with the other anterior teeth. Also, despite other anterior teeth, canine teeth don,t have pulp horns.

Because of these differences, the outline form of the access cavity and also the instrumentation techniques in them is somehow different from other maxillary inci-

* Corresponding author. E-mail: maryamk2325@gmail.com

sor teeth. The outline form of their access cavity is oval, in comparison with the Central maxillary incisors, which is triangular. (Hargreaves *et al.* 2016, Ash *et al.* 2007, Ingle *et al.* 2011, Seltzer *et al.* 1988)

Many studies in different parts of the world have shown that the anatomic characteristics along with the related root canal morphology of the teeth is various in different racial populations. (Cohen *et al.*2016 Ingle *et al.*2011) In the Caucasians only one root and one root canal configuration has been reported to exist in the maxillary canines, whereas in the Turkish populations an additional canal configuration has been reported in this tooth. (Vertucci *et al.* 1984 Caliskan *et al.*1995 Sert *et al.*2004) Studies on root canal anatomy and morphology of permanent canine teeth are limited. Therefore, this study was done to investigate the external and internal root canal anatomy of the extracted permanent maxillary canine teeth in an Iranian population using macroscopic observation along with the Staining, decalcification and clearing technique.

Materials and methods

With the approval of the University Ethics committee, approval code: *K/90/19* 100 permanent maxillary Canine teeth with completely formed apices which had been extracted because of different dental interventions such as progressive caries or periodontal diseases, complete or partial denture treatments and financially inability of the patients to treat the teeth were randomly collected from 5 dental centers within 5 different municipal districts of the city of Kerman, the capital city of the province; Kerman located in the southeast of the Islamic Republic of Iran. The side of the teeth, gender, and age of the patients had not been considered as a criterion. The attached soft tissues were removed from the surfaces of the extracted teeth by an ultrasonic scaler and then kept in 5.25% Sodium Hypochlorite (Samen-Mashad). The length of the teeth was measured from apex to the Cusp of the teeth, considering that in cases of root curvature this could underestimate root length up to 1mm. The direction of root curvature was also visually assessed and recorded in a table along with the length of the teeth. After determining macroscopic anatomical characteristics, the root canals of the teeth were stained, decalcified and finally cleared in order to study the internal anatomy of the samples.

For this purpose, access cavities to the pulp were prepared with a high-speed Turbine (Bien-Air, Swiss) and diamond burs, (Diatech-Germany). Then the organic pulp tissues of the samples were dissolved and removed by immersing the teeth in 5.25% Sodium Hypochlorite (Samen-Mashad) for nearly12 hours. Finally, all samples were washed and dried in the room temperature. The locations of the apical foramina for all Canine teeth were determined by putting a no 10 K file (Maillefer-Swiss) inside the canal, until it reached to the root apex. India ink (Shimin-Tehran) was injected into the pulp chambers of the teeth by an irrigating syringe and a 27Guage needle. The ink was moved into the canal system by negative pressure to the apical end of the teeth with the use of a central suction system . Then the stained samples were dried and demineralized by immersion in 14% Nitric acid solution (Shimin – Tehran) for almost 10 days. The acid solution was changed daily and, was checked for enough demineralization of the teeth by taking frequent X-rays. after enough

demineralization the samples were dehydrated in Ethanol (Taghtir- Iran) for 12 hours and finally all teeth were made transparent by immersion inside 5% Methyl Salicylate(Merck-Germany). The teeth were maintained within this solution until they completely became transparent. The stained, decalcified and cleared canine teeth were carefully observed under the Stereomicroscope (Olympus- Japan) at ×2 to ×3magnification. (Vertucci *et al.*1984 Caliskan *et al.* 1995 Sert *et al.*2004 Kuzekanani *et al.* 2015)*.

Results

All maxillary canine teeth had 1 root and one root canal and the average length for this tooth was 27.31 mm in this study. The curvature of the roots and related root canals in 32% of the cases was distally, in 8%: buccally, in 4%: mesially and in 3%: palatally. 53% of the teeth had straight roots and root canals. 25% of the teeth had lateral canals which in all of the cases were located in the apical thirds and were not observed in any sample in the middle and coronal thirds of the roots.

Discussion

There are several different techniques which help us to study the root canal anatomy and morphology of the teeth. Each technique has some advantages and some disadvantages.

Some of the most efficient and practical techniques for this purpose are: 1 preparing access cavities, putting files inside the diagnosed canals and taking radiographs. 2-Studying stained cross sections of different parts of the root canals under magnifications. 3- Studying the stained, decalcified and cleared (transparent) root canals and 4-Cone Beam Computed Tomography (CBCT). In this research we performed the third method which can detect and stain some areas of the root canals that are complex and not reachable and diagnosed by the files and other endodontic instruments, and be diagnosed on the simple radiographs. In a recent study, no significant statistical difference has been reported between the accuracy of the CBCT and the staining, decalcification and clearing methods in revealing the number and the morphology of the roots and root canals. (Dalili Kajan *et al.*, 2018) The clearing technique is more applicable than the CBCT method to study the root canal morphology of the teeth in experimental studies, but in the clinical studies and also clinical practice finding the additional canals and detecting morphological and anatomical variations and even canal obstructions, using the efficient CBCT technology is highly recommended. (Patel *et al.*, 2007, Versiani *et al.*, 2013, Kuzekanani *et al.*, 2017, Kuzekanani *et al.*, 2018, Mashyakhy, 2018, Mashyakhy, 2019)

Canine teeth are bulkier and more calcified in comparison with other anterior teeth. so more volume and higher concentration of the Nitric acid solution and also more time was needed for becoming decalcified .In our Study the average length of the Canines was 27.31 which is longer than the average international records which is 26.5 mms.(Hargreaves *et al.* 2016) Many investigators and clinicians have reported more than one root canal for the canine teeth in the literature and through the case

Table 1. Variations in root canal anatomy and morphology of Maxillary canine Teeth in different populations.

Author/year	Methodology	Country	No of samples	1 root and 1 canal	Accessory canals
Green/1956	Cross section/in vitro	USA	50	100%	----
Chapman/1969	Cross section/in vitro	UK	20	100%	12(60%)
Pindea/1972	Radiography/in vitro	Mexico	260	100%	77(29%)
De Deus/1975	Staining and clearing/in vitro	Brazil	73	100%	12(16.5%)
Vertucci/1984	Staining and clearing/in vitro	USA	100	100%	27(27%)
Caliskan/1995	SEM(Scanning Electrone Mycroscope)/in vitro	Turkey	100	93.5%	45.5%
Sert/2004	Staining and clearing/in vitro	Turkey	200	94%	57(28.5%)
Weng/2009	Staining and clearing/in vitro	China	65	75.5%	30(37.5%)
Uchiyama/2011	Staining and clearing/in vitro	Japan	250	98.5%	92(37%)
Somalinga/2014	CBCT/in vitro	India	250	81.6%	30(12%)
Plascencia/2017	CBCT/in vitro	Mexico	32	93.7%	43.7%

reports, (Caliscan *et al.*1995 Sert *et al* 2004Alapati *et al.*2006 Onay *et al.*2008 Weng *et al.* 2009 Uchiyama *et al* .2011 Somalinga *et al.* 2014 Plascencia *et al.* 2017) in contrast, more than one root and one root canal was not observed among randomly select-ed extracted canine teeth in this study. In agreement with the results of our study, many other investigators have not found more than one root and one root canals for Canine teeth in different parts of the world.(Green *et al.* 1956 Chapman *et al.* 1969 Pindea *et al.*1972 Dedeus *et al.*1975 Vertucci *et al.*1984) The results of the studies on the anatomic characteristics and the root canal morphology of the maxillary Canine teeth, along with the used techniques in different parts of the world has been sum-marized in the Table 1. Furthermore most of the studies and the texts report that dis-tally curved roots are more prevalent in Canines,(Amin sobhani *et al.* 2013Vertucci *et al.* 2005) also in contrast most of the cases, (53%) had straight roots and root canals ,followed by distally(32%), buccally(8%), mesially(4%) and palatally curved roots(3%) in this study. Any additional canal was not recognized for these teeth in this study, instead 25% of the samples had lateral canals which are a thorough challenge in Endodontics because they cannot be bypassed by endodontic instruments and some-times they may need apical surgeries to be sealed by retrograde material fillings such as amalgam, MTA and other retrofil materials and special care should be focused on chemical cleaning of these teeth while cleaning and shaping procedure. Also vertical compactions of warm and softened Guttapercha is a promising method to obturate and seal these lateral canals.(Hargreaves *et al.* 2016).

Conclusion

Based on the results of the current study all maxillary canine teeth had 1 root and one root canal.

The average length for this tooth was 27.31 mms. The curve of the roots in 32% of the cases was, distally, in 8%: buccally, in 4%: mesially and in 3%: palatally. 53% of the teeth had straight roots and root canals. 25% of the teeth had lateral canals which in all cases were located in apical thirds and were not observed in any case in the middle and coronal thirds of the roots.

Conflicts of interests

The authors have no conflicts of interests to be declared.

Acknowledgments

Special thank is dedicated to Dr. Mahdavi Jafari for hard work to finalize his research thesis.

Reference

Alapati S, Zaatar EI, Shyama M, Al-Zuhair N(2006) Maxillary canine with two root canals.*Med Princ Pract*,**15**:74–6.

Aminsobhani M, Sadegh N, Meraji H, Razmi H, Kharazifard MJ(2013)Evaluation of the root and canal morphology of mandibular permanent anterior teeth in an Iranian population by Cone-Beam Computed Tomography *Journal of Dentistry*, **4**:358–366

Ash M, Nelson SJ (2007) The permanent canines: maxillary and mandibular teeth, *in Wheeler's Dental Anatomy*, Physiology, and occlusion, 8th ed Elsevier, St. Louis, Mo, USA,91-214

Calişkan MK, Pehlivan Y, Sepetçioğlu F, Türkün M, Tuncer SS(1995) Root canal Morphology of human permanent teeth in a Turkish population *J of Endodontics*, **21**:200-4 PubMed

Chapman CE(1969) A microscopic study of the apical region of human anterior teeth. *J Br Endod Soc*,**3**:52-8.

Dalili Kajan Z, Taramsari M, Khosravi Fard N, Kanani M(2018**)** Accuracy of Cone-beam Computed Tomography in Comparison with Standard Method in Evaluating Root Canal Morphology: An *In Vitro* Study**.** *Iran Endod J*, 13**:181–187.**

De Deus QD(1975) Frequency, location, and direction of the lateral, secondary, and accessory canals. *J Endod*,**1**:361-6.

Green D. A(1956) stereomicroscopic study of the root apices of 400 maxillary and mandibular teeth *Oral Surg Oral Med Oral Pathol*,**9**:1224-32

Hargreaves KM, Cohen S (2016) *Pathways of the Pulp*, 11th ed. Mosby Inc, St.Louis. USA**,** 136-222

Ingle J, Bakland I(2011)*Endodontics*.7th ed.Hamilton:BCDecker,345-90

Kuzekanani M, Haghani J, Golbazkhanipour MR (2015) Root canal anatomy and Morphology of Maxillary incisor teeth in an Iranian population.*IJRD*,**6**:147-151

Kuzekanani M, Walsh LJ, Haghani J, Kermani AZ(2017) Radix entomolaris in the mandibular molar teeth of an Iranian population. *Int J Dent.*, **21**:1-5.

Kuzekanani M, Haghani J, Walsh LJ, Estabragh MA (2018). Pulp stones, prevalence and distribution in an Iranian population. *J Contemp Dent Practice*,**19**:60-5.

Mashyakhy M (2018) Prevalence of a second root and canal in mandibular and maxillary canines in a Saudi Arabian population: A cone-beam computed tomography study. *J Contemp Dent Practice*,**20**:773-777.

Mashyakhy M (2019) Anatomical analysis of permanent mandibular incisors in a Saudi Arabian population: An in Vivo cone-beam computed tomography study. *Nigerian journal of clinical practice*,**22**: 1611-1.

Onay OE, Ungor M.(2008) Maxillary Canines with two root canals. *Hacettepe Dis Hekimligi Fakultesi Dergisi*, **32**:20–4.

Patel S, Dawood A, Ford TP, Whaites E(2007)The potential applications of cone beam computed tomography in the management of endodontic problems. *Int EndodJ*,**40**:818–830.

Pineda F, Kuttler Y(1972) Mesiodistal and buccolingual roentgenographic investigation of 7,275 root canals.*Oral Surg Oral Med Oral Pathol*,**33**:101–10.

Plascencia H, Cruz A, Sánchez CAP, Díaz M, López C, Bramante CM , Bertram I. Moldauer BI, Zapata RO(2017) Micro-CT study of the root canal anatomy of maxillary canines. *J Clin Exp Dent* ,**9**:1230-6.

Sert S, Bayirli GS (2004)Evaluation of the root canal configurations of the mandibular and maxillary permanent teeth by gender in the Turkish population. *Journal of Endodontics*,**6**:391-8

Seltzer S(1988) *Endodontology*: Biologic considerations in endodontic procedure .2nd ed Philadelphia Lea&Febiger 1988 ;Chap 11: 410-433

Somalinga Amardeep N, Raghu S, Natanasabapathy V(2014)Root canal morphology Of Permanent maxillary and mandibular canines in Indian population using cone beam computed tomography.*Anatomy Research International*,**2**:1-7

Uchiyama M, Anzai M, Yamamoto A, Uchida K, Utsuno H, Kawase Y(2011) Root canal system of the maxillary canine. *Okajimas Folia Anat Jpn*,**87**:189-93.

Versiani MA,Pecora JD, Sousa-Neto MD(2013) Microcomputed Tomography analysis of the root canal morphology of single-rooted mandibular canines *Int Endod J*,**46**:800–80

Vertucci F(1984) Root canal anatomy of the human permanent teeth.*Oral Surg Oral Med Oral_Pathol*,**58**:589–99.

Vertucci FJ(2005) Root canal morphology and its relationship to endodontic procedures *Endodontic Topics*,**l**:1 3–29

Vertucci,FJ, Haddix JE (2016)"Tooth morphology and access cavity preparation," in *Pathways of Pulp*, K. M. Hargreaves and S Cohen,11th ed. Mosby Inc, St.Louis. USA,136-222

Weng XL, Yu SB, Zhao SL, Wang HG, Mu T, Tang RY, Zhou XD(2009)Root canal morphology of permanent maxillary teeth in the Han nationality in Chinese Guanzhong area: a new modified root canal staining technique *JEndodon*,**35**d:651-6.

Wikipedia. https://en.wikipedia.org/wiki/Maxillarycanine accessed; 2/05/2019.

Potential ability for implantation of mouse embryo post-vitrification based on Igf2, H19 and Bax Gene expression

Noer Muhammad Dliyaul Haq[1], Diah Pristihadi[1], Vista Budiariati[1], Ahmad Furqon[2], Mokhamad Fahrudin[1], Cece Sumantri[2], Arief Boediono[1,*]

[1] Department of Anatomy, Physiology and Pharmacology, Faculty of Veterinary Medicine
[2] Department of Animal Production and Technology, Faculty of Animal Science
[1,2] Bogor Agricultural University, Bogor 16680, Indonesia

Abstract

Vitrification is one of cryopreservation method for freezing cells without ice formation so that biological materials such as sperm, oocyte, or embryo, can be preserved and later can be used for a specific purpose including wildlife conservation efforts. Unfortunately, high concentration of cryoprotectan in vitrification process can cause osmotic stress and has high toxic levels that may affect embryo quality. The purpose of this research is to analyze the quality of post-vitrification embryos at morula and blastocyst stages based on morphometric variable, and Bax gene expression, futhermore potency of implantation of the post-vitrification embryo were also examined based on H19 and Igf2 gene expression. The results showed embryo viability post-vitrification decreased 5.67% and 6.02% in morula and blastocyst. Development ability from morula to blastocyst post-vitrification was also decreased by 10.15%. Morphometry analysis of morula post-vitrification showed decreased values of zona pellucida tickness (ZPT), zona pellucida tickness variation (ZPTV) and blastomeres area, while perivetellin space (PVS) area was increased compared to fresh morula. Blastocyst post-vitrification had increased values of ZPT, ZPTV, and PVS, while in ICM and the blastocoel were also decreased compared to fresh blastocyst. The result of relative levels mRNA of Igf2, H19, and Bax gene show no significant difference gene expression between fresh blastocyst, blastocyst post-vitrification, and morula post-vitrification group.

1. Introduction

Cryopreservation is cells freezing method that aims to reduce cell metabolism so that cells can be stored for a long time. Cryopreservation can be used to support the success of conservation by storing source of primary genetic material such as sperm for males and oocytes for females. In addition, storage of genetic material can also be carried out on embryos. The development of cryopreservation method that can be used to store genetic material are slow freezing and vitrification method (Best, 2015). Currently, many researchers prefer to do vitrification than slow freezing for genetic

* Corresponding author. E-mail: ab@apps.ipb.ac.id

material storage. The advantages of the vitrification method are lower costs and it does not require long time process compared to slow freezing method.

The results of the study by Li et al., (2014) showed that the vitrification method gave a higher post-warming survival rate of the embryos compared to the traditional method of slow freezing, but there are several things that should be considered before decided to use vitrification method. There are the toxicity of cryoprotectants and osmotic stress induced by replacement water content in cells with cryoprotectant. These effects may cause morphological and morphometric changes of mouse embryos post-vitrification (Homayoun et al., 2016). The morphological assessment and morphometric approach of the embryos was carried out to determine the quality of the embryos, including implantation capability and development prediction of embryo after embryo transfer.

In addition, previous study showed that vitrification in pig embryos causes changes of genome imprint expression (Bartolac et al., 2018). Genome imprinting is the expression of genes or parts of chromosomes that are derived by the parental allele. The maternal or the paternal alleles are found but only one allele is active, while the other alleles are silenced or inactive. The influential factor in the process of imprinting is the binding of the methyl group on DNA which causes genes to be inactive (Hitchin and Moore, 2004). The process of epigenetics is caused by three mechanisms, i.e. non-coding RNAs, histone modification and DNA methylation. During development of the pre-implantation embryo, the genome undergoes a demethylation and methylation process, but differentially methylated regions (DMRs) from the imprint gene are maintained. Disorders in gene imprint expression can be caused by exposure to the artificial environment during embryo culture and embryo manipulation that can lead to changes in methylation patterns, such as the development of extra embryonic tissue in parthenogenetic embryos (Marhendra and Boediono, 2010).

There are several imprint genes that influence the embryogenesis process including growth of the embryos, placenta and neonate. Specifically, genes expressed by paternal alleles such as Igf2, Peg1, Peg3, Rasgrf1, and Dlk1 act as growth promoters, while specifically genes expressed by maternal alleles act as growth inhibitor such as Igf2r, Gnas, Cdkn1c, H19, and Grb10. In addition, there are genes that influence neurological such as Nesp, Ube3a, and Kcnq1 (Plasschaert and Bartolomei, 2014). The imprint genes which have a function to maintain the growth and development of fetal and placental is the Igf2 and H19 genes. The aberration of gene imprint expression causes the condition of fetal and placental dysplasia which subsequently causes abnormal embryo development (Park et al., 2011). In addition, Ig2 and H19 gene expression at the stage of the preimplantation embryo were fluctuate. This was indicated by the repressed of H19 gene transcription in early develop embryo to stage 4 cells. The H19 gene was stable expressed at the morula stage and increased at the blastocyst stage. The Igf2 gene transcription was detected in all stages of preimplantation embryo development and increased at the 8 cell stage.

Embryos at blastocyst stage are more preferable to be performed vitrified than at 4-8 cell and morula stage. The results of the Ochota et al. (2014) on cat's embryo vitrification at the stages of 4-8 cells and morula showed that the ability of 4-8 cells and morula embryos to develop into blastocysts are 13% and 27% respetively. Based on those previous studies, the aim of this research was to analyze the effect of vitrifica-

tion in mice embryos at the morula and blastocyst stages based on Igf2, H19 and Bax expression genes.

2. Materials and Methods

2.1 Material and Media

The experimental animals used as sources of embryos are adult female DDY mice at 2 months of age. Mice were kept under controlled temperature of 22-25 °C and 12 hours light conditions (6:00-18:00). Food and water supplied ad libitum. Experimental procedures of research was approvel by the animal ethics committee Faculty of Veterinary Medicine, Bogor Agricultural University (No: 121/KEH/SKE//IV/2019).

The materials used in this research are pregnant serum gonadotrophin (PMSG) (Folligon, Intervet, Netherland), human chorionic gonadotrophin (hCG) (Chorulon, Intervet, Netherland), GMOP (Vitrolife, Sweden), G2 culture medium (Vitrolife, Sweden). Cryoprotectant used in vitrification-warming process obtained from Sigma-Aldrich (St. Louis, MO, USA) which are ethylene glycol (EG), dimethyl sulfoxide (DMSO) and sucrose.

Molecular analysis were done using the RNeasy mini kit (Qiagen), reverted Ace qPCR master RT mix with gDNA remover (Toyobo), iTaqTM SYBR Green Supermix with Rox PCR core reagent (Bio-Rad).

2.2 Embrio *In Vivo* Collection

The superovulation methods were carried out based on Eckardt and McLaughlin (2009). The embryos were collected on day 3 for the embryo at the morula stage, while the blastocyst stage embryo was collected on day 4. The embryos that have been obtained are transferred in drop of GMOP and the vitrification process was carried out.

2.3 Vitrification and Warming Process

The method and vitrification-warming media in this research were carried out based on the research report of Boediono (2005). The vitrification medium used is (V2) 10% EG, (V3) 15% EG + 15% DMSO + 0.5 M sucrose, while the warming medium is (V4) 0.5 M sucrose, (V5) 0.25 M sucrose and (V6) 0.1 M sucrose. Embryos vitrification further warming at room temperature, followed cultured in G2 medium.

2.4 Viability and Embryo Development Analysis

Analysis of viability of morula and blastocyst embryos were analyzed based on morphology and the ability of the embryo to return to its original shape (re-expansion). Morula embryos were cultured in G2 medium for 42 hours to determine the ability of the embryo to develop to blastocyst, while the blastocyst embryos were cultured in G2 medium for 24 hours to analyze the number of cells.

2.5 Numbers Cells of Blastocyst Embryos Analysis

Analysis of the number of cells in the blastocyst embryo was carried out based on the method of making chromosome preparations by Notosoediro et al. (2001). Staining was done using 5% Giemsa for 20 minutes.

2.6 Morphometric Analysis

Embryo morphometry analysis was carried out with Standard Cellens software. The method of analysis is carried out based on the method Molina et al. (2014) and Sun et al. (2005). Embryos morphometry analysis was carried out based on the parameters of zona pellucida thickness (ZPT), zona pellucida thickness variation (ZPTV), and periviteline space. Blastocyst embryos were analyzed of inner cell mass (ICM) and blastocoel area, while embryos of morula were analyzed for blastomer area.

2.7 Embryo RNA Extraction

Embryo RNA extraction method was carried out based on Bartolac *et al*. (2018). The morula and blastocyst embryos that cultured in G2 medium were collected in 8-10 embryos in one tube and RNA extraction was carried out based on the RNeasy mini kit (Qiagen) protocol. Furthermore, cDNA synthesis was performed based on Ace qPCR reverta protocol mix master RT with gDNA remover (Toyobo). cDNA concentration was measured using the nanodrop method.

2.8 Quantitative reverse transcriptase polymerase chain reaction (qRT-PCR) Analysis

For the analysis of qRT-PCR, the specific gene primers were manually designed and displayed in Table 1. The initial step was the 96-well microtiter plate filled with each cDNA sample and no-template control. qRT-PCR analysis was carried out with a program of 95 °C for 1 minute, 95 °C for 15 seconds, and 58 °C for 1 minute. The

Table 1. Spesific genes primer.

No.	Access number			Gene name	Product length (bp)
1	BC058615.1	Igf2	Forward	5'-GTCTTCATCCTCTTCCAGCC-3'	195
			Reverse	5'-CGGTCCGAACAGACAAACTG-3'	
2	BC025150.1	H19	Forward	5'-GCAGTCATCCAGCCTTCTTG-3'	190
			Reverse	5'-GAAGTCCCCGGATTCAAAGG-3'	
3	BC018228.2	Bax	Forward	5'-CAAGAAGCTGAGCGAGTGTC-3'	156
			Reverse	5'-CCCCAGTTGAAGTTGCCATC-3'	
4	BC138614.1	Actb	Forward	5'-CTGTATTCCCCTCCATCGTG-3'	181
			Reverse	5'-GTGTGGTGCCAGATCTTCTC-3'	

housekeeping gene used in this research is Actb gene. The 2Delta Ct (ΔCt) method is used to calculate the difference between the target gene and housekeeping genes: (2-$\Delta\Delta$Ct = [(ΔCt target gene) - (ΔCt housekeeping genes) sample] - [(ΔCt target gene) - (Δ Housekeeping CT gen) standard]).

2.9 Statistical Analysis

Statistical analysis in this research was carried out with SPSS software. Gene expression data were analyzed using a one-way ANOVA test, viability of the embryo was analyzed using the Wilcoxon test. Number of cells, ZPT, ICM, blastocoel and blastomer area were analyzed using t-independent test, while ZPTV, perivitelline space, and embryo development were analyzed using the mann-whitney test.

3. Results

Vitrification method widely used for storage of genetic material. In addition, vitrification in human embryos is also used as an alternative step to reduce the incidence of multiple pregnancies that can affect maternal or fetal development. Vitrification can be performed at different embryonic stages. The results showed that viability of morula and blastocyst stage post-vitrification was decreased 6.02% and 5.67% respectively (Table 2), but statistically did not show significant differences (p>0.05). This is confirmed by the ability of post-vitrified embryo re-expansion (Figure 1). In addition, Blastocyst rate in post-vitification morula embryos cultured in G2 medium also decreased by 10.15%, similar compared to fresh morula embryos (Table 3).

Post-vitrified embryo morphometry analysis is one of method that can be used to determine the quality of the embryo. Morphometry analysis in post-vitrified morula embryos showed decreased values of zona pellucida thicknes (ZPT), zona pellucida thickness variation (ZPTV) and blastomer area of 2.73 μm, 0.2% and 1504.83 μm^2 respectively, while in variable perivetellin space area showed increased of 2280,195

Table 2. Viability of post-vitrification at morula and blastocysts stage embryos.

Group	N	Viability (%) ± SE
Fresh morula	66	100 ± 0[a]
Post-vitrified morula	66	93,98 ± 2,72[a]
Fresh blastocyst	54	100 ± 0[a]
Post-vitrified blastocyst	54	94,33 ± 2,47[a]

Table 3. Ability development of post-vitrification morula embryo.

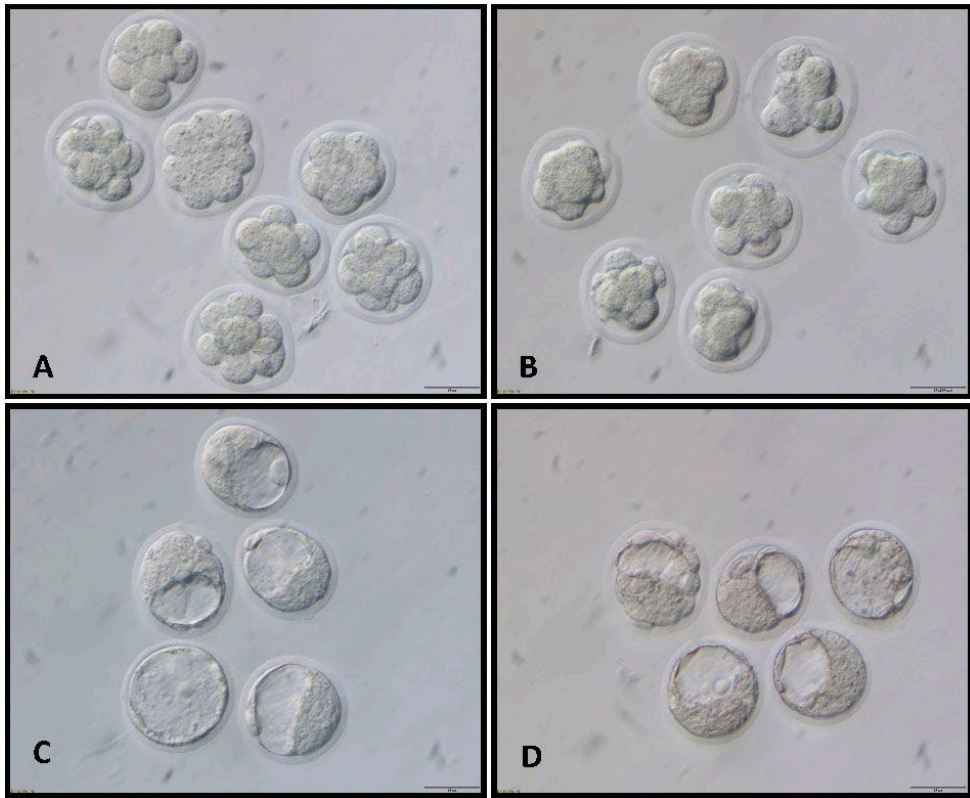| Group	N	Ability develop to balstocyst (%) ± SE
Fresh morula	70	94,29 ± 2,51[a]
Post-vitrified morula	62	82,14 ± 5,08[a]

Figure 1. Comparison of embryonic morphology (A) Fresh morula, (B) post-vitrified morula, (C) fresh blastosis, and (D) post-vitrified blastosis. Scale bar = 50 µm.

μm^2 compared to the fresh morula. In post-vitrified blastocyst embryos showed increased values of ZPT, ZPTV, and perivitellin space of 1.27 μm, 0.46% and 265.727 μm^2 repectively, while ICM and blastocoel area were decreased 710.16 μm2 and 84.29 μm^2 respectively compared to fresh blastocysts. Statistically the morphometric analysis result on post-vitrified embryos at the blastocyst stage showed no significant difference ($p>0.05$) compared to fresh blastocyst embryos (Table 4). the morphometric analysis results in post-vitrification embryos at the morula stage showed significant differences ($p<0.05$) in ZPTV, periveteline space, and blastomers variables, while in ZPT did not show significant differences ($p>0.05$) compared to fresh morula embryos (Table 5).

Advanced applications that can be performed on post-vitrified embryos which have good quality morphology and morphometry are embryo transfer (TE). The success of embryo transfer is influenced by several factors, such as genes expression that play an important role in embryogenesis. The results of the analysis of Igf2, H19, and Bax gene expression in post-virification embryos did not show significant differences ($p>0.05$) compared to fresh embryos. It attempted by the relative levels of the mRNA

Table 4. Morphometric analysis of post-vitrified blastocyst embryos.

Group	N	ZPT (μm) ± SE	ZPTV (%) ± SE	PVS (μm²) ± SE	ICM (μm²) ± SE	*Blastocoel* (μm²) ± SE
Fresh blastocyst fresh	45	12,83 ± 0,99 [a]	5,61 ± 0,19 [a]	880,785 ± 98,50 [a]	11613,56 ± 459,88 [a]	13936,69 ± 875,87 [a]
Post-vitrified blastocyst	50	14,10 ± 1,07 [a]	6,07 ± 0,15 [a]	1146,512 ± 135,73 [a]	10903,4 ± 458,26 [a]	13852,4 ± 787,73 [a]

ZPT: zona pellucida thickness; ZPTV: zona pellucida thicknss variation; PVS: perivitellin space; ICM: Inner Cell Mass. (a-b, p<0.05).

Table 5. Morphometric analysis of post-vitrified morula embryos.

Group	N	ZPT (μm) ± SE	ZPTV (%) ± SE	PVS (μm²) ± SE	*Blastomer* (μm²) ± SE
Fresh Morula	30	10,23 ± 0,93 [a]	6,91 ± 0,08 [a]	5553,53 ± 423,03[a]	22473,87 ± 389,78 [a]
Post-vitrified morula	28	7,50 ± 0,75 [a]	6,71 ± 0,10 [b]	7833,725 ± 911,4075 [b]	20969,04 ± 367,25[b]

ZPT: zona pellucida thickness; ZPTV: zona pellucida thicknss variation; PVS: perivitellin space; ICM: Inner Cell Mass. (a-b, p<0.05).

Table 6. Cells number of post-vitrified blastocyst.

Group	N	Cells number ± SE
Fresh blastocyst	9	63,67 ± 3,09[a]
Post-vitrified blastocyst	9	63,33 ± 3,35[a]

Table 7. Relative levels Igf2, H19, and Bax genes expression.

Group	ΔΔCt *Igf*2 ± SE	ΔΔCt *H19* ± SE	ΔΔCt *Bax* ± SE
Fresh Blastocyst	0,75 ± 0,31[a]	1,30 ± 0,61[a]	1,62 ± 0,79[a]
Vitirified Blastocyst	0,76 ± 0,68[a]	0,11 ± 0,04[a]	1,06 ± 1,04[a]
Vitrified Morula	1,24 ± 0,66[a]	1,19 ± 0,54[a]	0,68 ± 0,36[a]

expression in the Igf2 gene of 0.75 ± 0.31, 0.76 ± 0.68, 1.24 ± 0.66 and H19 gene of 1.30 ± 0.61, 0.11 ± 0.04, 1.19 ± 0.54, and Bax gene of 1.62 ± 0.79, 1.06 ± 1.04, 0.68 ± 0.36 in fresh blastocysts, post-vitrified blastocysts and post-vitrified morula respectively (Table 7). In addition, cells number analysis of post-vitrified blastocyst embryos showed a number of cells of 63.67 ± 3.09 and 63.33 ± 3.35 in fresh blastocyst embryos and vitrified blastocysts respectively, statistically not significantly different (p>0.05) compared with fresh embryos (Table 6).

4. Discussion

Vitrification method has been widely applied for animals and humans. This is because method has several advantages compared to slowfreezing cryopreservation, such as shorter time and simpler tools. Moreover, viability rate of post-vitrification embryos are higher compared to slow freezing cryopreservation methods (Li et al., 2014). In this research, the viability rate of post-vitrified embryos at the morula and blastocyst was similar compared to fresh embryos. The higher level of viability rate of post-vitrified embryos caused by no formation of ice crystals in cells during the vitrification process.

In general, cell freezing process can impact cell damage through two main pathways, which are mechanical damage that affects cell shape due to the formation of ice crystals and cell damage caused by toxicity from cryoprotectants and osmotic stress that occurs related to cryoprotectant concentration used in the cell cryopreservation process. Cryoprotectants used in the cryopreservation process of this study are dimethyl sulfoxide (DMSO), ethylene glycol (EG), and sucrose. Dimethyl sulfoxide (DMSO) and ethylene glycol (EG) are penetrating cryoprotectant, while sucrose is one of non-penetrating type cryoprotectant. Both types of cryoprotectants have a function to inhibit formation of ice crystals in the vitrification process. The difference of the two cryoprotectants is the size of the molecule. Penetrating cryopotectants are small molecules that able to pass cell membranes, while non-penetrating cryoprotectants are large molecules, so it will not penetrate cell membranes. In addition, non-penetrating cryoprotectants usually have lower toxic properties compared to penetrating cryoprotectant (Bhattacharya and Prajapati 2016).

Combination of penetrating and non-penetrating cryoprotectant on research is expected to reduce toxic and osmotic stress caused by penetring cryoprotectant. In the process of warming, sucrose solution plays a role as an osmotic buffer so that cryoprotectants can be released without spending excessive intracellular water. In addition, multilevel concentrations in sucrose solution can reduce membrane damage due to osmotic pressure (Dattena et al., 2004). Mouttham and Comizzoli (2017) report that sucrose is very effective in maintaining structural integrity and function of membranes. Other factors to the success of vitrification are the small volume of high concentrations and times of cryoprotectant exposure in the vitrification process (Liebermann, 2003).

Cryopreservation of biological materials consist of six important steps, starting with exposure biological material to cryoprotectants, freezing (slow/rapid) to sub-zero temperatures, storage, thawing/warming, dilution and removal of cryoprotectants and restoring biological material in environmental physiology (Liebermann, 2003). In this research, morula and blastocysts embryos post-vitrified were cultured in G2 medium. Morula stage embryos cultured for 42 hours after warming, whereas blastocyst embryos cultured for 24 hours after warming. At the morula post-vitrified, embryo culture aims to determine the ability of embryo develop to blastocyst. Hence, embryo culture is expected can perform a repairing mechanism. The results showed that post-vitrified morula embryos were able to develop to blastocysts. These results indicate that vitrification does not affect embryo metabolism.

Embryo metabolism is one of the factors that influence the ability of the embryo to develop into the next stage. Morbeck et al. (2014) explained that disorder of meta-

bolic and reductive-oxydative balance can inhibit embryonic development and potentially reduce embryo viability, fetus and postnatal development. Other researchers suggest that amino acid metabolism in embryos can be used as an approach to predict the ability of embryonic development. Post-freezing embryos that are able to develop to blastocyst stage show the same amino acid metabolism as fresh embryos, whereas non-developing embryos show metabolic homeostatic disorders (Stokes et al., 2007). On the other hand, there are other variables that can be used to determine the quality of the embryo, such as morphology and morphometry embryo. Morphology embryo analysis is very subjective and requires high skill to be able to distinguish embryo quality. Because of that, several researchers carried out embryonic morphometry analysis to predict the ability of embryo development and implantation.

Morphometry analysis on the research carried out after the warming process includes zona pellucida thickness (ZPT), zona pellucida thickness variation (ZPTV), perivitelline space, inner cell mass (ICM), and blastocoel area for post-vitrified blastocyst embryos, while morphometric analysis in post-vitrification morula embryos include ZPT, ZPTV, perivetillen space, and blastomeres. Zona pellucida thickness (ZPT) and zone pellucida thickness variation (ZPTV) are variables that can be used to predict the ability of the embryo for hatching and implantation. Zona pellucida serves to maintain the occurrence of poly-sperm fertilization. In addition, at the early stage of embryonic development, zona pellucida function is to maintain the integrity and transportation of the embryo through the fallopian tube. At the stage of the blastula, zona pellucida is depleted in preparation for implantation due to the effects of endometrial lysine and expansion of blastocyst.

The depletion zona pellucida correlated positively with embryonic development, but in some cases zona pellucida fail to rupture resulting in failed hatching of the blastocyst embryo (Sun et al., 2005). It can be caused by impaired secretion of trypsin-like proteases from the tropectoderm (TE) and the phenomenon of zona hardening. Cohen et al., (1989) explained that the thickness of the pellucida zone is not the same, some thinner parts than other parts. It allows the embryo to transport the membrane and secrete the substrate to lyse the local zona. In this research, vitrification of blastocyst embryos showed an increase in the value of ZPT and ZPTV, although statistically it did not show significantly differencent. Whereas the morula embryo showed a decrease in the value of ZPT and ZPTV, but only the value of ZPTV which showed statistically significant differences. Sun et al., (2005) explained that the high value of ZPTV increases the potential of the pregnancy rate in human embryos. Decreasing ZPTV values can be negatively correlated with patient age. In addition, high-grade embryos have higher ZPTV values than low-grade embryos.

The volume analysis of post-vitrified embryonic cells was also carried out in this research. Hnida et al., (2004) explained that the incidence of embryonic cell fragmentation associated with the blastomere volume. It is indicated by an increase in the incidence of fragmentation significantly in the blastomer which has decreased volume. In the results of this research there was a decrease in blastomer volume of post-vitrified morula embryos, ICM and blastocoel volume in blastocyst embryos. Whereas perivetilen space has increased volume in post-vitrified morula and blastocyst embryos. The decrease volume is possible due to substitution process of cryoprotectants with water in cells during warming process. These results were supported by an analysis of the number of cells in the post-vitrified blastocyst embryos that did not

show significant differences. Konc et al., (2014) explained that during the vitrification process, majority of cells undergo dehydration before starting ultrarapid freezing due to high concentrations exposure of cryoprotectant. It is needed for the stages of intracellular and extracellular glass formation in the vitrification process. Nonetheless, failure of vitrification can lead to increased incidence of necrosis and cell apoptosis.

Research result by Baust et al., (2001) showed an increase in apoptotic protease (caspase-3) activity of 3.3 fold after thawing compared to normal cells. Increased apoptotic activity occurred at 12 to 21 hours post-thawing, while increased necrosis activity occurred at 6 hours post-thawing. After that, the activity returned to normal at 48 hours post-thawing. Increased activity can be inhibited by the addition of molecules that can reduce sublethal hypothermic stress that occurs in cells due to the cryopreservation process. Sublethal stress possible associated with oxidative stress, adenylate depletion, production and accumulation of free radicals, cell dehydration, and upregulation of nitric oxide. The accumulation of these things able to initiate the occurrence of the apoptotic mechanism in several cellular systems. The success of vitrification in this research can also be seen from Bax gene expression which statistically did not show significant differences in post-vitrified embryos compared to fresh embryos. Bax is a pro-apoptotic protein and plays an important role in the process of apoptosis. Based on molecular mechanism, Bax and Fas complex receptors in the mitochondrial membrane will be stimulated by the Trp53 protein when the cells have DNA damage. Activation of Bax and Fas complex receptors will cause release of cytochrome c and caspase 3 activation. In some cases, apoptosis and anti-apoptotic genes in apoptotic pathways are stimulated by hyperglycemic stress conditions that cause increased DNA fragmentation (Fabian et al., 2009).

Furthermore, this research analyzed the potency for implantation ability in post-vitrified embryos based on Igf2 and H19 gene expression. The results showed that post-vitrified blastocyst embryos had similar Igf2 gene expression levels and increased expression in post-vitrified morula embryos compared to fresh embryos. Whereas H19 gene expression pattern showed an increased expression in post-vitrified morula and blastocyst embryos compared to fresh embryos. However, statistically it did not show a significant difference in Igf2 and H19 gene expression. This results can be caused by the vitrified close system method used in this research. The close system keeps the embryo indirect contact with LN_2, so that the physical shock effect of the embryo can be reduced. These results were supported by the research result Bartolac et al. (2018) which indicated that pig blastocyst embryos exposed to vitrification and warming cryoprotectants without being inserted into LN2 showed the same transcription level as fresh embryos.

Bartolac et al., (2018) explained that disruption of gene expression can be caused by cellular and molecular changes associated with contact embryo-LN_2. In addition, the vitrification process at room temperature is believed to reduce the toxic effects of cryoprotectants used. The results showed that post-vitrified embryos in this research had potential implantation capability after embryo transfer. The results of this research indicated that post-vitrification embryos was safe and could be applied to support the success of embryo transfer. It was shown by the ability of post-vitrified embryo development to the next stage and genes that influenced on fetal and placental development had a relative level of mRNA similar to fresh embryos. Changes in the transcription levels of Igf2 and H19 genes could be influenced by the embryo

culture system. It was shown by the results of research by Park et al. (2011) which explained that the transcription levels of the Igf2 and H19 genes in pig embryos in the blastocyst stage in vitro were higher than in vivo embryos.

Igf2 is a gene that is specifically expressed by the paternal allele and has a function to regulate the development of the placenta and fetus. Whereas, H19 is a gene that is specifically expressed by the maternal allele and its function is to inhibit the development of the placenta and fetus. Abberant of gene expression cause abnormalities in embryonic development, such as Beckwith-Wiedemann Syndrome (BWS) which causes excessive fetal growth or Silver-Russell Syndrome (SRS) which causes less optimal fetal growth (Plasschaert and Bartolomei, 2014). Sivastava et al., (2000) showed that the H19 promoter is control part of the monoallele expression of the Igf2 and H19 genes in different regulatory pathways. On the maternal allele, the H19 gene promoter is required as an insulator which functions to deactivate the Igf2 gene. Whereas in the paternal allele, the upstream element mediates epigenetic modification of the H19 promoter during development which results in H19 in the paternal allele being inactive.

Igf2 gene in the blastocyst embryo is strongly expressed in the inner cell mass (ICM). The Igf2 gene functions to stimulate the classic Erk1/2 pathway and activation of Akt kinase. Erk 1/2 activation serves as an important proliferative signal of the embryo to continue the cell cycle during embryonic development. Erk1/2 activation plays a role in the proliferation of polar tropectoderm cells (TE) and tropoblast cell formation, while activation of Akt signaling plays an important role in the success of implantation by maintaining cell survival ability, tropoblast invasion and induction of extracellular matrix remodeling (Thieme et al. 2012).

Based on these results, it can be concluded that vitrification in morula and blastocyst stage embryos did not affect embryo quality based on morphometric analysis and Bax gene expression. In addition, post-vitrified embryo still has potential ability for implantation. It is indicated by the levels of Igf2 and H19 gene expression which is almost the same as the fresh embryo. Nevertheless, confirmation of the implantation ability in post-vitrified embryos is needed by embryo transfer.

Acknowledgments

References

Bartolac L.K., Lowe J.L., Koustas G., Grupen C.G., Sjoblom C. (2018) Vitrification, not cryoprotectant exposure, alters the expression of developmentally important genes in *in vitro* produced porcine blastocysts. Cryobiology. 80: 70-76.

Baust J.M., Vogel M.J., Buskirk R.V., Baust J.G. (2001) A molecular basis of cryopreservation failure and its modulation to improve cell survival. Cell transplantation. 10: 561-571

Best B.P. (2015) Cryprotectant toxicity: fact, issues, and quetions. Rejuvenation research. 18(5): 422-436.

Bhattacharya S., Prajapati B.G. (2016) A review on cryoprotectant and its modern implication in cryonics. Asian Journal of Pharmaceutics. 10(3): 154-159

Boediono A. (2005) Kriopreservasi Embrio. Surabaya. Konas II PERMI & Temu Ilmiah II FER, 3-5 Februari.

Cohen J., Inge K.L., Suzman M., Wiker S.R., Wright G. (1989) Videocinematography of fresh and cryopreserved embryos: a retrospective analysis of embryonic morphology and implantation. Fertlity and Sterility. 51(5): 820-827

Dattena M., Accardo C., Pilichi S., Isachencko V., Mara L., Chessa B., Cappai P. (2004) Comparison of different vitrification protocols on viability after transfer of ovine blastocysts in vitro produced and in vivo derived. Theriogenology. 62: 481-493.

Eckardt S., McLaughlin K.J. (2009) Production of uniparental embryonic stem cell lines. Trends in Stem Cell Biology and Technology. 402: 19-38.

Fabian D., Cikos S., Koppel J. (2009) Gene expression in mouse preimplantation embryos affected by apoptotic inductor actinomycin D. Journal of Reproduction and Development. 55(5): 576-582

Hitchin M.P., Moore G. (2004) Genomic imprinting in fetal growth and Development. Reproductive Medicine Review. 11(1): 1-24

Hnida C., Engenheiro E., Ziebe S. (2004) Computer-controlled, multilevel, morphometric analysis of blastomere size as biomarker of fragmentation and multinuclearity in human embryos. Human Reproduction. 19(2): 288-293

Homayoun H., Zahiri S.H., Hemayatkhah J.V., Hassanpour D.A. (2016) Morphological and morphometric study of early-cleavage mice embryos resulting from in vitro fertilization at different cleavage stages after vitrification. Iranian Journal of Veterinary Research. 17(1): 55-58

Konc J., Kanyon K., Kriston R., Somoskoi B., Cseh S. (2014) Review article: Cryopreservation of embryos and oocyte in human assisted reproduction. BioMed Research International. 1-9

Li Z., Wang Y.A., Ledger W., Edgar D.H., Sullivan E.A. (2014) Clinical outcomes following cryopreservation of blastocysts by vitrification or slow freezing: a population-based cohort study. Human Reproduction. 29(12): 2794-2801.

Liebermann J. (2003) Review: Recent developments in human oocyte, embryo and blastocyst vitrification: where are we now?. Reproductive BioMedicine Online. 7(6): 623-633

Marhendra A.P.W., Boediono A. (2010) Perkembangan partenogenetik dari oosit mencit yang diaktivasi dengan ethanol dan 6_DMAP secara in vitro. Veterinaria Medica. 3(1): 69-74.

Moutcham L., Comizzoli P. (2017) Presence of sucrose in the vitrification solution and exposure for longer periods of time improve post-warming follicle integrity in cat ovarian tissues. Reproduction Domestic Animal. 52(2):224-229

Molina I., Lazaro-Ibanez E., Pertusa J., Debon A., Martinez-Sanchis J.V., Pellicer A. (2014) A minimally invasive methodology based on morphometric parameters for day 2 embryo quality assessment. Reproductive BioMedicine Online. 29: 470-480

Morbeck D.E., Krisher R.L., Herrick J.R., Baumann N.A., Matern D., Moyer T. (2014) Composition of commercial media used for human embryo culture. Fertility and Sterility. 102 (3): 759-766

Notosoediro P.N., Mohamad K., Boediono A. (2001) Abnormalitas jumlah kromosom embrio tahap blastosis pada mencit dan manusia. Media veteriner. 3: 62-65.

Ochota M., Wojtasik B., Nizanski W. (2016) Survival rate after vitrification of various stage of cat embryos and blastocyst with and without artificially collapsed blastocoel cavity. Reproduction in domestic animals. 51: 1-7.

Park C., Uh K., Mulligan B.P., Jeung E., Hyun S., Shin T., Ka H., Lee C. (2011) Analysis of imprinted gene expression in normal fertilized and uniparental preimplantation porcine embryos. Plos one. 6 (7): 1-10.

Plasschaert R.N., Bartolomei S. (2014) Genomic imprinting in development, growth, behavior, and stem cell. Development. 141: 1805-1813

Srivastava M., Hsieh S., Grinberg A., Williams-Simons L., Huang S., Pfeifer K. (2000) H19 and Igf2 monoallelic expression is regulated in two distinct ways by a shared cis acting regulatory region upstream of H19. Genes & Development. 14: 1186-1195.

Stokes P.J., Hawkhead J.A., Fawthrop R.K., Picton H.M., Sharma V., Leese H.J., Houghton F.D. (2007) Metabolism of human embryos following cryopreservation: Implications for the safety and selection of embryos for transfer in clinical IVF. Human Reproduction. 22 (3):829-835

Sun Y.P., Xu Y., Cao T., Su Y.C., Guo Y.H. (2005) Zona pellucida thickness and clinical pregnancy outcome following in vitro fertilization. International Journal of Gynecology and Obstetrics. 89: 258-262.

Thieme R., Schindler M., Ramin N., Fischer S., Muhleck S., FIscher B., Santos A.N. (2012) Insulin growth factor adjusment in preimplantation rabbit blastocysts and uterine tissues in response to maternal type 1 diabetes. Molecular and Cellular Endocrinology. 358:96-103.

Review

3D surface acquisition systems and their applications to facial anatomy: let's make a point

Daniele Gibelli, Annalisa Cappella, Claudia Dolci, Chiarella Sforza*

LAFAS, Laboratorio di Anatomia Funzionale dell'Apparato Stomatognatico, Dipartimento di Scienze Biomediche per la Salute, Università degli Studi di Milano, Milano, Italy

Abstract

In the last decades 3D optical devices have gained a primary role in facial anthropometry, where they find several applications from the anatomical research to clinics and surgery. With time the number of articles focusing on 3D surface analysis has raised, as well as validation studies which aim at verifying the reliability of different devices and methods of acquisition in comparison with other methods or direct anthropometry. This review aims at making a point in the field of 3D surface acquisition systems, describing the most used types of available devices and comparing the relevant outcomes in acquiring 3D facial models. Results show that currently stereophotogrammetric devices represent the gold standard, further improved by the diffusion of portable models. Caution should be given to the use of low-cost devices, more and more frequently described by literature, as often they do not meet the basic criteria for being applied to the anatomical study of face.

Introduction

The quantitative assessment of facial soft-tissue structures, their reciprocal relationships and relative proportions represent an important task in clinics (Hammond et al., 2004). Diagnosis, treatment planning and follow-up examinations all need some kind of measurements that should be performed taking their peculiar three-dimensional (3D) configuration into account (Schwenzer-Zimmerer et al., 2008; Pucciarelli et al., 2017; Kimura et al., 2019; Sforza et al., 2018).

3D optical scans are devices able to acquire a 3D model of an object through surface imaging. The introduction of this technology has represented a revolution in anthropometry: metrical assessment of face had been previously performed through direct measurements by calipers, a low-cost method which has the main limits of being time-consuming, to depend upon patients' cooperation and to have some problems in repeatability (Wong et al., 2008). Not even instruments developed in later times such as electromagnetic and electromechanic digitizers could overcome the lack of permanent records of the face, and the opportunity to replace wrong or missing values. On the other side, the acquisition of a virtual model of the face allows to perform reliable and repeatable measurements, and to assess a novel set of met-

* Corresponding author. E-mail: chiarella.sforza@unimi.it

rical parameters, including not only the traditional linear distances and angles, but also surface areas, volumes, differences between superimposed 3D models and geometric morphometric analyses (Winberg et al., 2006; Hong et al., 2017; Sawyer et al., 2009; Gibelli et al., 2015; Codari et al., 2015; Pucciarelli et al., 2017). Moreover, surface acquisition devices do not need physical contact with the face, thus avoiding the risk of skin compression (Douglas et al., 2003; Majid et al., 2005).

These methods of 3D acquisition have found several applications in a variety of disciplines involving the analysis of facial anatomy, from dentistry (Sterenborg et al., 2018) to aesthetic (Feng et al., 2019; Jimenez-Castellanos et al., 2016) and maxillofacial surgery (Sforza et al., 2018; Kimura et al., 2019), from the early diagnosis and follow-up of genetic and acquired pathologies (Pucciarelli et al., 2017; Dolci et al., 2018) to forensic anthropology (Gibelli et al., 2017a; Gibelli et al., 2017b).

In the last years the use of 3D surface acquisition systems has progressively increased, and devices improved as well: in the past 3D acquisitions could be performed only through static and expensive machines (de Menezes et al., 2010; Tzou et al., 2014) which limited the fields of applications and prevented the recruitment of some types of patients. Now the scenario is changing, with the introduction of modern portable and in some cases low-cost devices (Camison et al., 2018; Gibelli et al., 2018a; Gibelli et al., 2018c).

This review aims at taking stock of the situation in the field of soft tissue 3D facial imaging, describing the different types of available devices and the relevant advantages and limits. As the instruments are based on different technologies, should be used with dedicated protocols, and show specific limits, we will focus on those instruments that had been tested and used in our laboratory, thus providing also some practical information about 3D acquisition and reconstruction.

Stereophotogrammetry

Stereophotogrammetry is based on a light source (either patterned or conventional) to light the face, simultaneously acquired by two or more coordinated cameras oriented from different points of view (Majid et al., 2005; Wong et al., 2008; Plooij et al., 2009; Tzou et al., 2014). The device is able to record a dense polygon mesh together with facial texture and combines the quantitative mesh information with the qualitative reproduction of facial surface (Fig. 1). The finer the mesh, the better the outcome of facial acquisition. Generally facial stereophotogrammetric scans can reconstruct the face structure with a resolution of approximately 60 vertices/cm^2 in about 1.5-3.5 ms: the faster the scan, the less motion artifacts (Tzou et al. 2014; Gibelli et al., 2018b). Measurements obtained by stereophotogrammetry have a good precision and reproducibility, with random errors generally lower than 1.5 mm (Gibelli et al., 2018b). The position of some structures within the face such as the nostrils, ears and the chin region may limit the possibility of being viewed simultaneously by more than one camera. The problem can be partially resolved by increasing the number of cameras, with a higher monetary investment.

The chance of acquiring the entire face from different points of view at the same time and the high acquisition velocity render stereophotogrammetry the gold standard for facial scans, as it reduces at the minimum possible the bias due to involuntary
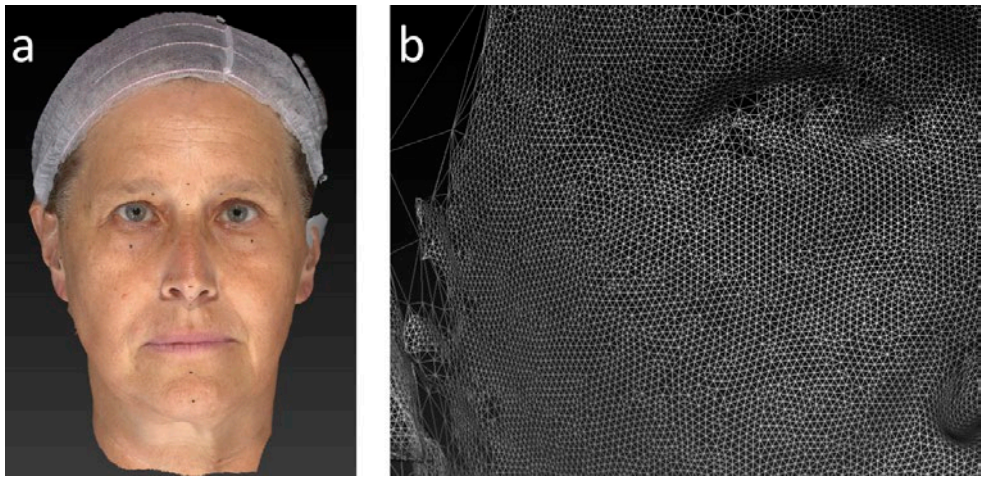
Figure 1. Example of textured scan (a) and mesh (b) of an acquisition by VECTRA M3 stereophotogrammetric device (Canfield Scientific, Inc.): the mesh is highly detailed and homogeneous, with defects in correspondence of hair and eyes.

movements (typically, eyes, nose and lips). Therefore, it is the ideal device for acquisition of not cooperative patients (such as children) and disabled persons with motor impairments.

Another advantage is the texture information which allows to label facial landmarks before the facial acquisition: previous landmarks labeling proved to improve accuracy in landmark recognition (Weinberg et al., 2004, Fig. 2).

The main limitations include the cost of the device (tens of thousands of euros circa), and the size of acquisition setting (Tzou et al., 2014) which sometimes prevent from acquiring patients who cannot be adequately hosted within the acquisition area (for example, patients in wheelchair). In addition, the devices are static, and therefore cannot be moved to meet permanently bedridden patients.

Laser scanner

Laser scanners acquire facial surface through a laser light and digital cameras. Accuracy and resolution are reported between 0.5 and 1 mm, with a mean scanning error of 1.1 mm (Fig. 3). During data acquisition, the laser light moves to scan the facial surface and approximately 10 s are necessary to obtain a complete facial image (Tzou et al., 2014; Gibelli et al., 2018c). As a consequence, the effect of possible involuntary facial movements is more evident than in stereophotogrammetry and may alter the final result (Schwenzer-Zimmerer et al., 2008). Critical parts for the acquisition are the ears, the nostrils and the chin; shadows and a dark complexion usually result in a hampered scan (Majid et al., 2005).

Some of the published studies based on acquisitions through laser scanner include two different captures from the right and left sides, simultaneously performed by
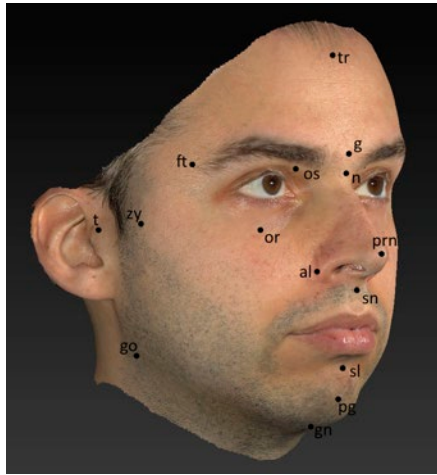
Figure 2. Example of landmarks usually labeled on the skin to improve anthropometrical analysis: tr: trichion; g: glabella; n: nasion; prn: pronasale; sn: subnasale; sl: sublabiale; pg: pogonion; gn: gnathion; os: sovraorbitale; or: orbitale; ft: frontotemporale; zy: zygion; t: tragion; go: gonion.
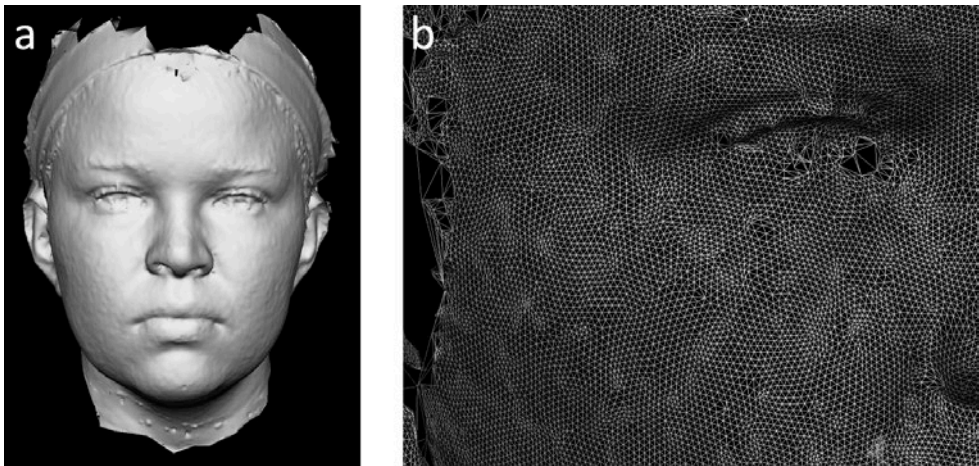

Figure 3. Example of scan (a) and mesh (b) of an acquisition by Vi910 laser scanner (Konica Minolta): the mesh is detailed, but affected by some not homogeneous areas due to involuntary facial movements during facial scan and between consecutive acquisitions.

two devices arranged in a pair (Kau and Richmond, 2008; Toma et al., 2009). This approach allows to reduce the influence of involuntary movements, but doubles the costs, as it requires two devices. However, recent literature observed that three consecutive models can be acquired separately (right side, frontal, left side), and merged, without appreciable modifications (De Angelis et al., 2009; Cattaneo et al., 2012;

Gibelli et al., 2018c). Clearly, in these cases the cooperation of the subjects is essential to limit motion artifacts due to the longer scan times.

The main limits of laser scanners are cost and the size of the device, as for the stereophotogrammetric ones: in addition, some models do not provide facial texture, preventing previous landmarks labelling. Laser scanner devices can be moved, although with difficulties because of their encumbrance.

The portable stereophotogrammetric devices

In the last years portable stereophotogrammetric devices have been introduced in commerce: these systems can obtain a facial model through a compact device and a laptop (Camison et al., 2018). In comparison with the static devices, the final acquisition is obtained through three consecutive scans (right side, frontal and left side) taken within a limited time period (Fig. 4). These new devices may extend the facial acquisition also to hospitalized patients as well as to subjects who cannot be hosted within the conventional stereophotogrammetric set.

The main weak point of these stereophotogrammetric instruments is the need for three consecutive facial scans, with an increment of facial involuntary movements and a less detailed final 3D model (Camison et al., 2018).

Two validation studies have been published in the last years, focusing on a portable stereophotogrammetric device. Camison et al. (2018) analyzed the repeatability of linear measurements between the portable device and a traditional static instrument. In addition, a superimposition procedure was performed registering the facial model
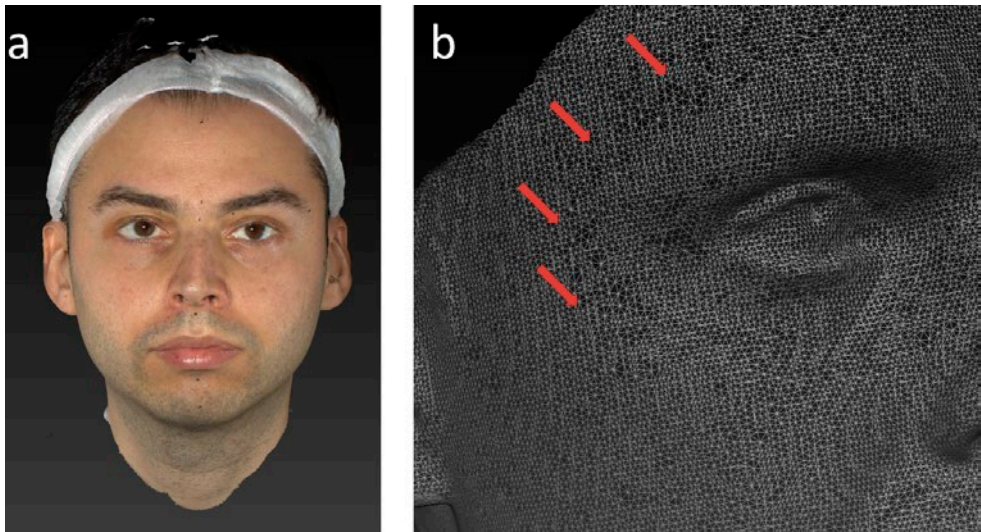

Figure 4. Example of textured scan (a) and mesh (b) of an acquisition by Vectra H2 portable device (Canfield Scientific, Inc.): the mesh is highly detailed; defects can be found in correspondence of areas shared by two consecutive scans (red arrows).
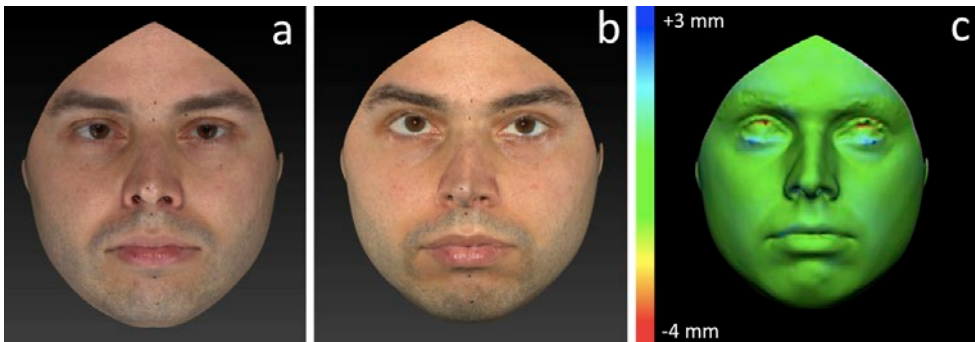
Figure 5. Example of 3D-3D superimposition between a scan from static VECTRA M3 system (a) and portable VECTRA H2 system (b), with chromatic sheet representing more concordant (green) and discordant (blue, red, yellow colors) areas between the two scans. As one can observe, most of facial surface is green indicating high concordance, but for eyes because of involuntary facial movements.

produced by the portable instrument onto that provided by a fixed one produced by another company (Camison et al., 2018). Their results confirmed that the stereophotogrammetric portable device is sufficiently accurate for most clinical applications.

Another validation study was published by Gibelli et al. (2018b): in this case, both the reference stereophotogrammetric static device and the portable one were produced by the same company. Again, the portable system was reliable in assessing linear measurements, angles and surface areas; however, volumetric measurements and 3D-3D registration procedures were affected by facial movements, increased by the need for consecutive captures (Fig. 5).

The major limits of the current instruments are represented by the necessary higher patient compliance, and by the cost (a few thousand euros circa): in addition, the device needs to be used with a high-performance laptop. Otherwise, it can be used storing the images on a memory card, for off-line elaborations, but it does not allow the operators to immediately verify the correctness of facial acquisitions.

Low-cost devices

Recently, novel and more economical portable devices have been developed, to widen the diffusion of 3D acquisition technology. An example is the Sense® 3D scanner, a hand-held scanner with a spatial x/y resolution of 0.9 mm and a depth resolution of 1.0 mm at 0.5 m (Fig. 6). It costs a few hundred of euros circa and can acquire a face in less than one minute (Fan et al., 2017).

However, at our knowledge, presently the Sense® device has been applied only in one published scientific article, where it was used to scan the face of a cadaver for the assessment of 3D modifications due to the decomposition process (Caplova et al., 2018). Only a validation study is available (Gibelli et al., 2018a): the device proved to give a reliable acquisition for the assessment of linear and angular measurements in case of inanimate subjects/objects (Caplova et al., 2018), but was is not reliable enough to be applied to clinical contexts.
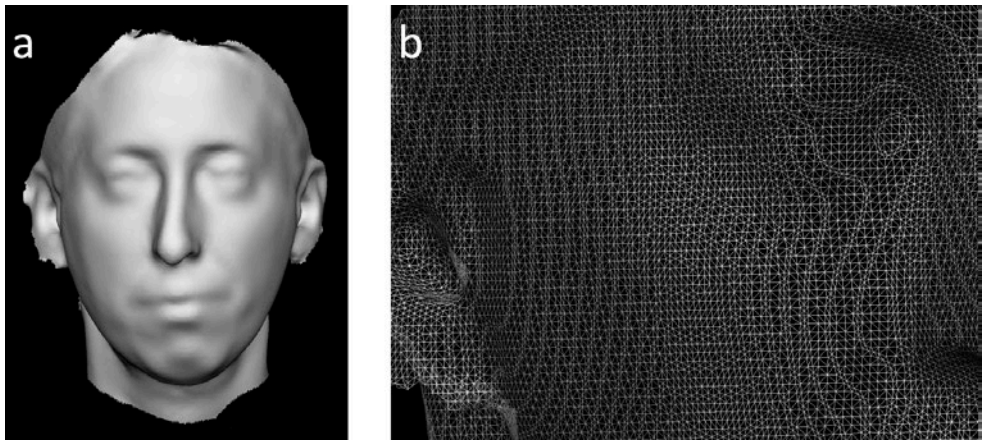
Figure 6. Example of textured scan (a) and mesh (b) of an acquisition by Sense laser scanner portable device: the mesh is less detailed than those obtained by the other facial scan methods.

Maués et al. (2018) compared facial scans obtained by a conventional fixed stereophotogrammetric device with the Microsoft Kinect® scanner. The relevant facial models were superimposed, and the distances between them were obtained. On average, the difference between the two methods was lower than 0.5 mm, but some areas had higher discrepancies. The authors concluded that the device showed a reasonable accuracy, thus proposing it as a possible resource for facial analysis.

Finally, in the last years other low-cost systems have been developed, including 3D acquisition applications for smartphones and tablets (Koban et al., 2014). However, they have not been validated for their application to research and clinical contexts.

Conclusion

3D optical surface acquisition systems have progressively widened their application fields. In addition, technology has improved with the development of novel devices which may be reliably used in the clinical context. The choice of the most appropriate instrument vary from time to time, in relation to its use and the characteristics of the patients to be analyzed. Validation studies are crucial to verify the reliability of novel procedures and to compare performances with gold standard methods.

References

Camison L., Bykowski M., Lee W.W., Carlson J.C., Roosenboom J., Goldstein J.A., Losee J.E., Weinberg S.M. (2018). Validation of the Vectra H1 portable three-dimensional photogrammetry system for facial imaging. Int. J. Oral Maxillofac. Surg. 47: 403-10.

Caplova Z., Gibelli D., Poppa P., Cummaudo M., Obertova Z., Sforza C., Cattaneo C. (2018). 3D quantitative analysis of early decomposition changes of the human face. Int. J. Legal Med. 132: 649-53.

Cattaneo C., Cantatore A., Ciaffi R., Gibelli D., Cigada A., De Angelis D., Sala R. (2012). Personal identification by the comparison of facial profiles: testing the reliability of a high-resolution 3D-2D comparison model. J. Forensic Sci. 57: 182-7.

Codari M., Pucciarelli V., Pisoni L., Sforza C. (2015). Laser scanner compared with stereophotogrammetry for measurements of area on nasal plaster casts. Br. J. Oral Maxillofac. Surg. 53: 769-70.

Dolci C., Pucciarelli V., Gibelli D., Codari M., Marelli S., Trifirò G., Pini A., Sforza C. (2018). The face in Marfan syndrome: a 3D quantitative approach for a better definition of dysmorphic features. Clin. Anat. 31: 380-6.

De Angelis D., Sala R., Cantatore A., Grandi M., Cattaneo C. (2009). A new computer-assisted technique to aid personal identification. Int. J. Legal Med. 123: 351-6.

De Menezes M., Rosati R., Ferrario V.F., Sforza C. (2010). Accuracy and reproducibility of a 3-dimensional stereophotogrammetric imaging system. J. Oral Maxillofac. Surg. 138: 84-8.

Douglas T.S., Martinez F., Meintjes E.M., Vaughan C.L., Viljoen D.L. (2003). Eye feature extraction for diagnosing the facial phenotype associated with fetal alcohol syndrome. Med. Biol. Eng. Comput. 41: 101-6.

Fan Y., Xu X., Wang M. (2017). A surface-based spatial registration method based on Sense three-dimensional scanner. J. Craniofac. Surg. 28: 157-60.

Feng J., Yu H., Yin Y., Yan Y., Wang Z., Bai D., Han X. (2019). Esthetic evaluation of facial cheek volume: a study using 3D stereophotogrammetry. Angle Orthod. 89: 129-37.

Gibelli D., Codari M., Rosati R., Dolci C., Tartaglia G.M., Cattaneo C., Sforza C. (2015). A quantitative analysis of lip aesthetics: the influence of gender and aging. Aesth. Plast. Surg. 39: 771-6.

Gibelli D., De Angelis D., Poppa P., Sforza C., Cattaneo C. (2017a). An assessment of how facial mimicry can change facial morphology: implications for identification. J. Forensic Sci. 62: 405-10.

Gibelli D., De Angelis D., Poppa P., Sforza C., Cattaneo C. (2017b). A view to the future: a novel approach for 3D-3D superimposition and quantification of differences for identification from next-generation video surveillance systems. J. Forensic Sci. 62: 457-61.

Gibelli D., Pucciarelli V., Caplova Z., Cappella A., Dolci C., Cattaneo C., Sforza C. (2018a). Validation of a low-cost laser scanner device for the assessment of three-dimensional facial anatomy in living subjects. J. Craniomaxillofac. Surg. 46: 1493-9.

Gibelli D., Pucciarelli V., Cappella A., Dolci C., Sforza C. (2018b). Are portable stereophotogrammetric devices reliable in facial imaging? A validation study of VECTRA H1 device. J. Oral Maxillofac. Surg. 76: 1772-84.

Gibelli D., Pucciarelli V., Poppa P., Cummaudo M., Dolci C., Cattaneo C., Sforza C. (2018c). Three-dimensional facial anatomy evaluation: reliability of laser scanner consecutive scans procedure in comparison with stereophotogrammetry. J. Craniomaxillofacial Surg. 46: 1807-13.

Hammond P., Hutton T.J., Allanson J.E., Campbell L.E., Hennekam R.C., Holden S., Patton M.A., Shaw A., Temple I.K., Trotter M., Murphy K.C., Winter R.M. (2004). 3D analysis of facial morphology. Am. J. Med. Genet. 126A: 339-48.

Hong C., Choi K., Kachroo Y., Kwon T., Nguyen A., McComb R., Moon W. (2017). Evaluation of the 3dMDface system as a tool for soft tissue analysis. Orthod. Craniofac. Res. 20(Suppl. 1): 119-24.

Jimenez-Castellanos E., Orozco-Varo A., Arroyo-Cruz G., Iglesias-Linares A. (2016). Prevalence of alterations in the characteristics of smile symmetry in an adult population from southern Europe. J. Prosthet. Dent. 115: 736-40.

Kau C.H., Richmond S. (2008). Three-dimensional analysis of facial morphology surface changes in untreated children from 12 to 14 years of age. Am. J. Orthod. Dentofac. Orthop. 134: 751-60.

Kimura N., Kim H., Okawachi T., Fuchigami T., Tezuka M., Kibe T., Amir M.S., Inada E., Ishihata K., Nozoe E., Nakamura N. (2019). Pilot study of visual and quantitative image analysis of facial surface asymmetry in unilateral complete cleft lip and palate. Cleft Palate Craniofac. J. 56: 960-9.

Koban K.C., Leitsch S., Holzbach T., Volkmer E., Metz P.M., Giunta R.E. (2014). 3D-imaging and analysis for plastic surgery by smartphone and tablet: an alternative to professional systems? Handchir. Mikochir. Plast. Chir. 46: 97-104.

Majid Z., Chong C.A., Ahmad A., Setan H., Setan H., Samsudin A.R. (2005). Photogrammetry and 3D laser scanning as spatial data capture techniques for a national craniofacial database. Photogramm. Rec. 20: 48-68.

Maués C.P.R., Casagrande M.V.S., Almeida R.C.C., Almeida M.A.O., Carvalho F.A.R. (2018). Three-dimensional surface models of the facial soft tissues acquired with a low-cost scanner. Int. J. Oral Maxillofac. Surg. 47: 1219-25.

Plooij J.M., Swennen G.R., Rangel F.A., Maal T.J.J., Schutyser F.A.C., Bronkhorst E.M., Kuijpers-Jagtman A.M., Bergé S.J. (2009). Evaluation of reproducibility and reliability of 3D soft tissue analysis using 3D stereophotogrammetry. Int. J. Oral Maxillofac. Surg. 38: 267-73.

Pucciarelli V., Bertoli S., Codari M., De Amicis R., De Giorgis V., Battezzati A., Veggiotti P., Sforza C. (2017). The face of Glut1-DS patients: a 3D craniofacial morphometric analysis. Clin. Anat. 30: 644-52.

Sawyer A.R., See M., Nduka C. (2009). 3D stereophotogrammetry quantitative lip analysis. Aesth. Plast. Surg. 33: 497-504.

Schwenzer-Zimmerer K., Chaitidis D., Berg-Boerner I., Krol Z., Kovacs L., Schwenzer N.F., Zimmerer S., Holberg C., Zeilhofer H.F. (2008). Quantitative 3D soft tissue analysis of symmetry prior to and after unilateral cleft lip repair compared with non-cleft persons (performed in Cambodia). J. Craniomaxillofac. Surg. 36: 431-8.

Sforza C., Ulaj E., Gibelli D., Allevi F., Pucciarelli V., Tarabbia F., Ciprandi D., Dell'Aversana Orabona G., Dolci C., Biglioli F. (2018). Three-dimensional superimposition for patients with facial palsy: an innovative method for assessing the success of facial reanimation procedures. Br. J. Oral Maxillofac. Surg. 56: 3-7.

Sterenborg B.A.M.M., Maal T.J.J., Vreeken R., Loomans B.A.C., Huysmans M.D.N.J.M. (2018). The facial effects of tooth wear rehabilitation as measured by 3D stereophotogrammetry. J. Dent. 73: 105-9.

Toma A.M., Zhurov A., Playle R., Ong E., Richmond S. (2009). Reproducibility of facial soft tissue landmarks on 3D laser-scanned facial images. Orthod. Craniofac. Res. 12:33-42.

Tzou C.H., Artner N.M., Pona I., Hold A., Placheta E., Kropatsch W.G., Frey M.

(2014). Comparison of three-dimensional surface-imaging system. J. Plast. Reconstr. Aesthet. Surg. 67: 489-97.

Winberg S.M., Naidoo S., Govier D.P., Martin R.A., Kane A.A., Marazita M.L. (2006). Anthropometric precision and accuracy of digital three-dimensional photogrammetry: comparing the Genex and 3dMD imaging systems with one another and with direct anthropometry. J. Craniofac. Surg. 17: 477-83.

Wong J.Y., Oh A.K., Ohta E., Hunt A.T., Rogers G.F., Mulliken J.B., Deutsch C.K. (2008). Validity and reliability of 3D craniofacial anthropometric measurements. Cleft Palate Craniofac. J. 45: 232-9.

Morphological assessment of Ear auricle in a group of Iraqi subjects and its possible role in personal identification

Sinan S. Farhan[1,*], Watheq M. Al-Jewari[1], Aiman Q. Afar Al-Maathidy[2], Aiman Al-Qtaitat[2]

[1] Department of Basic sciences, Faculty of Pharmacy, Al-Rafidain University College, Baghdad, Iraq
[2] Department of Anatomy and Histology, Faculty of Medicine, Mutah University, Al-Karak, Jordan

Abstract

Ear auricle had been studied many years ago for personal identification. Many studies in different countries had assessed the shape and measurements of parameters. Variance in dimensions of auricle within various age groups, race and genetic background recommended identification of normal range for auricle parameters; that is necessary for aesthetic purposes and anatomical standardization. **Materials and method:** Auricular dimensional parameters in 311 individuals in both right and left sides were measured using Vernier caliber; in addition to shape assessment, and lobular attachment status were recorded. **Results:** Nine parameters were evaluated for auricle morphometry in both sides. In one hand, significant differences were noticed regarding gender in ear height above tragus, tragus span and lobule height on other hand, no significant difference in parameters measurements according to lobule status. Comparing means of parameters among four shapes of auricle the study showed a statistical significance. Significant differences were recorded regarding gender with lobule status and gender with ear shape. Moreover, positive correlations were noticed among many parameters including, concha width and width of ear. **Conclusion:** This study represent a standardization of auricular dimensional parameters among Iraqi sample that is so beneficial in plastic surgery, hearing aids productions and personal identification. Taking in consideration, lobule status, gender, and shape of auricle.

Keywords

Ear auricle, morphometry, anthropometry, personal identification, ear lobule.

Introduction

The use of ear to identify human started since late 19th century when Alphonse Bertillon considered it as one of anthropometric measurements for identifying individuals, as ear print (Dhanda et al., 2011). Variations in ear morphology were assessed depending on its anatomical aspect that aimed mainly for identification of wrongdoer (Abbas and Rutty, 2005). The ear measurements vary according ethnic groups, which is important for treatment of auricular deformities and facial reconstruction procedures. Dimensions of auricle are so beneficial to plastic surgeon that needs normative data. In human, the ear composed of outer, middle and inner parts. External ear is formed by auricle and external acoustic meatus which is important in the forensic sciences for personal identification. Auricle was considered as a primary

* Corresponding author. E-mail: sinansubhi@gmail.com, sinan.subhi@ruc.edu.iq

feature of the human face and is particularly important in appearance (Purkait and Singh 2007; Sinnatumby, 2011). Certain studies on human ears suggested that there were morphological variations, but these data lacked inter- ethnic groups parameters, and these variations are important for the forensic sciences in human identification (Kapil et al., 2014; Chattopadhyay and Bhatia, 2009).

Ear print final individualization depended on specific ear details, like site, size, creases patterns and helix features. Ear parameters were assessed and they developed the Forensic Ear Identification research project (Meijerman et al., 2004). Familial relationships could be evaluated depending on ear characteristics, as ear morphology seems to be hereditary (Imhofer, 1906). For instance, the ear is classified into four shapes, which are triangular, rounded, oval and rectangular (Dhanda et al., 2011). Ear have its importance to the physiognomy and aesthetics of the face. Furthermore, people with congenital malformations or trauma of the ear usually uncomfortable. Surgery is needed to treat auricular defects, plastic surgeons require information about normal auricular dimension, but these data is different in various ethnic groups (Akpa et al., 2013; Kumar and Selvi 2016; Sadler, 2019).

This study aims to assess the morphometry and biometrics of external ear auricle, and to compare variations among, genders, shape of auricle and lobule attachment status in Iraqi subjects.

Subjects and methods

In this present longitudinal randomized study, a total of 311 pharmacy students were recruited for the study, having age 18-22years, at Al-Rafidain University College, Baghdad and approved by ethical committee in the university. All the subjects were normal healthy residents of Iraq, 157 male and 154 female, the study was conducted during the period of March 2018 to January 2019. The study purposes were explained to all subjects and a written informed consent was obtained from each subject. Medical history and clinical examination were obtained, none of those enrolled for the study have history of craniofacial trauma, ear diseases, congenital anomalies or surgery of the ear auricle (Verma et al., 2016). Measurements of parameters were obtained directly from both right and left ears by a single investigator (to eliminate error), by using a digital Vernier's caliper. Measurements were recorded in millimeter, to the nearest 0.1mm. Each subject measured twice for accuracy and to each dimension. Assessment of auricle shape and status of lobule either free or attached were evaluated by at two investigators and for both ears and once there was asymmetry, subject was excluded. Originally, the overall number of randomly selected students was 318; the number of excluded cases for different reasons was seven. The Anthropometric parameters that were measured includes the following anatomical landmarks (Kapil et al., 2014), and are illustrated in Figure 1:
1. Total Ear height: from highest to lowest point of Auricle.
2. Ear height above tragus: highest point of auricle to tragion.
3. Ear height below tragus: lowest point of auricle to intertragic incisures.
4. Tragus span: extends from intertragic incisure to tragion.
5. Width of Ear: distance from ear root to extreme helix convexity.
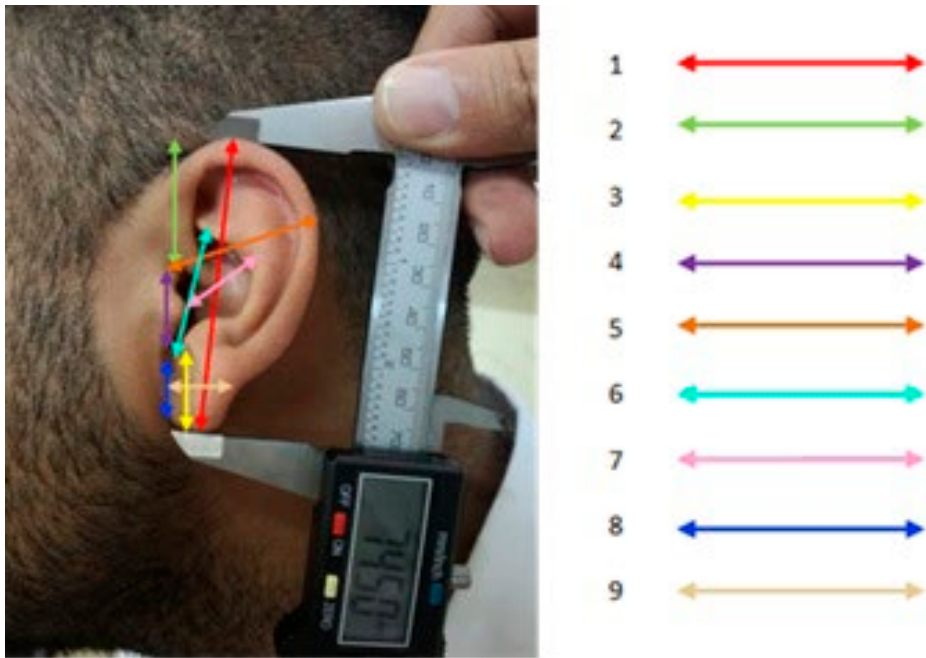6. Concha length: from intertragic incisure to cymba concha.

Figure 1. showing the recorded Anthropometric parameters of the auricle. Total Ear height (1), Ear height above tragus (2), Ear height below tragus (3), Tragus span (4), Width of Ear (5), Concha length (6), Concha width (7), Lobule height (8), Lobule width (9).

7. Concha width: extends from the antihelix concavity to tragus border.
8. Lobule height: from inferior site of the external ear attachment to the head (otoba-sion inferior) to the lower expansion to free margin of the ear lobe (subaurale).
9. Lobule width: from the most caudal attachment of the ear lobule to the head and to the outermost maximum transverse width of the ear lobule.

Statistics

The collected data was statistically analyzed using SPSS software v.20. T test ,one way ANOVA followed by post hoc test, chi square Fisher Exact and Pearson correla-tion test were used to compare the differences of parameters with significance value P<0.05.

Results

The measurements of nine parameters were assessed according to gender and lob-ule status (Free or Attached) and for both right and left ears and recorded in Table 1. Regarding gender, significant differences were noticed in the height above tragus, tra-gus span and lobule height. Conversely, no significances were seen in all parameters

Table 1. Ear morphometry for right (R) and left (L) ears (measurements in mm). The results were expressed as mean ±SD. significant difference for gender difference marked by * (P<0.05).

Parameter	Gender	Mean ± SD	Lobule	Mean ± SD
Total Ear height R	Female N=154	52.2 ± 5.6	Free (N=186)	52.7 ± 6.7
	Male N=157	53.3 ± 6.8	Att (N=125)	52.8 ± 5.5
Total Ear height L	Female	52.2 ± 5.7	Free	52.8 ± 6.8
	Male	53.4 ± 6.9	Att	52.9 ± 5.7
Ear height above tragus R	Female	46.7* ± 6.0	Free	47.7 ± 6.2
	Male	48.1 ± 5.7	Att	47.1 ± 5.4
Ear height above tragus L	Female	46.8* ± 6.0	Free	47.8 ± 6.1
	Male	48.3 ± 5.7	Att	47.2 ± 5.4
Ear height below tragus R	Female	32.0 ± 4.4	Free	32.3 ± 4.2
	Male	32.4 ± 3.8	Att	32.0 ± 4.0
Ear height below tragus L	Female	32.2 ± 4.4	Free	32.3 ± 4.7
	Male	32.0 ± 5.0	Att	31.8 ± 4.7
Tragus span R	Female	25.7* ± 4.1	Free	26.5 ± 4.4
	Male	26.9 ± 4.5	Att	26.1 ± 4.2
Tragus span L	Female	25.7* ± 4.6	Free	26.6 ± 4.5
	Male	27.0 ± 4.6	Att	26.0 ± 4.7
Width of Ear R	Female	33.0 ± 4.5	Free	33.5 ± 4.5
	Male	33.6 ± 4.3	Att	33.0 ± 4.2
Width of Ear L	Female	33.0 ± 4.4	Free	33.4 ± 4.4
	Male	33.5 ± 4.2	Att	33.1 ± 4.2
Concha length R	Female	20.5 ± 3.1	Free	20.8 ± 3.1
	Male	21.0 ± 3.0	Att	20.8 ± 3.1
Concha length L	Female	20.8 ± 3.0	Free	21.0 ± 3.0
	Male	21.2 ± 3.0	Att	20.9 ± 3.0
Concha width R	Female	32.6 ± 4.4	Free	33.2 ± 4.4
	Male	33.5 ± 4.4	Att	32.8 ± 4.3
Concha width L	Female	32.7 ± 4.4	Free	33.3 ± 4.4
	Male	33.6 ± 4.3	Att	33.0 ± 4.3
Lobule height R	Female	8.0* ± 2.1	Free	7.9 ± 1.9
	Male	7.6 ± 1.7	Att	7.7 ± 1.9
Lobule height L	Female	8.4* ± 1.9	Free	8.1 ± 1.8
	Male	7.8 ± 1.6	Att	7.9 ± 1.9
Lobule width R	Female	20.0 ± 3.3	Free	20.2 ± 3.4
	Male	20.3 ± 3.4	Att	20.0 ± 3.3
Lobule width L	Female	20.1 ± 3.1	Free	20.3 ± 3.0
	Male	20.3 ± 3.0	Att	20.0 ± 3.0

according to lobule status. All parameters in both right and left side and for different shapes showed significant differences by ANOVA test (Table 2). Therefore, Bonferroni post-hoc test was done to compare the mean differences in each shape with others (labeled by superscript a, b, c and d; Table 2) for significantly difference comparing oval, rectangular, round and triangular with each other when P<0.05 respectively. The percentages of female were higher in rectangular and then round in contrast to male that had higher percentage in oval and then triangular shapes (Table 3). High significant relationship was observed between shape of ear and gender of subject by using Chi square. Gender difference regarding lobule showed that 66% of male had free lobule compared to 54% of female with free lobule. An assessment of relation between lobule status and gender was done using Fisher Exact test and significant difference were found (Table 4). Pearson Correlations among various parameters showed positive and significance correlation in most of parameters (Table 5 and 6). Each of the following parameters (total ear height, height below tragus, tragus span, concha length and lobule width) showed significant correlation when compared to almost all other parameters.

Table 2. Ear morphometry for R and L according the shape of auricle. The results were expressed as mean ±SD. ANOVA test significance followed by Post hoc Bonferroni test which represented by a,b , c and d for significantly difference as compared to oval, round , rectangular and triangular respectively. Also lateralization significance (right and left) were demonstrated in total column and marked by * (P<0.05).

Parameter		Oval N=85 Mean ± SD	Round (N=47) Mean ± SD	Rectangular (N=68) Mean ± SD	Triangular (N=111) Mean ± SD	Total (N=311) Mean ± SD
Total Ear height	R	50.0 ± 4.6	51.5^c ± 7.5	57.2^{abd} ± 6.6	52.6^{ac} ± 5.0	52.8* ± 6.3
	L	50.0 ± 4.7	51.4^c ± 7.5	57.4^{abd} ± 6.7	52.8^{ac} ± 5.2	52.8 ± 6.4
Ear height above tragus	R	45.9 ± 4.5	48.5 ± 5.9	50.3^{ad} ± 7.4	46.4^c ± 5.0	47.4* ± 5.9
	L	45.9 ± 4.4	48.7 ± 5.9	50.5^{ad} ± 7.3	46.6^c ± 5.1	47.6 ± 5.8
Ear height below tragus	R	30.1 ± 2.9	33.1^a ± 4.2	34.9^{ad} ± 5.0	31.7^{ac} ± 3.2	32.2 ± 4.1
	L	30.2 ± 3.0	32.7^a ± 5.9	35.0^{ad} ± 5.0	31.5^c ± 4.1	32.1 ± 4.7
Tragus span	R	23.5 ± 2.6	27.3^{ac} ± 4.7	29.7^{abd} ± 4.3	25.9^{ac} ± 3.7	26.3 ± 4.3
	L	23.5 ± 3.6	27.4^{ac} ± 4.8	29.9^{abd} ± 4.4	26.0^{ac} ± 3.7	26.4 ± 4.6
Width of Ear	R	30.6 ± 2.7	34.7^{ad} ± 4.3	36.8^{abd} ± 4.3	32.6^{abc} ± 3.9	33.3 ± 4.4
	L	30.6 ± 2.7	34.5^a ± 4.5	36.4^{ad} ± 4.4	32.8^{ac} ± 3.8	33.3 ± 4.3
Concha length	R	19.1 ± 2.3	21.5^a ± 2.9	22.9^{ac} ± 3.0	20.4^{ac} ± 2.9	20.8* ± 3.1
	L	19.4 ± 2.5	21.7^a ± 2.8	22.9^{ad} ± 2.9	20.7^{ac} ± 2.7	21.0 ± 3.0
Concha width	R	30.3 ± 2.4	34.3^{acd} ± 4.9	36.8^{abd} ± 4.2	32.3^{abc} ± 3.7	33.0* ± 4.4
	L	30.6 ± 2.4	34.4^{acd} ± 4.7	36.8^{abd} ± 4.2	32.5^{abc} ± 3.8	33.2 ± 4.4
Lobule height	R	7.1 ± 1.8	8.0^a ± 1.4	8.2^a ± 1.9	8.1^a ± 2.1	7.8* ± 1.9
	L	7.3 ± 1.8	8.5^a ± 1.3	8.3^a ± 1.7	8.3^a ± 1.8	8.1 ± 1.8
Lobule width	R	18.0 ± 2.4	21.1^a ± 3.6	22.4^{ad} ± 3.4	20.0^{ac} ± 2.8	20.1 ± 3.4
	L	18.3 ± 2.1	20.9^{ac} ± 3.5	22.3^{abd} ± 3.1	20.0^{ac} ± 2.5	20.2 ± 3.0

Table 3. Distribution of gender according to ear shape. Significant difference was calculated using Chi square**.**

Gender	Shape				Total
	Oval (100%)	Round (100%)	Rectangular (100%)	Triangular (100%)	
Female	31(36%)	25(53%)	53(78%)	45(41%)	154
Male	54(64%)	22(47%)	15(22%)	66(59%)	157
Total	85(27.3%)	47(15.1%)	68(21.9%)	111(35.7%)	311 (100%)
The chi-square statistic showed P value < 0.00001					

Table 4. Relation between gender and lobule status using Fisher's Exact Test.

Gender	Lobule		Total
	Free	Attached	
Female	83(54%)	71(46%)	154(100%)
Male	103(66%)	54(43%)	157(100%)
Total	186	125	311
Fisher's Exact Test showed P value < 0.05			

Table 5. Pearson correlation for different parameters of right ear. significant difference marked by ** (P<0.05).

Pearson Correlation	Total ear height	Height above tragus	Height below tragus	Tragus span	Width of ear	Concha length	Concha width	Lobule height	Lobule width
Total ear height	1.00	.67**	.35**	.60**	.50**	.34**	.58**	.13	.45**
Height above tragus	.67**	1.00	.34**	.52**	.46**	.33**	.53**	.10	.41**
Height below tragus	.35**	.34**	1.00	.62**	.53**	.74**	.69**	.13	.76**
Tragus span	.60**	.52**	.62**	1.00	.70**	.61**	.85**	.18**	.71**
Width of ear	.50**	.46**	.53**	.70**	1.00	.62**	.79**	.07	.68**
Concha length	.34**	.33**	.74**	.61**	.62**	1.00	.72**	.13	.85**
Concha width	.58**	.53**	.69**	.85**	.79**	.72**	1.00	.11	.81**
Lobule height	.13	.10	.13	.18	.07	.13	.11	1.00	.16
Lobule width	.45**	.41**	.76**	.71**	.68**	.85**	.81**	.16	1.00

Discussion

The ear is an important part of the human face, functionally as well as esthetically. There is a wide range of normal variation in the shape of the external ear among populations. To strengthen the scientific basis for ear variations for identification, we

Table 6. Pearson correlation for different parameters of left ear. significant difference marked by ** (P<0.05).

Pearson Correlation	Total ear height	Height above tragus	Height below tragus	Tragus span	Width of ear	Con-cha length	Con-cha width	Lobule height	Lobule width
Total ear height	1.00	.67**	.30**	.57**	.55**	.32**	.58**	.10	.48**
Height above tragus	.67**	1.00	.30**	.51**	.52**	.32**	.53**	.07	.42**
Height below tragus	.30**	.30**	1.00	.50**	.56**	.61**	.57**	.13	.66**
Tragus span	.57**	.51**	.50**	1.00	.74**	.57**	.80**	.14	.68**
Width of ear	.55**	.52**	.56**	.74**	1.00	.71**	.88**	.10	.81**
Concha length	.32**	.32**	.61**	.57**	.71**	1.00	.68**	.15	.80**
Concha width	.58**	.53**	.57**	.80**	.88**	.68**	1.00	.11	.79**
Lobule height	.10	.07	.13	.14	.10	.15	.11	1.00	.16
Lobule width	.48**	.42**	.66**	.68**	.81**	.80**	.79**	.16	1.00

must understand more about how to select and use ear morphological features and know more about the factors that determine the range of racial variation. The Knowledge about the normal human ear dimensions and morphological features of various populations can be helpful from anthropological and forensic point of view to provide data procedures for the inclusion and exclusion of persons for identification based on ear variations (Verma et al., 2016). Furthermore, the data obtained from ear morphometric studies among populations will provide bases for ear reconstruction for plastic surgeons. Consequently, due to the complexity of the external ear, different anatomical landmarks of the external ear have been recorded in this study and in other various studies. Human ear shapes and variations can be useful for identification in the absence of fingerprints and facial recognition adopted software (Perpinan 1995; Asai et al., 1996; Sforza et al., 2009; Kalra et al., 2015; Verma et al., 2016; Japatti 2018). Age related changes showed a progressive increase of ear dimensions with age (Sforza et al., 2009). However, age related dimensional changes were not identical for all ear parameters (Japatti, 2018). Childhood and adolescent growth patterns were faster than those reported after adulthood. It is well accepted that the mature height of ear in males occurs at 13 year of age and in females at 12 years (Kalra et al., 2015). It has been stated that beyond 20 years of age, any size increase was basically attributable to secondary elongation of the earlobes due to gravitational forces (Verma et al., 2016). Therefore, all the subjects recruited in this study were mature males and females above external ear maturity age and less than 22 years old. All measurements were obtained directly from subjects, as it is the ideal anthropometry technique, although, indirect anthropometric techniques such as photography are also frequently used. Additionally, to eliminate inter-observer error, this is higher than intra-observer error (Petrescu et al., 2018). The entire sets of measurements were done by a single investigator, who has expertise in anthropometric measurements.

In the last few years, ear dimensions have been investigated in various ethnic groups, using direct as well as indirect anthropometry and photography (Japatti 2018). Indian ear biometric studies showed clear variations among the different eth-

nicity of the population (Kapil et al., 2014; Verma et al., 2016). Indian male parameters by Kapil et al. (2014) showed higher values in ear height, ear width, concha length and lobule height and lower values in the remaining parameters in comparison with the male Iraqi results obtained above. For example, the total ear height mean among male Indians was 64.2 mm, which is higher than the Iraqi males (53.4 ± 6.9 mm). These differences might be related to smaller sample size in their study (n=100), and in addition to race variation. Moreover they found that subjects with free lobule (65.14%) and (34.85%) for attached lobule in contrast to our study that revealed free lobule (59.8%) and (40.2%). Furthermore, another Indian ear biometric study by Kalra et al., (2015) showed the ear total height 57.7mm, which is also higher than our obtained data. However, ear width of male in our results was 33.6 mm, proximate to Indian study Purkait (2007) and lower than that of another Indian study (Kapil et al., 2014). On the other hand, Osunwoke et al., (2018) found that Nigerian subjects had total ear height 54.3 ± 4.120 and the width of ear was 31.4 ± 2.5mm. These findings are also higher than our obtained results for total ear height and lower for width of ear, 52.8 ± 6.3 and 33.3 ± 4.8, respectively. In their study, another difference regarding the auricle shape, which was lowest percentage of triangular shape among Nigerians in contrast to our sample that showed highest percentage of triangular shape. They also claimed that no significant difference between ear shape and gender, which disagreed with our findings that showed a significant difference between gender and lobule shape. Additionally, they stated that right ear parameters are larger than left ear parameters, which is inconsistence with ours, as we found most of the parameters are higher in the left than in the right, although a few records showed proximity of both sides, and a few measurements showed higher in the right (Table 2). These findings could be explained by the use of more number of variables in our study, as we used nine, compared to only two variable used in their study.

Comparing total ear height and width of ear among Iraqi population with other populations from different countries, the total ear height values of Iraqis' appear the smallest of all. However, the width of ear is among the smallest of all obtained data. Irrespective of the ethnicity of the study population, male showed higher values of both ear height and width compared to females (Ito et al., 2001; Azaria et al., 2003; Brucker et al., 2003; Bozkir et al., 2006; Sharma et al., 2007; Murgod et al., 2013; Purkait and Singh 2014). In our results, males were found to have marginally longer and wider ears as compared to females. Further gender comparison in our data demonstrates that males have slightly higher values in all parameters compared to females, excluding the lobule height which is higher in females. These results agreed partly with Murgod et al., (2014) which stated that lobe width and height were higher in females. Moreover, another study by Kalra et al., (2015) showed that total ear height and lobule height had higher values than our results but ear width and lobule width had lower values than ours and for both males and females. Although, our findings did not show any significance difference between genders regarding ear height and width, however lobule height showed a significance in both right and left side between males and females. Various previous studies have reported ear symmetry with different findings (Azaria et al., 2003; Sforza et al., 2009; Alexander et al., 2010). Comparing the parameters between right and left ear, our data showed no significant difference between both sides, which support symmetry between right and left ears. However, in several studies significant asymmetry was noted in total ear

height and width (Barut et al., 2006; Murgod et al., 2013). On the other hand, Petrescu et al., (2018) suggested that the shape of the ear is mainly determined by the proportions of its different dimensions, less than their absolute values and claimed that concha width and concha length had positive correlation with ear width and height respectively. In addition, they noted that of the 28 possible correlations between dimensional parameters of the ear only three parameters in the right ear and four in the left ear are significant. In contrast, our findings revealed many correlations in both right and left ears among various parameters (Table 5 and 6), particularly width of ear and concha width as they have significant and highly positive correlation with almost all parameters (Pearson correlation value is more than 0.5). These correlations could be useful in reconstructive plastic surgery, by measuring a group of parameters and estimate the remaining parameters. Additionally, Acar et al., (2017) who studied Turkish and African sample found a significant difference according to lateralization in ear lengths of Turkish male and African female individuals. In contrast to our results that found ear length in both male and female had significant difference according to lateralization. The ear classified by Dhanda et al., (2011) into four shapes triangular, rounded, oval and rectangular. Verma et al., (2016) stated that most common shape of north India was oval shape in contrast to round that had lowest percentage. These findings disagree with ours, as highest percentage was the triangular shape and agreed with lowest percentage that was the round in the total subjects. However, the highest proportion among males was the triangular, and among females was the rectangular. On the other hand, ear lobule attachment was found to be an interesting indicator in population genetics (Bhasin, 1969). In present study our population showed more percentage of free ear lobe among both males and females. These results were in accordance with Kapil et al., (2014) and contrary to others (Sharma et al., 2007; Verma et al., 2016). These differences might be attributed to different ethnic and genetic backgrounds of study populations.

In conclusion, throughout this study, different anatomical variations were observed in all subjects and in different parameters that can be used for personal identification especially for forensic and reconstruction purposes. According to our knowledge no previous study was done in Iraq to standardize ear parameters and assess the percentage of different auricle shapes. Consequently, we think that the information obtained are important for providing valid and objective reference of ear morphometry among the study subjects in Iraq. Nevertheless, we believe that an extensive larger sample, including different regions, should be examined in detail to further validate the findings of this study and come to definitive conclusions over Iraqis.

Funding sources

None.

Conflict of interest

The authors declare no conflict of interest

References

Abbas A. and Rutty G.N. (2005) Ear piercing affects ear prints: The role of ear piercing in human identification, J. Forensic Sci. 50(2):386–392

Acar M., Burcin S., Ulusoy M., Akkubak M. (2017) Comparison of some Morphometric Parameters of the Ear on Turkish and African Students. Asian Journal of Biomedical and Pharmaceutical Sciences. 7(60):8-12

Akpa A, Ibiam A, Ugwu C. (2013) Anthropometric study of the pinna among south East Nigerians. J. of expt. Res. 1:47-50

Alexander K. S., Stott D. J., Sivakumar B., Kang N. (2010) Morphometric study of the human ear. J. Plast. Reconstr. Aesthet. Surg. 20:1–7.

Asai, Y.; Yoshimura, M.; Nago, N. & Yamada, T. (1996) Why do old men have big ears? Correlation of ear length with age in Japan. B. M. J., 312(7030):582.

Azaria R, Adler N, Silfen R, Regev D, Hauben DJ. (2003) Morphometry of the adult human earlobe: A study of 547 subjects and clinical application. Plast. Reconstr. Surg. 111(7):2398-402.

Barut C., Aktunc E. (2006) Anthropometric measurements of the external ear in a group of Turkish primary school students. Aesth. Plast. Surg. 30: 255–259.

Bhasin MK. (1969) Ear lobe attachment among the Newars of Nepal. Hum. Hered. 19:506-08.

Bozkir MG, Karakaş P, Yavuz M, Dere F. (2006) Morphometry of the external ear in our adult population. Aesthetic Plast. Surg. 30:81-85.

Brucker MJ., Patel J., Sullivan PK. (2003) A morphometric study of the external ear: Age and sex related differences. Plast. Reconstr. Surg. 112:647-652.

Chattopadhyay P.K, Bhatia S. (2009) Morphological examination of ear: a study of an Indian population. Legal Medicine. 11:S190–193.

Dhanda V, Badhan JS, Garg RK. Studies on the development of latent ear prints and their significance in personal identification. Problems of Forensic Sci. 2011;138:285–95

Imhofer R. (1906) Die Bedeutung der Ohrmuschel fur die Feststellung der Identität. Arch Kriminol. 26:150-163

Ito I, Imada M, Ikeda M, Sueno K, Arikuni T, Kida A, et al. (2001) A morphological study of age changes in adult human auricular cartilage with special emphasis on elastic fibers. Laryngoscope 111:881-286.

Japatti SR, Engineer PJ, Reddy B M, Tiwari AU, Siddegowda CY, Hammannavar RB. (2018) Anthropometric assessment of the normal adult human ear. Ann. Maxillofac. Surg. 8:42-50.

Kalra D, Anshu K. and Goel S. (2015) Anthrometric measurements of external ear:An in vivo study. International Journal of Enhanced Research in Medicines & Dental Care. 2(3):10-16

Kapil V, Bhawana J, Kumar V. (2014) Morphological variations of ear for individual identification in forensic cases: a study of an Indian population. Res. J. Forensic Sci. 2(1):1–8.

Kumar B and Selvi G. (2016) Morphometry of the ear pinna in sex determination. Int. J. of Anatomy and Res. 4:2480-2484.

Meijerman L., Sholl S., De Conti F., et al. (2004) Exploratory study on classification and individualization of earprints, Forensic Sci. Int. 140: 91–99

Murgod V., Angadi P., Hallikerimath S., Kale A. (2013) Anthropometric study of the external ear and its applicability in sex identification: assessed in an Indian sample. Austr. J. Forensic Sci. 45: 431-444

Osunwoke EA, Vidona WB, Atulegwu GC. (2018) Anthropometric study on the anatomical variation of the external ear amongst Port Harcourt students, Nigeria. Int. J. Anat. Var. 11(4):143-146.

Perpinan MA. (1995) Compression neural networks for feature extraction: Application to human recognition from ear images (M.S. Thesis). Madrid: Technical University.

Petrescu L., Gheorghe A., Tirgoviste C. Petrescu C. (2018) Anthropometric investigation of external ear morphology, as a pattern of uniqueness, useful in identifying the person. Proc. Rom. Acad., Series B 20(2):95–104

Purkait R and Singh P (2007). Anthropometry of the normal human auricle: a study of adult Indian men. Aesthetic Plast. Surg. 31(4):372-9

Purkait R. (2007). Ear biometric: An aid to personal identification, Anthropologist Spl. 3, 215–218

Sadler T. (2019) , Langman's Medical Embryology , 14th Edition , Wolters Kluwer. China

Sforza C., Grandi G., Binelli M., Tommasi D.G., Rosati R., Ferrario V.F. (2009) Age- and sex-related changes in the normal human ear. Forensic Sci Int. 30: 187(1-3):110.e1-7

Sharma A., Sidhu N.K., Sharma M.K., Kapoor K., Singh B. (2007) Morphometric study of ear lobule in Northwest Indian male subjects. Anat Sci Int. 82:98-104.

Sinnatumby C., (2011), Last's anatomy Regional and Applied , 12th edition, Elsevier Limited, London.

Verma P, Sandhu K, Verma G, et al. (2016) Morphological variations and biometrics of ear-an aid to personal identification. J Clin Diag Res. 10(5): ZC138–ZC142

Morphological Analysis of Palmaris Longus Muscle And Its Anatomic Variations: A Cadaveric Study In North India

Monika Lalit[1], Sanjay Piplani[2], Anupama Mahajan[1], Poonam Verma[1]

[1] Department of Anatomy, SGRDIMS&R, Amritsar, Punjab, India
[2] Department of Pathology, SGRDIMS&R, Amritsar, Punjab, India

Abstract

Palmaris longus is classified as a phylogenetically retrogressive muscle having a short belly with a long tendon. It varies in the incidence of its absence, form, attachment, duplication and its ability of having accessory slips and substitute structures. The muscle is of interest to hand surgeons because a number of cases have been reported with complaints of a volar distal forearm swelling and median nerve compression symptoms. Therefore, the present study was performed with the purpose to determine the morphology and the variations of PL in North Indian population. Material for the present study consisted of 62 limbs(20 Male and 11 Female) which were made available through a series of dissections performed for first year medical students at SGRDIMSAR, Amritsar, Punjab. The morphology and variations of PL and its relation with neighbouring structures were noted. The data thus collected was stored and compared to other studies. Of 62 limbs dissected 55(88.70%) showed normal morphology of palmaris longus muscle as per the standard textbook. 5 limbs(8.06%) showed complete agenesis. 1(1.61%) limb exhibited a fleshy fusiform PLM. A Reversed palmaris longus muscle(RPLM) along with accessory PL(1.61%) was observed in the same limb. Variations of the PL tendon may even confuse an experienced surgeon. Thus, it is important for the reconstructive surgeons or radiologists to be aware of the possibility of variations and its impact on the structures present at the wrist area especially one that might contribute to median or ulnar nerve compression.

Introduction

Palmaris Longus is a slender fusiform muscle of the forearm, located just under the skin, subcutaneous fat and forearm fascia, superficial to Flexor Digitorum Superficialis (FDS) and between Flexor Carpi Radialis (FCR) laterally & Flexor Carpi Ulnaris (FCU) medially. (Ellis et al., 2005) The short muscular belly and the long tendon is characteristic of phylogenetic retrogressive degeneration of this muscle (Sebastin et al., 2005) which is evidenced by palmar aponeurosis representing the distal part of its tendon. (Bergman et al., 1984)

The muscle is subject to many variations both in morphology and number ranging from complete agenesis to duplication, triplication, variable location and accesso-

* Corresponding author. E-mail: monika.lalit@yahoo.com

ry slips. (Reimann et al., 1944;) The prevalence of the PL agenesis has been well-documented by many authors in different ethnic groups or populations. (Sebastin et al., 2005) It may have a proximal tendon or a distal tendon, or have a fleshy central belly with proximal and distal tendons, it maybe digastric or fleshy throughout or its tendon may be split and sometimes it maybe degenerated to such an extent it that may be simply represented by a tendinous band. (Reimann et al., 1944;) Generally variations in palmaris longus anatomy are thought to be asymptomatic. several authors have described variations of the reversed palmaris longus, many of which may cause symptomatic median nerve compression (Schlafly & Lister, 1987; Meyer and Pflaum, 1987; Depuydt et al., 1998; Schuurman & Van Gils, 2000).

Normally the fleshy part of Palmaris longus muscle arises from the medial epicondyle of humerus and tendinous part gets inserted into palmar aponeurosis. (Ellis et al., 2005) When it is tendinous proximally and has a fleshly distal belly it is called reverse PL or PL inversus. (Cope et al., 2009) A reversed palmaris longus, possessing a distal musculo-tendinous junction, was first reported by Captain John T. Morrison in 1916 as an incidental, post-amputation find-ing. (Morrison, 1916) The reversed muscle belly can hypertrophy or divide distally into 2 or 3 separate attachments. Accessory digitations have also been reported to insert most commonly deep to the flexor retinaculum (Bencteux et al., 2001).

The knowledge of such variations is not only desirable, but also essential as these have important influences on the predisposition to illness, clinical examination, investigations and patient management including operative surgery. Moreover, there are no comprehensive studies in the recent past on these variations hence the study was undertaken to have better understanding on their incidence and morphology. The present study was performed with the purpose to determine the morphology and anatomical variations of PLM and its impact on the neighboring nerves and more importantly its surgical significance in North Indian population.

Materials and methods

Material for the present study consisted of 62 limbs of North Indian origin of different age group and sex (20 Male and 11 Female). The limbs were made available through a series of dissections performed over a period of 6 years during the years 2014-19 for first year medical students at Sri Guru Ram Das Institute Of Medical Sciences and Research (SGRDIMSAR), Amritsar, Punjab. The flexor compartment of the forearm of the upper limb was dissected using standard procedure. (Romanes C J, 2012) A vertical incision was made in the center of the anterior surface of the forearm from the cubital fossa to the distal transverse crease of the wrist. Skin and superficial antebrachial fascia of the flexor compartment of the forearm was dissected layer-by-layer and lifted to expose the underlying superficial flexor muscles of the forearm. The origin, course and insertion (Morphology) of Palmaris longus Muscles (PLM) were observed. Variations of PLM and its relation with neighboring structures were noted. Photographs were taken to document the observed variations. The data thus collected was stored and compared with other studies. The presence, absence and morphological variations of PL, its nerve supply and its relation to flexor retinaculum and neighboring structures were noted.

Results

Out of 62 limbs dissected, 55(88.70%) limbs showed the typical anatomical features of the Palmaris longus muscle as described in the standard textbook being muscular in origin and tendinous in insertion and also being supplied by the median nerve (Figure 1).

Complete agenesis of the PLM was observed in 5 limbs (8.06%), of which, unilateral absence was found in 3 male subjects (7.5%), 2 on right side & 1 on left side and 2 female subjects (9.09%), both on left side. (Figure 2). Their numbers, incidence and laterality are shown in Table 1.

A Fleshy Fusiform PLM (1.61%) was also observed in the right UL of a 60-year-old male cadaver being muscular and fleshy in the proximal 2/3 and tendinous in
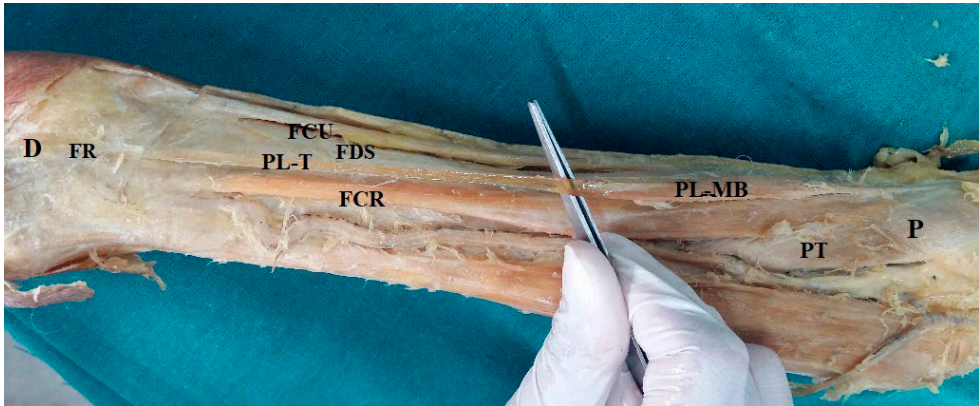
Figure 1. Showing Normal Palmaris Longus Muscle with Proximal Muscle Belly and Distal Tendon In the Left Upper Limb. P- Proximal; D-Distal; PL-Palmaris Longus; PT-Pronator Teres; FCU- Flexor Carpi Ulnaris; FCR-Flexor Carpi Radialis; FDS- Flexor Digitorum Superficialis; FR- Flexor Retinaculum.
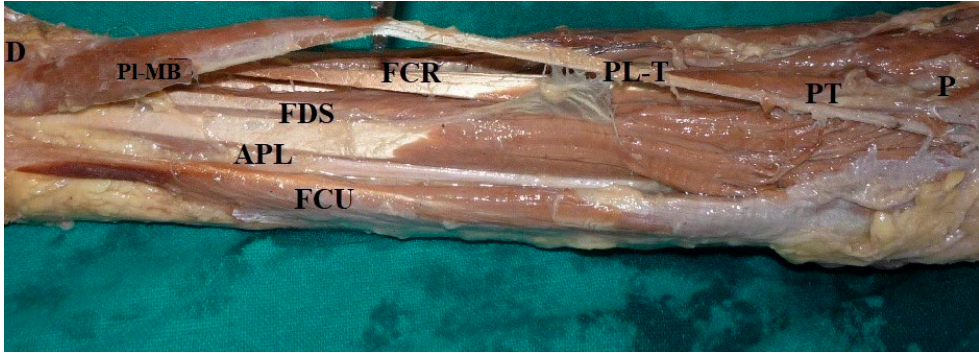

Figure 2. Showing Agenesis/Absent Palmaris Longus Muscle In the Right Upper Limb. P- Proximal; D-Distal; PT-Pronator Teres; FCU- Flexor Carpi Ulnaris; FCR-Flexor Carpi Radialis; FDS- Flexor Digitorum Superficialis; FR- Flexor Retinaculum.

Table 1. Morphology of Palmaris Longus Muscle & its incidence.

S. No.	Morphology & Variations	Number of Varia-tions	Side		Number of Limbs	Incidence (%)
			Right	Left		
1.	Normal	55	27	28	55	88.70%)
2.	Agenesis	5	2(M)	3(1M, 2F)	5	8.06%-(62 Limbs) M-7.5%-(40 Limbs) F-9.09%-(22 Limbs)
3.	Fleshy Fusiform PLM	1	1M	-	1	1.61%
4.	Accessory	1	1M	-	1	1.61%
5.	Bifid Reverse/ Inverted PLM	1	1M	-		

M-Male, F-Female.

the distal 1/3 part of the UL. The length of the MB was 16.4 cm and its width was 2.9 cm and the length of the tendon was 6.2 cm and it measured 0.47 cm at its widest part. The tendon was seen inserted into flexor retinaculum. No such variations were observed on the left side (Figure 3).

One limb exhibited an Accessory PLM (1.61%) on the right side of a 54-year-old male cadaver. The APLM was located medial to RPL and Lateral to FCU. It originated with a long, thick tendon from the medial epicondyle of the humerus which prolonged downward and forward in the forearm. Some of these bundles were attached to the flexor retinaculum, while others were seen inserted into the proximal points of origin of the muscles of the hypothenar muscles. The length of the APLM was found to be 23.6cm and width was measured as 0.8 cm (Figure 4).

Figure 3. Showing Fleshy/Fusiform Palmaris Longus Muscle with 2/3rd Proximal Long Muscle Belly and 1/3rd Distal Tendon In the Right Upper Limb. P- Proximal; D-Distal; PL-MB-Palmaris Longus-Muscle Belly; PL-T- Palmaris Longus-Tendon; PT-Pronator Teres; FCU- Flexor Carpi Ulnaris; FCR-Flexor Carpi Radialis; FDS- Flexor Digitorum Superficialis.

Figure 4. Showing Accessory Palmaris Longus Muscle (APLM) In the Right Upper Limb. P- Proximal; D-Distal; APL-Accessory Palmaris Longus; RPL-MB- Palmaris Longus -Muscle Belly; RPL-T- Reverse Palmaris Longus-Tendon; PT-Pronator Teres; FCU- Flexor Carpi Ulnaris; FCR-Flexor Carpi Radialis; FDS- Flexor Digitorum Superficialis.
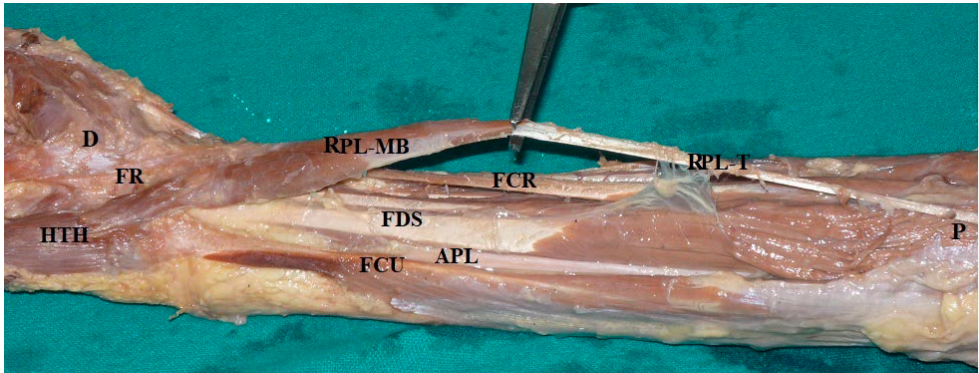

Figure 5. Showing Reverse Palmaris Longus Muscle (RPLM) In the Right Upper Limb. P- Proximal; D-Distal; RPL-MB- Reverse Palmaris Longus Muscle; RPL-T-Reverse Palmaris Longus Tendon; FCU- Flexor Carpi Ulnaris; FCR-Flexor Carpi Radialis; FDS- Flexor Digitorum Superficialis; APL-Accessory Palmaris Longus; FR- Flexor Retinaculum; HTH- Hypothenar Muscle.

A variant Bifid inverted or Reverse Palmaris Longus muscle (RPLM) was also discovered in the same right forearm of a 54-year-old male cadaver having APLM. The RPLM originated from the medial epicondyle of the humerus, being tendinous in the proximal 2/3 and muscular in the distal 1/3 part. The length of the proximal tendon was 18.0 cm that coursed superficial to FDS and changed to a muscular belly in distal 1/3rd of forearm. The length of the muscle belly (MB) was 10 cm and width at its middle part was found to be 2.2 cm. MB passed superficial to flexor retinaculum and bifurcated into a muscular and a fascial slip (Figure 5).

Discussion

Though Numerous variations of Palmaris longus muscle are reported in literature being variable both in number and form. Bergman has classified the PL variations as: Complete agenesis, Variation in location and form of its fleshy part, Aberrancy of attachment at its origin or insertion, Duplication and Triplication, Accessory slips, Replacing elements of a similar form or position. (Bergman et al., 1984). In the present study, Table 1 depicts the complete agenesis of the PLM was observed in 5 limbs (8.06%), of which, unilateral absence was found in 3 male subjects (7.5%), 2 on the right side and 1 on the left side and 2 female subjects (9.09%) on the left side (Figure 2).

Agenesis of the palmaris longus has been attributed to Mendelian principles, its absence is autosomal dominant and its presence is autosomal recessive. (Michael & Shaw, 1978). The prevalence of agenesis of the PL has been extensively studied following the first report of its absence recorded as early as 1559 by Colombo in De Re Anatomica Libri. (Realdi Columni C, 1559). An average of 10% absence has been universally accepted. An extensive research of 1600 cadaveric limbs conducted by Reimann and colleagues in 1944 found that incidence of agenesis of PL was 12.9% and an additional 9% had noticeable variations in the location and form of the muscle belly. (Reimann et al., 1944). In another study of 276 cadavers, palmaris longus was observed bilaterally in 216 (78.3%) cases, 17 (6.1%) cases on right side and 19 (6.9%) cases on left side whereas it was found absent on both the sides in 24 (8.7%) cases. (George, 1953) In a study of 800 living subjects the palmaris longus was absent on both the sides in 7.7% of cases, absent on the right side in 4.5% and on the left side in 5.2%. (Bergman et al., 1984) Schaeffer (1909) also reported its absence in 10% cases either unilaterally or bilaterally. According to Troha et al., (1990), Wehbe & Mawr, (1992), Thompson et al. (2001), Roohi et al. (2007) and Kose et al. (2009), In White Caucasians, Indian Dravidian, Malaysian and Turkish the prevalence of agenesis of PL ranges between 16-26.6% and as low as 4% in Mongloids in a study by Sebestin et al. (2005).

Kapoor et al. (2008) studied palmaris longus muscle in Indian population and found a bilateral absence of 17.2% with unilateral absence in left arm 6.2% and 3% in right arm. There is also mention of racial and ethnic population variation in frequency of prevalence of PL muscle as it has been reported that bilateral absence of palmaris longus occurs in 8-16% of individuals and unilateral in 4-14%. (Vanderhooft, 1996) As can be depicted from Table 2 that the frequency of agenesis of PL recorded in the present study is more than observed by Adachi (1910), Ceyhan & Mavt (1997), Igbigbi & Ssekitoleko (1998), Mbaka & Ejiwunmi (2009), and Gangata (2009) for other populations of the world. Some authors suggested that apart from its ethnic and racial variations, its absence is more common in women, bilateral absence being more common, and that unilateral absence occurs more frequently on the left side. (Schaffer, 1909) The present study supports the findings being unilateral absence more common on left side in females however no bilateral agenesis was found in the present study. From a viewpoint of phylogeny, it is notable that this almost functionless muscle is present in about 90 per cent of humans and is best developed in those where the forelimbs are used for ambulation. (Humphary, 1872) Degeneration has proceeded much further in the group of animals generally considered as phylogenetic forebears. (Jones, 1941). Some remnant of it is usually present in the gibbon and orangutan but less often in

Table 2. Showing incidence of Palmaris Longus Muscle (PLM) agenesis among different ethnic groups and populations.

S. No.	Author	Year	Ethnic group or population	Incidence (%)
1	Reimann et al.	1944	North America	12.9%
2	George	1953		24 (8.7%) cases BL 17 (6.1%) on Lt side 19 (6.9%) on Rt side
3	Adachi	1909	Japanese,	3.4% in Japanese,
4	Schaeffer	1909	-	10%
5	Troha et al.	1990	North American Caucasians	24%
6	Wahbe & Mawr	1992	Pennsylvania	23%
7	Vanderhooft	1996		8-16% BL 4-14%.UL
8	Ceyhan & Mavt	1997	Korean	0.6%
9	Igbigbi & Ssekitoleko	1998	Ugandas	1.02%
10	Thomposn et al.	2001	Northern Ireland	25%
11	Sebastin et al.	2005	Chienese	3.3% UL, 1.2% BL (4.6%)
12	Roohi et al.	2007	Malaysian	9.3%
13	Kapoor et al.	2008	Indian Delhi	17.2%-Bl, 6.2%-Ul-Lt., 3%-Ul-Rt.
14	Kose et al.	2009	Turkish	26.6
15	Mbaka & Ejiwunmi	2009	Yorubas	6.7%
16	Gangata	2009	Zimbabweans, Congolese	1.5% 3.0%
17	Present Study	2019	North India	8.06% (3.22%)-Rt. (4.83%)- Lt.

the chimpanzee and ape, and it is only present in about 25 per cent of gorillas. In this respect the palmaris longus belongs to a group of muscles which are more degenerate in the Apes and monkeys than in man. (Keith, 1899) According to developmental basis the PLM, as a skeletal muscle, originates from the mesoderm of the myotomes of the somites and these precursors follow an intrinsic program which allows them to differentiate into muscle cells, this process is controlled by environmental signals. During the early embryogenesis the absence of such signals in the ectoderm leads to premature differentiation of the precursors, which in turn may cause agenesis or incomplete genesis of the respective muscles (Holinshed, 1964).

Concerning the kind of muscle, PLM may be fleshy throughout its entire length or may have muscle belly located centrally in the forearm and tendon above & below or may be reduced to a mere tendinous band. (Bergman et al., 1984) In the present study a fleshy fusiform muscle having proximal 2/3rd MB and a distal 1/3rd Tendon PL was

Table 3. Showing incidence of accessory Palmaris Longus Muscle among different populations .

S. No.	Author	Population	Year	Incidence (%)
1.	Gruber	Russians	1868	3.1%
2.	Koganei et al	Japan	1903	1.9%
3.	Adachi	Japan	1910	2.1%
4.	Reimann et al	Americans	1944	0.8%
5.	Sato et al	Japanese	1974	2.5%
6.	Teingo et al	Itlay	2006	1 Accessory PL
7.	Present Study	North India	2019	1 Accessory PL

Table 4. Showing work reported by various authors on Reverse Palmaris Longus Muscle (RPLM).

S. No.	Worker/authors	Population	Year	No. of cases of RPLM
1.	Reimann et al	North America	1944	
2.	Schlafly & Lister	American	1987	1 bifid
3.	Meyer & Pflaum	American	1987	1
4.	Regan et al	British-Buckinghamshire	1988	1 bifid RPL
5.	Giunta et al	German	1993	1
6.	Depuydt et al	Netherlands	1998	2
7.	Schuurman &Van Gils	Netherlands	2000	4 (3F/1M)
8.	Yildiz et al.	Turkey	2000	3 Headed bilateral accessory muscle
9.	Oommen & Rajarajeshwari	South India/Manglore	2002	1
10.	Rawat & John.	Ludhiana/Punjab	2003	1
11.	Seyhan et al.	Turkey	2005	1three headed
12.	Natsis et al.	Greece	2007	Three headed PL
13.	Nayak et al.	South India/Karnatka	2008	1
14.	Present Study	North India	2019	1 Bifid Reverse palmaris longus

observed. (Figure 3) In this variation compression of both ulnar and median nerves in the forearm can occur.

An accessory PLM was observed having its origin from medial epicondyle of humerus and insertion at FR and being tendinous throughout its course. (Figure 4) A look at the comparative analysis of Table 3 elucidates that the incidence of APLM was found to be more than Reimann et al (1944) and less than the work done by Adachi (1910), Gruber (1868) and Sato et al., (1974). It is in concordance with the findings of Koganei et al. (1903) and Tiengo et al. (2006). Rubino et al (1995) reported a case where an individual had a small accessory muscle that originated from PL tendon.

The developmental basis for such type of variation is that the forearm muscles develop from a single precursor mass which divides into superficial component giving rise to the pronator teres, flexor carpi radialis, flexor carpi ulnaris and the PL. The deep component gives rise to the deep flexors of the forearm. The additional or accessory PLM can be embryologically explained on the basis of additional cleavage of the superficial mass (Holinshed, 1964).

A variant Bifid inverted or Reverse Palmaris longus muscle being tendinous in the proximal 2/3 and muscular in the distal 1/3 part was observed in the same Right limb of a 54 year old male cadaver having APLM and has been reported earlier. (Lalit and Singla 2014) A RPLM possessing a distal musculo-tendinous junction, was first reported by Captain John T. Morrison in 1916 as an incidental, post-amputation finding. (Morrison, 1916) It was originally described as musculus PL inversus and later was recognised as the term reverse PL. (Natsis, 2007). (Figure 5) Bifid RRL has also been reported by Schlafly & Lister (1987) and Regan et al (l988). Natsis (2007) reported a case where a female cadaver had three headed (radial, central and ulnar) reverse palmaris longus in the left forearm. Though three headed RPLM has also been reported by Yildiz et al. (2000) and Seyhan et al. (2005). A glance at Table 4 reveals the work done by Meyer & Pflaum (1987), Guinta et al. (1993), Depuydt et al. (1998), Oommen and Rajarjeshwari (2002), Rawat and John (2003) and Nayak et al. (2008) on RPLM. Schuurman and Van Gils (2000) also identified four patients in Netherlands who had reverse palmaris longus muscle causing activity related compression of the median nerve. Georgiev et al. (2009) reported a case of reverse palmaris longus with muscular belly at proximal end and the two tendons distally on his left forearm. The primitive function of PL is flexion of the metacarpo-phalangeal joints by means of a tendon that fans out in the palm to be inserted by a slip to the base of each proximal phalanx. In the development of the forelimb as a prehensile organ this function has been taken over by the intrinsic muscles of the hand and the palmaris longus muscle has become degenerated. This retrogression is considered to be due to the gradual development of prehension, achieved by diversion of muscular power for the independent motion of parts of hand. (Humphary, 1872)

Conclusion

PLM variations are described as one of the most common muscular variations in the human body, and their presence has specific clinical significance. Variations of PLM could cause nerve compression with slow progressive symptoms such as carpal tunnel syndrome more frequently than acute nerve compression. These symptoms include oedema on the palmar surface of the wrist, weakness and reduction of muscular strength, pain and numbness in the area. In clinical practice, the variant PLM could be incidentally found during clinical examination without provoking clinical symptoms and may simulate a soft tissue tumor. Therefore, the possible presence of PLM variations and their impact (particular RPLM) on the structures present at the wrist area must be considered by clinicians, hand surgeons, radiologists and all those who are involved in patient care during clinical examination of the forearm, during surgical interventions in that region, or while searching for an entrapment site of the median and ulnar nerve.

Conflict of interest

None

References

Adachi B. (1910) Beiträge zur anatomie der Japaner. XII Die Statistik der Muskelvari-
    etäten. Z Morphol Anthropol. 12: 261–312.

Bergman R.A., Thompson S.A., Afifi A.K. (1984) Catalog of human variation. Urban &
    Schwarzenberg: Baltimore.

Bencteux P., Simonet J., El Ayoubi L., Renard M., Attignon I., Dacher J.N., Thiebot J.
    (2001) Symptomatic palmaris longus muscle variation with MRI and surgical cor-
    relation: report of a single case. Surg Radiol Anat. 23(4): 273-275.

Ceyhan O., Mavt A. (1997) Distribution of agenesis of the palmaris longus muscle in
    12-18 years old age groups. Indian J Med Sci. 51: 156-60.

Cope J.M., Looney E.M., Craig C.A., Gawron R., Lampros R., Mahoney R. (2009)
    Median nerve compression and reverse palmaris longus. Int J Anat Var. 2: 102-04.

Depuydt K.H., Schuurman A.H., Kon M. (1998) Reversed palmaris longus muscle
    causing effort-related median nerve compression. J Hand Surg Br. 23(1): 117-119.

Ellis H., Healy J.C., Johnson D., Williams A. (1995) In: Standring S Edinburg, edi-
    tor. Gray's Anatomy: The Anatomical Basis of Clinical Practice. 39th Ed. Elsevier
    Churchill Livingstone, Philadelphia. Pp. 873-887.

Gruber W. (1868) Über die varietäten des musculus an palmaris longus. Mem I'Acad
    Imp Sci St Petersbourg. 7(11): 1–26.

George R. (1953) Co-incidence of palmaris longus and plantaris muscles. Anat Rec.
    116(4): 521-523.

Giunta R., Brunner U., Wilhelm K. (1993) Bilateraler reverser Musculus Palmaris
    longus –seltene Ursache eines peripheren N.-medianus-kompressions syndroms.
    Unfallchirurg. 96: 538-540.

Gangata H. (2009) The Clinical Surface Anatomy Anomalies of the palmaris longus
    muscle in the Black African population of Zimbabwe and a proposed new testing
    technique. Clin Anat. 22: 230-5.

Georgiev G.P., Jelev L., Ovtscharoff W.A. (2009) Unusual combination of muscular
    and arterial variations in the upper extremity: a case report of a variant palmaris
    longus and an additional tendinous portion of the flexor carpi ulnaris together
    with a persistent median artery. 3: 58-61.

Humphary G.M. (1872) The muscles of vertebrates. J Anat and Physiol. 6: 293-376.

Holinshed W.H. (1964) Anatomy for surgeons Vol.3 Second Edition New York, Harp-
    er and Row. Pp. 412.

Igbigbi P.S., Ssekitoleko H.A. (1998) Incidence of agenesis of the palmaris longus
    muscle in Ugandans. West Afr J Anat. 6: 21-3.

Jones F.W. (1941) The principles of anatomy as seen in the hand. Second Edition. Lon-
    don; Bailliere, Tindall and Cox.

Keith A. (1899) On the chimpanzees and their relationship to the gorilla. Proc Zool
    Soc London. 296-314.

Koganei Y., Arai H., Shikinami J. (1903) Varietätenstatistik der musculn. Tokyo Igak-
    kai Zasshi. 7:127–131.

Kapoor S.K., Tiwari A., Bhatia R., Tantuway V., Kapoor S. (2008) Clinical relevance of palmaris longus agenesis: common anatomical aberration. Anat Sct Int. 83: 45-48.

Kose O., Adanir O., Cirpar M., Kurklu M., Komurcu M. (2009) The prevalence of absence of the palmaris longus: A study in Turkish population. Arch Orthop Trauma Surg. 129: 609-11.

Lalit M., Singla R.K., Piplani S. (2014) Bifid inverted palmaris longus muscle – a case report. Eur J Anat. 18(3):341-3.

Morrison J.T. (1916) A palmaris longus muscle with a reversed belly, forming an accessory flexor muscle of the little finger. J Anat Physiol. 50(4): 324-326.

Michael F.H., Shaw E.F. (1978) Anatomical variations of the palmaris longus causing carpal tunnel syndrome. J Plastic and Reconstructive Surgery. 62: 798-800.

Meyer F.N., Pflaum B.C. (1987) Median nerve compression at the wrist caused by a reversed palmaris longus muscle. J Hand Surg Am. 12(3): 369-371.

Mbaka G.O., Ejiwunmi A.B. (2009) Prevalence of palmaris longus absence: A study in the Yoruba population. Ulster Med J. 78: 90-3

Nayak S.R., Krishnamurthy A., Ramanathan L.A., Prabhu L.V., Kumar C.J., Tom D.K., Joy T. (2008) Multiple muscular anomalies of upper extremity: A cadaveric study. Rom J Morphol Embryol. 49(3): 411-415.

Natsis K. (2012) Fleshy palmaris longus muscle- a cadaveric finding and its clinical significance: A case report. Hippokratia. 16(4): 378-380.

Oommen A., Rajarajeshwari T. (2002) Palmaris Longus-upside down. JASI. 51(2): 232-233.

Realdi Columni C. (1559) De Re Anatomica Libri.Venice: ex typographia N. Beuilacquae.

Reimann A.F., Daseler E.H., Anson B.J., Beaton L.E. (1944) The Palmaris longus muscle and tendon. A study of 1600 extremities. Anat Rec. 89: 496-505.

Regan P.J., Roberts J.O., Bailey B.N. (1988) Ulnar nerve compression caused by a reversed palmaris longus muscle. J Hand Surg Br.13(4): 406-407.

Rubino C., Paolini G., Carlesimo B. (1995) Accessory slip of the palmaris longus muscle. Ann Plast Surg. 35: 657-659.

Rawat J.S., John B. (2003) Reverse palmaris longus muscle: a case report. Indian J orthop. 37: 13.

Roohi S.A., Choon-Sian L., Shalimar A., Tan G.H., Naicker A.S. (2007) A Study on the absence of palmaris longus in a multiracial population. Malaysian Ortho J. 1:126-8.

Romanes G.J. (2012) Cunninghams Manual of Practical Anatomy Vol 1. 15th Edition. India. Oxford Medical Publications. 74-75.

Schaeffer J.P. (1909) On the variations of the palmaris longus muscle. Anat Rec. 3: 275-278.

Sato Y., Takeuchi R., Umeno K., Chen S., Takafuji T. (1974) A contribution to the study of the M palmaris longus. Acta Anat Nippon. 19: 318–319.

Schlafly B., Lister G. (1987) Median nerve compression secondary to bifid reversed palmaris longus. J Hand Surg Am. 12(3): 371-373.

Schuurman A.H., Van Gils A.P. (2000) Reversed palmaris longus muscle on MRI: report of four cases. Eur Radiol. 10(8): 1242-1244.

Sebastin S.J., Puhaindran M.E., Lim A.Y., Lim I.J., Bee W.H. (2005) The prevalence of absence of the palmaris longus-a study in a Chinese population and a review of the literature. J Hand Surg Br. 30(5): 525-7

Seyhan T. (2005) Median nerve compression at the wrist caused by reversed 3-headed palmaris longus muscle: case report and review of literature. Am J Orthop. 34(11): 544-546.

Troha F., Baibak G.J., Kelleher J.C. (1990) Frequency of the palmaris longus tendon in North American Caucasians, Ann Plast Surg. 25(6): 477–478.

Thompson N.W., Mockford B.F., Cran G.W. (2001) Absence of the palmaris longus muscle: A population study. Ulster Med J. 70: 22-4.

Tiengo C., Macchi V., Stecco C., Bassetto F., De Caro R. (2006) Epifascial accessory palmaris longus muscle. Clin Anat. 19: 554-557.

Wehbe M.A., Mawr B. (1992) Tendon graft donor sites. J Hand Surg. 17A: 1130-2.

Vanderhooft E. (1996) The frequency of and relationship between the palmaris longus and plantaris tendons. Am J Orthop. 1: 38-41.

Yildiz M., Sener M., Aynaci O. (2000) Three headed reversed palmaris longus muscle: A case report and review of literature. Surg Radiol Anat. 22: 217-219.

Main perforators of the upper limb: still birth study

Aymn A. Khanfour

Faculty of medicine, Alexandria University, Egypt

Abstract

Background: Perforator flaps are an excellent reconstructive option for functional upper limb reconstruction. **Aim of the work:** This study aimed to identify the main anatomical sites, number and length of the main perforators of the upper limb for better surgical reconstruction interventions. **Material and methods:** The material of this work included twelve fresh stillbirths. Red-colored latex was injected into the abdominal aorta. Dissection was done at the sub-fascial level of the upper limb. **Results:** Results showed that the most common sites of brachial artery perforators were located at a mean distance of 1.73 ±0.52 cm measured from the tip of the coracoid process. More than one third of ulnar perforators (35%) were located within 40 mm proximal to the pisiform. More than half of the distal forearm radial artery perforators (68%) were located within 22 mm proximal to the distal wrist crease. About (40%) of the posterior interosseous artery were located within 40 mm proximal to the ulnar head. Dorsal metacarpal artery perforators were found in the mid metacarpal region proximal to junctuate tendinae while the proper digital arteries give rise to multiple cutaneous perforators along their course on the sides of each digit. **Conclusion:** Detailed anatomy of the main perforators of the upper limb concerning its accurate site measured from fixed specific bonny points, number and length of their pedicles are very essential in the success of the different flap techniques. **Recommendations:** A wide scale of the stillbirth cases may give more standard values as regard the location of the main perforators of the upper limb. A combined adult cadaveric study could be advised to be compared with the main values with those of the stillbirths.

Abbreviations

Brachial artery perforators (BAP), Radial artery perforators (RAP), Ulnar artery perforators, Posterior interosseous artery perforators (PAP), Dorsal metacarpal artery perforators (DAP), Digital artery perforators (DAP)

Introduction

Trauma contributes to one of the main causes of defects in the upper and lower limbs. Limb injuries most likely lead to complicated defects, so it may be demanding to reconstruct tissue loss. (Spyropoulou and Jeng 2010)

The replacement of the soft tissue in the upper limb is a common challenge that surgeons face after burns, trauma and infection. Reconstruction quality has an impor-

Corresponding author. E-mail: aymn222@hotmail.com

tant effect on the functional outcome of the patient. (Appleton and Morris 2014, Peng, Li et al. 2019)

In the upper limb, there are several choices for the restoration of soft tissue, including skin grafting, local flaps, regional flaps and free flaps. (Levin and Erdmann 2001) Fascio-cutaneous flaps are provided by discrete perforator arteries which can be elevated in different areas of the human body and are regularly used in fundamental plastic surgery. (Tinhofer, Tzou et al. 2017)

In the past, numerous local and free flaps have been reported with more or less consistent morbidity of the donor site. The latest implementation of the perforator-based flap idea has resulted in an evolution in the reconstruction of the upper extremity, wonderful results at the receiving site, as well as minimizing and attaining this in the easiest manner possible. (Innocenti, Baldrighi et al. 2009, Chaput, Herlin et al. 2015).

For functional upper limb reconstruction, perforator flaps are an outstanding reconstructive choice. The upper limb keystone perforator flaps are focused on propeller flaps such as the brachial artery perforators, ulnar artery perforators, radial artery perforators, interosseous artery perforators, metacarpal artery perforates and digital artery perforators. (Sinna, Qassemyar et al. 2011, Hussein Mahmoud, M Khedr et al. 2019)Flap safety concerns depend on the degree of the perforator's intentional twist. (D'Arpa, Cordova et al. 2011, Thomas, Calcagno et al. 2019).

Microsurgery provided a strong tool for the plastic surgeon. In cases of complex defects that cannot be covered by the simpler options of reconstructive surgery, new advances in microsurgery can almost provide a solution. (Levin and Erdmann 2001, Spyropoulou and Jeng 2010).

Aim of the work

This study aimed to identify the main anatomical sites, number and length of the main perforators of the upper limb for better surgical reconstruction interventions.

Materials and methods

The material of this work included twelve stillbirth upper limbs obtained from the Dissecting Room of Anatomy Department, Faculty of Medicine, Alexandria University.

In this study, a midline abdominal incision was done, cutting through all layers, followed by reflecting the intestine to expose the abdominal aorta. Irrigation of the abdominal aorta with warm saline to dislodge blood clots after ligation of its distal segment.

The red-color latex was injected into the abdominal aorta until resistance was felt or the backflow of the dye occurred. The upper limbs were then dissected 48 hours after injection to allow the latex to regain firm rubbery consistency. A vertical midline skin incision was done along the course of the main arteries of the upper limb. Dissection was done at the sub-fascial level with reflection of the flaps. (Morris S 2006).

The data included the site of the main perforators in relation to fixed anatomical landmarks, in addition to their number, length of the pedicle and the main source vessel.

Measurements were done using manual Smith Vernier caliper and a ruler and were photographed and statistically analyzed.

Statistical analysis

The data was collected, processed and entered into the personal computer. Statistical analysis was done using Statistical Package for Social Sciences (SPSS/version 20) software. The arithmetic mean, standard deviation were used to the numerical measurements.

Results

I. Brachial artery perforators (BAP)

The length of the arms of the stillbirth specimens was measured from the tip of the acromion process to the mid-elbow point. It ranged from 5.0 to 6.9 cm with a mean value of 5.93± 0.56 cm.   The number of BAP perforators ranged from 2 to 6 with a mean value of 4.21± 1.72 (Fig. 1, 8). The most common sites of BAP were pre-
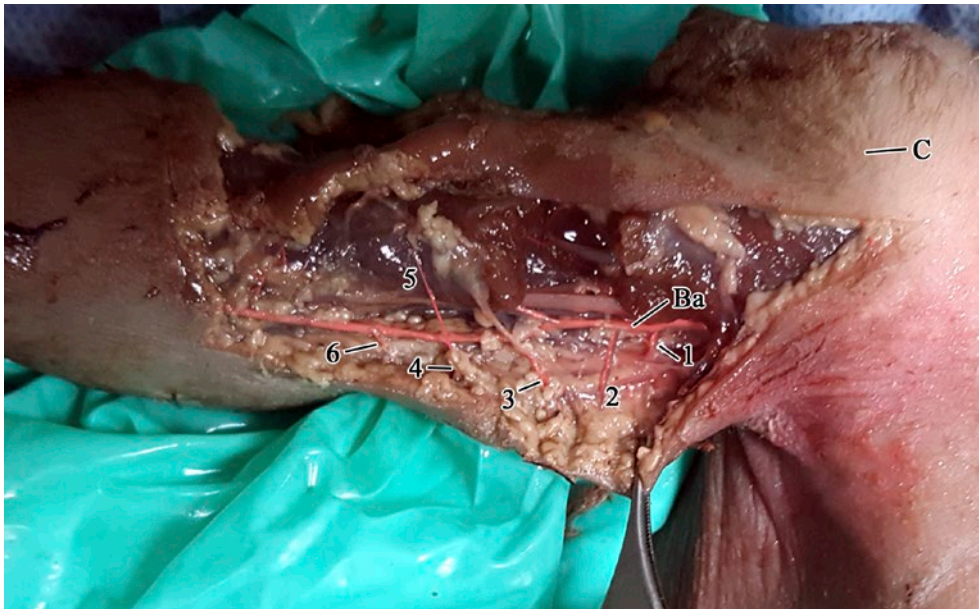
Figure 1. A photograph of a right arm of a stillbirth showing the brachial artery (Ba) and its perforators 1-6 (**C:** site of palpation of the tip of the coracoid process).
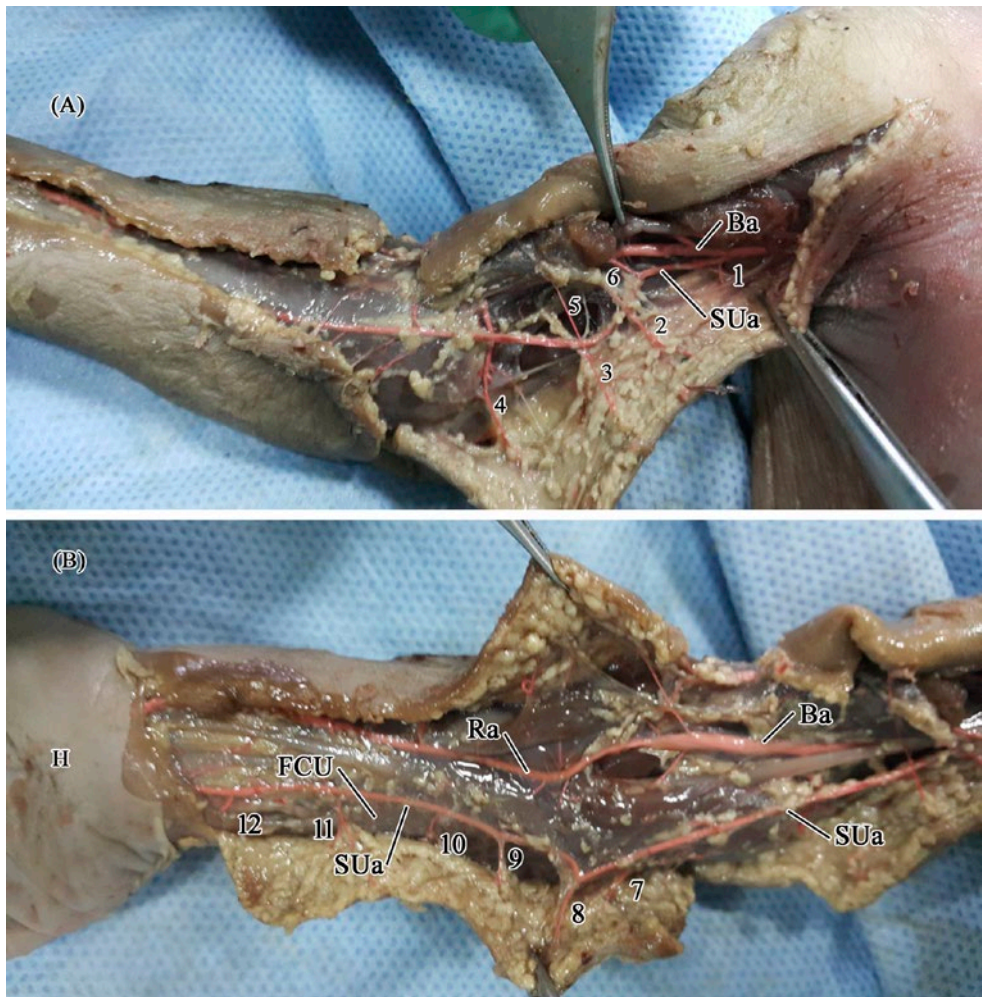
Figure 2. Picture (A): A photograph of a right upper limb of a stillbirth showing the superficial ulnar artery (SUa) arising from the brachial artery (Ba) in the upper third of the arm. **Picture (B):** Follow up of the same specimen in **picture (A)** where the superficial ulnar artery (SUa) continues to the forearm in a superficial course. (1-6: superficial ulnar artery perforators in the arm –7-12: superficial ulnar artery perforators in the forearm. (**H:** Hand - **Ra:** Radial artery – **FCU:** Flexor carpi ulnaris).

sent at a mean distance of 1.73 ±0.52 cm measured from the tip of the coracoid process (Fig. 9). The mean length of BAP was 2.13 ±0.42 cm.

In one specimen out of the twelve specimens (8.33%), the ulnar artery originated in the upper third of the arm on both the right and left sides of the brachial artery (Fig. 2). In such a case, the part of the ulnar artery in the arm gave 3 to 4 perforators at a distance 2 -3 cm from the coracoid process. The mean length of the ulnar artery perforators in the arm was 2.51 ±0.32 cm.
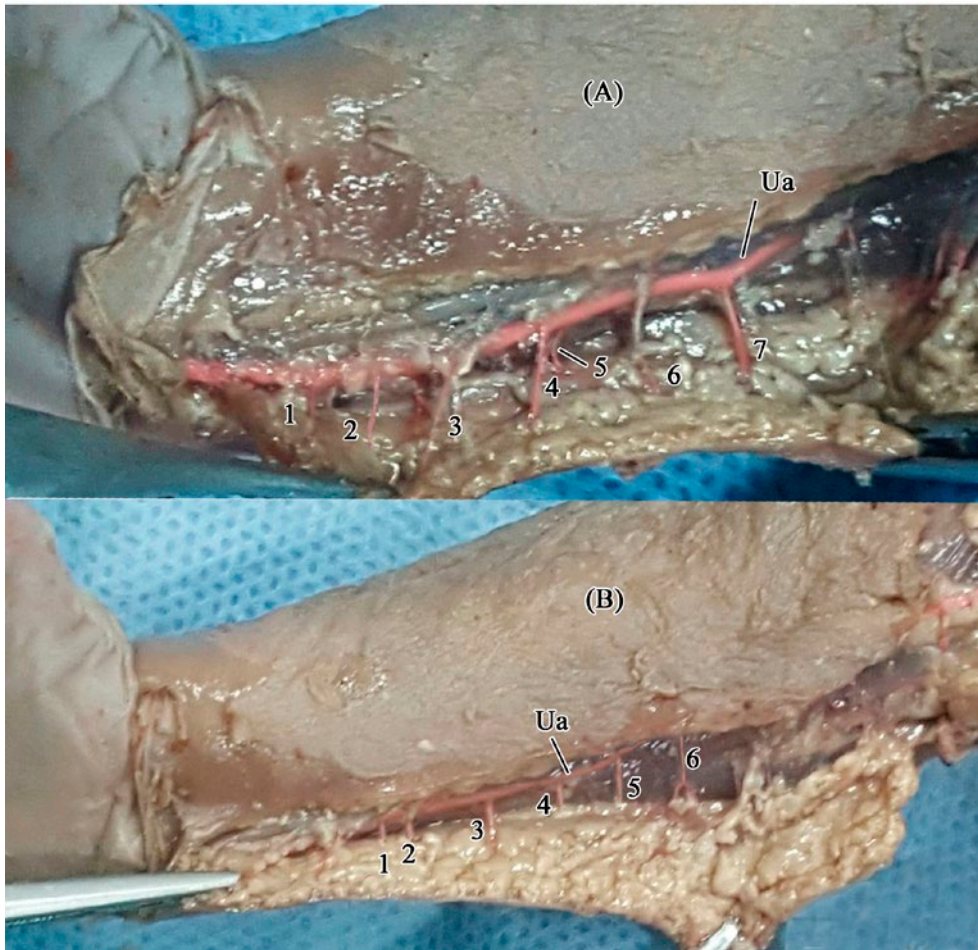
Figure 3. A photograph of a right forearm of a stillbirth showing the ulnar artery (Ua) and its perforators (1-7 in **picture A** & 1:6 in **picture B**) (note the concentration of the perforators in the lower third of the forearm).

II. Ulnar artery perforators (UAP)

The length of the forearms of the stillbirth specimens was measured from the mid-elbow point to the mid-wrist point. It ranged from 4.2 to 7.8 cm with a mean value of 6.1 ± 1.15 cm. The number of UAP ranged from 6 to 12 with a mean value of 9.63 ± 2.14 (Fig. 3,8). The largest number of perforators were within 16.0 mm proximal to the pisiform, while the second largest number of perforators were in area 28 to 36 mm proximal to the pisiform. Taken together, more than one third of forearm perforators (35%) were located within 40 mm proximal to the pisiform (Fig. 9). About 90 % of UAP were found online drawn from the pisiform to the medial epicondyle or just medial to it. The mean length of the UAP was 1.28 ± 0.37 cm.

Figure 4. A photograph of a left forearm of a stillbirth showing the radial artery (Ra) and its perforators (1-6). The insert picture demonstrates the method of measuring of the distance of each perforator from the distal wrist crease. (**FCR:** Flexor carpi radialis – **FDS:** Flexor digitorum superficialis)**.**

Figure 5. A photograph of the dorsum of a right forearm of a stillbirth showing the posterior interosseous artery perforators (1-7). The insert picture demonstrates the method of measuring the distance of each perforator from the ulnar head. (**ECU:** Extensor carpi ulnaris – **EDM:** Extensor digiti minimi).
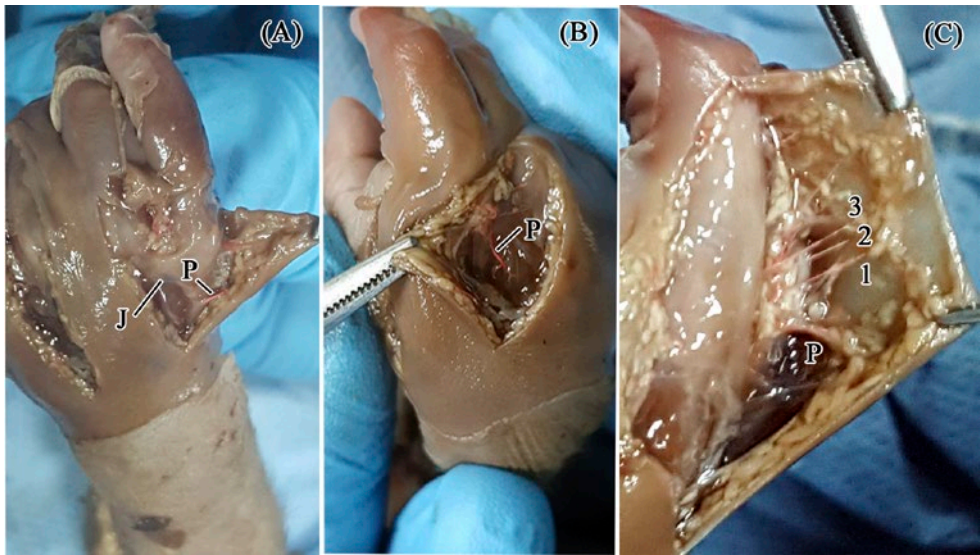
Figure 6. A photograph of the dorsum of a right hand of a stillbirth showing the junctuate tendinae (J) **(picture A)**, main dorsal metacarpal artery perforator (P) **(pictures A, B and C)** and other dorsal metacarpal artery perforators 1- 3 **(Picture C)**.
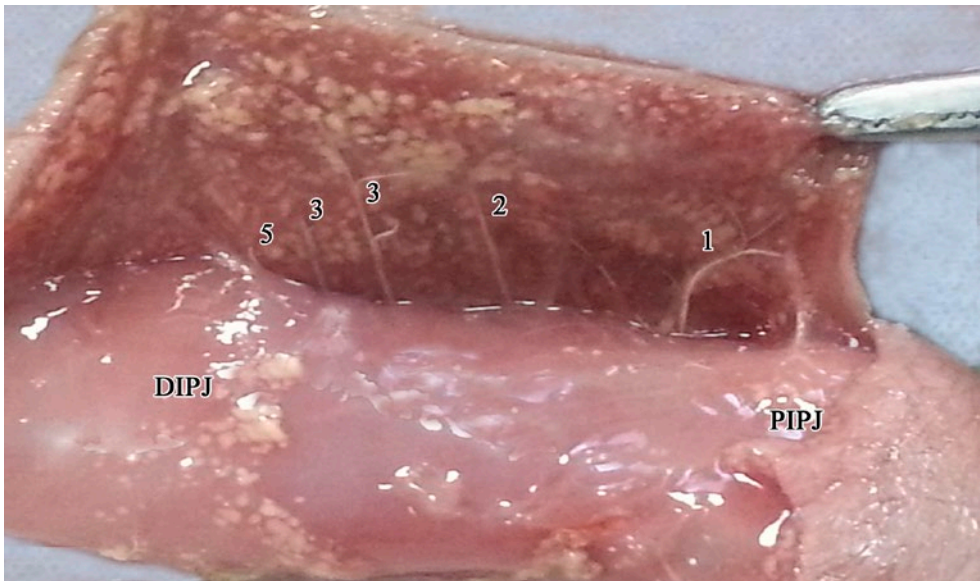
Figure 7. A photograph of a stillbirth intermediate digit of the index finger (lateral view) showing digital perforators (1-5) on the lateral side of the digit (**PIPJ:** Proximal interphalangeal joint – **DIPJ:** Distal interphalangeal joint).
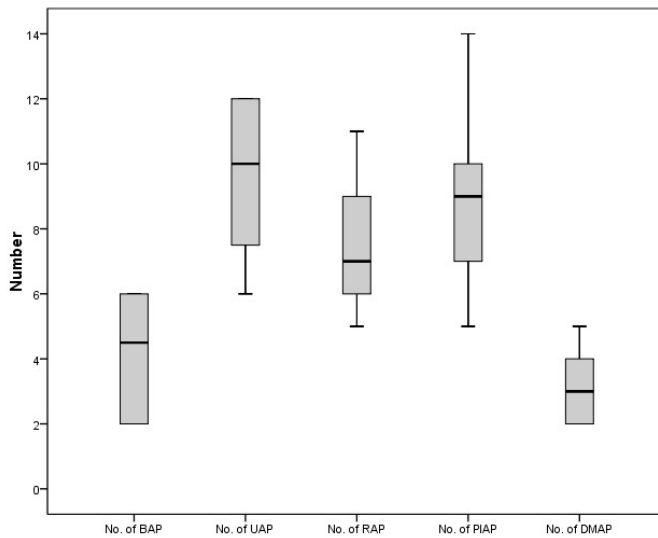
Figure 8. Box Plot showing the number of the main perforators of the upper limb.
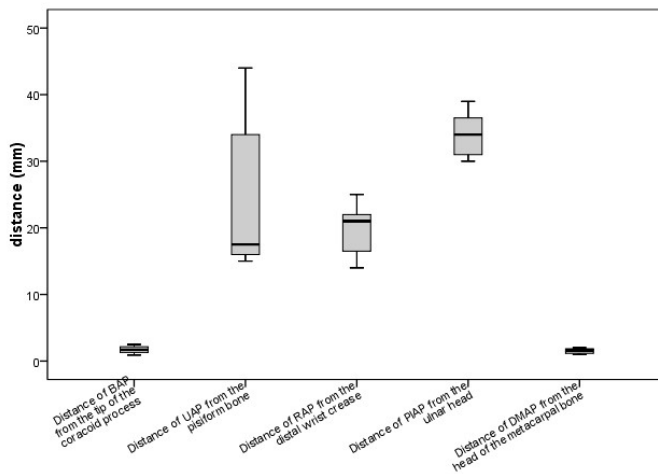
Figure 9. Box Plot showing the different distances of the main perforators of the upper limb from fixed anatomical landmarks.

III. Radial artery perforators (RAP)

The number of RAP ranged from 5 to 11 with a mean value of 7.63±1.74 (Fig. 4,8).
The largest number of perforators were found within 15 mm proximal to the distal wrist crease, while the second largest was in area 15 to 22 mm proximal to the dis-

tal wrist crease. Taken together, more than half of the distal forearm perforators (68%) were located within 22 mm proximal to the distal wrist crease (Fig. 9). The mean length of the RAP was 1.21 ± 0.28 cm.

All distal RAP were septal or direct cutaneous arose between flexor carpi radialis and brachioradialis, while proximal perforators arose between pronator teres and brachioradialis.

IV. Posterior interosseous artery perforators (PIAP)

The number of PIAP ranged from 4 to 15 with a mean value of 8.83±2.33 (Fig. 5,8)

The PIAP arose between extensor carpi ulnaris and extensor digiti mini. The largest number of perforators was 30 mm proximal to the ulnar head, and the second largest number was in area 30 to 40 mm proximal to the ulnar head. Taken together, more than one third of forearm perforators (40%) were located within 40 mm proximal to the ulnar head (Fig 9). About 95 % of PIAP were found in a line drawn from inferior radioulnar joint to the lateral epicondyle in supination or just radial to it. The mean length of PIAP perforator was 1.53 ± 0.34 cm

V. Dorsal metacarpal artery perforators (DMAP)

The length of the hand of all specimens was measured from the head of the third metacarpal bone to the proximal line of the carpal bones. It ranged from 1.5 to 3.1 cm with a mean value of 2.12 ± 0.54 cm (Fig. 6,8). The number of DMAP ranged from 2 to 6 with a mean value of 3.17±1.05. These perforators were roughly found in the mid metacarpal region proximal to junctuate tendinae (connective tissues that link the tendons of the extensor digitorum) (Fig. 9). The mean length of the DMAP was 0.52 ± 0.07 cm.

VI. Digital artery perforators (DAP)

Axial vessels in the hand and digits gave rise to both volar and dorsal DAP.

The proper digital arteries gave rise to multiple cutaneous perforators along their course ranged from 4-6 with a mean value 4.67±0.87 (Fig. 7). Many of the cutaneous digital artery perforators originated from the lateral aspect of the finger distally, forming the basis for the digital artery perforator flap design.

Discussion

In the last years, a wide range of propeller flaps were used to cover a broad range of defects. Indeed, these flaps allow for considerable freedom in the design and coverage of many complex defects. However, dissecting a perforator is not an easy task, it determines the success rate of the performed procedure. (Hussein Mahmoud, M Khedr et al. 2019)

Liu, Y. et al (2017) (Liu, Zang et al. 2017)considered the fact that perforators of the arm are more on the medial side and have long pedicles. They added the techniques of tissue expansion and perforator flap surgery. Pre-expansion in the presence

of lengthy pedicles improves the size of the flap, remodels the vasculature of the flap and decreases the morbidity of the donor site. This fact is also supported by Peng, J. Q. et al (2019). (Peng, Li et al. 2019)Another tool for demonstration of the main perforators of the upper limb was done by Dalla Pozza, E. et al (2018) (Dalla Pozza, Bassiri Gharb et al. 2018)on nine hand allografts. They injected blue ink through the brachial artery to assess the perfusion of the skin flaps. Results demonstrated sizable perforators from the brachial, superior ulnar collateral, radial, ulnar and posterior interosseous arteries. Concerning the brachial artery, the average stained area of the medial arm flap was between 85.7 and 93.9 percent indicating predominant medial side perforators. Sun, R. et al (Sun, Ding et al. 2016)added that color Doppler sonography facilitates the preoperative assessment of the origin, course, variations and locations of the main arterial pattern of the upper limb.

In the present study, the most common sites of BAP were present at a mean distance of 2 cm ± 0.5 cm from the tip of the coracoid process. The mean length of the BAP was relatively long 2.13 ±0.42 cm. This fact is beneficial in functional and aesthetic outcomes in patients with soft tissue defects on the head and neck, axilla, chest wall and upper extremity.(Liu, Zang et al. 2017)

Vascular anomalies of the upper limb are not uncommon. Panagouli, E. (2009) (Panagouli, Tsaraklis et al. 2009)reported a superficial origin of the ulnar artery in the upper part of the arm during anatomical dissection of a female Caucasian cadaver. A case of bifurcation of the brachial artery into a common radial-interosseous trunk and the superficial ulnar artery was reported by Narayanan, S. et al (2017) (Narayanan and Murugan 2017).

Baral, P. et al (2009) (Baral, Vijayabhaskar et al. 2009)concluded that single neurovascular variation is common but multiple vascular anomalies on the same upper limb is a very rare case. These variations include the branching pattern of the main arteries of the upper limb, the radial origin of the common interosseous artery and the dominant arteries that share in the formation of the palmar arches.

In the present study, a superficial origin of the ulnar artery was found in only one case of the twelve stillbirth cadavers (8.33%). The presence of a superficial position of the ulnar artery could enable the surgeons to raise a long free ulnar forearm flap for reconstructive surgeries of the head and neck. (Narayanan and Murugan 2017)

Hekner, D. D. et al (2016) (Hekner, Roeling et al. 2016)investigated the distal forearm vascular anatomy to optimize the choice between the free flap of the radial forearm and the free flap of the ulnar forearm and to choose the best site for harvesting the flap. Seven fresh cadavers were injected through the radial and ulnar arteries with epoxy resin (Araldite) and dissected the perforating arteries. The number of clinically relevant radial and ulnar artery perforators in the distal forearm was not significantly different. Most perforators were in the proximal half of the distal one-third, making this portion likely the safest flap harvest place. More perforators were detected on the ulnar side than on the radial side near the wrist, i.e. most distally. Ulnar artery stained 77 percent of the forearm's skin surface, indicating that the ulnar forearm free flap is more suitable for the restoration of large defects than the radial forearm free flap.

On the other hand, Kimura, T. et al (2017) (Kimura, Ebisudani et al. 2017) performed a study on twenty-nine human cadaveric forearms. All radial and ulnar arteries cutaneous perforators were analyzed for total number and distribution. The radial artery's cutaneous perforators were more than that of the ulnar artery, and both were

concentrated in the distal one-third of the forearm. When harvesting forearm flaps, this data could be useful. These findings are also confirmed by Tiengo, C. et al 2007 (Tiengo, Macchi et al. 2007)

The present study, in agreement with the previous studies as regard the concentration of the RAP and UAP in the lower third of the forearm. However, it disagrees with Kimura, T. et al (2017) (Kimura, Ebisudani et al. 2017) where the number of UAP is more than RAP. This means that there are great personal variations as regards the number of perforators of both radial and ulnar arteries, a fact to be considered in surgical interventions.

Liu, P. et al (2015) studied fifteen fresh human cadaveric hands using latex perfusion for micro-anatomical analysis. In the distal second dorsal metacarpal artery, they found two main clusters of arterioles that can be helpful in repairing finger defects from the second webspace border to the midpoint of the second metacarpal bone at a comparative range of 40.8 and 68.6 percent. There were no significant differences in the distribution of the skin perforators from the second dorsal metacarpal artery, either radial or ulnar. (p = 0.779).(Liu, Qin et al. 2015)

In the present study, both the anatomical position (proximal to junctuate tendinae) and the number of the DMAP allow it to have a longer arc of rotation of the standard DMAP flap because of its more distal pivot point.

In a study performed by Usami, S. et al (2018) (Usami, Inami et al. 2018)on thirty-two finger dorsum defects in 32 patients, they concluded that there are multiple perforators in the finger and thumb dorsum region from the proper digital artery. These perforators are suitable for pedicle free-style perforator flaps.

Compared with the present work, many of the cutaneous DAP originated from both sides of the finger distally, forming the basis for the digital artery perforator flap design. In clinical applications, this fact improves flap flexibility and reliability.

Conclusion

Detailed anatomy of the main perforators of the upper limb concerning its accurate site measured from fixed specific bonny points, number and length of their pedicles are very essential in the success of the different flap techniques. Vascular variations are not an uncommon finding of the upper limb.

Acknowledgments:

Refrences

Appleton, S. E. and Morris, S. F. (2014). Anatomy and physiology of perforator flaps of the upper limb. Hand Clin **30**(2): 123-135, v.

Baral, P., et al. (2009). Multiple arterial anomalies in upper limb. Kathmandu Univ Med J (KUMJ) **7**(27): 293-297.

Chaput, B., et al. (2015). Thinning: The Difference between Free and Propeller Perforator Flaps. Arch Plast Surg **42**(2): 241-242.

D'Arpa, S., et al. (2011). Freestyle pedicled perforator flaps: safety, prevention of complications, and management based on 85 consecutive cases. Plast Reconstr Surg **128**(4): 892-906.

Dalla Pozza, E., et al. (2018). Procurement of Extended Vascularized Skin Flaps from the Donor Enables Hand Transplantation in Severe Upper Extremity Burns: An Anatomical Study. Plast Reconstr Surg **142**(2): 425-437.

Hekner, D. D., et al. (2016). Perforator anatomy of the radial forearm free flap versus the ulnar forearm free flap for head and neck reconstruction. Int J Oral Maxillofac Surg **45**(8): 955-959.

Hussein Mahmoud, W., et al. (2019). Propeller Flaps in Different Parts of Body: A Retrospective Study.

Innocenti, M., et al. (2009). Local Perforator Flaps in Soft Tissue Reconstruction of the Upper Limb.

Kimura, T., et al. (2017). Anatomical Analysis of Cutaneous Perforator Distribution in the Forearm. Plast Reconstr Surg Glob Open **5**(10): e1550.

Levin, L. S. and Erdmann, D. (2001). Primary and secondary microvascular reconstruction of the upper extremity. Hand Clin **17**(3): 447-455, ix.

Liu, P., et al. (2015). The second dorsal metacarpal artery chain-link flap: an anatomical study and a case report. Surg Radiol Anat **37**(4): 349-356.

Liu, Y., et al. (2017). Pre-expanded Brachial Artery Perforator Flap. Clin Plast Surg **44**(1): 117-128.

Morris S, T., M., Geddes, C.R.. (2006). Vascular anatomical basis of perforator skin flap. Cirugía Plástica Ibero-Latinoamericana **32**(4).

Narayanan, S. and Murugan, S. (2017). Bifurcation of brachial artery into a common radial-interosseous trunk and superficial ulnar artery: a rare variation. Anat Sci Int.

Panagouli, E., et al. (2009). A rare variation of the axillary artery combined contralaterally with an unusual high origin of a superficial ulnar artery: description, review of the literature and embryological analysis. Ital J Anat Embryol **114**(4): 145-156.

Peng, J. Q., et al. (2019). [Effect of skin soft tissue expansion on repair of large area of scars on extremities]. Zhonghua Shao Shang Za Zhi **35**(4): 308-310.

Sinna, R., et al. (2011). [About perforator flaps...20 years later]. Ann Chir Plast Esthet **56**(2): 128-133.

Spyropoulou, A. and Jeng, S.-F. (2010). Microsurgical coverage reconstruction in upper and lower extremities. Seminars in plastic surgery **24**(1): 34-42.

Sun, R., et al. (2016). Color Doppler Sonographic and Cadaveric Study of the Arterial Vascularity of the Lateral Upper Arm Flap. J Ultrasound Med **35**(4): 767-774.

Thomas, W. W., et al. (2019). Incidence of inadequate perforators and salvage options for the anterior lateral thigh free flap. Laryngoscope.

Tiengo, C., et al. (2007). The proximal radial artery perforator flap (PRAP-flap): an anatomical study for its use in elbow reconstruction. Surg Radiol Anat **29**(3): 245-251.

Tinhofer, I. E., et al. (2017). Vascular territories of the medial upper arm-an anatomic study of the vascular basis for individualized flap design. **37**(6): 618-623.

Usami, S., et al. (2018). Coverage of the dorsal surface of a digit based on a pedicled free-style perforator flap concept. J Plast Reconstr Aesthet Surg **71**(6): 863-869.

Effect of Melamine Administration during Pregnancy on Foetal Bone Ossification

Yasin I. Tayem[1,*], Sindhan V. Veeramuthu[1], Aisha N. Rashid[1], Reginald P. Sequeira[1], Raouf A. Fadel[2]

[1] Department of Pharmacology and Therapeutics, Arabian Gulf University, Manama, Kingdom of Bahrain
[2] Department of Anatomy, Arabian Gulf University, Manama, Kingdom of Bahrain

Abstract

Aim: We aimed to study the effects of prenatal administration of two doses of melamine on foetal ossification centers in rats. **Methods**: Positively-mated, virgin, adult female Sprague-Dawley rats (n=24) were treated from day 6 to day 20 of gestation with solvent (control), melamine 300 mg/kg/day (group 1) or melamine 450 mg/kg/day (group 2). On day 21, half of the fetuses were examined for bone ossification abnormalities. **Results**: A total of 109 foetal skeletons were examined. The percentage of incomplete or absent bones in the entire skeleton was significantly less in group 1 and group 2 compared to control. These findings were more prominent in group 2 compared to group 1. Likewise, ossified centers were fewer in the sternum and metacarpal bones in group 1 and group 2 compared to control. No abnormal ossification was observed in metatarsal, skull, pubic or rib bones. Regarding the vertebral *centrae*, a significant increase in the number of absent or delayed bones was noticed only in group 2 compared to control. Specifically, the abnormalities were observed in the thoracic and sacral *centrae*. Similarly, group 2 was associated with fewer ossified centers in vertebral arch compared to control. The abnormal ossifications were observed in sacral and coccygeal bones. The only observed abnormality in vertebral ossification in group 1 was in coccygeal arch, compared to control. **Conclusions:** Prenatal administration of melamine caused dose-dependent retardation in bone ossification, which mainly affected the sternum, metacarpal, vertebral *centraee* and arch.

Keywords

Melamine, Gestational Exposure, Foetal Ossification, Teratogenicity, Rats.

1. Introduction

Melamine is a heterocyclic nitrogenous compound that is widely used in industry especially for manufacturing dining wares. It is also an ingredient in other essential products such as paints, coatings and glue. In food industry, due to its apparent high amino group content, some manufacturers intentionally add melamine to food products, such as pet food and powdered milk, in order to deceptively inflate their protein content aiming to generate more revenues (Tyan et al, 2009). The illegal addition of melamine to pet food resulted in a global outbreak of melamine poisoning in cats and dogs in several countries world-wide during 2004 and 2007 (Brown et al, 2007). A year later, a catastrophic melamine poisoning was reported in China were tens of thousands of infants and children were admitted to hospitals with acute renal failure and nephrolithiasis due to the ingestion of melamine-tainted infant formulae. Unfor-

* Corresponding author. E-mail: yasiniyt@agu.edu.bh

tunately, a few children lost their lives as a result of this incident (Chiu, 2008). This outbreak in humans dominated the food safety news for several years thereafter and attracted intense health concerns worldwide.

Previous animal studies have demonstrated that toxicity resulting from acute exposure to melamine is considered low at small doses (Zhang et al, 2012). Indeed, experiments on mice have revealed that melamine has a high lethal dose 50 (LD50) which ranged from 3.2 g/kg to 7.0 g/kg (Skinner et al, 2010). However, subacute and chronic exposure to melamine could lead to serious toxic effects which include infertility, urinary stone formation, hematuria, proteinuria, oliguria, renal failure, hepatic impairment, and transitional cell carcinoma in ureter and urinary bladder [Dai et al, 2015; Hau et al, 2009; Hu et al, 2012; Xu et al, 2013; An and Sun, 2017; Ogasawara, et al 1995; Reimschuessel et al, 2010). Acute renal failure and urinary stone formation remain the most serious toxicities resulting from exposure to melamine. Gao et al conducted a prospective cohort study on young children who had history of melamine poisoning as a result of ingestion of contaminated powdered milk. The authors reported that after 18 months of follow up, more than 90% of the participants spontaneously passed a stone and a significant proportion of the children had hematuria and proteinuria (Gao et al, 2016).

Data on the impact of melamine exposure during pregnancy on fetal ossification is scarce. As far as we know, only one study appeared in the literature which explored this topic. In this investigation, Kim and his colleagues reported a delay in fetal bone ossification at maternal doses beyond 400 mg/kg. Indeed, at 800 mg/kg dose, the investigators showed incomplete ossification in many bones including sternum, metacarpal, metatarsal, coccygeal and sacral vertebrae (Kim et al, 2011). Therefore, the main aim of this study was to extensively investigate the effect of exposure of pregnant dams to different doses of melamine on bone ossification in their offspring.

2. Materials and Methods

2.1. Animals

Ethical approval was obtained from the Institutional Research and Ethics Committee at the Arabian Gulf University in Bahrain (Approval number 17-PI-12/2013). Nulliparous, virgin, female Sprague-Dawley rats (n=24) weighing 180–250grams were kept in separate cages in a pathogen-free environment. Prior to starting the experimental work, the rats were acclimated for one week in the animal facility under ambient temperature of 25C°, 12-hour light-dark cycles, and *ad libitum* access to standard rodent chow and purified water. Following acclimatization, one fertile male rat was placed in each cage with two female rats for mating. Pregnancy was confirmed by microscopic examination of a smear taken from vaginal lavage every morning and the day on which the spermatozoa were detected was designated as the first day of gestation.

2.2. Experimental design

Starting from the 6th until the 20th day of gestation, pregnant dams were treated once daily by oral gavage and were randomly allocated into three experimen-

tal groups: Control (n=8) received the solvent 1% carboxymethylcellulose in water, group 1 (n=8) and group 2 (n=8) were administered melamine at doses of 300 mg/kg/day or 450 mg/kg/day, respectively.

On day 21 of pregnancy, the rats were euthanized by ether inhalation and laparotomy was performed. During this procedure, the fetuses were collected from the uterine horns, and immediately euthanized by ether. Then they were eviscerated and immersed for 30 seconds in hot water to facilitate skin removal. Approximately one half of the fetuses, randomly collected from each mother, were stained by Alizarin red to examine them for bone ossification abnormalities as previously described by our group (Fadel et al, 2012). Briefly, the specimens were initially kept in 95% ethanol for 2 to 3 days, after which they were washed with 1% KOH solution for a few days. Once the skeleton was distinctly visible, the specimens were transferred into a fresh KOH solution mixed with a few drops of Alizarin red stain. Following successful staining, the fetuses were kept in solutions containing 30%, 50% and 70% glycerin then finally in 100% glycerin solution with added thymol to prevent fungus growth.

Examination of bone ossification centers in the rat fetuses was systematically carried out by using a dissecting microscope. The chart which was used to record observations included the bones which are expected to be ossified in a rat fetus on day 20 of gestation which include skull, mandible, hyoid, sternum, ribs, forelimbs, hind limbs, vertebral column and hip as previously described (Nash et al, 1989). The examined bones were categorized into two groups: complete or absent, where the latter included bones which were either totally non-ossified or incompletely ossified.

2.3. Statistical analysis

The data were analyzed by using the Statistical Package for Social Sciences software (SPSS-23) using Pearson's Chi-Square test. Statistical significance was set at p value less than 0.05.

3. Results

A total number of 109 Alizarin red stained fetal skeletons were examined for bone ossification; control (n=39), group 1 (n=38) and group 2 (n=32). The following bones were evaluated during this study (Table 1): skull bones (frontal, parietal, interparietal, supraoccipital, exoccipital, basiocciptal, nasal, lacrimal, premaxilla, maxilla, zygoma, squamosal, tympanic bulla, basisphenoid, presphenoid and alisphenoid), mandible, hyoid body, hyoid arch, sternum, ribs, clavicle, scapula, humerus, radius, ulna, metacarpus, hand phalanges, femur, tibia, fibula, metatarsus, foot phalanges, ilium, ischium and pubis. Vertebral column examination included both vertebral *centrae* as well as vertebral arches. In both parts, we examined the cervical, thoracic, lumbar, sacral and coccygeal vertebrae.

3.1. Entire skeleton

The total number of bones (n=21,146) in the entire skeleton were examined. The number of incomplete or absent bones in group 1 was 707 (9.59%) which was sig-

Table 1. Effect of maternal melamine ingestion on bone ossification in 21-day rat fetuses.

Bones	Group	Absent/delayed ossification	Complete ossification	Total number of bones
Entire skeleton	Control	646 (8.54%)	6920 (91.46%)	7566
	1	707 (9.59%)*	6665 (90.41%)	7372
	2	662 (10.66%)**#	5546 (89.34%)	6208
Sternum	Control	66 (33.85%)	129 (66.15%)	190
	1	47 (24.1%)*	148 (75.9%)	195
	2	44 (22.56%)*	151 (77.44%)	160
Metacarpal	Control	157 (40.26%)	233 (59.74%)	390
	1	185 (48.7%)*	195 (51.3%)	380
	2	154 (48.13%)*	166 (51.87%)	320
Metatarsal	Control	142 (36.41%)	248 (63.59%)	390
	1	153 (40.16%)	228 (59.84%)	381
	2	133 (41.43%)	188 (58.57%)	321
Skull bones	Control	20 (10.26%)	175 (89.74%)	195
	1	17 (14.78%)	98 (85.22%)	115
	2	24 (15%)	136 (85%)	160
Pubis	Control	16 (20.51%)	72 (92.31%)	78
	1	8 (10.53%)	68 (89.31%)	76
	2	0 (0%)	64 (100%)	64
Ribs	Control	0 (0%)	1014 (100%)	1014
	1	0 (0%)	988 (100%)	988
	2	0 (0%)	832 (100%)	832
Vertebral *centrae*	Control	99 (9.79%)	912 (90.21%)	1011
	1	105 (10.62%)	884 (89.38%)	989
	2	131 (15.75%)***#	701 (84.25%)	832
Thoracic *centrae*	Control	52 (10.26%)	455 (89.74%)	507
	1	54 (10.91%)	441 (89.09%)	495
	2	80 (19.23%)***##	336 (80.77%)	416
Lumbar *centrae*	Control	1 (0.43%)	233 (99.57%)	234
	1	2 (0.88%)	226 (99.12%)	228
	2	3 (1.56%)	189 (98.44%)	192
Sacral *centrae*	Control	1 (0.64%)	155 (99.36%)	156
	1	3 (1.97%)	149 (98.03%)	152
	2	7 (5.47%)*	121 (94.53%)	128
Coccygeal *centrae*	Control	46 (39.32%)	71 (60.68%)	117
	1	46 (40.35%)	88 (77.19%)	114
	2	41 (42.71%)	55 (57.29%)	96

Bones	Group	Absent/delayed ossification	Complete ossification	Total number of bones
Vertebral arch	Control	137 (6.76%)	1891 (93.24%)	2028
	1	140 (7.09%)	1836 (92.91%)	1976
	2	141 (8.47%)*	1523 (91.53%)	1664
Cervical arch	Control	19 (2.94%)	527 (81.58%)	646
	1	18 (3.38%)	514 (96.62%)	532
	2	12 (2.68%)	436 (97.32%)	448
Thoracic arch	Control	0 (0%)	1041 (100%)	1041
	1	0 (0%)	988 (100%)	988
	2	0 (0%)	832 (100%)	832
Lumbar arch	Control	0 (0%)	468 (100%)	468
	1	0 (0%)	456 (100%)	456
	2	2 (0.52%)	382 (99.48%)	384
Sacral arch	Control	13 (4.17%)	299 (95.83%)	312
	1	10 (3.29%)	294 (96.71%)	304
	2	31 (12.11%)***##	225 (87.89%)	256
Coccygeal arch	Control	100 (42.74%)	134 (57.26%)	234
	1	119 (52.19%)*	109 (47.81%)	228
	2	103 (53.65%)*	89 (46.35%)	192

Chi-Square, *$p < 0.05$, **$p < 0.01$, ***$p < 0.001$, compared to control, #$p < 0.01$, ##$p < 0.001$ compared to group 1. Group 1: melamine 300 mg/kg/day, group 2: melamine 450 mg/kg/day.

nificantly higher compared to control ($p < 0.05$). A similar observation was noticed in group 2 where the number of abnormally ossified bones reached 662 (10.66%) which was also statically significant compared to control ($p < 0.01$). More ossification abnormalities were detected in group 2 compared to group 1 ($p < 0.05$).

3.2. Sternum, forelimbs and hind limbs

A total of 585 sternum bones were analyzed. In comparison with control group, 47 bones (24.1%) were absent in group 1 compared to 44 bones in group 2 (22.56%). In both groups, the number of non-ossified bones was statistically significant compared to control ($p < 0.05$) but no difference was observed between melamine-exposed groups.

Regarding the forelimbs, melamine was found to affect metacarpal ossification. A total of 1092 metacarpal bones were examined. At lower dose of melamine used, 186 bones (48.82%) were absent ($p < 0.05$). Similarly, at the highest dose, 155 metacarpal bones were absent (48.29%), a finding that was statistically significant compared to the control group ($p < 0.05$). However, no difference was noticed between the two melamine-treated groups.

No significant decrease in the number of ossification centers was detected in metatarsal, skull, pubis or rib bones in all the groups.

3.3. Vertebral *centrae*

In the vertebral *centrae*, we evaluated a total of 2832 bones (13 thoracic, 6 lumbar, 4 sacral and 2 coccygeal in each skeleton). Overall, no decrease in the number of ossified centers was observed in group 1. However, a significant decrease was observed in group 2 (131, 15.75%) compared to control ($p< 0.001$) and group 1 ($p< 0.01$). In the thoracic *centrae*, 1418 bones were analyzed. Defective ossification was observed in 80 bones (19.23%) which was significantly more than control ($p< 0.001$) and group 1 ($p< 0.001$). For the sacral *centrae*, 436 bones were examined. Likewise, group 2 showed a higher rate of missing bones (7, 5.47%) which was remarkably higher compared to control ($p< 0.05$) but not different than group 1. For the lumbar and coccygeal *centrae*, no notable findings were observed.

3.4. Vertebral arch

A total of 5668 vertebral arch bones were examined (14 cervical, 26 thoracic, 12 lumbar, 8 sacral, and 4 coccygeal). Overall, the total number of non-ossified bones in the entire vertebral arch in group 2 was 141 (47%) which was significantly more than the control group ($p< 0.05$). Nevertheless, no notable difference between group 2 and group 1 was reported. In the sacral arch, we examined a total of 872 bones. The number of ossification centers was fewer in group 2 compared to control ($p< 0.001$) and group 1 ($p< 0.001$). Similarly, in the coccygeal bones, we examined 654 bones. Less ossification was recorded both in group 1 ($p< 0.05$) and group 2 ($p< 0.05$) compared to control. However, no difference was observed between the two melamine-treated groups. For the thoracic, lumbar and cervical parts of the vertebral arch, no positive findings were reported.

4. Discussion

Most research on melamine focused on renal stone formation and nephrotoxicity since they are the major causes of mortality and morbidity (Hau et al, 2009; Lam et al, 2009). However, only one study has addressed the effects of melamine on fetal bone ossification (14). In that particular study, Sprague-Dawley dams were treated with 200, 400 or 800 mg/kg/day and bone ossification in their fetuses was examined. The outcomes of that study reported notable results at 800 mg/kg/day only. In a recent study, our group has demonstrated that melamine negatively affected intrauterine growth in Sprague-Dawley fetuses when pregnant rats were exposed to 300 and 400 mg/kg/day (unpublished data). In the current study, we observed that melamine resulted in a significant decrease in the number of ossified centers in certain parts of the skeleton at lower doses than previously reported (Kim et al, 2011).

Analysis of the data on the entire skeleton revealed that the number of incomplete or absent bones was statistically significant in group 1 and group 2 compared to the control fetuses. In addition, we reported more ossification abnormalities in group 2

compared to group 1, indicating a dose-dependent pattern. These findings suggest that both melamine doses resulted in detrimental effects on the number of ossified centers-a finding which contradicted the reports of Kim and co investigators who concluded that no adverse effects on ossification were observed at dose of 400 mg/kg/day.

Our findings on individual bone groups showed that the number of ossification centers was significantly fewer in fetal sternum and metacarpal bones at both melamine doses studied. Although Kim et al showed that melamine remarkably affected sternum and metacarpal ossification, these changes were detected only at a dose of 800 mg/kg/day while no significant changes were observed at doses of 200 and 400 mg/kg. In addition, Kim and colleagues reported that metatarsal bone ossification was adversely affected, a finding that was not reported in our study.

Regarding the data on vertebral *centrae*, the negative impact of melamine was noticed at 450 mg/kg dose and changes were observed in thoracic and sacral regions. Since the cervical *centrae* are not normally ossified at this gestational age, none of the bones in this part were appreciated in all the groups. In the vertebral arch, however, changes were observed at both doses of melamine. Specifically, at 300 mg/kg, less ossification was observed in the coccygeal arch. However, at 400 mg/kg, the number of ossified bones was significantly less in the coccygeal and sacral regions. Compared to our findings, Kim and co investigators reported that changes in vertebral ossification were seen at 800 mg/kg melamine dose and that the changes were noticed in the sacral and coccygeal parts only. Again, that group reported no ossification defects at melamine doses less than 400 mg/kg/day.

In conclusion, Maternal exposure to melamine during pregnancy delayed fetal bone ossification. Although some of these adverse consequences were observed at 300 mg/kg, they were more prominent at 450 mg/kg/day. More specifically, the sternum, metacarpal, and parts of the vertebral *centrae* and arches were markedly affected.

5. Acknowledgments

6. Reference

An L, Sun W. (2017) A Brief Review of Neurotoxicity Induced by Melamine. Neurotox Res. 32: 301-309.

Brown CA, Jeong KS, Poppenga RH, Puschner B, Miller DM, Ellis AE, Kang KI, Sum S, Cistola AM, Brown SA. (2007) Outbreaks of renal failure associated with melamine and cyanuric acid in dogs and cats in 2004 and 2007. J Vet Diagn Invest, 19: 525-31.

Chiu MC. (2008) Melamine-tainted milk product (MTMP) renal stone outbreak in humans. Hong Kong Med J, 14(6):424-6.

Dai X, Zhang M, Lu Y, Miao Y, Zhou C, Sun S, Xiong B. (2015) Melamine Impairs Female Fertility via Suppressing Protein Level of Juno in Mouse Eggs. PLoS One. 10: e0144248.

Fadel RA, Sequeira RP, Abu-Hijleh MF, Obeidat M, Salem AH. (2012) Effect of pre-natal administration of therapeutic doses of topiramate on ossification of ribs and vertebrae in rat fetuses. Rom J Morphol Embryol, 53: 321-7.

Gao J, Wang F, Kuang X, Chen R, Rao J, Wang B, Li W, Liu H, Shen Q, Wang X, Xu H. (2016) Assessment of chronic renal injury from melamine-associated pediatric uro-lithiasis: an eighteen-month prospective cohort study. Ann Saudi Med. 36: 252-7.

Hau AK, Kwan TH, Li PK. (2009) Review Melamine toxicity and the kidney. J Am Soc Nephrol. 20: 245-50.

Hau AK, Kwan TH, Li PK. (2009) Review Melamine toxicity and the kidney. J Am Soc Nephrol. 20: 245-50.

Hu P, Wang J, Zhang M, Hu B, Lu L, Zhang CR, Du PF. (2012) Liver involvement in melamine-associated nephrolithiasis. Arch Iran Med. 15: 247-8.

Kim SH, Lee IC, Lim JH, Shin IS, Moon C, Kim SH, Park SC, Kim HC, Kim JC. (2011) Effects of melamine on pregnant dams and embryo-fetal development in rats. J Appl Toxicol. 1: 506-14.

Lam CW, Lan L, Che X, Tam S, Wong SS, Chen Y. (2009) Diagnosis and spectrum of melamine-related renal disease: plausible mechanism of stone formation in humans. Clin Chim Acta. 402: 150–155.

Nash JE, Persaud TV. (1989) Influence of nicotine and caffeine on skeletal develop-ment in the rat. Anat Anz. 168: 109-26.

Ogasawara H, Imaida K, Ishiwata H, Toyoda K, Kawanishi T, Uneyama C, Hayashi S, Takahashi M, Hayashi Y. (1995) Urinary bladder carcinogenesis induced by mel-amine in F344 male rats: correlation between carcinogenicity and urolith forma-tion. Carcinogenesis 16: 2773-7.

Reimschuessel R, Puschner B. (2010) Melamine toxicity--stones vs. crystals. J Med Toxicol. 6: 468-9.

Skinner CG, Thomas JD, Osterloh JD. (2010) Review Melamine toxicity. J Med Toxicol. 6: 50-5

Tyan YC, Yang MH, Jong SB, Wang CK, Shiea J. (2009) Melamine contamination. Anal Bioanal Chem. 395: 729-35.

Xu X, An L, Mi X, Zhang T. (2013) Impairment of cognitive function and synaptic plasticity associated with alteration of information flow in theta and gamma oscil-lations in melamine-treated rats. PLoS One. 8: e77796.

Zhang Q, Gamboa da Costa G, Von Tungeln LS, Jacob CC, Brown RP, Goering PL. (2012) Urinary biomarker detection of melamine- and cyanuric acid-induced kid-ney injury in rats. Toxicol Sci. 129: 1-8.

Morphometric Analysis of Body and Odontoid Process of Axis Vertebrae in North Indians: An Anatomical Perspective

Monika Lalit[1,*], Sanjay Piplani[2], Jagdev S. Kullar[3], Anupama Mahajan[1]

[1] Dept. of Anatomy, SGRDIMS&R, Amritsar
[2] Dept. of Pathology, SGRDIMS&R, Amritsar
[3] Dept. of Anatomy, Govt. Medical College, Amritsar

Abstract

Axis, the second cervical vertebra forms a pivot on which the atlas rotates carrying the head. Though this region is very small but can cause serious complications due to complex anatomy of the cranio-cervical junction. Odontoid fractures compose 7-20% of all cervical spine fractures. The vertebral artery may also be at risk as it is present on under surface of axis. Thus, thorough understanding of the anatomy of body of axis and its odontoid process(dens) is required in screw placement or other surgical interventions. Therefore, aim of the present study was to measure and present the detailed morphometric parameters of body of axis and its odontoid process. 60 dry axis vertebrae were obtained for anatomic evaluation focused on body and odontoid process. The morphometric measurements included linear measurements focused on length, breadth and height of body and odontoid process. Vertebral body length, superior width, inferior width, anterior height and posterior height were found to be 15.10 ± 1.56mm, 15.48 ± 2.09mm,15.83 ± 2.12 mm, 19.28 ± 2.24 and 16.26 ± 1.73mm. Odontoid process height, diameter, maximum and minimum width were found to be 16.36 ± 1.68 mm, 10.74 ± 1.06 mm, 9.85 ± 1.08 mm and 8.79 ± 1.17 mm respectively. Morphological features of dens included its macroscopic appearance and shape of ventral and dorsal facets. Most common shapes of ventral and dorsal facets were found to be vertical elliptical 83.3 % and horizontal elliptical 76.66% respectively. The knowledge of these parameters is important for the surgeons while operating around axis in spinal surgical procedures like anterior atlanto-axial fixation, anterior odontoid screw fixation or odontoidectomy procedures.

Introduction

Axis, the second cervical vertebra, is moulded in a special way, so as to allow greater range of motion at the atlantoaxial joints (Madawi et al., 1997) and forms a pivot on which the atlas rotates carrying the head. (Bryce, 1915) It thus, acts as an axle for rotation of the atlas and head around the strong dens (odontoid process), which projects cranially from the superior surface of the body. (Anson & Rea,1966) The Odontoid Process or Dens is a large blunt tooth-like process which projects supe-

* Corresponding author. E-mail: monika.lalit@yahoo.com

riorly approximately 1.5 cm from the body of the axis. (Williams etal. 2005) It develops in the position of the centrum of the atlas and consists of a thick part, termed the head and a constricted part, the neck. (Bryce, 1915) The anterior aspect bears an ovoid articular facet for articulation with the anterior arch of the atlas to form the atlantodental articulation. The body or corpus of axis is deeper in front than behind and prolonged downward anteriorly so as to overlap the upper and front part of the third cervical vertebra. (Williams etal. 2005) Its undersurface is concave from before backwards and convex from side to side. (Anson & Rea,1966) The body consists of partly fused centra of the atlas and axis, and a rudimentary disc between them which usually remains detectable deep within the body of axis throughout life. There has been an increasing interest in the anatomical study of the axis and the point of interest often being screw fixation in cases of dens fractures (Xu et al. 1995) that comprise 7-20% of all cervical spine fractures. (Montesano et al., 1991; Castillo & Mukherji, 1996; Apfelbaum et al, 2000; Ochoa, 2005) Anderson and D'Alonzo have published a classification of odontoid fractures where Type II and III fractures are among the common fractures of the odontoid process. (Anderson and D'Alanzo, 1974) The knowledge about course of the vertebral artery in relation to axis is also very important because here the vertebral artery is present partially or completely on undersurface of axis while in others it is located entirely in relation to transverse foramen. (Gupta & Goel, 2000) This vital artery may be at risk during the operations especially with the lateral or posterolateral approaches, which are carried out to treat instability of the cranio-cervical junction. Other pathological processes like tumours, degenerative and inflammatory diseases, infections, vascular problems, congenital malformations are also associated with this junction. (Mummaneni & Haid, 2005) Thus Both, odontoid fractures, and craniovertebral junction pathologies may require surgical procedures, including anterior craniovertebral junction stabilization, odontoid screw fixation and transoral odontoidectomy. Such surgical approaches need the correct and common landmarks for placing materials like screws and plates. (Naderi et al, 2006) Structural features of the materials used in the surgery such as the thickness of the screw and screw length, also need accurate morphometric knowledge. These facts require thorough understanding of the anatomy of body of axis and its odontoid process. Therefore, aim of the present study was to measure and present the detailed morphometric parameters of body of axis and its odontoid process. The knowledge of these parameters will be helpful in safe and effective implementation of new interventional techniques or screw placement surgeries.

Material and Methods

Material for the present study comprised of 60 axis vertebrae, obtained by maceration of the cadavers, made available for the purpose of dissection, in the department of anatomy, Government Medical College, Amritsar. The vertebrae were complete in all respects so as to give the correct measurements. All the axis vertebrae were thoroughly boiled, cleaned and numbered from 1-60. Each bone was meticulously examined and fourteen parameters were studied including both morphometric and morphological features. The morphometric measurements included linear measurements, focused on length, breadth and height of body and odontoid process of axis verte-

brae (Table 1). (Gilad and Nissan 1985; Schaffler et al., 1992; Xu et al., 1995) All the measurements were made using a vernier caliper accurate to 0.1 mm. Morphological features of odontoid process (OP) (Dens) of axis included macroscopic appearance of odontoid process, shape of ventral facet on the OP and shape of dorsal facet on OP (Table 4). (Koebke, 1979) All the values were statistically analysed and compared with other studies. (Table 2, 3, 4).

Following are the measured and observed parameters of body and odontoid process (OP) of Axis vertebrae in present study:

Vertebral Body

1) Vertebral Body Length (VBL): It was measured as anteroposterior diameter across the base of vertebral body and shown as AB =VBL (Figure 1)
2) Vertebral Body Superior Width (VBSW): The diameter was measured as the transverse width of the base of superior aspect of vertebral body and shown as CD=VBSW (Figure 1)
3) Vertebral Body Inferior Width (VBIW): The diameter was measured as the transverse width of the base of inferior aspect of vertebral body and shown as C'D'=VBIW (Figure 1)
4) Vertebral Body Anterior Height (VBAH): It is measured in the anterior midline of vertebral body from the inferior anterior edge to the superior border, which was defined by a line drawn at the superior aspect of the superior articular facets and marked as A'B'=VBAH (Figure 2)
5) Vertebral Body Posterior height (VBPH): Posterior vertebral body height was measured in the posterior midline of the vertebral body from the posterior inferior edge to the superior border and shown as A"B"=VBPH (Figure 1)

Odontoid Process (Dens)

6) Odontoid Process Height (OPH): It was measured from the superior border of the superior articular facets to the superior most point of the odontoid process and shown as QR= OPH (Figure 2)

Table 1. The results of the measured parameters of body and Odontoid Process (OP) of axis vertebra in the present study.

S. No.	Parameters	Mean (mm)	Range (mm)	S.D
1.	Vertebral Body Length (VBL)	15.10	9.30-14.00	1.56
2.	Vertebral Body Superior Width (VBSW)	15.48	10.20-18.40	2.09
3.	Vertebral Body Inferior Width (VBIW)	15.83	12.80-20.40	2.12
4.	Vertebral Body Anterior Height (VBAH)	19.28	15.30-25.20	2.24
5.	Vertebral Body Posterior height (VBPH)	16.26	13.40-19.80	1.73
6.	Odontoid Process Height (OPH)	16.36	13.60-19.40	1.68
7.	Odontoid Process Diameter (OPD)	10.74	7.10-12.90	1.06
8.	Odontoid Process Maximum width (OPAW)	9.85	7.40-13.00	1.08
9.	Odontoid Process Minimum width (OPIW)	8.79	4.90-10.60	1.17
10.	Atlanto-odontoidal Facet Width (AOFW)	7.89	4.90-9.40	1.15
11.	Atlanto-odontoidal Facet Height (AOFH)	8.87	5.90-12.90	1.77
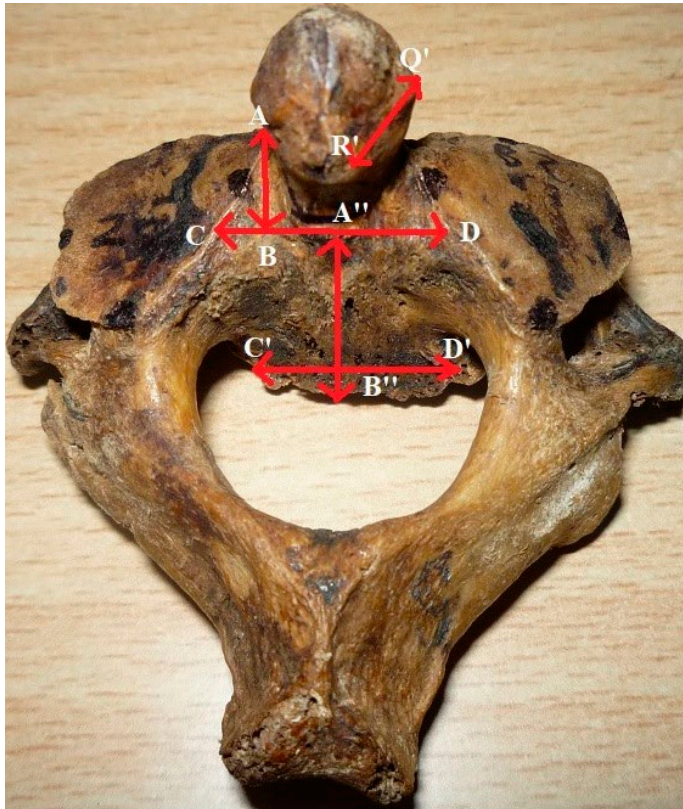
Figure 1. Superoposterior view of axis vertebra showing-
    AB: Vertebral Body Length (VBL)
    CD: Vertebral Body Superior Width (VBSW)
    C′D′: Vertebral Body Inferior Width (VBIW)
    A″B″: Vertebral Body Posterior height (VBPH)
    Q′R′: Odontoid Process Diameter (OPD)

7) Odontoid Process Diameter (OPD): It was taken as anteroposterior measurement from anterior surface to the posterior surface of odontoid process and shown Q′R′=OPD (Figure 1)

8) Odontoid Process Maximum width (OPAW): It was measured as the maximum transverse width on the anterior surface from one end to another end and shown as q″r″=OPAW (Figure 2)

9) Odontoid Process width (OPIW): It was measured as the minimum width on the anterior surface from one end to another end at the junction of dens with the vertebral body and shown as q′r′=OPIW (Figure 2)

10) Atlanto-odontoidal Facet Width (AOFW): It is the maximum transverse diameter of atlantodental facet of axis and shown as c′d′=AOFW (Figure 2)

11) Atlanto-odontoidal Facet Height (AOFH): It is the maximum diameter from superior margin of facet to inferior margin of axis and shown as a′b′=AOFH (Figure 2)
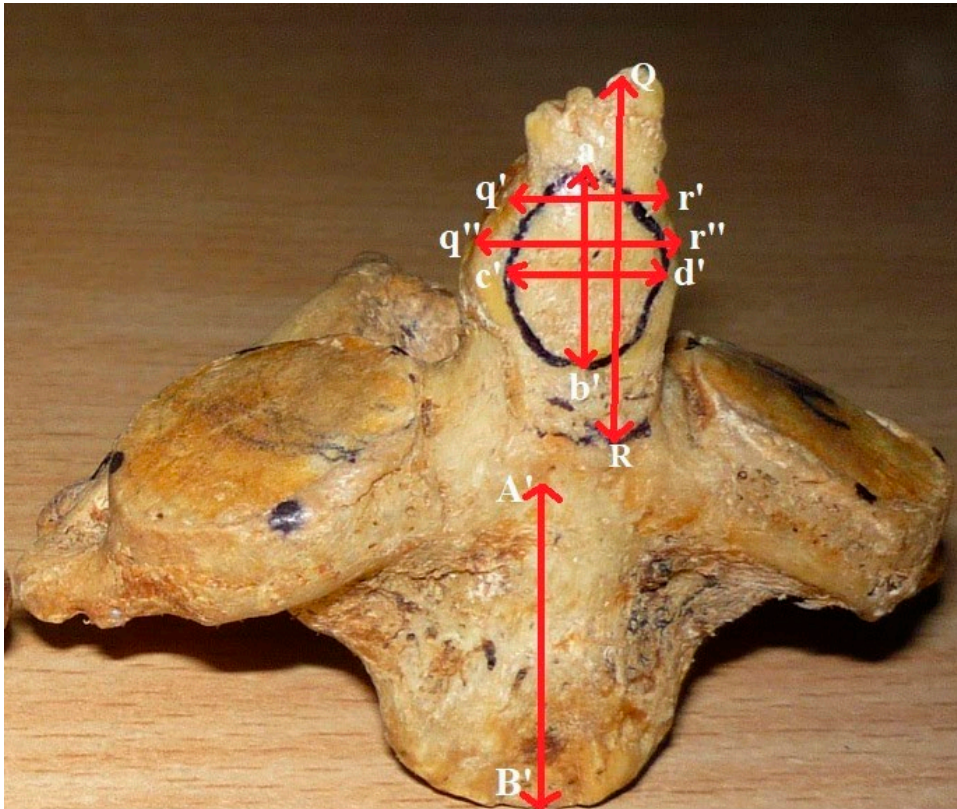
Figure 2. Anterior view of axis vertebra showing-
   A'B': Vertebral Body Anterior Height (VBAH)
   QR: Odontoid Process Height (OPH)
   q"r": Odontoid Process Maximum width (OPAW)
   q'r': Odontoid Process Minimum width (OPIW)
   c'd': Atlanto-odontoidal Facet Width (AOFW)
   a'b': Atlanto-odontoidal Facet Height (AOFH)

Morphological features of odontoid process of axis

12) Macroscopic appearance of odontoid process: It was observed ss Lordotic, Kyphotic and Straight.
13) Shape of ventral facet on odontoid process: It was observed as Vertical, elliptical and Oval.
14) Shape of dorsal facet on odontoid process: It was observed as Vertical, elliptical and Round.

Table 2. Comparison of results of body of axis reported in the present study and series reported in the literature.

Worker & Year	Population	N	VBL Mean(mm) & S.D Range (mm)	VBSW Mean(mm) & S.D Range (mm)	VBIW Mean(mm) & S.D Range (mm)	VBAH Mean(mm) & S.D Range (mm)	VBPH Mean(mm) & S.D Range (mm)
Anderson 1883 [20]	Belfast	23	15.6 (14-17)	19.0 (14-21)	-	19.5 (18-22)	-
Francis 1955 [18]	White Males	109	16.1±1.3 (13-19)	19.5±1.7 (15-24)	-	39.9±2.4 (33-47)	-
	White Females	27	14.7±1.1 (13-17)	17.9±1.5 (15-22)	-	36.6±2.0 (32-40)	-
	Negro Males	135	17.3±1.4 (14-21)	20.3±1.2 (17-24)	-	38.6±2.4 (33-43)	-
	Negro Females	57	15.6±1.3 (13-19)	18.6±1.4 (16-22)	-	35.7±2.4 (31-40)	-
Gilad & Nissa1985 [14]	Israel	130	-	12.6±2.1	15.3±1.6	16.6±2.5	19.0±3.2
Mazzara & Fielding 1988 [19]	American	103	19.0± 2.2 (12-30.2)	22.8±1.5 (19.0-26.5)	-	-	-
Schaffler et al 1992 [15]	Black & White Males	59	-	-	-	24.3±1.9 (19.6-30.1)	20.4±1.9 (15.8-25.3)
	Black & White Females	59	-	-	-	22.6±2.0 (18.1-27.0)	18.9±1.9 (15.0-25.5)
Xu et al. 1995 [5]	Ohio Males	30	16.1±1.5 (14-20)	19.0±2.0 (14-23)	-	21.1±1.7 (18-24)	16.5±1.6 (14-20)
	Ohio Females	20	15.0±1.7 (12-18)	18.7±2.5 (15-25)	-	19.5±1.7 (17-23)	15.3±1.1 (14-18)
Doherty & Heggeness 1995 [23]	American	-	-	-	18.7	23.3	-
Kandziora et al 2001 [21]	European	-	16.7±1.30 (13.6-20.0)	-	15.9±1.45 (12.2-20.1)	21.9±1.67 (17.0-28.4)	17.8±1.45 (11.4-22.10)
Naderi et al 2006 [13]	Turkish	80	15.8±1.7 (12.5-20.2)	-	18.1±1.8 (14.7-24.7)	23.2±2.4 (17.8-34.5)	17.9±2.2 (13.6-27.5)
Gosavi & Swami, 2012 [22]	Maharashtrian	-	-	-	15.99	20.49	-
Present Study 2019	North Indians	60	15.1± 1.56 (9.30-14.00)	15.48±2.09 (10.20-18.40)	15.83±2.12 (12.80-20.40)	19.28±2.24 (15.30-25.20)	16.26±1.73 (13.40-19.80)

Vertebral Body Length-VBL, Vertebral Body Superior Width-VBSW, Vertebral Body Inferior Width VBIW, Vertebral Body Posterior height-VBPH, Vertebral Body Anterior Height-VBAH

Table 3. Comparison of results of odontoid process of axis reported in the present study and series reported in the literature.

Worker & Year	Population	N	OPH Mean (mm) & S.D Range (mm)	OPD Mean (mm) & S.D Range (mm)	OPAW Mean (mm) & S.D Range (mm)	OPIW Mean (mm) & S.D Range ()	AOFW Mean (mm) & S.D Range (mm)	AOFH Mean (mm) & S.D Range (mm)
Francis 1955 [18]	White Males	109	17.5±1.7 (14-22)	12.2±1.0 (10-14)	10.7±0.8 (9-13)	-	8.7±1.3 (6-14)	10.6±1.9 (6-16)
	White Females	27	16.6±1.7 (13-19)	11.1±0.9 (10-13)	10.1±0.6 (8-11)	-	8.2±1.0 (6-10)	10.3±1.7 (8-14)
	Negro Males	135	16.7±1.6 (13-21)	11.8±0.8 (10-13)	10.4±0.8 (9-12)	-	9.0±1.1 (7-12)	11.3±1.9 (8-17)
	Negro Females	57	15.9±1.5 (13-20)	10.8±0.9 (9-13)	10.0±0.(9-12)	-	8.8±1.0 (6-10)	11.1±2.1 (7-15)
Tulsi 1978 [28]	Australian Males	59	14.4±2.19 (11.5-18)	10.29±0.63 (9-12)	-	-	-	-
	Australian Females	48	13.7±1.19 (11-16)	9.54±0.68 (8-11.5)	-	-	-	-
Mazzara & Fielding 1988 [19]	American	103	15.4±2.4 (7-22)	11.0±1.0 (8-13)	10.5±1.0 (8.8-14.5)	-	8.7±1.4 (5-13.3)	11.0±2.4 (7-19)
Schaffler et al 1992 [15]	Black & White Males	59	14.7±1.7 (11.3-20.3)	11.0±0.9 (8.2-12.8)	11.0±1.2 (8.1-14.7)	9.5±0.9 (8.0-11.7)	-	-
	Black & White Females	59	14.0±1.4 (10.9-17)	10.1±0.7 (8.5-11.5)	10.7±1.0 (8.8-13.0)	9.1±0.9 (7.4-12.2)	-	-
Xu et al 1995 [5]	Ohio Males	30	15.5±1.8 (11-18)	10.3±0.7 (7-11)	10.0±0.9 (8-15)	8.7±1.2 (6-10)	-	-
	Ohio Females	20	14.6±1.5 (12-17)	9.6±0.9 (8-11)	9.6±0.8 (8-11)	8.3±0.6 (7-9)	-	-
Kandziora et al 2001 [21]	European	-	20.3±1.90 (15.2-25.4)	10.9±0.8 (8.8-13.9)1	10.8±0.84 (8.6-13.6)	9.7±0.79 (7.8-13.2)	-	-
Naderi et al 2006 [13]	Turkish	-	15.5±1.8 (11.5-19.8)	11.3±1.0 (9.3-13.8)	10.5±0.9 (8.0-12.5)	9.3±0.9 (7.5-12.9)	8.8	10.5
Senegul &Kodiglu 2006 [29]	Turkish	-	14.5	11.2	11.2	-	-	-
Gosavi , Swamy 2012 [22]	Maharashtrian	100	14.86	9.92	9.28	-	-	-
Present Study 2019	North Indian	60	16.36±1.68 (13.60-19.40)	10.74±1.06 (7.10-12.90)	9.85±1.08 (7.40-13.00)	8.79±1.17 (4.90-10.60)	7.89±1.15 (4.90-9.40)	8.87±1.77 (5.90-12.90)

Odontoid Process Diameter-OPD, Odontoid Process Height-OPH, Odontoid Process Maximum width-OPAW, Odontoid Process Minimum width-OPIW, Atlanto-odontoidal Facet Width-AOFW, Atlanto-odontoidal Facet Height-AOFH

Table 4. Macroscopic appearance of dens and shape of ventral and dorsal facet in the present study.

Features	Type	N	%	N	%
	Present study (2019) **N=60** **North Indians**			**Koebke (1979) [16]** **N=52** **German**	
Macroscopic appearance of odontoid process	Lordotic	44	73.33	Most common	
	Kyphotic	10	16.66	4	-
	Straight	6	10.00	-	
Shape of ventral facet on odontoid process	Vertical Elliptical	50	83.30	-	
	Oval	10	16.66	-	
Shape of dorsal facet on odontoid process	Horizontal Elliptical	46	76.66	-	70
	Round	14	23.33	-	30

Results

The present study showed the vertebral body length (VBL), vertebral body superior width (VBSW) and vertebral body inferior width (VBIW) to be 15.1$\pm$1.56mm, 15.48$\pm$2.09mm, 15.83$\pm$2.12mm respectively. Vertebral body anterior height (VBAH) and vertebral body posterior height (VBPH) were 19.28$\pm$2.24mm, 16.26$\pm$1.73mm respectively. (Table 1)

Odontoid process height (OPH) and diameter (OPD) were measured as 16.36$\pm$1.68mm and 10.74$\pm$1.06mm respectively. Odontoid process maximum width (OPAW) and minimum width (OPIW) were found to be 9.85$\pm$1.08mm and 8.79$\pm$1.17mm. Facet for atlanto-odontoidal articulation included measurement of its width (AOFW) and height (AOFH) which were found to be 7.89$\pm$1.15mm and 8.87$\pm$1.77mm respectively. (Table 1)

On the basis of macroscopic features of odontoid process, the most common type was viewed as lordotic (73.33%) followed by kyphotic 16.66% and then straight 10.00%. (Table 4) On the gross appearance of ventral and dorsal facets present on odontoid process, the vertical elliptical shape was found to be 83.30% and oval shape was 16.66% for the ventral facets whereas for the dorsal facets the most common shape was found to be horizontal elliptical 76.66% and round shape was found to be 23.33%.(Table 4)

The results of parameters of vertebral body and odontoid process of axis vertebrae are shown in (Table 1), the comparative data in (Table 2 & Table 3) and the results of macroscopic appearance of OP and shape of dorsal and ventral facets and its comparison are shown in (Table 4).

Discussion

The body of second cervical vertebra and its odontoid process has been the focus of a variety of spinal surgical procedures like anterior atlanto-axial, anterior

occipito-cervical fixation, anterior odontoid screw fixation, odontoidectomy and other surgical procedures. (Naderi et al., 2006) The parameters in the present study like vertebral body length (VBL), vertebral body superior width (VBSW), vertebral body inferior width (VBIW), vertebral body anterior height (VBAH) and vertebral body posterior height (VBPH) were measured and compared with those reported in previous studies by other authors. (Table 2) These series of measurements of axis vertebrae can be taken into consideration during the anterior plating of the C2 body using screws to detect the screw length. (Naderi et al., 2006) These parameters may also be helpful for anthropologists and forensic experts in knowing the racial differences. As stated by Wood Jones (1938), in Australian natives, axis of cervical vertebrae was especially small.

It is depicted from Table 2 that in the present study, the mean value of VBL was 15.1mm. Francis (1955) measured the same parameter with its value 14.7mm in white females (Francis, 1955) and Xu et al (1995) found this parameter as 15.0mm in Ohio females. whereas Mazzara & Fielding (1988) reported VBL as 19mm in American population.

VBSW in the present study was found to be 15.48mm. (Table 2) Gilad & Nissan (1985) reported this parameter to be 12.6mm in Israel population. However, the findings in the present study are, to some extent, smaller than the results reported by Anderson (1883), Francis (1955), Mazzara & Fielding, 1988, Xu et al. (1995).

Table 2, in the present study, shows that VBIW was 15.83mm and these values are in line with results reported by Gilad & Nissan (1985), Kandziora et al (2001), Gosavi & Swami, (2012). Doherty & Heggeness (1995) and Naderi et al (2006) reported this parameter as 18.7 mm and 18.1 mm respectively. This parameter can be taken into consideration during the anterior plating of the C2 body using screws to detect the screw length.

The mean value of VBAH in the present study (Table 2) was 19.28mm which concurs well with the findings of Anderson (1883) in Belfast and Xu et al (1995) in Ohio females. The total height of axis. (DH+VBAH) reflects the length of screw necessary for anterior trans-odontoid screw fixation which was found to be 35.64mm in the present study. This parameter was reported to be 37.8 mm by Heller et al (1992), 39.9 mm by Doherty & Heggeness, (1995) and 38.7 mm by Naderi et al. (2006). Therefore a 36 mm screw seems to be appropriate in most cases. (Naderi et al., 2006) Francis (1955) reported the same parameter in a range of 31-47mm in White & Negro males and females whereas Cyriax (1920) found this to be as 39.22mm.

The present study revealed VBPH as 16.26 mm which is parallel with the values given by Xu et al (1995) in Ohio males as 16.5mm. Gilad & Nissan (1985) measured this height as 19.00mm, (Table 2). Schaffler et al. (1992) found this value in a range of 15.0-25.5mm in Black & White males and females. Xu et al. (1995) found this in a range of (14-20) mm in Ohio males and females. Kandziora et al. (2001) reported this parameter to be 17.8mm while Naderi et al. (2006) found this value as 17.9mm.

Hypertrophic dens of axis is known to cause atlanto-dental instability and neurological complications. (Singh, 1998) Osteoarthritis of atlantoaxial joint is associated with upper cervical myelopathy. Patients usually have hypertrophic dens having anteroposterior diameter as 15-16mm. Association between atlanto-dental instability and formation of pseudotumor around dental process has also been reported. (Okada et al., 2000) Odontoidectomy procedures can be performed using a transoral route

or less commonly using a posterolateral approach. Regardless of the approach used for odontoidectomy, some anatomic data may help the surgeon during the surgical procedure. Thus odontoid process (OP) of axis was studied for OP height (OPH), OP diameter (OPD), OP maximum width (OPAW) and OP minimum width (OPIW). (Table 3) Facet for atlanto-odontoidal articulation includes measurement of its width (AOFW) and height (AOFH). Odontoidal facet dimensions are useful in evaluating sexual dimorphism. In males it is found to be more as compared with females. (Schaffler et al., 1992) Os-odontoideum may be a profound medicolegal importance as it could be due to fracture of dens in early life and confused with congenital absence and hypoplastic dens. (Tulsi, 1978)

It is interpreted from Table 3 that the OPH in the present study was 16.36mm. Our results are in line with the results reported by Francis (1955) in white females and Negro males and females both, Mazzara & Fielding 1988, Xu et al. (1995) and Naderi et al. (2006). This is, to some extent, larger than the results reported by Tulsi (1978), Schaffler et al. (1992), Senguel & Kodiglu (2006), Gosavi & Swamy (2012). On the other hand, the height of OP was reported to be 20.3 mm by Kandziora et al (2001).

The OPD, as depicted from Table 3, in the present study was found to be 10.74mm which supports the findings given by Francis (1955), Mazzara & Fielding (1988), Schaffler et al (1992), Xu et al (1995), Kandizora et al (2006), Naderi et al 2006 and Gosavi & Swamy (2012). It was reported to be 10.29mm and 9.54mm in Australian males and females respectively by Tulsi (1978). (Tulsi, 1978). On the other hand Francis (1955) reported the same parameter to be 12.2mm in white males. (Francis, 1955)

Table 3 also depicts the values of maximum (OPAW) and minimum (OPIW) width of odontoid process of axis as 9.85mm and 8.79mm respectively. OPAW and OPIW showed no major difference when compared with the works done by various authors.

A transoral odontoidectomy requires the detachment of the OP from the atlanto-odontoidal joint. A glance at table 5 elucidates that both AOFW and AOFH were found to be 7.89mm and 8.87mm respectively in the present study. There values were found to be consistent with the works done by Francis, (1955), Mazzara & Fielding, (1988) and Naderi et al. (2006)

The odontoid process is prone to numerous developmental anomalies or variations and many of these are so bizarre that there is no problem in identifying them as such. These variations may be observed regarding the relation of height of OP to anterior arch of atlas like hypoplastic odontoid process when the odontoid tip lies below the level of the superior margin of the anterior arch of atlas or hypertrophic OP where it may even invaginate the foramen magnum and compress the brain stem. (Wackenheim & Wenger, 1973) The Variations may also be observed with regard to longitudinal orientation of the dens and most common being Os Odontoideum in which a variable portion of the upper part of the dens is demarcated from the rest of the bone. (Trivedi, 2003)

A well marked movement of flexion and extension can be realised only in presence of lordotic dens. Kromptic –Nemanic and Keroes (1973) proposed a functional adaption of odontoid process to the degree of cervical lordosis and bending of base of skull. (Koebke, 1979) Thus, Macroscopic classification of dens was also done on the basis of ventral and dorsal facets present on the dens. The comparative data from table 4 depicts that in the present study the most common type of dens on macroscopic appearance was viewed as lordotic which stood equivalent to that of Koebke

(1979). Gross appearance of ventral facets & dorsal facets on odontoid process of axis were also observed. (Table 3) For ventral facets the vertical elliptical shape was found to be (83.30%) and oval shape (16.66%). However, not much quantitative anatomic data was available in the accessible literature except for the types given by Koebke (1979). For dorsal facets the most common shape was found to be horizontal elliptical in (76.66%) of cases which is in accordance with work of Koebke (1979). The observations thus obtained in axis in the present study tallied with the results of previous workers with slight differences, which could be due to racial factors, living habits, native place or different environmental or working conditions.

Conclusion

This study provides information regarding the morphometric dimensions of body of axis and its odontoid process which is critical to safe and effective implementation of the new orthopaedic interventional techniques, to predict the screw size in anterior trans-odontoid screw fixation for odontoid fractures or occipito-cervical fixation procedures. However, the preoperative use of computed tomography is recommended to avoid variation-related complications. The study may also be helpful for anthropologists and forensic experts in knowing the racial differences.

Conflict of Interest

The authors declare that they have no conflict of interest.

References

1) Anderson R.J. (1883) Observations on the diameter of human vertebrae in different regions. J Anat and Physiol. 17: 341-344.
2) Anson B.J., Rea R.L. (1996) Axial skeleton – cervical vertebrae. In: Morris Human Anatomy – A complete systematic treatise. 12th edition. New York, Toronto, Sydney, London: The Blakiston division McGraw Hill Book Company. Pp.142-147.
3) Anderson L.D., D'Alanzo R.T.(1974) Fractures of the odontoid process of the axis. J Bone Joint Surg (Am). 56A: 1663-1674.
4) Apfelbaum R.I., Lonser R.R., Veres R., Casey A. (2000) Direct anterior screw fixation for recent and remote odontoid fractures. Neurosurg Focus. 8(6): Article 2.
5) Bryce T.H. (1915) Osteology the skeleton – Vertebral calumn. In: Schaffer EA, Symington J, Bryce TH, Editors. Quains elements of anatomy. 11th edition. London: Longmans Green and Co. Pp.5-34.
6) Cyriax E.F. (1920) On current absolute and relative measurements of human vertebrae. J Anat. LIV: 305-308.
7) Castillo M., Mukherji S.K. (1996) Vertical fractures of the dens. AJNR. 17: 1627-1630.
8) Doherty B.J., Heggeness M.H. (1995) Quantitative anatomy of second cervical vertebra. Spine. 20(5): 513-17.

9) Francis C.C. (1955) Dimensions of cervical vertebrae. Anat Rec. 122: 603-609.

10) Gilad I., Nissan M. (1985) Sagittal evaluation of elemental geometrical dimensions of human vertebrae. J Anat. 143: 115-120

11) Gupta S., Goel A. (2000) Quantitative anatomy of the lateral masses of the atlas and axis vertebrae. Neural India. 48: 120-125.

12) Gosavi S., Swamy V. (2012) Morphometric anatomy of the axis vertebra. Eur J Anat. 16(2): 98-103.

13) Heller J.G., Alson M.D., Schaffler M.B., Garfin S.R. (1992) Quantitative Internal Dens Morphology. Spine. 17: 861-866.

14) Koebke J. (1979) Morphological and functional studies on the odontoid process of the human axis. Anat Embryol. 155: 197-208.

15) Kandziora F., Schulze-Stahl N., Khodadadyan-Klostermann C., Schröder R., Mittlmeier T. (2001) Screw Placement in transoral atlantoaxial plate systems: An anatomical study. J Neurosurg (Spine). 95: 80-87.

16) Mazzara J.T., Fielding J.W. (1988) Effect of C_1-C_2 rotation on canal size. Clinical Orthopaedics. 237: 115-119.

17) Montesano P.X., Anderson P.A., Schlehr F., Thalgott J.S., Lowrey G. (1991) Odontoid fractures treated by anterior odontoid screw fixation. Spine. 16(30): S33-S37.

18) Madawi A.A., Solanki G., Casey A.T.H., Crockard H.A. (1997) Variations of the groove in the axis vertebra for the vertebral artery - Implications for instrumentation. J Bone and Joint Surgery. 79-B(5): 820-823.

19) Mummaneni P.V., Haid R.W. (2005) Atlantoaxial fixation: overview of all techniques. Neurol India. 53: 408-15.

20) Naderi S., Arman C., Guvencer M. et al. (2006) Morphometric analysis of the C2 body and the odontoid process. Turkish Neurosurgery. 16(1): 14-18.

21) Okada K., Sato K., Abe E. (2000) Hypertrophic dens resulting in cervical myelopathy. Spine. 25(10): 1303-1307.

22) Ochoa G. (2005) Surgical management of Odontoid fractures. Injury. 36: SB54-SB64.

23) Schaffler M.B., Alson M.D., Heller J.G., Garfin S.R. (1992) Morphology of the dens-A quantitative study. Spine. 17(7): 738-743.

24) Singh D.R. (1998) Clinical significance of the cranio-vertebral junction anomalies. J Anat Soc India. 47(2): 80-90.

25) Sengul G., Kodiglu H.H. (2006) Morphometric anatomy of atlas and axis vertebra. Turkish neurosurgery. 16(2): 69-76.

26) Tulsi R.S. (1978) Some specific anatomical fractures of the atlas and axis: Dens, epitransverse process and articular facets. Aust NZJ Surg. 48(5): 570-574.

27) Trivedi P., Vyas K.H., Behari S. (2003) Congenital absence of posterior elements of C_2 vertebra: A case report. Neurology India. 51: 250-251.

28) Wood-Jones F. (1938) The cervical vertebrae of the Australian native. J Anat. 72: 411-415.

29) Wackenheim A., Wenger J.J. (1973) Variations in the height of the odontoid process. Neuroradiology. 5: 140-141.

30) William M., Newell R.L.M., Collin P. (2005) The back: cervical vertebrae. In: Standring S, Ellis H, Haely JC, Johson D, Williams A, Gray's Anatomy. 39th edition. Edinburg, London: Elsevier Churchill Livingstone. Pp.742-746.

31) Xu R., Nadaud M.C., Ebraheim N.A., Yeasting R.A. (1995) Morphology of the second cervical vertebra and the posterior projection of the C_2 pedicle axis. Spine. 20(3): 259-263.

Anatomic variations of the upper biliary confluence and intra-hepatic ducts in East-central Tunisian population

Mohamed Salah Jarrar[1,2,*], Wafa Masmoudi[1], Mohamed Hedi Mraidha[1], Nader Naouar[2], Malek Barka[1], Sabri Youssef[1], Fehmi Hamila[1], Slah-Eddine Ghannouchi[2], Rached Letaief[1]

[1] Department of General and Digestive Surgery, Farhat Hached University Hospital, Sousse
[2] Department of Anatomy, Faculty of Medicine, Sousse

Abstract

Introduction The anatomy of the biliary tract includes a considerable number of variations that may be explained by the hepato-biliary tract embryology. The in-depth knowledge of this anatomy is essential for a good interpretation of conventional radiology imaging, and, especially for a good practice of hepato-biliary surgery. Several imaging techniques allow us to study the biliary tract anatomy. Our **purpose** is to study of modal anatomy (most frequent) and anatomic variations of biliary tract through interpretation of post-operative cholangiograms. **Materials and Methods** It is a retrospective monocentric observational study. It concerned every patient who had a hepato-biliary and/or pancreatic surgery in Farhat Hached University Hospital from 2007 till 2016, and who have had at least one post-operative cholangiography. A data form has been filled for every patient. **Results** Out of a total population of 293 patients, we encountered 17.4% of variations of the upper biliary convergence divided into 7 patterns. Concerning intrahepatic bile ducts, we observed branching variations for segments 4, 5, 6 and 8 in respectively 3.5%, 4.1%, 1.7% and 1.7% of cases. **Conclusion** Both intra- and extrahepatic biliary anatomy is complex with the existence of many common and uncommon anatomic variations. Intra-operative cholangiography constitutes an accurate tool to detect these anatomic variants and is therefore crucial in the practice of hepato-biliary surgery especially after the advent of a variety of new techniques in this field. However, it also necessitates a more widespread and appropriate knowledge of these anatomic variations.

Keywords

Anatomic variations, Cholangiography, Intrahepatic ducts, Upper biliary confluence.

Authors' contribution

Mohamed Salah Jarrar wrote the paper, interpreted the cholangiograms and drew the figures.

Wafa Masmoudi did the data collection and the statistical analysis.

Mohamed Hedi Mraidha, Malek Barka and Sabri Youssef interpreted the cholangiograms.

Rached Letaief interpreted the cholangiograms and revised the paper.

Fehmi Hamila interpreted the cholangiograms and revised the paper.

Nader Naouar revised the paper.

Slah-Eddine Ghannouchi revised the paper.

* Corresponding author. E-mail: hammadi.jarrar@gmail.com

Introduction

Accurate assessment of the hepatic vascular and biliary anatomy is essential to ensure safe and successful hepatobiliary surgery. If bile duct anatomy is misrecognized, intra-operative difficulties and complications may occur. Variations in the anatomy of the biliary tree have long been recognized. Couinaud (1957) described bile ducts anatomic variations since 1957. Thereafter, many other authors proposed other classifications, with a more complex anatomy each time, to match modern surgery requirements (Chaib, 2014; Champetier, 1994; Huang et al., 1996; Jurkovikj, 2011; Karakas et al., 2008; Kim et al., 2010; Kitami et al., 2006; Ohkubo et al., 2004)These new classifications revealed significant variability in frequencies which led to questioning the validation of the frequencies of main variations for different geographical populations. Knowledge on true frequencies for each geographical and racial population has a great meaning, as it may influence surgical practice.

In this research, we tried to study biliary anatomy of a Tunisian population of the Center-east and to determine the frequencies of anatomic variations of the upper biliary confluence (UBC) and intrahepatic biliary tree through post-operative cholangiographies.

Materials and Methods

It is a retrospective monocentric observational study. This study concerned every patient who had a hepatobiliary and/or pancreatic surgery. It included patients hospitalized since January 1st 2007 until December 31st 2016, going thus through a period of ten years. The patients were operated on in Farhat Hached University Hospital or in another hospital and transferred afterwards to our Center, and have had at least one postoperative cholangiography.

Were not included in our study: patients operated on for a hepatobiliary pathology and who didn't have a post-operative cholangiography, files that were incomplete, non-interpretable cholangiograms, incomplete cholangiograms (Hepatectomy, Technical problem, artefacts…), and other means of biliary imaging such as magnetic resonance imaging (MRI) and endoscopic retrograde cholangiopancreatography (ERCP).

Post-operative cholangiography is performed through a cystic duct drain, a T-tube drain, or other drainage tubes such as Pezzer's tube. A preliminary or initial radiograph of the abdomen (scot film) is taken in the supine position with the right upper quadrant of the abdomen centered to the midline of the grid. A water soluble organic contrast medium is gently and slowly introduced, employing general asepsis precautions. First images of the common bile duct filling are taken after a small injection (about 2 milliliters). These sequences are best for visualizing common bile duct content. Fractional injections of the contrast medium are continued gradually (about 3 to 5 milliliters) until contrast medium squirts into the duodenum. In the next sequence, filling is continued until intra-hepatic bile ducts are visualized. The patient is then adjusted in the right posterior oblique (RPO) position to obtain a lateral projection of the common bile duct off the spine and to demonstrate the branching of the hepatic ducts in this plane. Indeed, it is crucial for accurate interpretation of cholangiograms to understand that at a supine position, right hepatic bile ducts are overlapping while
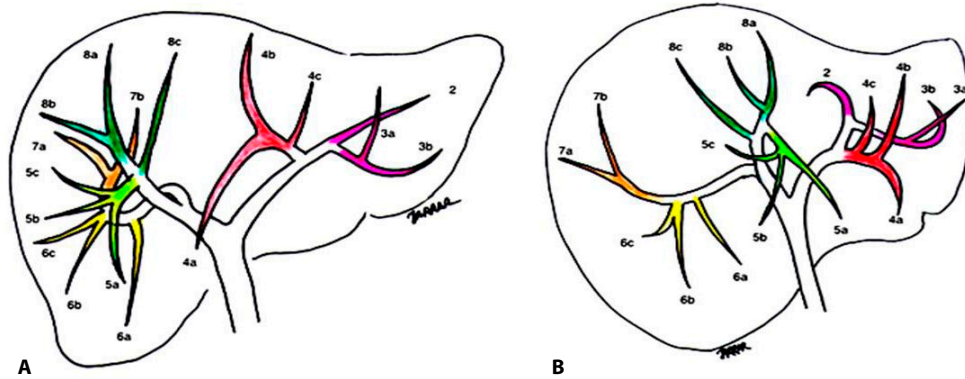
Figure 1. Intra-hepatic bile ducts view according to patient's position. a. Supine position. b. Right posterior oblique position. Numerals refer to Couinaud's segments: 3a: superior branch, 3b: inferior branch, 4a: inferior branch, 4b: superior branch, 4c: dorsal branch, 5a: ventral branch, 5b: dorsal branch, 5c: lateral branch, 6a: ventral branch, 6b: dorsal branch, 6c: lateral branch, 7a: ventral branch, 7b: dorsal branch, 8a: ventral branch, 8b: lateral branch, 8c: dorsal branch.

left hepatic ducts are visible. On the contrary, in the RPO position, left hepatic ducts are overlapping and right hepatic ducts are individualized better (figure 1) (Hautefeuille, 1998). We studied anatomic variants of intra and extra-hepatic bile ducts, intraoperative difficulties and post-operative course. We filled in a data form for every patient's file. This data form was specially conceived for the purpose of this study and consisted of two sections. The first section included information about the patient, the surgery and the hospital stay. The second one concerned the analysis of the post-operative cholangiography. We established a layout of modal anatomy and anatomic variations based on the classification of Couinaud (1957), picked arbitrarily as reference. Interpretation of the cholangiograms was reviewed systemically by a surgeon and an anatomist with a 10-year-expertise, and we referred to a third party in case of disagreement. We studied variations of the upper biliary confluent. Different patterns for each item have been drawn to help fill in the form. A white page was added to draw an eventual variation that was not described in the pre-existent patterns.

Results

Throughout the period between the 1st of January 2007 and the 31st of December 2016, we counted 351 files of patients operated for a hepatobiliary and/or pancreatic pathology and who have had postoperative cholangiography. Among them, 58 did not respond to inclusion criteria or had non-inclusion criteria. We kept thus 293 exploitable files.

Sixty-eight point six percent (68.6%) of the population were women (n=201), and 31.4% were men (n=92) with a sex ratio M/F of 0.46. In our population, the mean age was 49 years, the minimum age was 11 and the maximum age was 89.

Table 1. Surgical indications.

Diagnosis	n	%
Cholecystolithiasis	45	15.3%
Acute cholecystitis	42	14.3%
Acute pancreatitis	14	4.7%
Hydatid cyst	100	34.1%
Common bile duct lithiasis	7	2 %
Cholecystolithiasis+ common bile duct lithiasis	31	10.5%
Acute lithiasic cholangitis	22	7.5%
Acute cholecystitis + acute cholangitis	6	2%
Hydatid cholangitis	14	4.7%
Mirizzi's syndrome	3	1%
Bilio-enteric fistula	3	1%
Others	6	2%

Table 2. Surgical procedures.

Surgical procedure	n	%
Cholecystectomy	276	94.2%
Choledocotomy	85	29%
Cyst unroofing	92	31.4%
Internal transfistulary drainage	11	3.7%
Pericystectomy	9	3.1%
Perdromo procedure	7	2.4%
Bipolar drainage	5	1.7%
Antrectomy+ gastrojejunostomy	1	0.3%
Blio-enteric fistula disconnexion	2	0.7%
Peritoneal lavage	1	0.3%

One hundred five (35.8%) of our patients had a laparoscopic surgery while 188 (64.2%) had an open surgery. Tables 1 and 2 summarize the surgical indications and procedures.

A cystic duct drain (Pedinielli drain) was used in 201 procedures (68.6%) and a Kehr's T-tube was used in 88 procedures (30%). Other types of drainage were also used: fistula drainage (n=3; 1%) and Pezzer tube (n=1; 0.3%).

The upper biliary confluence (UBC) had a modal presentation (type A) according to Couinaud classification (1957) in 242 cholangiograms (82.6%). In 51 patients (17.4%), we encountered 7 other branching patterns listed in figure 2:
• Type B=APL (trifurcation): 18 cases (6.1%)
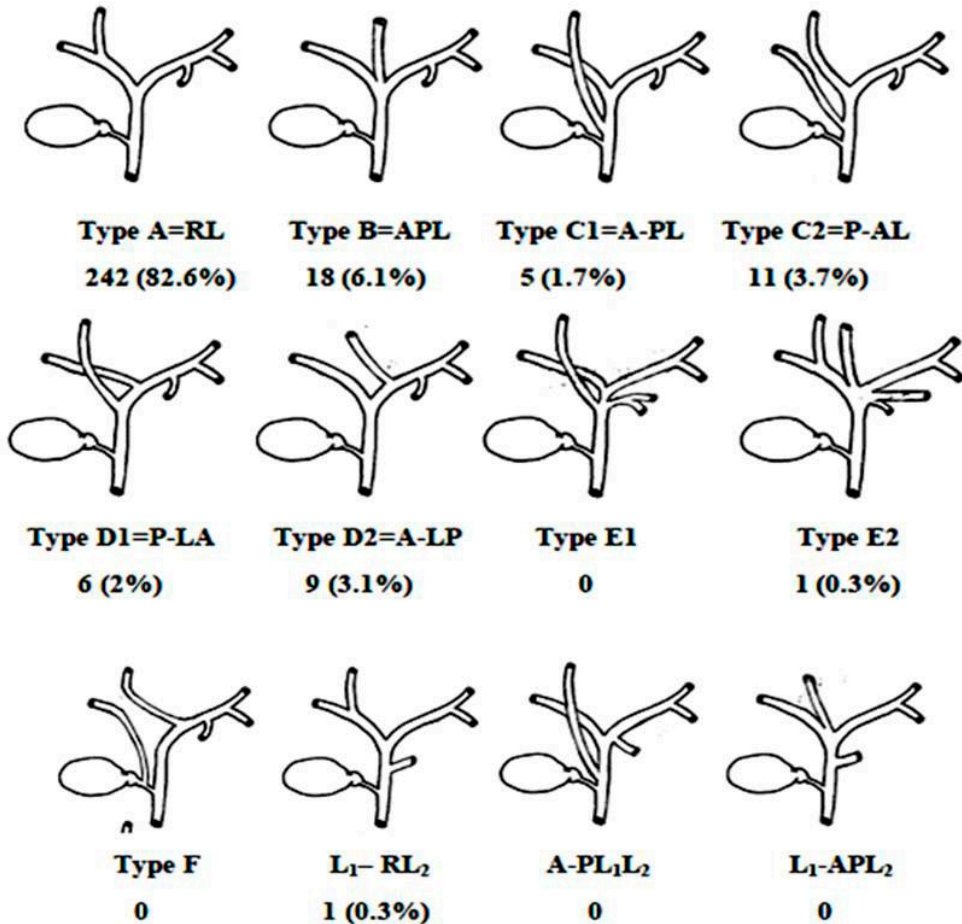
Figure 2. UBC branching. A: right anterior hepatic duct, P: right posterior hepatic duct, L: left hepatic duct. When the branches come off at different levels, a hyphen is inserted between the appropriate letters. For example, "A-PL" indicates that the first branch from below is A (right anterior duct) and that the next branches are P (right posterior duct) and L (left hepatic duct) at the same level.

- Type C1=A-PL: 5 cases (1.7%)
- Type C2=P-AL: 11 cases (3.7%)
- Type D1=P-LA: 6 cases (2%)
- Type D2=A-LP: 9 cases (3.1%)
- Type E2: 1 case (0.3%)
- Type L_1-RL_2: 1 case (0.3%).

The fifth segment duct was unseen in 3 cases (1%), the sixth segment in 2 cases, segment VIII duct was not visualized on cholangiograms in 2 cases and the fourth segment duct was unseen in 5 cases.

When seen, the intra-hepatic ducts presented 8.8% of variations:
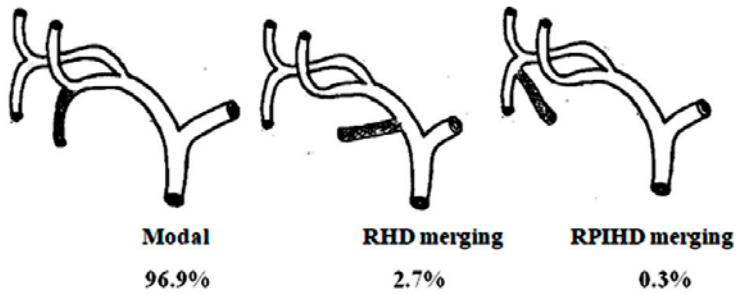
Figure 3. Fifth segment duct branching. RHD: Right hepatic duct; RPIHD: Right postero-inferior hepatic duct.
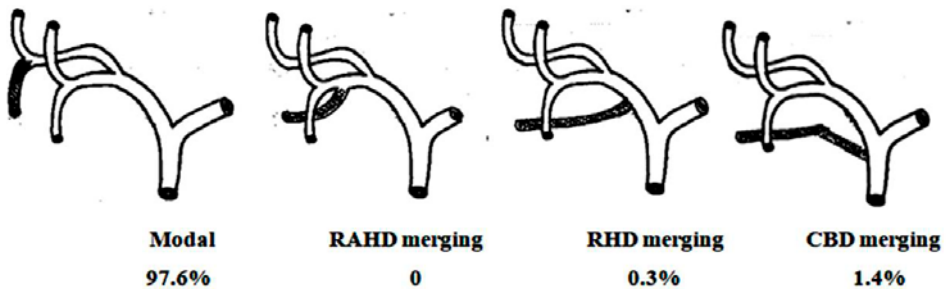
Figure 4. Sixth segment duct branching. RAHD: Right anterior hepatic duct; RHD: Right hepatic duct; CBD: Common bile duct.
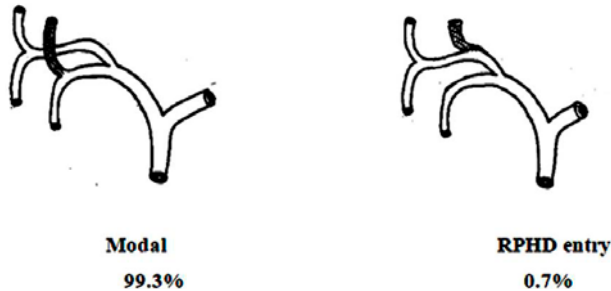
Figure 5. Eighth segment duct branching. RPHD: Right posterior hepatic duct.

- The fifth segment duct had a modal presentation in 281 cholangiograms (95.9%). It had a branching in the right hepatic duct in 8 cases, and in the right postero-inferior hepatic duct in 1 case (figure 3).
- The sixth segment duct had a modal presentation in 286 cholangiograms (98.3%). It had a branching in the right hepatic duct in 1 case, and in the common bile duct in 4 cases (figure 4).
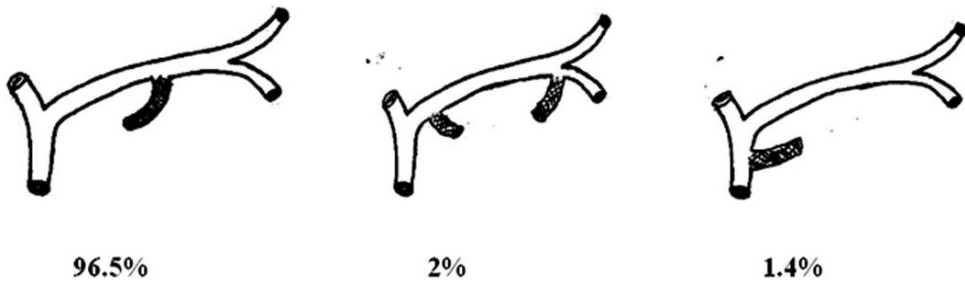
Figure 6. Fourth segment duct branching.

- Beside the modal presentation of the eighth segment duct in 288 cases (98.3%), we observed 2 cases of right posterior hepatic duct entry (0.7%) (figure 5).
- The fourth segment duct had a modal presentation in 278 cholangiograms (96.5%) (figure 6).

Discussion

Variations in the anatomy of the bile ducts have long been recognized. Clinical radiological diagnostics, gastro-enterological and surgical practice often encounter findings of variable anatomy and topography of the elements that create the biliary tree. Several authors helped defining the notions of normal (modal) and accessory or aberrant anatomy, by different imaging modalities such as ERCP, magnetic resonance cholangiography (MRC), intraoperative cholangiography and also by corrosion cast studies on autopsy specimens (Huang et al., 1996). In our study, evaluation was focused on the post-operative cholangiograms of a Tunisian population of the Center-east.

We listed a total of 51 patients (17.4%) with anatomic variations of the UBC and 8.8% of variation of intra-hepatic ducts.

The mean age in literature varied in North-African studies from 35 to 46 years (Abdelgawad and Eid, 2012; Elhjouji et al., 2009; Tawab and Taha Ali, 2012). In other international studies it varied from 30 to 57 years with a range of 16 to 89 years (Choi et al., 2003; Cucchetti et al., 2011; Deka et al., 2014; Karakas et al., 2008; Ohkubo et al., 2004). The age of our 293 subjects ranged from 11 to 89 years, with a mean of 49 years. We found no correlation between age and the presence of anatomic variants. This is perfectly explained if we admit the embryological development aberrations to be the origin of variations.

Few data are available about the regional, ethnical disparities or other demographical characteristics regarding hepatic biliary abnormalities. Living donor liver transplantation surgery is being widely performed in the Far East where organ donations do not compensate the requirement. Therefore, the majority of the studies on liver variations were performed on Asian race. For the specific subtype Asian race, no major differences were found in regard to frequencies of variations and modal anatomy was predominant with a frequency of 63-73% (Karakas et al., 2008). In their study of an Anatolian Caucasian population, Karakas et al. (2008) noted that modal

anatomy frequency was significantly lower than that of Asian population (55% versus 63–73%), but was very similar to North Americans (57%). In a meta-analysis of literature, Cucchetti et al. (2011) showed that Europeans and Americans share similar prevalence rates of typical biliary anatomy. From an ethnicity point of view, this finding is not surprising since both populations can be considered Caucasian. On the contrary, Asians seem to have a slightly higher prevalence of typical anatomy. This meta-analysis is concordant with Karakas' results (2008), but also states that these differences should be taken into account with caution, in regard to interpretation bias. This same study though, did not include in its pool any African, or Middle-East population, probably due to lack of studies about them. Indeed, only a few authors in these regions studied the subject, and our research seems to be the first to study a Tunisian population. Modal anatomy in North African population according to these studies varied from 60% to 80%, but population size was limited to a small sample (20 to 106 subjects) which might not be representative of general population. Table 3 compares some of the North African studies with our present study.

The upper biliary confluence (UBC) anatomy has been subject to a prolific research. Different classifications of anatomic variants have been described: Couinaud (1957), Champetier (1994), Huang et al. (1996), Choi et al. (2003) and Ohkubo et al. (2004).

Huang classification would be considered "the simplest" and was the most widely used system by authors. It is based on the variable insertion of right posterior hepatic duct and is composed of five distinct anatomic types. Champetier classification (1994), in comparison to Huang classification, deals only with the variations and not with the dominant (modal) Huang type A. It has an additional type (E) in which both right posterior hepatic duct and right anterior hepatic duct open to cystic duct (figure 7).

Choi et al. (2003) added in his classification two patterns including accessory ducts as well as one variation of the LHD. Ohkubo et al. (2004) divide the bile ducts according to the position of the right posterior hepatic duct insertion relative to portal vein level; so types A to C are supraportal, and types D and E are infraportal patterns.

An Indian study by Deka et al. (2014) tried to compare these different classifications and states that Ohkubo classification system is the most applicable as it considers most clinically relevant variations pertinent to hepatobiliary surgery, unclassified variants were the least, and both right and left ductal systems could be classified. We used Couinaud classification as reference in our research rather than the others classifications that were conceived for the purpose of living-donor liver transplant. The drawback of Couinaud classification is that is does not take into account accessory

Table 3. Modal anatomy and variations of upper biliary confluence according to North African authors.

Series	Country	n	Modal anatomy	Anatomic variations
Elhjouji (2009)	Morocco	70	72.9%	27.1%
Abdelgawad (2012)	Egypt	20	80%	20%
Tawab (2012)	Egypt	106	63.2%	36.8%
Barsoum (2013)	Egypt	50	60%	40%
Our series	**Tunisia**	**293**	**82.6%**	**17.4%**

Table 4. Upper biliary confluence variants according to authors.

Series	n	Country	Type A (%)	Type B (%)	Type C1 (%)	Type C2 (%)	Type D1 (%)	Others (%)
Huang (1996)	958	Taiwan	63	19	11	6	-	2
Ohkubo (2004)	110	Japan	65	5	12	7	-	11
Choi (2003)	293	South Korea	64	9	11	6	-	7
Karakas (2008)	112	Turkey	55	14	21	10	-	
Deka (2014)	299	India	57.8	8	3	6.6	17,4	35.5
Cuccettti (2011)	200	Italy	64.5	14		8	12	1.5
Tawab (2012)	106	Egypt	64	10	17	7	-	2
Our series	**293**	**Tunisia**	**82.6**	**6.1**	**1.7**	**3.7**	**2**	**3.7**

ducts. An accessory bile duct is an additional bile duct draining the same area of the liver, whereas an aberrant bile duct is the only bile duct draining a particular hepatic segment. In our study, modal anatomy (Couinaud type A) of the UBC was present in 82% of cases, which is a higher rate than of that described in most literature articles. Couinaud type B, or the so called triple confluence was the second most frequent modality (6.1%). Table 4 shows the frequency of different variations of the UBC in different studies.

Most of the authors did not study separately intra-hepatic segmental bile ducts and focused only on right hepatic duct, left hepatic duct, right anterior hepatic duct and right posterior hepatic duct variations as these two were the most relevant elements in surgical practice.

Huang et al. (1996), Champetier (1994), Choi et al. (2003), Ohkubo et al. (2004) and Karakas et al. (2008) did not include segmental bile ducts variants in their classifications concerning the right liver.

Concerning the left liver, Ohkubo's left intra-hepatic ducts classification was mainly about segment IV branching patterns (Ohkubo et al., 2004). However, when two or more segment IV ducts are present and drain separately into the left ductal system, classification is not possible. This specific aspect was studied by Kawarada et al. (2000) who also proposed a separate classification based on cast studieshilar bile duct carcinoma can easily spread to the bile duct branches of the caudate lobe (B1.

Huang et al. (1996) also described variants of the left intra-hepatic ducts, his classification has the advantage of including segment I duct variations. He is the only author known to us that has described segment I duct variants.

Very rare are segments II and III ducts variants. Only Choi type 6 (figure 58) and Huang type B5 (figure 57) describe a pattern in which segments II and III ducts drain separately in the common bile duct, these variants were up to 1% and 3% respectively.

Using the classifications mentioned above would lead to several cases of unclassified variants, a situation which we mended by adding another section for segmental ducts variants, following the description of Valette and De Baere (2002).

In our study, 4.4% of population had variants only in the intra-hepatic bile tracts (UBC excluded). Five point eight percent had variants in both intra-hepatic and extra-

Table 5. Frequency of intra hepatic bile ducts variations according to authors.

	Seg V	Seg VI	Seg VIII	Seg IV	Seg II and III	Seg I
Valette (2002)	9%	12%	20%	30%	-	-
Ohkubo (2004)	-	-	-	24%	-	-
Choi (2003)	-	-	-		1%	
Huang (1996)	-	-	-	24%	3%	17%
Our series	3%	1.7%	0.7%	3.4%	-	-

hepatic bile tracts. Segment V duct variants were up to 3%, segment VI duct variants 1.7%, segment VIII duct 0.7% and segment IV duct 3.4%. We didn't encounter segment II and III ducts variants.

Table 5 summerizes frequencies of intra-hepatic bile ducts according to some authors.

Recent technical advancement of various types of hepatectomy, such as laparoscopic hepatectomy and donor hepatectomy for living-donor liver transplant, has increased the number of surgical plans that can be made only after surgeons have achieved a complete understanding of the branching of the bile duct. Variations of the bile duct would be essential for the screening of donors and the selection of methods of hepatectomy. If variations of the bile duct would not be confirmed or would be overlooked prior to surgery, this would lead to the occurrence of bile duct complications in both recipients and donors. On the other hand, some variants such as short right hepatic duct were predictors of a more complex surgery (bench ductoplasty or multiple anastomoses) (Ayuso et al., 2004; Barsoum et al., 2013; Catalano et al., 2008; Karakas et al., 2008). However, an insufficient number of studies have been conducted to examine whether variations of biliary tree affect the outcomes and the course of daily-routine procedures such as laparoscopic cholecystectomy and whether this would increase risks for injury to the bile ducts.

We believe our study has a few points that add to its pertinence. It has, indeed, included a large population sample, representative of the Tunisian Center-east (293 patients). It is the first study, to our knowledge, to be conducted in our country, and one among few in North-Africa. This work may seem at first, to be mainly about anatomy, but it also takes interest in its practical repercussions and it treats about a subject of current "trend" that is hepatobiliary surgery; a field with constant development and updates each day. We used as support to our text original sketches and figures, along with literature figures, and we enriched it with original iconography of the collected cholangiograms.

The main limitation of this study is interpretation bias. Indeed, cholangiograms interpretation was sometimes difficult due to poor quality, technical limitations, artefacts, incomplete or severed images, as most of these cholangiograms were not applied for identification of bile duct anatomy, but for suspicion of common bile duct stone. Many non exploitable cholangiograms were excluded reducing thus the population size. Interpretation is also operator-dependent. In a study led by a United Kingdom team (Sanjay et al., 2012), it was proven that accuracy of detection of both

normal and variants of normal anatomy was poor in all grades of surgeon irrespective of a policy of routine or selective IOC. Some authors would have cholangiograms interpreted by two independent experienced investigators and sometimes a third investigator was consulted in case of disagreement (Choi et al., 2003). In our case, interpretation was systematically reviewed and corrected by a 10-year-experience surgeon and anatomist and we referred to a third party in case of disagreement. The second limitation of this study is methodological. Indeed, it is a retrospective, non-randomized study, using a data collection sheet filled from medical records that were not all complete and exploitable. Sometimes, we found insufficient clinical, radiological and operative data. Difficulties were also encountered during data collection due to incomplete or sometimes unavailable files (archiving issues). We suggest that large-scale prospective control study should be needed.

Conclusion

Both intra- and extra-hepatic biliary anatomy is complex with the existence of many common and uncommon anatomic variations. Intra- and post-operative cholangiography constitutes an accurate tool to detect these anatomic variants and is therefore crucial in the practice of hepatobiliary surgery especially after the advent of a variety of new techniques in this field. Other means of biliary mapping such as MRC and ERCP are also available for pre-operative diagnosis. However, all these thechniques necessitate a more widespread and appropriate knowledge of anatomic variations.

Acknowledgement

References

Abdelgawad MS, Eid M (2012) Biliary tract variants in potential right lobe living donors for liver transplantation: Evaluation with MR cholangiopancreatography (MRCP). Egypt J Radiol Nucl Med 43: 53–57

Ayuso JR, Ayuso C, Bombuy E et al (2004) Preoperative evaluation of biliary anatomy in adult live liver donors with volumetric mangafodipir trisodium enhanced magnetic resonance cholangiography: MRC Evaluation of Biliary Anatomy in LLDs. Liver Transpl 10: 1391–1397

Barsoum NR, Samie AA, Adel L, Asaad RE (2013) Role of MRCP in assessment of biliary variants in living donor liver transplantation. Egypt J Radiol Nucl Med 44: 131–136

Catalano OA, Singh AH, Uppot RN et al (2008) Vascular and Biliary Variants in the Liver: Implications for Liver Surgery. RadioGraphics 28: 359–378

Chaib E, Kanas AF, Galvão FHF, D'Albuquerque LAC (2014) Bile duct confluence: anatomic variations and its classification. Surg Radiol Anat 36: 105–109

Champetier J. Les voies biliaires (1994) Anatomie Clinique - Tronc. Springer, Paris

Choi JW, Kim TK, Kim KW et al (2003) Anatomic variation in intrahepatic bile ducts: an analysis of intraoperative cholangiograms in 300 consecutive donors for living donor liver transplantation. Korean J Radiol 4: 85–90

Couinaud C (1957) Le foie. Etudes natomiques et chirurgicales. Masson, Paris

Cucchetti A, Peri E, Cescon M et al (2011) Anatomic variations of intrahepatic bile ducts in a european series and meta-analysis of the literature. J Gastrointest Surg 15: 623–630

Deka P, Islam M, Jindal D et al (2014) An analysis of biliary anatomy according to different classification systems. Indian J Gastroenterol 33: 23–30

Elhjouji A, Ali AA, Alahyane A et al (2009) Variations anatomiques des voies biliaires et conséquences chirurgicales: à propos de 19 cas. J Afr Hépatol Gastroenterol 3: 137–142

Hautefeuille P (1998) Reading the anatomy of cholangiograms. J Chir 135: 275–278

Huang TL, Cheng YF, Chen CL et al (1996) Variants of the bile ducts: clinical application in the potential donor of living-related hepatic transplantation. Transplant Proc 28 :1669–1670

Jurkovikj D (2011) Some Anatomic-Topographic Features of Common and Right Hepatic Ducts and their Constituents. Maced J Med Sci 4: 44-53

Karakas HM, Celik T, Alicioglu B (2008) Bile duct anatomy of the Anatolian Caucasian population: Huang classification revisited. Surg Radiol Anat 30: 539–545

Kawarada Y, Das BC, Onishi H et al (2000) Surgical anatomy of the bile duct branches of the medial segment (B4) of the liver in relation to hilar carcinoma. J Hepatobiliary Pancreat Surg 7:480–485

Kim SY, Byun JH, Lee SS et al (2010) Biliary Tract Depiction in Living Potential Liver Donors: Intraindividual Comparison of MR Cholangiography at 3.0 and 1.5 T. Radiology 254: 469–478

Kitami M, Takase K, Murakami G et al (2006) Types and frequencies of biliary tract variations associated with a major portal venous anomaly: analysis with multidetector row CT cholangiography. Radiology 238 :156–166

Ohkubo M, Nagino M, Kamiya J et al (2004) Surgical Anatomy of the Bile Ducts at the Hepatic Hilum as Applied to Living Donor Liver Transplantation: Ann Surg 239: 82–86

Sanjay P, Tagolao S, Dirkzwager I, Bartlett A (2012) A survey of the accuracy of interpretation of intraoperative cholangiograms. HPB 14: 673–676

Tawab MA, Taha Ali TF (2012) Anatomic variations of intrahepatic bile ducts in the general adult Egyptian population: 3.0-T MR cholangiography and clinical importance. Egypt J Radiol Nucl Med 43: 111–117

Valette PJ, De Baere T (2002) Biliary and vascular anatomy of the liver. J Radiol 83: 221–234

Stability analysis of occipitocervical fixation by occiput-C2 pedicular screws construct. A human cadaveric study

Ayman Ahmed Kkanfour[1],*, Tarek Elfiky[2], Hesham Elsaghir[2], Waleed Sabbah[2]

[1] Department of Anatomy and Embryology, Faculty of medicine, Alexandria University, Alexandria, Egypt
[2] Spine Unit, Department of Orthopaedics & Traumatology , Al-Hadra University Hospital, Alexandria University, Alexandria, Egypt

Abstract

Objective: The present study aims to evaluate the stability provided by occipitocervical (OC) fixation using occipital plate and C2 pedicular screws. **Methods:** The study included 6 formalin preserved whole human cadaveric specimens. Occipito-cervical fixation was performed using occipital plate and C2 pedicle screws connected by rods. Specimens were manually loaded by the maximum possible flexion, extension and axial rotation. Assessment of stability of fixation was done after 100, 500, 1000, 2000 and 3000 cycles. In the first 3 specimens (group 1), repetitive loading was planned to be initially applied in flexion and extension. If there was no failure of the construct at 3000 cycles, loading has to be continued in axial rotation. In the second 3 specimens (group 2), repetitive loading was planned to be applied initially in axial rotation up to 3000 cycles. If there was no failure of the construct, loading has to be continued in flexion and extension. **Results:** group 1 showed no implants failure apparently or radiologically after 3000 loading cycles. However, failure occurred at different sites when axial rotation loading was applied at 500, 700 and 900 cycles respectively by axial rotation loading cycles. On the other hand, when axial rotation was initially applied to group 2, failure occurred at 1050, 1000 and 800 respectively cycles before applying flexion and extension loading. **Conclusions:** Our study revealed that occiput-C2 pedicle screw construct, without supplementary C1 lateral mass provided stability in flexion and extension loading. However, repeated axial rotation loading causes failure of construct.

Keywords

Cadaveric, Biomechanics, Occipitoatlantoaxial fixation, Occipital screw, C2 pedicle screw.

Authors' role

Tarek Elfiky: Dissection and instrumentations of the specimens and writing the manuscript, Waleed Sabbah Ayman: Stability testing and writing the manuscript. Ayman Ahmed Kkanfour: preparation of the specimens, critical revisions and dissection and exposure, Hesham Elsaghir: study design and critical revisions

Introduction

The occipitocervical (OC) region is the most mobile part of the cervical spine, with 50% of flexion and axial rotation occurring at the atlantooccipital and atlanto-

axial joints. The OC junction is stabilized only by capsuloligamentous and muscular structures. As a result, its stability is vulnerable to a multitude of disorders to include infection, trauma, tumor, inflammatory, and other degenerative conditions.[1,2]

Historically, stabilization of this junction dates back to 1927 when Foerster used a fibular strut graft construct.[3] Since then, other nonrigid methods of stabilization have been used, including wire fixation, pin fixation, hook constructs, and others with onlay bone graft and halo immobilization.[4] However, these techniques have been shown to be biomechanically inferior to procedures that offer segmental fixation.[5,6] Surgical fixation has advanced during the past decades, and occipital plate-rod-screw instrumentations are currently the most widely used method. These techniques use C2 pedicle screws with and without C1 lateral mass screws that are then incorporated into occipital plate fixation with occipital screws.[7-9] Special considerations are necessary for surgery because of the unique neurologic, musculoskeletal, and vascular anatomy of the spine, and the need to restrict all planes of motion.[10] Proper stabilization system in this unique transitional area must be able to resist loads in the different axis of motion (flexion, extension, lateral flexion, rotation, distraction and axial loading), until solid fusion is obtained.[11] Several biomechanical and finite element studies have compared the stability of various occipitoatlantoaxial stabilization techniques.[10,12-15] However, to date there are no consensus about the standard occiput to C2 fixation and the necessity of routine incorporation of C1 lateral mass screws into (OC) instrumentation constructs.[16,17]

The present study aims to evaluate the stability provided by OC fixation using occipital plate and C2 pedicular screws.

Material and methods

The study included 6 formalin preserved whole human cadaveric specimens obtained from the dissecting room of the Anatomy Department at our institute. Occipitocervical fixation using occipital plate and C2 pedicle screws connected by rods was performed in all specimens. The cadavers included 6 males, with different ages. However, the exact age of the cadaveric specimens was not available from the records. This study protocol was approved by the institutional review board and ethics committee.

Specimen preparation

All specimens were dissected, instrumented and tested in prone position. A midline vertical incision was done at the occipitocervical region. Dissection was done with preservation of the facet joints and osteoligamentous structures. (Nondestructive stability testing).

Methods of fixation

1. Occipital fixation was performed with an occipital plate using 2 bicortical screws (4.5 ×12mm). The occipital plate has 4 rigidly locked holes for midline screws placement and arms that extend laterally, which contain bilateral slots for rods attachment.

2. Cervical fixation was performed with bilateral C2 pedicular screws which were 3.5 mm in diameter.

3. Adequacy of screws placement was assessed in all specimens before testing using portable x-ray machine.

4. The rods were inserted in the slots of the screws that are placed on the lateral wing of the plate and the slots of the pedicle screws in C2, and final tightening of the nuts was performed.

The dissection and fixation were carried out by a senior consultant spine surgeon.

Methods of Appling forces

1. The specimens were manually loaded by the maximum possible flexion, extension and axial rotation, with the head lying free at the edge of the table.

2. Assessment of stability of fixation was done after 100, 500, 1000, 2000 and 3000 cycles, and any construct failure was documented.

3. In the first 3 specimens (group 1), repetitive loading was planned to be initially applied in flexion and extension. If there was no failure of the construct at 3000 cycles, loading has to be continued in axial rotation.

4. In the second 3 specimens (group 2), repetitive loading was planned to be initially applied in axial rotation up to 3000 cycles. If there was no failure of the construct, loading has to be continued in flexion and extension. (Fig. 1)

The manual loading was applied by a spine fellow.
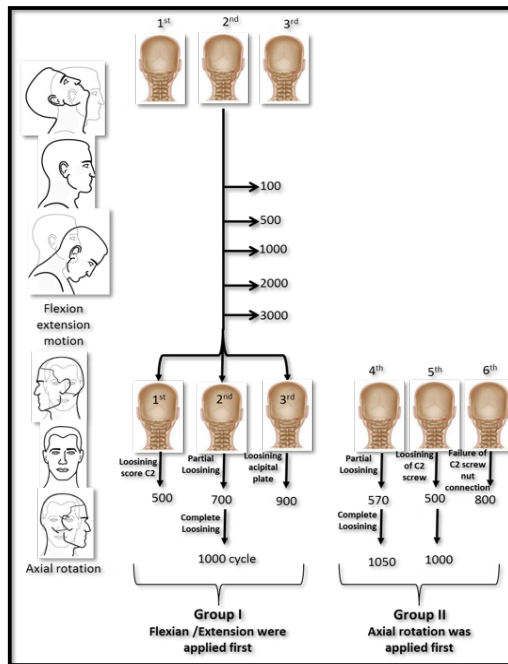
Figure 1. Flow chart summarizing the methods of applying loading and the results.

Methods of Radiological evaluation

Lateral radiographs of cervical spine were done in neutral, flexion, and extension after instrumentation to all specimens and after 100, 500, 1000, 2000 and 3000 loading cycles, and any construct failure was documented.

Method of statistical analysis

After data collection, the results were tabulated and analyzed. Descriptive statistics were used for parameters which did not need statistical analysis. SPSS software (v 9.4) software was used for the analysis.

Results

The maximum possible flexion, extension and axial rotation were performed in all specimens, with some difficulty, because of their stiffness as a result of formalin preservation. The first 3 specimens (group 1) showed no implants failure apparently or radiologically after 3000 loading cycles. However, failure occurred at different sites when axial rotation loading was applied at 500, 700 and 900 cycles respectively.

On the other hand, when axial rotation loading was initially applied to the second 3 specimens (group 2), failure occurred at 570, 500 and 800 cycles respectively before applying flexion extension loads (Fig. 1, Table 1,2).

Sites of failure

As shown in table 2, loosening of C2 screw occurred in 4 specimens, while occipital plate loosening occurred in one specimen and loosening of screw nut connection in one specimen.

Case illustrations are shown in figures 2, 3 and 4.

Table 1. Distribution of cadaveric occipitocervical stability regarding axial rotation loading.

Number of cycle	Number of success	Percent
100	6	100
500	5	83.3
1000	3	50
2000	0	0
3000	0	0
Total	6	100

Table 2. Distribution of the cadaveric occipitocervical stability after rotation loading and the sites of failure.

Case No.	No. of cycle till Partial failure	No. of cycle till complete failure	Site of failure
1	-	500	Loosening of C2 screw
2	700	1000	Loosening of C2 screw
3	-	900	Loosening occipital plate
4	570	1050	Loosening of C2 screw
5	500	1000	Loosening of C2 screw
6	-	800	Failure of C2 screw nut connection

A   B

Figure 2. The first specimen from group 1. Flexion and extension loading were applied first till 3000 cycles, and fixation remain stable. After that, axial rotation was applied till 500 cycles when loosening of C2 screw occurred.

Discussion

This study was to evaluate the stability of OC fixation using occipital plate and C2 pedicle screws in 6 human cadavers under flexion, extension and axial rotation loading. Our results showed that axial rotation and not flexion and extension loading affect the stability of the contract.

Clinical studies have demonstrated that the occipital plate combined with pedicle screws provided a high fusion rate and maintained alignment in the OC region, in both elderly and pediatric patients.[18,19] Hankinson et al have reported a 100% occipitoatlantoaxial fusion rate in pediatric patients.[19] Furthermore, Oda et al showed,

A   **B**
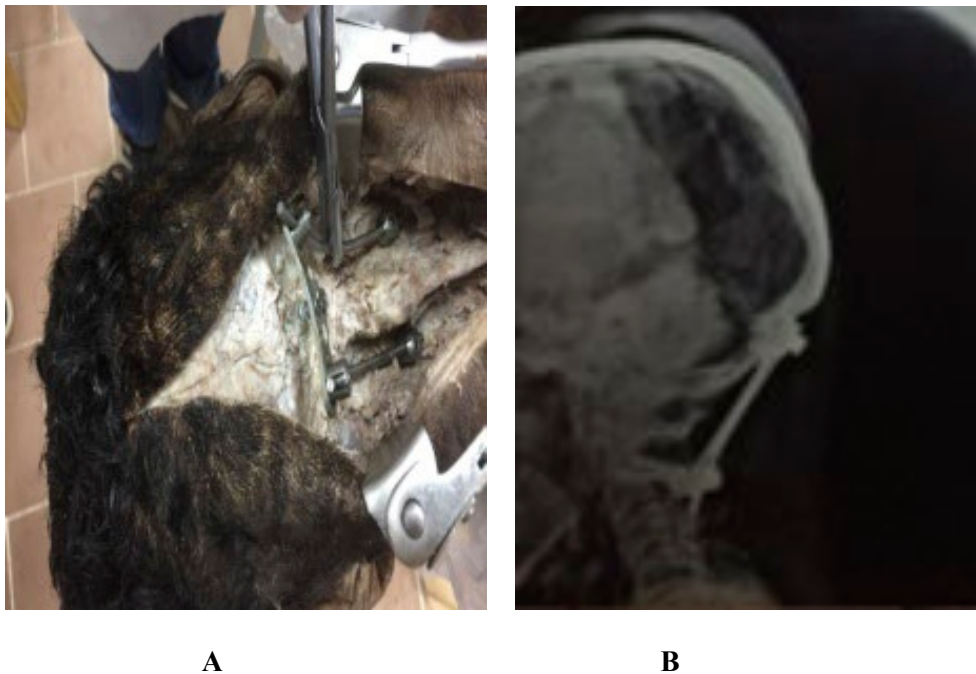
Figure 3. The third specimen from group 1. Flexion and extension loading were applied first till 3000 cycles and fixation remained stable. After that, axial rotation was applied till 900 cycles when occipital screw loosening occurred.

in their cadaveric models, that the combination of occipital screws and C2 pedicle screws provided the highest stability among other constructs.[5]

Several techniques of C2 fixation have been evaluated. In addition to being a challenging screw insertion technique, the transarticular screw has the greatest risk of injuring the vertebral artery during placement. The C2 pars screw has the same high risk of vertebral artery injury without the biomechanical strength of C2 pedicle screws. The pedicle screw technique may have a slightly less risk of vertebral artery injury. The C2 laminar screw technique theoretically has the least risk of vertebral artery injury. However, difficulty in rod contouring can also present a challenge. Moreover, the presence of laminae is a prerequisite for using the crossing C2 laminar screws. [20]

A debate of inclusion of lateral mass C1 to the construct existed. In their biomechanical study, Wolfla et al showed that the placement of C1 lateral mass screws did not increase occipitocervical construct stability when compared with construct without of C1 lateral mass screws. The authors, however, used C2 pars screws, but not pedicle screws.[16] On the other hand, in their nonlinear finite element model, Liu et al revealed that the addition of supplemental C1 lateral mass screws to occiput-C2 fixation not only enhances greater stability, especially during axial rotation, but also has the advantage of distributing the stress evenly and reduces the risk of construct

A   B
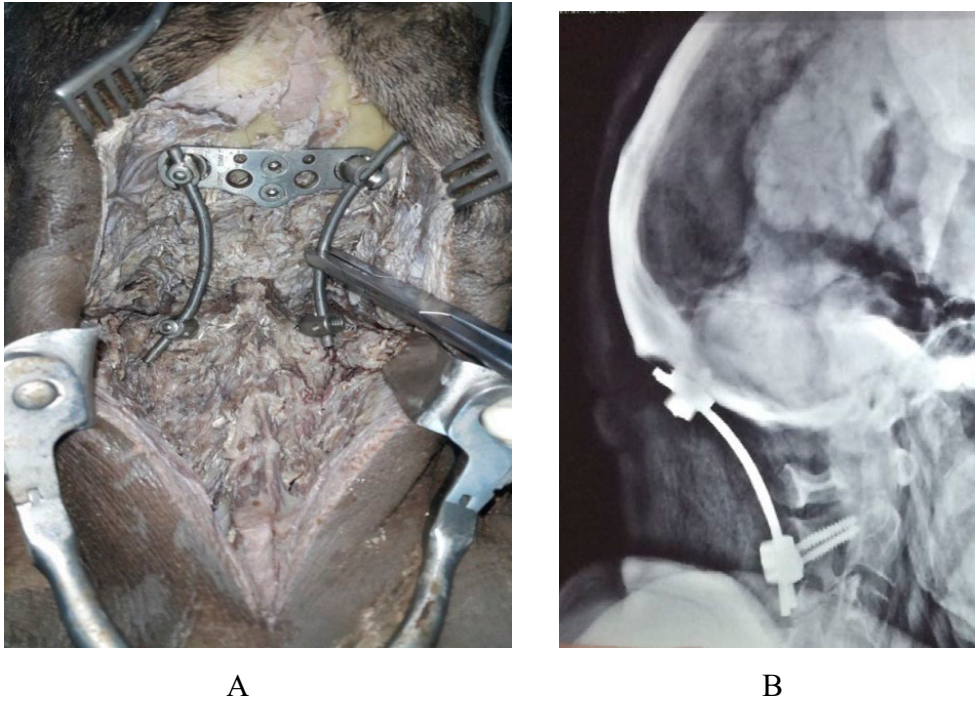
Figure 4. The Second specimen from group 2. Axial rotation loading was applied first till 1050 cycles, when loosening of C2 screw occurred.

failure due to occipital screw pullout and rod fracture.[17]   We agree with them that this method may be a reasonable option in some selected cases in severe rheumatoid arthritis, the chronic smoker, tuberculosis, osteopenia, or osteoporosis in elderly patients, where the bone mineral density is of poor quality and screw purchase is weaker, and it may promote a high OC fusion rate. Their study design was, however, only a computational simulation with all its limitations. It should be noted, however, that the placement of C1 lateral mass screws is technically demanding and susceptible to possible complications such as vertebral artery injury, blood loss, and longer overall operative time.[19]

Our results showed the occiput-C2 construct can tolerate flexion extension loading more than rotational loading. Liu et al study results indicated that the addition of supplemental C1 lateral mass to the construct may offer similar stability in flexion but greater stability in extension, lateral bending, and axial rotation in comparison to the occiput-C2 fixation.[17]

Our data indicated that most of the construct failure occurs at C2 (loosening of C2 screws occurred in 4 specimens, loosening of C2 screw nut connection in one specimen, while occipital plate loosening occurred in only one specimen). However, several studies have shown that OC instrumentation failure most commonly occurs at the occipital screw and superior part of the rod. [17,21] Bhatia et al reported 4% patients

undergoing fixation had rod fracture in the stress region of rod curvature or occipital screw pullout.[21] They explain this observation by the low holding capacity of the occipital screw because of its short purchase length, compared to C2 pedicle screw. Moreover, the occipital screw and superior part of the rod bear main part of stress.[17] We were unable to explain this difference. However, our occipital screws were applied bicortically. Obtaining purchase of the ventral cortex would provide the screw with increased strength of fixation and pullout strength. However, the concept of bicortical occipital screws may be taken cautiously during surgery for adjacent structures concerns.

Since our results indicated that occiput-C2 construct can tolerate flexion extension loading and not axial rotation, we would recommend immobilization, at least at the early postoperative period, in a way that allow flexion and extension, but restricts axial rotation.

The results of our study should be kept within the context of its limitations. The limitations of our study are that it is a cadaveric, in vitro design, which may not truly reflect clinical application, the relatively small numbers of specimens, the lack of lateral pending loading testing, and the lack of destructive tests.

In addition, the experiment has been done using formalin preserved cadavers, which are not the standard cadavers used for biomechanical studies. Formalin hardens the tissues including joint capsules and ligaments leading to loss of pliability of the joints and the elastic properties of the ligaments. Hence the actual stability to the joint, offered by the capsuloligamentous structures might not be accurately assessed by the experiment. If the study had been performed using fresh frozen cadavers (not available in our department) which are brought to room temperature during the study, that would replicate the living tissues, the results would reflect the actual stability of the C0-C2-C2 joint complex.

Furthermore, the OC junction complex has been subjected to manual loading by the same person for all 6 specimens. Even if it was done by the same person, the amount of force applied by manual loading may not going to be consistent in each cycle and may vary to a significant extent between cadavers.

However, the cadaveric biomechanical data could be useful to adequately test and validate the biomechanical principles for further understanding of occiput- C2 pedicle screw constructs. In addition to the biomechanical stability, there are several factors that could determine the choice of the OC construct, including the patient's clinical situation, the structural regional anatomy, especially the vertebral artery, the size of the C2 pedicle, the presence or absence of a C2 lamina and surgeon preference. We believe that the choice of the OC instrumentation should depend on the clinical situation, including the previously mentioned factors, and not only on the biomechanical considerations.

Conclusion

Our study revealed that occiput-C2 pedicle screw construct, without supplementary C1 lateral mass provided stability in flexion and extension loading. However, repeated axial rotation loading causes failure of construct. Therefore, we could suggest immediate postoperative restriction of axial rotation while flexion extension motion could be allowed.

Conflict of interest

None of the authors have any conflict of interest. None declared.

References

1. Vaccaro AR, Lim MR, Lee JY. Indications for surgery and stabilization techniques of the occipito-cervical junction. Injury 2005; 36(2 Suppl): B44–53.
2. Deutsch H, Haid RW, Rodts GE, et al. Occipitocervical fixation: long-term results. Spine (Phila Pa 1976) 2005; 30:530–5.
3. Foester O. Die Leitungsbahnen des Schmerzgefuhls und die Chirurgische Behandlung der Schmerzzustande. Berlin: Urban und Schwarzenberg, 1927.
4, Wertheim S, Bohlman H. Occipito-cervical fusion: indications, technique, long-term results in thirteen patients. J Bone Joint Surg Am 1987; 69: 833–6.
5. Oda I, Abumi K, Sell LC, et al. Biomechanical evaluation of five different occipito-atlanto-axial fixation techniques. Spine (Phila Pa 1976) 1999; 24:2377–82.
6. Sutterlin CE, Bianchi JR, Kunz DN, et al. Biomechanical evaluation of occipitocervical fixation devices. J Spinal Disord 2001; 14:185–92.
7. Winegar CD, Lawrence JP, Friel BC, et al. A systematic review of occipital cervical fusion: techniques and outcomes. J Neurosurg Spine 2010; 13:5-16.
8. Smucker JD, Sasso RC. The evolution of spinal instrumentation for the management of the occipital cervical and cervicothoracic junctional injuries. Spine (Phila Pa 1976) 2006; 31(11 Suppl): S44-52.
9. Vender JR, Rekito AJ, Harrison SJ, et al. The evolution of posterior cervical and occipitocervical fusion and instrumentation. Neurosurg Focus 2004;16: E9.
10. Helgeson MD, Lehman RA Jr, Sasso RC, et al. Biomechanical analysis of occipitocervical stability afforded by three fixation techniques. Spine J 2011; 11:245–50.
11. Logroscino CA, Genitiempo M, Casula S. Relevance of the cranioaxial angle in the occipitocervical stabilization using an original construct: a retrospective study on 50 patients. Eur Spine J (2009) 18 (Suppl 1):S7–S12.
12. Takigawa T, Simon P, Espinoza OA, et al. Biomechanical comparison of occiput-C1-C2 fixation techniques: C0-C1 transarticular screw and direct occiput condyle screw. Spine (Phila Pa 1976) 2012; 37:E 696–701.
13. Anderson PA, Oza AL, Puschak TJ, et al. Biomechanics of occipitocervical fixation. Spine (Phila Pa 1976) 2006; 31:755–61.
14. Gabriel JP, Muzumdar AM, Khalil S, et al. A novel crossed rod configuration incorporating translaminar screws for occipitocervical internal fixation: an in vitro biomechanical study. Spine J 2011; 11:30–5.
15. Cai X, Yu Y, Liu Z, et al. Three-dimensional finite element analysis of occipitocervical fixation using an anterior occiput-to-axis locking plate system: a pilot study. Spine J 2014; 14:1399–1409.
16. Wolfla CE, Salerno SA, Yoganandan N, et al. Comparison of contemporary occipitocervical instrumentation techniques with and without C1 lateral mass screws. Neurosurgery 2007; 61(3 Suppl):87-93.
17. Liu H, Zhang B, Lei J, et al. Biomechanical Role of the C1 Lateral Mass Screws in Occipitoatlantoaxial Fixation: A Finite Element Analysis. Spine (Phila Pa 1976) 2016; 41:E1312-E1318.

18. Clarke MJ, Toussaint LR, Kumar R, et al. Occipitocervical fusion in elderly patients. World Neurosurg 2012; 78:318–25.
19. Hankinson TC, Avellino AM, Harter D, et al. Equivalence of fusion rates after rigid internal fixation of the occiput to C-2 with or without C-1 instrumentation. J Neurosurg Pediatr 2010; 5:380–4.
20. Nassos JT, Ghanayem AJ, Sasso RC, et al. Biomechanical evaluation of segmental occipitoatlantoaxial stabilization techniques. Spine (Phila Pa 1976). 2009; 34:2740-4.
21. Bhatia R, Desouza RM, Bull J, et al. Rigid occipitocervical fixation: indications, outcomes, and complications in the modern era. J Neurosurg Spine 2013;18:333–9.

Original research article

Anatomical and Congenital Variations of Styloid Process of Temporal Bone in Indian Adult Dry Skull Bones

Kalyan Chakravarthi Kosuri[1,*], Venumadhav Nelluri[2], Siddaraju KS[3]

[1] Associate Professor, Department of Anatomy, Varun Arjun Medical College, Banthra-Shajahanpur - 242307, Uttar Pradesh, India
[2] Assistent professor, Department of Anatomy, Melaka Manipal Medical College (MMMC), Manipal University, Manipal, and Karnataka, India
[3] Lecturer, Department of Anatomy, KMCT Medical College, Manassery, Calicut, Kerala, India

Abstract

Background: Styloid process of temporal bone is clinically significant, because of anatomical or congenital variations in length, number, angulations as well as close proximity to many of the vital neurovascular structures in the neck. Abnormal or congenital variations of the styloid process may compress adjacent neurovascular structures and leads to symptoms of stylalgia (Eagle's syndrome). **Aim:** Accordingly this study was aimed to evaluate the anatomical and congenital variations of styloid process of temporal bone in Indian adult dry skull bones. **Materials and Methods:** This study was carried out on 110 dry human skulls irrespective of age and sex at Varun Arjun medical college- Banthra,-UP, Melaka Manipal Medical College-Manipal and KMCT Medical College, Manassery- Calicut. All the skulls were macroscopically inspected for the anatomical and congenital variations of styloid process of temporal bone. Photographs of the anatomical and congenital variations were taken for proper documentation. **Results:** Out of 110 dry human skull bones we noted very rare unusual unilateral triple styloid processes in one skull bone, unusual bilateral double styloid processes in one skull bone and unilateral double styloid processes in right side of one skull bone. **Conclusion:** Congenital double, triple and elongated styloid process noted in this study can leads to styloidogenic jugular compression syndrome or stylo-carotid artery syndrome or disturb the biomechanics of temporomandibular joint or compress/ irritate nearby neurological structures trigger a series of symptoms such as dysphagia, odynophagia, facial pain, ear pain, headache, tinnitus and trismus. Proper knowledge and diagnosis of anatomical and congenital variations of styloid process of temporal bone is important to anaesthetists, dentists, neurosurgeons and otolaryngologists, orthopaedic surgeons, clinical anatomist, Radiologists, forensic experts Architectures and morphologists which may increase the success of diagnostic evaluation and surgical approaches to the region.

* Corresponding author. E-mail: kalyankosuric@gmail.com

Introduction

Styloid process of temporal bone is a slender bony projection from the inferior surface of the temporal bone, averaging from 2 to 2.5 cm in length when it exceeds the 4 cm length it is assigned the term elongation is considered an anomaly. The elongation of styloid process was first described in 1652 by Italian surgeon Pietro Marchetti. Embryologically it developed from the second pharyngeal/brachial arch called as the Reichert's cartilage because it is of cartilaginous origin. The styloid process provides attachments of two ligaments stylohyoid and stylomandibular ligaments and three muscles stylopharyngeus, stylohyoid and styloglossus muscles. Many important neurovascular structures are presented adjacent to the styloid process.

Styloid process laterally covered by parotid gland, facial nerve crosses its base, external carotid artery crosses its tip and medially, it is separated from beginning of internal jugular vein by stylopharyngeus. Lateral to the stylomastoid foramen, tympanomastoid suture lies which accommodates auricular branch of vagus nerve. Internal carotid artery, internal jugular vein and, vagus, spinal accessory and hypoglossal cranial nerves lie on its medial side. In close proximity is the glossopharyngeal nerve laying in the posterolateral wall of tonsilar fossa (Patil S et al., 2014). Styloid process is usually extends downwards, due to anatomical and congenital variations in length or number and angulations may compress adjacent neurovascular structures.

Stylomastoid foramen intervenes between styloid and mastoid processes; the foramen transmits facial nerve and stylomastoid artery. Any abnormal or congenital variations of styloid process or ossified ligamentous structures around area of stylomastoid foramen may partially or completely compress the facial nerve and leads to Bell's palsy is a condition that causes weakness or paralysis of the muscles in the face. Considering the various relations of styloid process with important neurovascular structures and its morphological variations, this study was aimed to evaluate the anatomical and congenital variations of styloid process in Indian dry adult skulls.

Materials and Methods

This study was carried out on 110 dry human adult skulls irrespective of age and sex at Varun Arjun medical college- Banthra,-UP, Melaka Manipal Medical College-Manipal and KMCT Medical College Manassery- Calicut. All the skulls were macroscopically inspected for the anatomical and congenital variations of styloid process of temporal bone. Photographs of the anatomical and congenital variations were taken for proper documentation.

Results

Out of 110 dry human skulls bones the following anatomical and congenital variations of styloid process of temporal bone were noted-
- **CASE-I:** Very rare unusual unilateral triple styloid processes were noted in left side of one skull bone. In which one styloid process with a length of 2.4cm projected from the anterior surface (non articular part of mandibular fossa) and lower
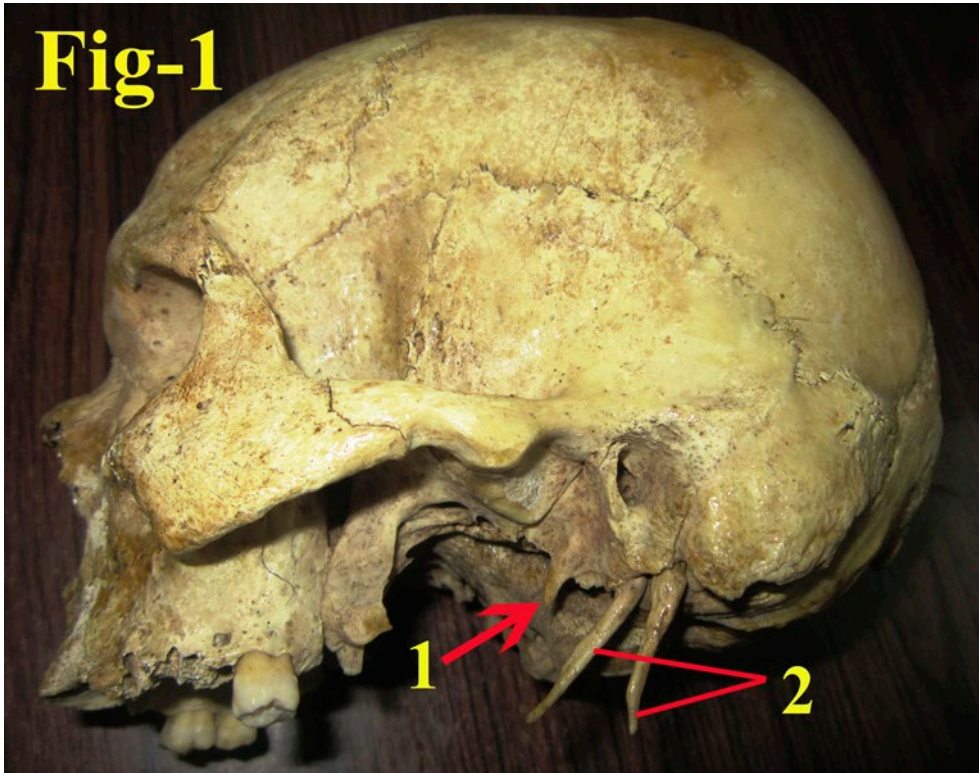
Figure 1. Left lateral view of skull showing unilateral Triple styloid processes. 1- Styloid process (bony projection) projected from the anterior surface (non articular part of mandibular fossa) and lower border of tympanic part of temporal bone; 2- Elongated double styloid processes.

border of tympanic part of temporal bone and another two styloid processes were elongated (each 7.3cm length) and projected from the inferior surface of the temporal bone. (Fig. 1)

- **CASE-II:** Unusual bilateral double styloid processes were noted in one skull bone. In which one styloid process with a length of 2.8 cm each projected from the anterior surface and lower border of tympanic part of respective temporal bone (non articular part of mandibular fossa) and another one styloid processes was elongated with a length of each 6.8 cm each projected from the inferior surface of the respective temporal bone. (Fig. 2)

- **CASE-III:** Unilateral double styloid processes were noted in right side of one skull bone. Double styloid processes were elongated and projected from the inferior surface of the temporal bone. In which one styloid process with a length of 5.9 cm extended downwards and forwards and another styloid process is slender and sharp with a length of 5 cm extended backwards. (Fig. 3)

- The length of styloid process (distance between base and tip of the styloid process) were measured with the help of digital vernier calipers.
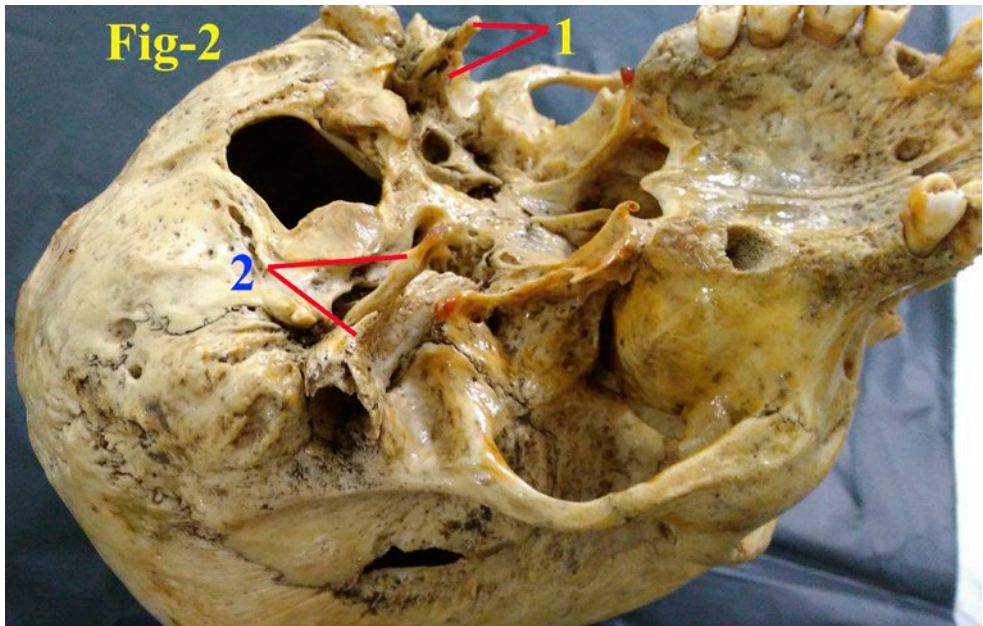
Figure 2. Basal view of skull showing bilateral double styloid processes. 1. Right side- double processes; 2. Left side- double styloid processes.

Discussion

Stylohyoid chain includes the styloid process, stylohyoid ligament, and the lesser horn of the hyoid bone which develops from the Reichert cartilage of the second brachial arch. Anatomical or congenital variation in the length/number of the styloid process and its stylohyoid chain or abnormal ossification of stylohyoid chain components is said to have profound anatomical, anthropological as well as of clinical importance. Such abnormalities may compress or irritate nearby neurovascular structures trigger a series of symptoms such as dysphagia, odynophagia, facial pain, ear pain, headache, tinnitus and trismus. This set of symptoms associated with the elongated styloid process is called Eagle's syndrome was first described by Watt W. Eagle in the year 1937 (Kim E et al., 2008). Two types of Eagle syndrome have been described the first type includes cervicofacial pain aggravated by swallowing and the sensation of a foreign body in the throat after tonsillectomy. The second type is the "stylo-carotid artery syndrome", and is attributed to impingement of the internal carotid arteries, extra cranially by the styloid process this can cause compression when turning the head, resulting in a transient ischemic accident or stroke (Chuang WC et al., 2007; Eagle WW, 1949; Farhat HI et al., 2009).

Dashti SR et al reported symptomatic jugular vein obstruction in association with Eagle syndrome (styloidogenic jugular compression syndrome). He reported two bilateral novel cases presenting with symptoms of increased central venous pressure related to jugular venous outflow obstruction caused by osseous impingement of the
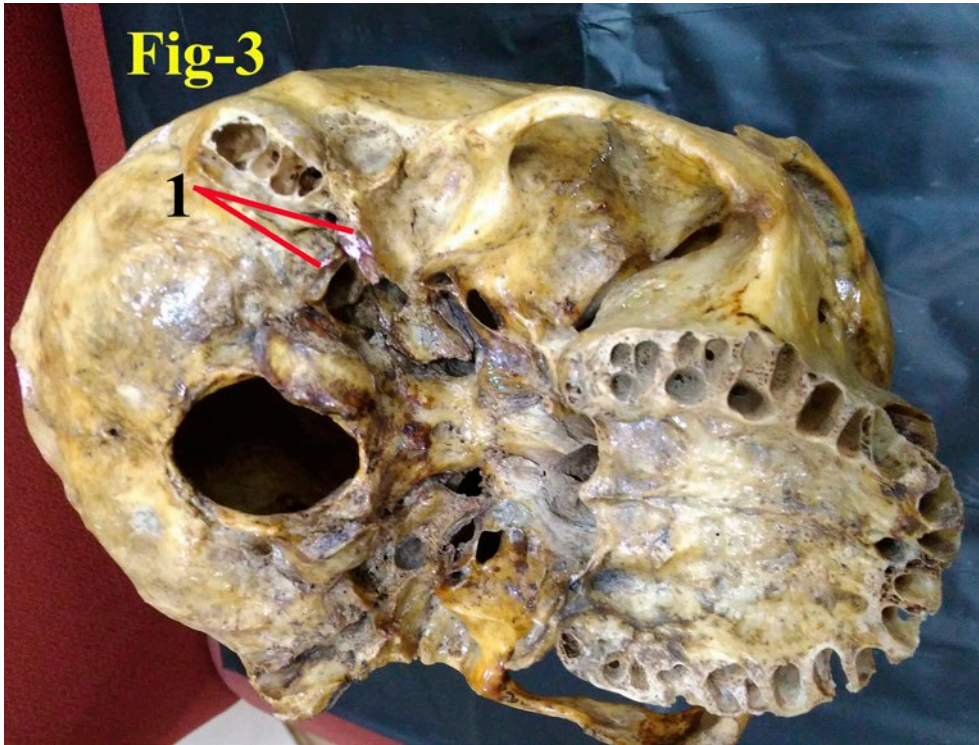
Figure 3. Basal view of skull showing unilateral double styloid processes. 1. Right side- double styloid processes.

jugular veins between the transverse process of atlas and a prominent, posteriorly located styloid process. In such cases patients may experience symptomatic central venous hypertension and may be predisposed to venous stasis and cerebral venous sinus thrombosis (Dashti SR et al., 2012). In the present study we noted elongated double styloid process in which one styloid process extended downwards and forwards and another styloid process is slender with sharp edges extended backwards (CASE-III). Such congenital double elongated styloid process may leads to styloidogenic jugular compression syndrome or stylo-carotid artery syndrome. The knowledge of the congenital double elongated styloid process and the structures related to it noted in this study can helps in proper diagnosis and treatment of eagle's syndrome.

Normal range of the length of the styloid process differs among the studies in the literature. Eagle reported the normal length of styloid process as 2.5 cm; other authors measured the length as 3 cm. It has been reported that it is probably symptomatic when the length exceeds 4cm (Monsour P A, Young W G. 1986). Massey et al reported 11 cases of styloid process having length of more than 4 cm out of 2000 cases studied (Massey EW, 1978). Harma et al reported 4 -7% for elongated styloid process (Harma R. Stylalgia, 1966). Cawich et al presented post mortem study elonga-

tion was seen four times more in males than females and in 75% of cases the elonga-
tion was bilateral (Cawich SO et al., 2009). Prabhu et al reported a case of bilateral
elongated styloid process with the length of 60 and 59 mm on the right and left side,
respectively (Prabhu LV et al., 2007). Paraskevas et al presented a case of the dried
skull with an elongated right styloid process with a length of 58 mm (Paraskevas G
K et al., 2009). Ishwar et al reported a bilaterally elongated styloid process in dried
skull measuring 60 mm (Ishwar B et al., 2013). The elongation of styloid process is
which can be accompanied by calcification of the stylohyoid and stylomandibular
ligaments, Guarna M et al reported abnormally elongated styloid process (70 mm on
the left side) was due to ossification of the stylohyoid ligament (Guarna M and Agli-
ano M, 2018). Sanjeev I K et al reported elongated styloid process of 8 cm length in
which styloid process proper was 5 cm long and remaining 3 cm was ossified stylo-
hyoid ligament (Sanjeev Iranna Kolagi et al,. 2010). In another case, he reported on
left side of a male cadaver the styloid process was 6.3 cm long. Very rare and unu-
sual unilateral triple styloid process noted in our study (CASE-I), in which one sty-
loid process projected from the anterior surface (non articular part of mandibular
fossa) and lower border of tympanic part of temporal bone with a length of 2.4 cm,
such congenital variations may disturb the biomechanics of temporomandibular joint.
The auriculotemporal nerve is branch from posterior division of mandibular nerve,
it supplies cutaneous sensitivity from the auriculotemporal area, including roof and
anterior wall of external acoustic meatus, tragus, anterior portion of the ear, skin of
temple, cuticular layer of tympanic membrane, articular branch to temporo-mandib-
ular joint, and also carries parasympathetic fibres to the parotid gland. The auricu-
lotemporal nerve arises as two roots unite to form a trunk passes between the neck
of the mandible and the sphenomandibular ligament and then turn superiorly, poste-
rior to its condylar head. The auriculotemporal nerve can be damaged or compressed
between anomalous styloid process (projecting from the anterior surface and lower
border of tympanic plate (CASE-I)) and temporomandibular joint results in auricu-
lotemporal neuralgia. And another two styloid processes were elongated and project-
ed from the inferior surface of the temporal bone with a length of 7.3 cm each (CASE-
I), surprisingly stylomastoid foramen intervenes between them such congenital vari-
ations may leads to compression of facial nerve and can results in symptoms of Bell's
palsy. Unilateral triple styloid process noted in our study (CASE-I) may be due to
errors of embryologic cleavage of Reichert cartilage of the second brachial arch dur-
ing development. To the best of our knowledge, triple and double styloid processes
observed in this study have not been cited in modern literature. Such multiple styloid
processes presented in this study may create a diagnostic problem for the radiolo-
gist examining for foreign bodies or may compress neurovascular structures and can
cause serious implications in any surgical intervention in the region, and may lead to
false radiological or neurological differential diagnosis. So it is important that clini-
cians and radiologists should keep this entity in mind as it may increase the success
of diagnostic evaluation and surgical approaches to the region.

Unusual bilateral double styloid process noted in our study (CASE-II), in which
one styloid process projected from the anterior surface (non articular part of man-
dibular fossa) and lower boarder of tympanic part of respective temporal bone with
a length of 2.8 cm each. Another styloid process was elongated and projected from
the inferior surface of the respective temporal bone with a length of 6.8 cm each.

The deep cervical facia or facia colli invests the muscles of the neck and fills up the interval between muscles, vessels and cervical viscera. The deep cervical facia generally described to possess three layers from outside inwards- investing, pretracheal and vertebral. When we see the vertical extent of investing facia traced above at the lower pole of parotid gland, it splits superficial and deep layers (parotid fascia). The superficial layer is strong, passes superficial to the gland, is attached to the lower margin of zygomatic arch and blends with the epimysium of the masseter to form a strong parotid-masseteric fascia. The deep layer passes medial to the gland and is attached to the lower boarder of the tympanic plate and the styloid process of temporal bone. Here the deep layer is thickened to form stylomandibular ligament which extends from the tip of the styloid process to the angle of mandible. Anomalous styloid process projecting from the anterior surface and lower border of tympanic plate noted in our study may the results of calcification and ossification of the deep layer of the parotid fascia attached to the lower boarder of the tympanic plate. Clinically the relation of tip of the stylohyoid process is important, course of it situated in between external and internal carotid arteries, anteriomedially it is related to facial nerve, medially with accessory and vagus nerves any pressure at the surrounding area of tonsilar fossa or manipulations around the neck area may lead to fracture of such double styloid process leading to many clinical signs. Knowledge of the existence of such congenital variation or elongated styloid process is important for dentist otolaryngologist, surgeon, and radiologist.

Conclusion

We believe that the present study has provided some important data which will contribute to the scientific literature, providing the anatomical data of styloid process of temporal bone in the in Indian adult dry skull bones. To the best of our knowledge, triple and double styloid processes observed in this study have not been cited in modern literature. Proper knowledge and diagnosis of anatomical and congenital variations of styloid process of temporal bone not only enlightening for the anaesthetists, dentists, neurosurgeons and otolaryngologists, orthopaedic surgeons, also vital for the clinical anatomist, Radiologists, Forensic experts Architectures and morphologists.

Funding

None.

Conflict of interest

None declared.

Ethical approval

Not required.

References

Chuang WC, Short JH, McKinney AM, Anker L, Knoll B, McKinney ZJ. (2007) Reversible left hemispheric ischemia secondary to carotid compression in Eagle syndrome: Surgical and CT angiographic correlation. AJNR Am J Neuroradiol 28: 143- 145.

Cawich SO, Gardner M, Shetty R, Harding HE. (2009) A post mortem study of elongated styloid Processes in a Jamaican population. The Internet Journal of Biological Anthropology.   Volume 3: Number 1.

Dashti SR, Nakaji P, Hu YC, Frei DF, Abla AA, Yao T, Fiorella D. (2012) Styloidogenic jugular venous compression syndrome: Diagnosis and treatment. Case report. Neurosurgery. 70(3): E795-799.

Eagle WW. (1949) Symptomatic elongated styloid process: Report of two cases of styloid process–carotid artery syndrome with operation. Arch Otolaryngol. 49: 490–503.

 Farhat HI, Elhammady MS, Ziayee H, Aziz-Sultan MA, Heros RC. (2009) Eagle syndrome as a cause of transient ischemic attacks. Case report. J Neurosurg. 110: 90-93.

Guarna M, Agliano M. (2018) An abnormally long styloid process with ossification of the stylohyoid ligament. Int J Anat Res. 6(2.1):5101-03.

Harma R. Stylalgia. (1966) clinical experiences of 52 cases. Acta Otolaryngol. suppl 224: 149+.

Ishwar B, Gavishiddappa H , Balasaheb P, Balappa B, Ambadasu B. (2013) Bilateral elongated styloid process: its anatomical embryological and clinical implications Int J Med Res Health Sci. 2(2):273-276.

Kim E, Hansen K, Frizzi J. (2008) Eagle Syndrome: case report and a review of literature. Ear Nose Throat J. 87, 631-633.

Monsour P A, Young W G. (1986) Variability of styloid process and stylohyoid ligament in panoramic radiographs. Oral Med Oral Path. 61: 522-526.

Massey EW. (19780 Facial pain from an elongated styloid process. (Eagles syndrome). South Med J. 71: 1156–1159.

Prabhu LV, Kumar A, Nayak SR, Pai MM, Vadgaonkar R, Krishnamurthy A, Madhan Kumar SJ. (2007) An unusually lengthy styloid process.Singapore Med J. 48(2):34-36.

Paraskevas G K, Raikos A, Lazos LM, Kitsoulis P (2009) Unilateral elongated styloid process: a case report. Cases Journal. 2:9135.

Patil S, Ghosh S, Vasudeva N. (2014) Morphometric study of the styloid process of temporal bone. J Clin Diagn Res. Sep; 8(9):AC04-6.

Sanjeev Iranna Kolagi , Anita Herur and Ashwini Mutalik. (2010) Elongated styloid process-report of two rare cases. Int J Anat Var. 3: 100–102.

Original Research Article

Anomalous Renal Vasculature Existing With Congenital Anomalies of Kidneys, Ureters and Suprarenal Glands: A Cadaveric Study

Kalyan Chakravarthi Kosuri[1,*], Siddaraju KS[2], Venumadhav Nelluri[3]

[1] Associate professor, Department of Anatomy, Varun Arjun Medical College, Banthra-Shajahanpur, Uttar Pradesh, India
[2] Lecturer, Department of Anatomy, KMCT Medical College, Manassery, Calicut, Kerala, India
[3] Assistent professor, Department of Anatomy, Melaka Manipal Medical College (MMMC), Manipal University, Manipal, and Karnataka, India

Abstract

Variations in the renal vessels have been observed frequently in routine dissection and surgical practice, but existing with congenital anomalies of kidneys or ureters or suprarenal glands is very rare. Accordingly the aim of this study was designed to evaluate the prevalence of anomalous renal vasculature existing with congenital anomalies of kidneys, ureters and suprarenal glands. This study was carried out on 48 human cadavers (including dissected cadaveric specimens) irrespective of age and sex used for routine dissection of abdomen conducted for medical undergraduates teaching purpose. The kidneys, ureters and suprarenal glands along with their arteries were exposed and the anomalous variations of renal vasculature existing with congenital anomalies of kidneys or ureters or suprarenal glands were observed. Photographs of the anomalous and developmental variations were taken for proper documentation. Out of 48 human cadavers following anomalous / developmental variations were noted- unilateral retro aortic left real vein, extra-hilar artery (branch of renal artery that presents an extra hilar penetration) to the superior pole of left kidney, existing with very rare and unusual double suprarenal gland with unusual blood supply was noted in one cadaver. Bilateral double renal arteries existing with unusual incomplete double ureters on right side and incomplete triple ureters on left side were found in one cadaver. Left triple renal arteries, right double renal arteries existing with bilateral polycystic kidneys with distended ureters were found in one cadaver. Double extra-hilar arteries to the superior pole of right kidney, existing with unusual blood supply to the right suprarenal gland and right testis was found in one cadaver. Bilateral Early division of renal artery existing with bilateral polycystic kidneys fond in one cadaver. Anatomical and developmental variations of renal vasculature, ureters, kidneys and their relationship to surrounding structures are clinically significant as they interferes several operative procedures like kidney transplantation, surgical reconstruction of the abdominal aorta, interventional radiologic procedures and urologic operations; hence detection of the possible developmental variations of the renal vasculature, ureters, kidneys and their relationship to surrounding structures is clinically necessary for adequate surgical management to preserve renal functions.

* Corresponding author. E-mail: kalyankosuric@gmail.com

Introduction

The urinary system includes pair of kidneys and their ureters, urinary bladder and urethra. The kidneys are essential excretory organs, situated retro-peritoneally in the posterior abdominal wall, which elaborate urine and eliminate nitrogenous waste products of protein metabolism from the blood and maintain electrolyte and water balance. The ureters are the muscular tubes which convey the urine from the corresponding kidney to the urinary bladder for temporary storage. Each kidney is supplied by one renal artery which is a lateral branch of abdominal aorta immediately below the level of superior mesenteric artery at the upper lumbar level (L1-L3). Suprarenal or Adrenal glands are a pair of retro-peritoneal endocrine glands situated near superior pole of corresponding kidney. Each gland consists of outer cortex which synthesizes three types of steroid hormones from plasma cholesterol: glucocorticoids, mineral corticoids, and sex steroids; and inner medulla under direct control of the central nervous system and synthesizes catecholamines along the sympathetic nervous system. Variations in the renal vessels have been observed frequently in routine dissection and surgical practice, but such occurrence existing with congenital anomalies of kidneys or ureters or suprarenal glands is rare. Accordingly this study was designed to evaluate the anatomical and developmental variations of renal vasculature existing with congenital anomalies of kidneys or ureters or suprarenal glands.

Materials and Methods

This study was carried out on routine human cadaveric dissection of abdomen (including dissected cadaveric specimens) conducted for medical undergraduates at Varun Arjun medical college- Banthra,-UP, KMCT Medical College, Manassery- Calicut and Melaka Manipal Medical College-Manipal. The kidneys, ureters and suprarenal glands along with their arteries were exposed and the anatomical and developmental variations of renal vasculature existing with congenital anomalies of kidneys or ureters or suprarenal glands were observed. Photographs of the anatomical and developmental variations were taken for proper documentation.

Results

Out of 48 human cadavers (including dissected cadaveric specimens) irrespective of age and sex, dissected during the medical undergraduates teaching purpose the following developmental variations of renal vasculature existing with congenital anomalies of kidneys or ureters or suprarenal glands were noted -

Case - I: Left retro aortic real vein, extra -hilar branch of left renal artery to the superior pole of left kidney, existing with very rare and unusual double suprarenal gland with unusual blood supply was noted in one cadaver (Fig. 1, Fig. 2 and Fig. 3).
• Left real vein (7.2 cm) found larger than right renal vein (1.1 cm). Left real vein after emerging from hilum of left kidney it descends obliquely and joined the inferior vena cava by passing behind the abdominal aorta.
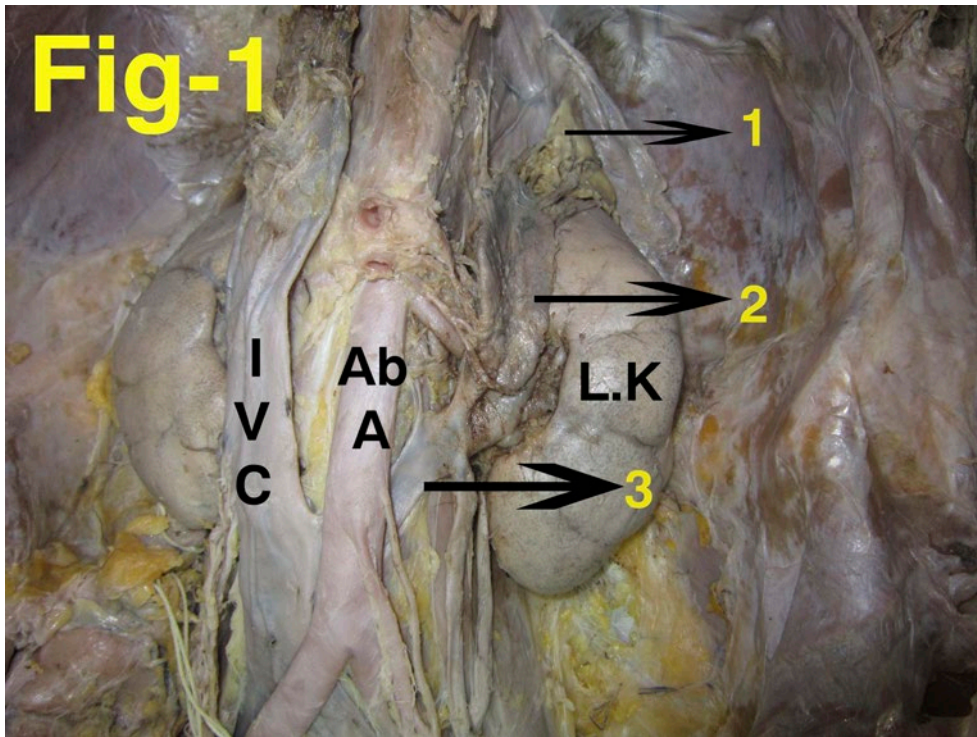
Figure 1. Showing left retro aortic real vein existing with double suprarenal glands. 1 and 2- left double suprarenal glands; 3- Left retro aortic real vein; IVC- Inferior Vena Cava; AbA- Abdominal Aorta; L.K- Left Kidney.

- Out of two suprarenal glands one was located across the hilum and on the anterior surface of left kidney, another suprarenal gland was found on the upper pole of the same kidney. Left suprarenal gland located across the hilum received blood supply from the left renal artery by two branches. Surprisingly another left suprarenal gland located on the upper pole of kidney received blood supply from the suprarenal gland located across the hilum by three branches.

Case - II: Bilateral double renal arteries existing with unusual incomplete double ureters on right side and incomplete triple ureters on left side were noted in one cadaver (Fig. 4).

Case - III: left triple renal arteries, right double renal arteries existing with bilateral polycystic kidneys with distended ureters were noted in one cadaver (Fig. 5).

Case - IV: Double extra-hilar arteries to the superior pole of right kidney, existing with very rare and unusual blood supply to the right suprarenal gland and testis was noted in one cadaver (Fig. 6 and Fig. 7).

- A common trunk originated from the right renal artery gave off double extra-hilar arteries to the superior pole of right kidney and a lower suprarenal branch to the right suprarenal gland. Surprisingly the middle suprarenal branch originated from
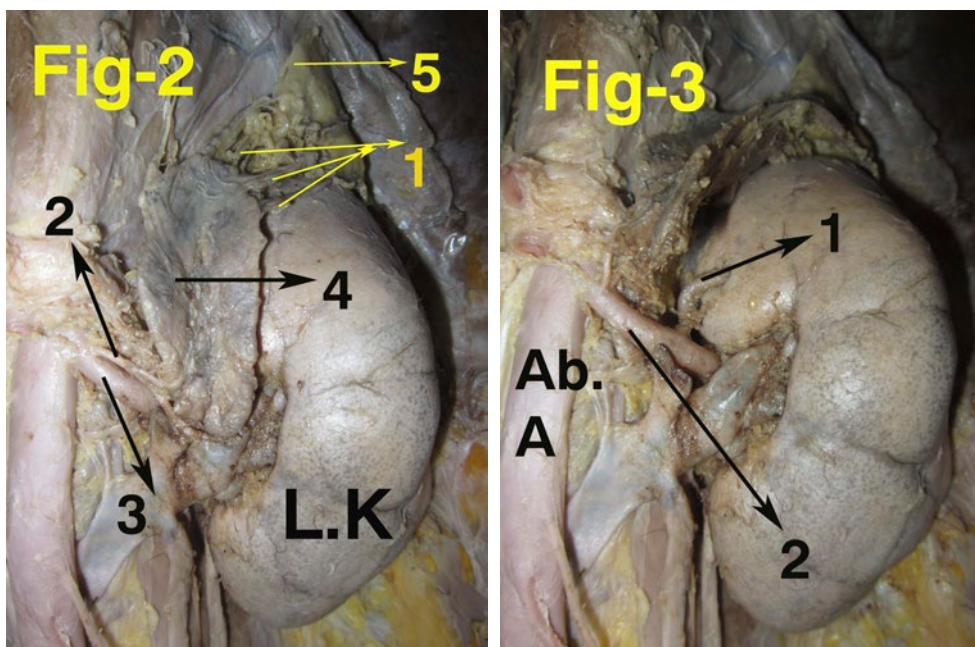
Figure 2. Showing unusual blood supply of left double suprarenal glands. 1- Three suprarenal branches originating from the suprarenal gland located across the hilum of left kidney; 2- Suprarenal branches originating from the left renal artery; 3- Left renal artery; 4- Suprarenal glands located across the hilum and on the anterior surface of left kidney; 5- Suprarenal glands located upper pole of the left kidney; L.K- Left Kidney.

Figure 3. Showing extra -hilar branch of left renal artery. 1- extra -hilar branch of left renal artery to the superior pole of left kidney; AbA- Abdominal Aorta. ; 2- Left renal artery.

the abdominal aorta after supplying suprarenal gland, within the gland it gave off a testicular artery which descends in front of the hilum of the right kidney.

Case-V: Bilateral Early division of renal artery existing with bilateral polycystic kidneys fond in one cadaver (Fig. 8 and Fig. 9).

Discussion

During the embryological period the metanephric kidneys lies in the pelvic cavity and obtain their blood supply from the median sacral artery. As the kidneys ascend, and reaches the iliac fossa blood supply is obtained from the common and internal iliac arteries. As the kidneys ascend further and reach undersurface of the diaphragm blood supply is obtained from the lowest supra-renal artery and this branch persists after birth as the permanent renal artery. Accessory renal arteries are common, and usually arise from abdominal aorta above or below the main renal artery they are regarded as persistent embryonic lateral splanchnic arteries. Rarely, accessory renal arteries arise from the celiac trunk, superior mesenteric arteries, inferior mesenteric
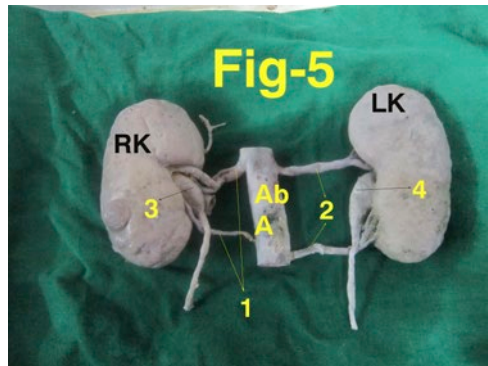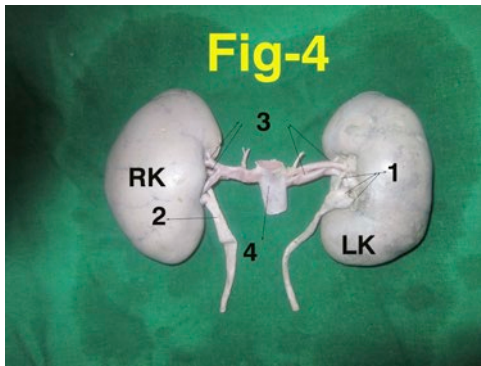
Figure 4. Showing Bilateral double renal arteries existing with double and triple incomplete ureters. 1- Left incomplete triple ureters; 2- Right incomplete double ureters; 3- Bilateral double renal arteries; 4- Abdominal Aorta; LK- Left Kidney; RK- Right Kidney.

Figure 5. Showing Bilateral accessory renal arteries existing with bilateral polycystic kidneys with distended ureters were. 1- Right triple renal arteries; 2- Left double renal arteries; 3 and 4- distended ureters; LK- polycystic Left Kidney; RK- polycystic Right Kidney.
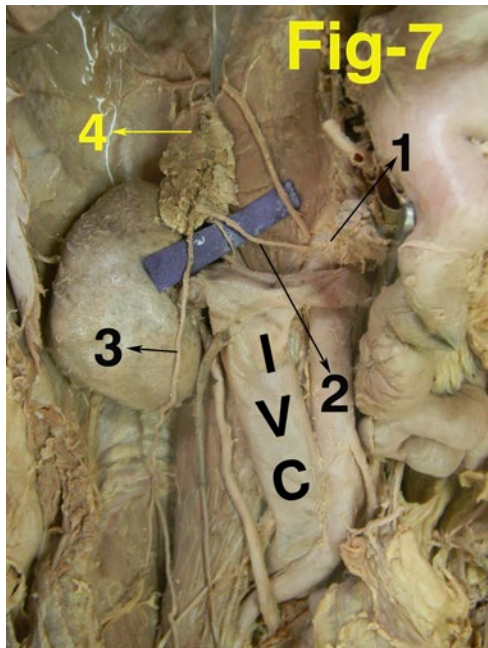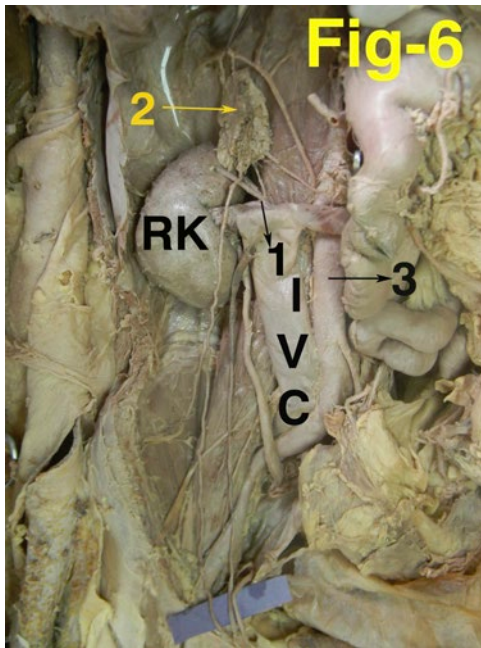
Figure 6. Showing double extra-hilar arteries to the superior pole of right kidney. 1- Common trunk originated from the right renal artery gave off double extra-hilar arteries to the superior pole of right kidney and a lower suprarenal branch to the right suprarenal gland; 2- Right suprarenal gland; 3- Abdominal Aorta; IVC- Inferior Vena Cava.

Figure 7. Showing unusual blood supply to the right suprarenal gland and testis. 1- Abdominal Aorta; 2- middle suprarenal branch; 3- testicular artery; 4- Right suprarenal gland; IVC- Inferior Vena Cava.
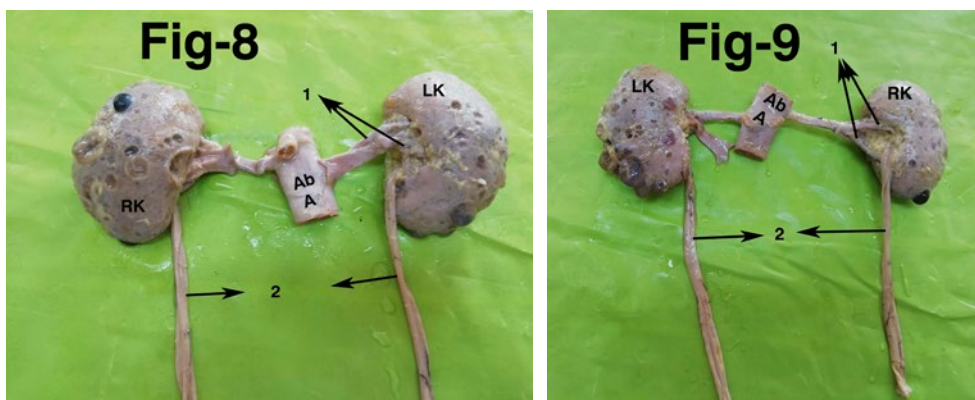
Figure 8. Front view showing Bilateral Early division of renal arteries existing with bilateral polycystic kidneys. LK- polycystic Left Kidney; RK- polycystic Right Kidney; AbA- Abdominal Aorta; 1- Early division of left renal artery;2- Ureters.

Figure 9. Posterior view showing Bilateral Early division of renal arteries existing with bilateral polycystic kidneys. LK- polycystic Left Kidney; RK- polycystic Right Kidney; AbA- Abdominal Aorta; 1- Early division of right renal artery;2- Ureters.

arteries, and the area near the aortic bifurcation, common iliac arteries or the median sacral artery (Kawamoto S et al., 2004; Urban BA et al., 2001; Pozniak MA., 1998). Incidence of accessory renal arteries had been variously re-ported as 50% (Helstrom 1927) 25% (Edsman 1954) and 30% (Henry Gray 2005). Pollak R et al reported 23% double renal arteries, 4% triple arteries, and 1% quadruple arteries in a cadaver study (Pollak R et al., 1986). In angiographic study Ozkan et al. reported multiple arteries in 24%, bilateral multiple arteries in 5%, and early division in 8% of cases, bilateral aberrant renal arteries were found in 13-16 % of cases (Ozkan et al., 2006). Adult polycystic kidney is an autosomal dominant disease with high penetrance and occurs in 1 out of 400 to 1000 persons and accounts for 5 to 10% of chronic renal failure (Sujatha K et al., 2017). In our study in one specimen bilateral early division of renal artery was present with bilateral polycystic kidneys. Saldarriaga B. et al reported one additional artery 22.3 and two additional arteries 2.6% (Saldarriaga B. et al., 2008). Hemanth Kommuru reported one additional artery 18.5%, two additional arteries 9.7% (Hemanth Kommuru et al., 2012). Renal artery variation including their number, source of origin and course are very common, but left triple renal arteries, right double renal arteries existing with bilateral polycystic kidneys with distended ureters in one cadaver noted in our study are very rare.

Kosuri Kalyan Chakravarthi et al. reported a case of left triple renal arteries in which two originated from the abdominal aorta and one originated from the common trunk gave off accessory renal artery to the left kidney, inferior mesenteric, and left testicular arteries (Kosuri Kalyan Chakravarthi et al., 2013). Where as in our study an unusual common trunk originated from the right renal artery gave off double extrahilar arteries to the superior pole of right kidney and a lower suprarenal branch to the right suprarenal gland, such anatomical variations awareness may provide safety

guidelines for endovascular procedures like therapeutic embolization and angioplasties and helps in the management of renal vascular hypertension. Interestingly in the same case the middle suprarenal branch originated from the abdominal aorta after supplying right suprarenal gland, within the gland it gave off a right testicular artery which descends in front of the hilum of the right kidney. Surgeons should have a thorough knowledge regarding such rare anatomical variations of origin and unusual course of the testicular arteries as any injury to this artery during surgery might cause testicular atrophy.

In 5th week of intrauterine life from dorsomedial side of caudal part of the mesonephric duct gives rise to a diverticulum know as the ureteric bud. The ureteric bud grows head wards and forms a dilation, later it was covered by a cap like investment known as metanephric blastema, where it divides many times and   gives rise to the major and minor calyces and the collecting tubules of the kidney. The stalk of the ureteric bud forms the ureter and its dilated end persists as the pelvis of the kidney. Duplicated ureter occurs approximately 1% of the population, Siomou E et al, and Inamoto K et al reported the duplex collecting system (Siomou E et al., 2006; Inamoto K et al., 1983). Kosuri Kalyan Chakravarthi et al. reported a case of unilateral double ureters descended from the separate renal pelvis (double pelvis) originated from the upper and lower renal poles of the right kidney joined at the middle in a Y-shaped manner (Kosuri Kalyan Chakravarthi et al.,2013). Unusual Y- shaped incomplete double (bifid) ureters on right side and incomplete triple ureters on left side found in this study probably due to double/triple ureteric buds arising from the caudal part of the mesonephric duct. Alexander et al has reported a case of duplex ureter which got damaged during laparoscopic hysterectomy and was diagnosed postoperatively (Alexander et al., 2010). Bilateral double renal arteries existing with unusual developmental abnormalities of ureters noted in this study should keep in mind by the urologists, technicians and clinicians for therapeutic and surgical interventions to avoid complications.

Suprarenal gland develops from two sources-the cortex of the gland developed from the mesoderm and the medulla from the neuro-ectoderm of the neural crest. The cortex is formed of two parts: a thick fetal cortex surrounded by a second thin layer of cells that will later form the definitive cortex. Within two or three weeks after birth, fetal cortex totally disappears and the definitive cortex differentiates into three zones of cells. In adrenogenital syndrome or any form of adrenocorticotropic hormone stimulation accessory suprarenal tissues are found around the main gland or in relation to the structures formed from the urogenital ridge. Unilateral double suprarenal glands noted in this study were close to the left kidney. Ectopic adrenal tissue has been reported in the testis, spermatic cord, broad ligament, kidney, retrocaval space, celiac region, lungs, central nervous system, colon, pancreas and gallbladder such abnormalities may undergo malignant transformation or become hormonally functional (Ayala AR et al., 200; Leibowitz J et al., 1998). Kirici et al reported a case of ectopically located adrenal gland in the right retrocrural space with compressive symptoms (Kirici et al., 2001). Alexander L Shifrin et al reported adrenal tumor from the aberrant adrenal gland located under hepatic segment (Alexander L Shifrin et al., 2011). Suprarenal gland is supplied by superior, middle and inferior suprarenal arteries. Superior suprarenal artery usually arise from the posterior division of inferior phrenic artery, Merklin and Michel, Gagnon, studies have

shown that superior suprarenal is arising directly from aorta, celiac trunk, and superior polar artery (Merklin R.J et al, 1958). Middle Suprarenal Artery arise from the abdominal aorta, Gagnon have shown the origin from the renal artery and Hollinshed and Cunningham have observed that the middle suprarenal is absent in some cases (Gagnon R, 1964; Gagnon R, 1957; Hollinshed W.H , 1952; Romanes G. J, 1978). Inferior suprarenal artery arise from the renal artery, Gerard et al reported in 23% of cases the inferior suprarenal artery is double, one arising from aorta and other from the renal artery (Gerard G, 1913). Where as in our study superior, middle suprarenal arteries were absent on the left side and inferior suprarenal artery originated from the left renal artery by two branches supplied the accessory suprarenal gland located across the hilum of left kidney. Surprisingly another left suprarenal gland located on the upper pole of kidney received blood supply from the accessory suprarenal gland located across the hilum by three branches. To the best of our knowledge, double suprarenal glands with unusual blood supply observed in this study have not been cited in modern literature.

The inferior vena cava is developed from a vast network of three pairs of veins including the posterior cardinal, subcardinal, and the supracardinal veins. During the development of the IVC, The subcardinal and supracardinal veins form an anastomotic communication network of veins that course along the ventral (pre-aortic) and dorsal (post-aortic) aspect of the abdominal aorta. The portion of pre-aortic anastomotic communication persists as the normal left renal vein. If the post-aortic anastomotic communication persists then the left renal vein is posterior to the aorta, forming a retro aortic left renal vein. Reed et al reported incidence of retro aortic left renal vein anomaly was1.8%, Trigaux et al reported 3.7%, and Satyapal et al reported 0.5% (Reed MD et al., 1982; Trigaux JP et al., 1998; Satyapal KS et al., 1998). In our study the retro aortic left renal vein (with a length of 7.2 cm) after emerging from hilum of left kidney it descends obliquely and joined the inferior vena cava close to the bifurcation of abdominal aorta. Retro aortic left renal vein anomaly is a relatively uncommon condition it may be compressed between aorta and vertebrae and leads to retrograde venous return which results in increases the pressure of gonadal veins leading to varicosity of veins, haematuria, pain, thrombosis and nutcracker syndrome (left renal vein hypertension). Combination of unilateral left retro aortic real vein, extra -hilar artery (branch of renal artery that presents an extra hilar penetration) to the superior pole of left kidney, existing with very rare and unusual double suprarenal gland with unusual blood supply noted in case-I made this study more unique.

Conclusion

To the best of our knowledge, anomalous renal vasculature existing with congenital anomalies of kidneys, ureters, suprarenal glands, and testicular artery observed in this study have not been cited in modern literature. Such anatomical and developmental variations knowledge is immensely important because of its implications in segmental resections, renal transplantation, and surgical reconstruction of the abdominal aorta, interventional radiologic procedures, urologic operations and gonadal surgeries.

Funding

None.

Conflict of interest

None declared.

Ethical approval

Not required.

References

Ayala AR, Basaria S, Udelsman R, Westra WH, Wand GS. (2000) Corticotropin-independent Cushing's syndrome caused by an ectopic adrenal adenoma. J Clin Endocrinol Metab. Aug; 85(8):2903-06.

Alexander L Shifrin, Min Zheng, Jerome J Vernick. Ectopic adrenocortical adenoma. (2011) World Journal of Endocrine Surgery. January-April; 3(1):1-2

Alexander P. B. Dalzell, Richard G. Robinson, Kirsten M. Crooke. (2010) Duplex ureter damaged during laparoscopic hysterectomy. Pelviperineology. 29: 88

Edsman G. (1954) *Acta. Radiol. Stockh*. 42: 26-32.

Gagnon R. Middle Suprarenal artery in man. (1964) A statistical study of two hundred human adrenal glands. Rev. Canad.Biol. 23:461.

Gagnon R. (1957) The arterial supply of human adrenal gland. Rev. Canada.Biol. 16:421- 423.

Gerard G. (1913) Sur les variations d origine et de nombre des Arteres genitales internes de 1'homme. Bibl Anat. 23:206-220.

Gray's anatomy (2005) *The anatomical basis of clinical prac-tice*, 39th edition, 1274.

Helstrom J. (1927) *Act. Chis. Scand*. 61, 289 -330.

Hemanth Kommuru, Sree Lekha D, Jothi S.S, Rajeswararao N, And Sujatha N. (2012) Presence Of Renal Artery Variations And Its Surgical Correlation. International Journal of Medical and Clinical Research. 3(5):176-179.

Hollinshed W.H. (1952) Anatomy of endocrine Glands, Surg. Clin. North Americ. 32:1115- 1140.

Inamoto K, Tanaka S, Takemura K, Ikoma F. (1983) Duplication of the renal pelvis and ureter: associated anomalies and pathological conditions. Radiat Med. 1: 55-64.

Kawamoto S, Montgomery RA, Lawler LP, Horton KM, Fishman EK. (2004) Multidetector row CT evaluation of living renal don bn ors prior to laparoscopic nephrectomy. Radiographics. 24: 453-466.

Kirici Y, Mas MR, Saglamkaya U, Oztas E, Ozan H. (2001) Accessory suprarenal gland: Report of a case. Surg Radiol Anat Jun. 23(3): 201-03.

Kosuri Kalyan Chakravarthi, Karuneswari Devi P, Uma MN. (2013) Congenital Unilateral Double Renal Pelvis and Double Ureters Associated with Triple Renal veins and Left Retro Aortic Renal Vein. Int. J. Chemical and Life Sciences. 02: 1159- 62.

Kosuri Kalyan Chakravarthi. (2013) Unilateral Multiple Variations of Renal, Phrenic, Suprarenal, Inferior mesenteric and Gonadal arteries. J Nat Sc Biol Med. 2013. 5(1):173-5.

Leibowitz J, Pertsemlidis D, Gabrilove JL. (1998) Recurrent Cushing's syndrome due to recurrent adrenocortical tumor fragmentation or tumor in ectopic adrenal tissue? J Clin Endocrinol Metab. Nov; 83(11): 3786-89

Merklin R.J and Michel's N.A. (1958) The variant Renal and Suprarenal blood supply with data on the inferior phrenic, ureteral and gonadal arteries. Jr Int.college Surg. 29: 41-75.

Ozkan U, Oguzkurt L. (2006) Renal artery origin and variations: Angiographic evaluation of 855 consecutive patients. Diagn Interv Radiol. 1: 183-186.

Pozniak MA, Balison DJ, Lee FT, Tambeaux RH, Uehling DT, Moon TD. (1998) CT angiography of potential renal transplant donors. Radiographics. 18: 565–587.

Pollak R, Prusak BF, Mozes MF. (1986) Anatomic abnormalities of cadaver kidneys procured for purposes of transplantation. Am Surg. 52: 233-235.

Reed MD, Friedman AC, Nealey P. (1982) Anomalies of the left renal vein: analysis of 433 CT scans. J Comput Assist Tomogr. 6:1124-6.

Romanes G. J. (1978) Cunningham's Textbook of Anatomy (Oxford Medical Publications), Ed.11.

Saldarriaga B, Perez A.F, Ballesteros L.E. (2008) A direct anatomical study of additional renal arteries in a Colombian mestizo population. 67(2): 129-13.

Satyapal KS, Kalideen JM, Haffejee AA, Singh B, Robbs JV. (1999) Left renal vein variations. Surg Radiol Anat. 21: 77-81.

Siomou E, Papadopoulou F, Kollios KD, Photopoulos A, Evagelidou E, Androulakakis P, et al. (2006) Duplex collecting system diagnosed during the first 6 years of life after a first urinary tract infection: a study of 63 children. Journal of Urology. 175: 678-81.

Sujatha. K, Shakuntala Rao. (2017) A human cadaveric study on incidence, prevalence and morphology of cystic kidneys-with emphasis on its embryological, pathological and clinicalsignificance.IntJAnatRes. 5(4.1):4437-4440

Trigaux JP, Vandroogenbroek S, De Wispelaere JF, Lacrosse M, Jamart J. (1998) Congenital anomalies of the inferior vena cava and left renal vein: evaluation with spiral CT. J Vasc Interv Radiol. 9:339-45.

Urban BA, Ratner LE, Fishman EK. (2001) Three dimensional volume-rendered CT angiography of the renal arteries and veins: normal anatomy, variants, and clinical application. Radiographics. 21: 373–386.

Instructions for the Authors

Submission: Original research or review papers and letters (not longer than two printed pages including up to one figure and one table) dealing with the entire field of anatomy, histology and embryology of vertebrates, with special regard to human and veterinary medicine and including medical education, anatomical case reports and history of medicine and biology in those fields, written in English, should be sent preferentially by email to: Prof. Domenico Ribatti, Dipartimento di Scienze Mediche di Base, Neuroscienze ed Organi di Senso, Università degli Studi di Bari, Piazza Giulio Cesare, 11, Policlinico, 70124 Bari (Italy), email <domenico.ribatti@uniba.it>. Texts should be in Word or RTF format; tables in Word or Excel format; see below for the format of tables and figures. In case the Authors would use mail instead of email to deliver the manuscript they should add the text and figures stored on a CD-ROM.

Proofs: Proofs will be sent to the corresponding author and should be returned within 10 days of receipt.

Arrangement: manuscripts should be typed double spaced with wide margins. All manuscripts should be introduced by a title page and all - except letters - should have a summary in the page following the title one. The text of research manuscripts should develop through Introduction, Materials and Methods, Results, Discussion, Acknowledgements. The references should start on a separate page and should be followed, on separate pages, by the captions for figures and tables.

Title page: the first page should indicate the title (in low case, except the initial of the first word), the Authors' names (full first name, middle initial and full surname of each Author) and departmental and institutional affiliation, a running title not exceeding 50 characters including spaces, up to six key words, full address with e-mail and number of telephone and fax of the corresponding Author.

Summary: except for letters, a summary should precede the text, not exceeding 250 words and free of abbreviations and references.

Introduction: should explain the scientific background purpose of the research.

Materials and methods: should present all the information useful for the repetition of the experiments.

Results: should present all experimental data and describe original observations, without references; the illustrations and tables should be recalled at the appropriate points. *Discussion:* should give the Authors' interpretation of the results and the conclusions of the research. *Acknowledgments:* should state also financial support and declaration of conflict of interest, if any.

References: the list should include all and only those publications which are cited in the text, and should be arranged in alphabetical order. References must always include the surname and initials of the name of all Author(s), year of publication in parentheses, and full title; see also separate instructions for formatting references and citations.

Articles in journals will be referred by the surname and initials of the name of all Author(s), year of publication, full title of the paper, title of the journal abbreviated according to international nomenclature, volume, first and the last page of the paper as follows:

Haider S.G., Passia D., Overmeyer G. (1986) Studies on the fetal and postnatal development of rat Leydig cells employing 3 beta-hydroxysteroid dehydrogenase activity. Acta Histochem. 32 (Suppl.): 197-202.

Monographs and books will be referred by the surname and initials of the Author(s), year of publication, full title, publisher, place of publication, as follows:

Matthews D.E., Farewell V.T. (1985) Using and understanding medical statistics. Karger, Basel.

Chapters of books will be referred by the surname and initial of Author(s), year of publication, title of the article, the word "in" followed by colon and the surname and initials of the editor(s) of the book, title of the book, publisher, place of publication and page numbers, as follows:

Cottingham S.L., Pfaff D. (1986) Interconnectedness of steroid-binding hormones: existence and implications. In: Gauten D., Pfaff D. Current Topics in Endocrinology, Vol. 7, Morphology of the hypothalamus and its connections. Springer, Berlin. Pp. 223-250.

In the citations in the text, the names of Authors must be followed by the year of publication. In case of more than two Authors, only the first one is named, followed by "et al.".

Captions for figures: the captions should make the figures self-explicative without referring to the text and without repeating extensively what is given in the Results section. The magnification of photomicrograph should be indicated by a scale bar in the lower right corner. If quantitative data are represented (as graphs etc.), the meaning of the error bars needs to be defined (standard deviation, standard error, 95% confidence limits or else).

Tables: when quantitative data are represented, the meaning of the indicated variance values needs to be defined (standard deviation, standard error, 95% confidence limits or else). Tables should be provided as Word or Excel files, NOT as images.

Figures: electronic images should be presented as high resolution images (not less than 300 dpi at the final size intended for the print) in TIFF, PDF or Photoshop format; drawings should be in EPS-modifiable or PDF format. Alternatively the Authors may provide high quality half tone or colour photomicrographs, professional level art work and graphic; line drawings should not exceed 28 x 36 cm. Lettering and labels must be readable after reduction; when printed, an illustration or group of illustrations should not exceed 19.2 cm long by 12.2 wide.

Page charge: Authors should be charged € 40.00 (+ VAT) per printed page. Illustrations will be printed in b/w on paper version, in full colour on online version. The printer, before typesetting, will send by fax or mail a quotation of the full cost in charge of the Author. If requested, the Editors may furnish a pro-forma invoice. Payment is requested before printing.

Reprints: Each author will receive a printed copy of the issue, plus the electronic version of the article published in PDF format.

Detailed instructions for reference formatting

FORMAT CITATIONS ACCORDING TO THE JOURNAL RULES:
• single author: Smith, 2012
• two authors: Smith and Brady, 2012
• three or more authors: Smith et al., 2012
• separate with semicolon multiple references in the same parentheses
• order multiple references in the same parentheses in progressive chronological order, and those of the same year in alphabetical order (*e.g.*: Smith, 2000; Brady and Smith 2007; Smith and Brady 2007; Brady, 2010)
• cite authors in parentheses [*e.g.*: someone made this statement (Smith, 2012)]; if the author name is part of a sentence, then insert the year ofr publication in parentheses [*e.g.*: Smith (2012) made this statement]

FORMAT REFERENCES ACCORDING TO THE JOURNAL RULES:
• complete list of all authors, whatever their number
• point after each initial of each author's name
• point at the end of the abbreviated words of the Journal title, not at the end of non-abbreviated words (e.g. J. Biol. Chem. // Nature)
• no comma after Journal title
• no issue number when the numbering of pages is continuous throughout a volume; indicate the issue only if the numbering of pages starts at 1 in each issue
• colon + space after Journal volume
• last page in full, as well as the first page, for all items
• no bold, no italic

LIST MULTIPLE REFERENCES OF THE SAME (FIRST) AUTHOR AS FOLLOWS:
a. Author alone, in chronological order (starting from the text, they are searched as "Author, year of publication")
b. Author and coauthor, in alphabetical order of second author and then in chronological order (starting from the text, they are searched as "Author and Coauthor, year of publication")
c. Author and more than one coauthor, in chronological order independent of the name of the second and other authors (starting from the text, they are searched just as "Author et al., year of publication")

REMOVE ALL HYPERLINK FROM THE TEXT AND REFERENCE LIST.

(continued)